The Effects of Mobile Phone Radiation on The Human Central Nervous System

A thesis submitted in fulfilment of the requirements for the degree of Doctor of Philosophy

Mr Nicholas Perentos
B. Eng.

School of Electrical and Computer Engineering
Science, Engineering and Technology College
RMIT University

November 2008

Declaration

I certify that except where due acknowledgment has been made, the work is that of the author alone; the work has not been submitted previously, in whole or in part, to qualify for any other academic award; the content of the thesis is the result of work which has been carried out since the official commencement date of the approved research program; and, any editorial work, paid or unpaid, carried out by a third party is acknowledged.

Mr Nicholas Perentos

November 04, 2008

Acknowledgments

The work presented in this thesis has been made possible with the input, guidance and support of a number of people with whom I was fortunate enough to cross paths with.

I would like to thank my senior supervisor, Professor Irena Cosic, for believing in me and providing me with this fantastic opportunity to undertake a PhD. I would also like to acknowledge Irena for the original idea based on which this thesis has been formed.

I am indebted to Steve Iskra who has been an endless source of knowledge in so many areas and from whom I have learned, I hope, to be more thorough, meticulous and precise in my work.

To Professor Rodney Croft I would like to express my gratitude for opening the doors to the Brain Sciences Institute to me, for his endless guidance in so many aspects of my work and for ultimately sparking the motivation in me to be as best a researcher as I can.

A warmhearted thank you goes to Ray McKenzie who has always been supportive and willing to discuss and guide me in most of the difficulties I have faced throughout this degree.

Thank you also to my second supervisor Dr Dean Cvetkovic and Dr Sarah Loughran for proof-reading large parts of my thesis and suggesting ways to improve the content. Thank you also to Dr Sumie Leung, Dr Vanessa Cropley, Maia Sauren and Kyrie Hadjilouizou for making work days more fun!

Last, I would like to thank my father, mother and brother for their unconditional support, each in their own way, throughout the years of my undergraduate and postgraduate studies.

Abstract

Mobile telephony has been introduced to the public as early as 1993. User numbers have been growing ever since and recent estimates put the Global Systems for Mobile Communication (GSM) users in excess of 2 billion. It is arguable that the perceived benefits that society enjoys from wireless technologies have been many and may include increased business productivity and easy access to emergency services. On the other hand, there are perceived risks associated with the use of these devices, one of them being the possibility of adverse health effects that may arise from the exposure to the electromagnetic energies that mobile phone devices emit.

To address these concerns, there is ongoing scientific research in the area. A large portion of this research has concentrated on detecting changes in brain function, predominantly through electroencephalography, both during and shortly after brief (less than 40 minutes) exposures to the radiation. Trends in findings point to spectral increases in the alpha band frequency range, (8-12 Hz) of the electroencephalogram. The evidence however is currently inconclusive; some of the reasons for this being constraints imposed by statistical issues, absence of any replication studies, diversity in methodological designs and inadequate characterizations of exposure dose.

The current thesis reports the following original contributions:

- Comparison of pulsed RF with continuous RF at identical instantaneous peak field intensities.
- Investigation of non linear features of brain signals during and shortly after GSM like electromagnetic exposures and
- Investigation of the effects of ELF battery generated fields on brain activity.

Abstract

Following a small pilot study, a larger one was conducted which employed a single day fully counterbalanced, double blind, cross-over design and recruited seventy-two healthy volunteers. It incorporated three active exposures a continuous RF, pulsed RF and a pulsed low frequency exposure and a sham exposure with each one lasting for twenty minutes.

The results suggest that alpha band EEG activity is reduced under continuous and pulsed-RF as well as pulsed-low frequency exposures. The effect appeared stronger under the pulse modulated exposures thus reinforcing the general finding in literature that field pulsing is necessary to induce effects. The non linear analysis of EEG measures revealed no changes under any of the active exposures. It was therefore concluded that if any non linear changes do occur, the Approximate Entropy method was not sensitive enough to detect them.

It was also identified through experimental measurements that the observed effect on the EEG was very close to the noise limit of the experimental setup. This observation can perhaps account for the largely variable results that are observed throughout the relevant literature. Another possible reason for the variation in findings is that the variability of the resting EEG may be large enough to mask the radiation induced effect in a random manner. If the latter is true, then it would be very difficult for studies to show any more consistency than what is presently observed.

In conclusion, an interaction of low-level RF and low frequency radiation with the human resting EEG was demonstrated. The significance of these effects with respect to health, if any, is not immediately obvious. Further research is needed to demonstrate the effects with more consistency and to identify whether the observed changes may lead to any adverse health effects. A possible avenue that might have the potential of demonstrating more repeatable effects is one based on case studies where a single subject is tested repeatedly providing the opportunity to observe repeatable effects. A vigilance controlled resting EEG could also provide a more robust measurement environment as opposed to the pure resting EEG which is more prone to vigilance lapses especially under extended recording periods.

List of Figures

List of Tables

Nomenclature

3G Third Generation

AAFT Amplitude Adjusted Fourier Transform Method

ApEn Approximate Entropy

CDMA Code Division Multiple Access

CW Continuous

DNA deoxyribonucleic acid

DTX Discontinuous Transmission

EEG Electroencephalogram

ELF Extremely Low Frequency

EM ElectroMagnetic

EMF ElectroMagnetic Field

ERP Event Related Potential

FEM Finite Element Method

FIT Finite Integration Technique

fMRI Functional Magnetic Resonance Imaging

GSM Global System for Mobile

IARC International Agency for Research on Cancer

IEGMP Independent Expert Group on Mobile Phones

MEG Magnetoencephalogram

PET Positron Emission Tomography

PM Pulse Modulated

RF radio frequency

SAR Specfic Absorption Rate

TDMA Time Division Multiple Access

UMTS Universal Mobile Telecommunications Service

UMTS Universal Mobile Telecommunications Service

W-CDMA Wideband Code Division Multiple Access

Contents

1. Introduction

This Chapter introduces the research area of interaction between electromagnetic fields and the human body, and the necessary background knowledge. A general preamble is followed by the introduction of the relevant basic concepts regarding mobile telephony, the interaction between electromagnetic energy and biological tissue, and electroencephalography. The need for research is identified, research aims are formulated and the original contributions of the thesis are listed. Finally, the outline of the thesis is reported.

1.1. General background

The Global System for Mobile (GSM) communications has been in use by the public for more than a decade. Its use extends in most countries of the world, while users are estimated in excess of 2 billion [7]. The health impact of such a widely used technology is one that must be considered carefully, since any adverse effects that might arise from its use could potentially influence large portions of the public. A substantial amount of research has been performed thus far, however it has not become clear yet whether any biological effects arise from the exposure to the electromagnetic (EM) radiation emitted by GSM telecommunications devices. This uncertainty is causing public concern that encompasses the use of mobile telephones, as well as the installation and operation of mobile phone base stations within communities. These concerns have attracted the attention of authorities and the scientific community who responded through several expert reports. The

reports conclude that any health or biological effects are very unlikely but the possibility cannot be excluded entirely [24, 2, 63, 118]. As such, the current opinion of experts, one that is also reflected in relevant guidelines and standards, is that more research is required if irrefutable conclusions are to be drawn.

Before the introduction of mobile telephony, a substantial amount of research investigating biological effects on the human body arising from exposures to electromagnetic fields had already been performed [2]. This research, although relevant, cannot be generalized to mobile telephony use due to differences in the characteristics of the potential stressor. The characteristics of interest are the exposure intensity, the spectral content, and the spatial distribution of the fields. To establish relevance to mobile phone exposures, investigations need to replicate all these aspects. For example, the results of studies that have assessed the influence on human electrophysiological parameters from high voltage fields originating from electricity power lines (very strong fields, largely homogeneous within the spatial constraints of a human body, and extremely low frequencies $\approx 50 - 60$Hz) would most likely relate poorly to results with mobile phone exposures (weak fields, largely inhomogeneous $\geq 100\%$ variation with the spatial constraints of the human body, and radiofrequencies ≈ 1 GHz).

Nevertheless, a considerable amount of research has examined the effects of mobile phone-like radiation on the human body [2]. This radiation must adhere to restrictions as outlined in the relevant guidelines and standards[1]. The imposed restrictions are based on established mechanisms of interaction, and at frequencies such as those emitted by mobile phones the main mechanism of interaction is the one of tissue heating. They are therefore set to limit tissue heating to levels well below those that can be tolerated by the human body. For this reason, the majority of research on mobile phone radiation-induced effects has focused on alternative potential mechanisms of interaction which are commonly classified as non-thermal. There have been suggestions that the pulsed

[1]Two sets of major guidelines exist, one issued by the International Commission for Non-Ionizing Radiation Protection (ICNIRP), and another issued by the Institute of Electrical and Electronics Engineers, (IEEE), (references [2] and [6] respectively). The Australian Radiation Protection and Nuclear Safety Agency, (ARPANSA) standard is based on these guidelines and is the one followed in Australia, [3].

nature of mobile phone signals may be a necessary feature of the low-level signal for a biological effect to arise [58].

Research investigating mobile phone-like radiation can be classified as *in vitro*, *in vivo*, and epidemiological.

In vitro studies can detect effects in tissues extracted from the organism. They can examine changes at physically small scales (e.g. molecular level), so they are best suited in assessing potential mechanisms of interaction. They include protein activation analysis, blood brain barrier permeability analysis, cellular membrane effects and DNA damage [2, 117]. At intensities similar to those emitted by GSM mobile phone handsets, *in vitro* studies have not demonstrated biological effects reliably, thus none of the proposed mechanisms reported have been widely accepted [2, 117]. On the contrary, such mechanisms may not exist since the energy levels that are available to biological tissue from such exposures are within the normal thermal energy variation that is observed in biological tissue and are therefore inadequate to elicit meaningful biological changes [24].

In vivo studies investigate effects on living organisms. They have been conducted on both humans and animals. In such studies, subjects are exposed to controlled electromagnetic fields. Subsequently, and/or simultaneously various biological function indicators are monitored [51]. These include neurophysiologic parameters such as brain parameters during wake and sleep states, event-related potentials and performance tasks, and parameters relating to the autonomous nervous system such as temperature, skin impedance, heart and blood flow parameters. Such studies are suitable for assessing immediate or short term effects can be assessed. Due to the proximity of the mobile phone handset to the user's head effects relating to brain function are the ones most widely studied. A finding that has been repeatedly reported is that of increased alpha band brain wave activity under the RF radiation of GSM phones. However it is not clear yet what consequence this change has to normal brain functioning and health [133].

The epidemiological field is another important category of electromagnetic radiation research. It

is particularly useful in identifying long term effects of the GSM exposures on the human body (rodent based epidemiological studies do exist as well) such as cancer incidence. It is also uniquely appropriate in assessing effects arising from long term exposure. One such example is the Interphone study conducted by the International Agency for Research on Cancer (IARC) in which large sample sizes were employed and several endpoints were studied. These were brain tumors, salivary gland tumors, acoustic neuromas, other head and neck tumors, leukemia and lymphomas. One 'arm' of the interphone study concluded that the use of a cell phone for 10 years or more did not increase acoustic neuroma risk over that of short-term users [25]. Difficulties arise when doing such large scale investigations due to the widespread use of mobile phones, making it difficult to obtain control groups (groups of people that do not use mobile phones at all). Exposure assessment and monitoring in epidemiological studies is also problematic [61].

Research investigating biological effects of mobile phone radiation has only considered the RF component of exposures. Perhaps the equally important low frequency components that are generated by GSM handset devices, called ELF fields have yet to be studied as a sole[2] stressor. This constitutes a gap in knowledge that requires further attention.

The work of this thesis focuses on the neurophysiology aspect of *in vivo* studies. Specifically, the resting brain electroencephalogram is investigated under GSM mobile phone radiation, following several studies indicating that certain aspects of the EEG change under the influence of the radiation (see reference [133] for a review). The exposures used in this thesis include both pulsed and continuous radio frequency fields as well as, for the first time, extremely low frequency fields. The studies were designed in such a way so as to establish relevance to GSM handset usage. Specifically this was achieved by reproducing all aspects of electromagnetic fields associated with GSM handset usage. The studies were optimized for the detection of possible short term, transient effects on the EEG.

[2]In some cases the combination of RF and ELF fields have been studied, e.g. [35].

1.2. Basic concepts

The interdisciplinary nature of this research, combining concepts from neurophysiology, electromagnetics, engineering and environmental health, requires at the very least basic understanding in all these scientific areas. To perform scientifically sound research all aforementioned aspects need to be carefully considered, an idea also reflected by the literature inclusion criteria that formed the review by Valentini et al. [133]. This section introduces some concepts that are required to understand the content of this thesis.

1.2.1. Mobile telephony

Wireless technologies extend from broadcast services such as radio and television, to mobile telephony, and to the more recently introduced wireless data and internet services. Some popular mobile telephony technologies are the GSM system, Code Division Multiple Access (CDMA) system and the UMTS third generation networks (3G) which are based on the Wide-band CDMA technology [11]. Although public concern does exist for both mobile telephony as well as wireless data and internet services (not so much for commercial radio and TV), this thesis is only concerned with the first.

GSM, CDMA and W-CDMA technologies use electromagnetic radiation energy to perform all necessary communications between terminals. In this context, terminals are the handset devices of users and the base stations. Due to the limited electromagnetic spectrum available to each of these technologies, there is a need to somehow reuse the allocated resources. This is achieved using the cellular based network structure, where certain sections of the spectrum are used in spatially confined areas called cells, see Figure 1.1. Adjacent cells would use another set of frequencies and once all frequencies are assigned to a cluster of cells, then the same cell-frequency allocation pattern is repeated at a neighboring cluster. This allows frequencies to be reused as many times as necessary provided that cells with the same frequency channels, called co-channels, have sufficient

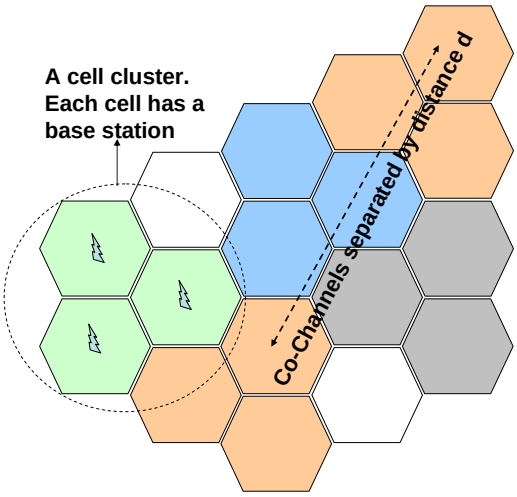

Figure 1.1.: A structural depiction of a cellular network. Adjacent cells operate at different sets of frequencies and thus do not interfere with each other. Co-channels operate using the same set of frequencies, but interference is avoided due to adequate spatial separation. This way the cellular system allows efficient reuse of the allocated frequency spectrum.

spatial separation. Each cell has a base station with which all Mobile Stations (mobile phone handsets) within its boundaries communicate using electromagnetic signals. A person found inside the physical area of a GSM cell will be exposed to the radio frequency emissions from its base station, and a person inside the same area using a mobile phone handset will additionally be exposed to the radiation that is emitted by his/her handset. It is these two emissions that attract public concern. In this thesis we are concerned with the emissions of handsets rather than base stations, and specifically emissions coming from GSM mobile phone handsets. As a general rule users are exposed to higher levels of radiation from handsets rather than base stations due to the increased proximity of handsets to the body.

The GSM system was first introduced in the early nineties in Europe [23]. It is the most widely used mobile telephony system with current users estimated at around two billion [7]. The widespread use of this technology is the main reason for choosing to investigate GSM related possible bio-effects instead of any other telecommunications system. Some of the major relevant characteristics of this

technology are discussed in the rest of Section 1.2.1.

1.2.1.1. Frequency Spectrum

Two of the major GSM bands currently in use are the GSM-900 and GSM-1800. GSM-900 uses the 890 - 915 MHz band to send information from Mobile Stations to Base Stations, (uplink direction), and the 935 - 960 MHz band for the opposite direction, (downlink), totaling to 124 channels. GSM-1800 uses 1710 - 1785 MHz band to send information from the Mobile Stations to the Base Stations and 1805 - 1880 MHz for the opposite direction totaling to 374 channels. It is important to be aware of the electromagnetic frequencies that each technology uses because as previously mentioned, different frequencies can interact with living tissue in different ways.

1.2.1.2. Time Division Multiple Access Technology (TDMA)

To maximize the usage of spectral resources, frequencies in a cell are used by more than one Mobile Station. This is achieved through the Time Division Multiple Access (TDMA) technology. TDMA allows for 8 users to transmit at different time intervals but in the same frequency band. To achieve this, transmission from each Mobile Station must be switched on and off at precise intervals so as not to interfere with the other users' transmissions. Each time interval (called time slot) has a duration of 576 μs which is equivalent to a repetition rate of 1736 Hz. A set of 8 time slots forms a frame, which is 4.6 ms long and is equivalent to repetition rate of 217 Hz. A set of 26 frames form a multiframe. In this, 25 out of 26 time slots are active giving a repetition rate of 8.3 Hz. The switching of the RF radiation at these regular intervals introduces the pulsed nature of the radiation. In contrast, and as their name suggests, CDMA and W-CDMA (Code Division rather than Time Division) technologies use digital codes to allow for multiple user access. As a result, in the absence of the TDMA structure pulsing of the RF fields is also absent. This is an important distinction between these technologies since it has been proposed that the pulsed nature of the

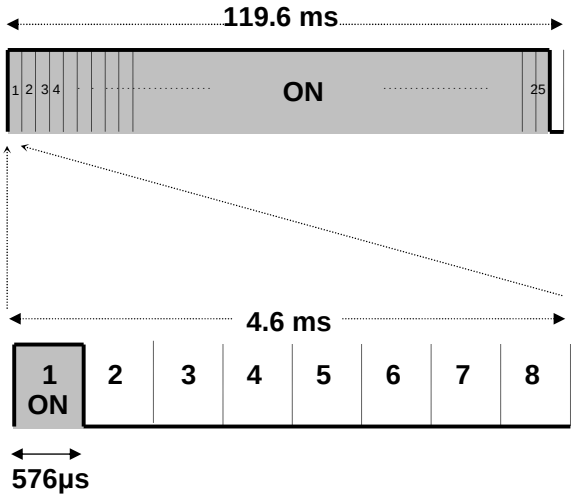

Figure 1.2.: The signal transmitted from a handset to a base station has the time frame structure depicted here. In this case time slot one is active. For another user transmitting in the same frequency band, one of the seven remaining time slots would have to be used. Twenty six frames make up a multiframe. The 26^{th} frame is always off giving rise to the 8.3 Hz frequency component.

GSM signals can be important in biological effect induction [58]. If this is true then W-CDMA and CDMA technologies would not be capable of inducing such an effect.

1.2.1.3. Discontinuous Transmission Mode (DTX)

As mentioned in Section 1.2.1.2, the modulation of the radiofrequency signal is a deciding factor of frequency content of the field. Additional modulation components are introduced during the Discontinuous Transmission Mode, (DTX). In a typical phone conversation, for most of the time only one of the parties will be talking while the other will be listening. This allows the mobile station of the listening party to minimize transmission since it has less information to transmit. As a result, more low frequency modulated components are introduced on the RF signal since transmissions become less regular. A DTX frame is made of 4 multiframes, see Figure 1.3. In each one there is one time slot active which is used to transmit signaling, (not speech), information to the

MFr1	0	1	2	3	4	5	6	7	8	9	10	11	12	13	14	15	16	17	18	19	20	21	22	23	24	25
MFr2	26	27	28	29	30	31	32	33	34	35	36	37	38	39	40	41	42	43	44	45	46	47	48	49	50	51
MFr3	52	53	54	55	56	57	58	59	60	61	62	63	64	65	66	67	68	69	70	71	72	73	74	75	76	77
MFr4	78	79	80	81	82	83	84	85	86	87	88	89	90	91	92	93	94	95	96	97	98	99	100	101	102	103

Figure 1.3.: The structure of a DTX multiframe. Unshaded regions represent frames of no transmission, whereas shaded ones represent frames with single slots active. DTX results in a 90% reduction on average emissions.

base station. In the third multiframe there are 8 speech frames active in which background noise information is transmitted. As a result, the DTX structure introduces an extra spectral frequency component, that of 2.1 Hz along with associated harmonics.

1.2.1.4. Maximum power levels and interference minimization

Base Station and Mobile Station transmissions need to adhere to safety standards that define maximum ambient energy field levels (reference levels) and maximum induced energies in human tissue (basic restrictions) [2]. Basic restrictions were established based on known health effects and mechanisms of interaction, and reference levels are derived from these basic restrictions so as to represent worst case scenarios. For example, at frequencies relating to GSM-900, a maximum electric field of 42 V/m is defined as the reference level and 2 Watts (W) of absorbed energy per kilogram of tissue for the area of the human head and torso is defined as the basic restriction level [2]. The compliance of mobile phone handsets to maximum allowed emissions is usually established before these are made available to the public. Apart from the aforementioned, electromagnetic energy transmission from cellular based communications systems are limited by another factor. To achieve functional cellular based systems co-channel interference needs to be minimized, (see Figure 1.1). For this reason Mobile Stations and Base Stations need to transmit the minimum energy possible and in this way they indirectly minimize user exposure. However adequately nominal co-channel interference could still be achieved at levels that exceed exposure limits. Therefore the fact that

cellular based systems need to minimize transmissions is no assurance that resulting exposures are within limits.

1.2.1.5. Interaction between tissue and electromagnetic energy

This section describes the relevant mechanisms of interaction between biological tissue and electromagnetic fields. These interactions vary between different frequency ranges of the electromagnetic field. Two major guideline documents suggest maximum energy fields. These are the ICNIRP Guidelines and the IEEE C95.1 [6, 2]. The relevant exposure limits found in the above guidelines have been set based on established biological mechanisms of interaction. No speculative or disputed effects are taken into account. Safety factors are built into these standards so permitted exposures are well below those levels at which biological effects are observed.

Mobile phone handsets emit two kinds of electromagnetic radiations, an RF one used for transmitting information and an ELF which is a by-product of the operation of the battery and electronics [87].

The main exposure metric defined in standards for the frequency range of 100 kHz to 3 GHz is the Specific Absorption Rate (SAR), Equation 1.1. SAR is defined in the ICNIRP guidelines as the rate at which energy is absorbed in body tissues, in watts per kilogram (W/kg), where σ is the conductivity of tissue (S/m), ρ is the mass density of tissue (kg/m3) and E is the electric field strength (V/m).

$$SAR = \frac{\sigma |E|^2}{\rho} \tag{1.1}$$

The limits based on SAR values are in place to prevent tissue heating effects from taking place. It has been observed in controlled experiments that 4 W/kg of whole body exposure and for a sufficient exposure period (~30 minutes), produces a temperature increase of 1°C, a level at which established biological effects begin to take place [2]. A safety factor of 50 is built in standards bringing the

maximum permissible exposure level for the general public down to 0.08 W/kg. Through a similar approach, a basic restriction level of 2 W/kg is defined for the localized head and trunk exposures. Additional exposure metrics apply for sub-ranges. For example in the range of 100 kHz to 5 MHz there are limits set to prevent electrostimulation effects. For amplitude modulated or pulsed fields, in the range of 200 MHz to 6.5 GHz, there are limits set to prevent thermoelastic effects such as the microwave hearing effect [2].

With respect to exposures coming from mobile phone handsets, the most relevant exposure limit is that of head and trunk localized exposure. This clearly follows from the fact that mobile phone handsets are usually held against the head and from the fact that GSM mobile phone handset antennas produce highly localized exposures [79]. As a comparison, a whole body exposure would be more appropriate if one was considering exposures from base stations where it is most likely that the whole body is exposed to similar levels of radiation.

It has been mentioned in Section 1.2.1.3 that GSM handsets produce low frequency fields (under 100 kHz) when in operation. The main mechanism of interaction between biological tissue and low frequency electromagnetic energy is that of nerve stimulation arising from current induction in tissues. It is measured by current density, J, defined as current flow per unit area of biological tissue, (A/m2). Sufficiently intense ELF fields can cause peripheral nerve and muscle tissue stimulation. Such effect is observed at around 100 mA/m^2 (for frequencies between a few Hz up to 1 kHz). Again a safety factor of 50 is embodied in standards for general public exposure bringing the limits down to 2mA/m2 (for frequencies between a few Hz up to 1 kHz).

1.2.1.6. Basic restrictions and reference levels

SAR and current density are termed as “Basic Restrictions” and refer to field or energy values inside the exposed tissue. In most cases it is inconvenient, if not impossible, to obtain such measures since invasive methods of measurement would be required. Therefore direct assessment of compliance

with basic restrictions is not usually feasible. Instead, computational modeling can be performed. For this reason exposure guidelines define more usable exposure assessment metrics which do not require measurements within the exposed tissue. These are termed reference levels and are based on measurements of ambient (free space) electromagnetic fields in close proximity to the exposed tissue. Reference levels are established via extrapolation from single frequency laboratory measurements and by mathematical modeling. They were determined based on maximum energy coupling conditions and therefore represent worst case scenarios [2].

1.2.2. Electroencephalography

Since mobile phone handsets are often held closest to the user's head than to any other body part, it follows that the head and in particular the brain would be exposed to the high SAR values. For this reason there has been a reasonable amount of research (see Chapter 2) that investigated effects on brain function under GSM handset exposure. Also, since the brain controls most peripheral body functions such as breathing, heart rate, arousal, vigilance etc, changes in brain function are required to elicit peripheral function changes. Thus if changes are observed in the brain under exposure to GSM-like EMF a possible physiological basis for peripheral changes would also exist. Several different ways of monitoring brain function exist such as functional Magnetic Resonance Imaging (fMRI), Positron Emission Tomography (PET), Magnetoencephalogram (MEG) and Electroencephalogram (EEG). Among these, electroencephalography is the most accessible and the one most widely used across several fields of study. As opposed to PET, fMRI and MEG it is relatively low-cost to implement, does not require any special infrastructure (apart from the electronic amplifiers), and substantial amount of studies have already looked at EEG variables under EMF exposure. Even though the EEG lacks in spatial resolution, its superior time resolution provides the unique opportunity of assessing brain electrical activity with a millisecond resolution. The EEG is a record of electrical activity fluctuations of large ensembles of neurons in the brain.

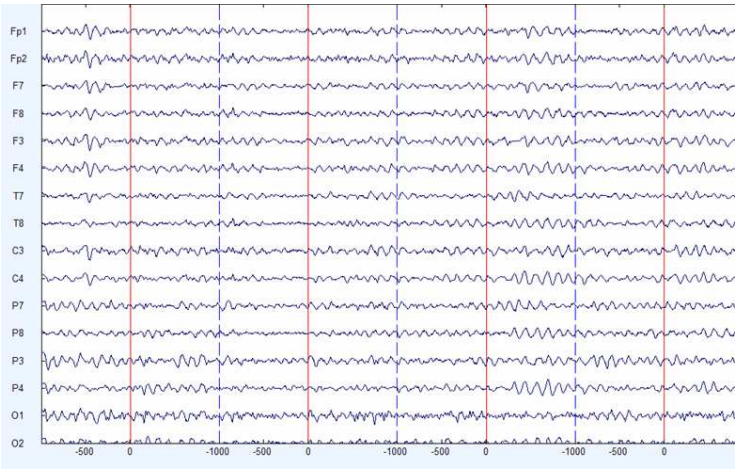

Figure 1.4.: An EEG recording of a human subject at rest with eyes closed. Alpha band oscillations, driven simply by closing the eyes, are visible throughout.

In general, these voltage fluctuations represent variations in electrical potential between different measurement points on the scalp, and represent changes in membrane potentials of underlying nerve cells and impulses from various neurogenerators [73].

Two major aspects of brain recordings are the Event Related Potentials (ERP) and resting EEG activity. ERPs relate to specific responses to external stimulus (sometimes occurring in specific time windows with relation to the stimulus). ERPs have been a popular tool for the investigation of possible EMF effects on the brain.

The spontaneous EEG is a measure of EEG activity which does not relate to any particular time event. An example is the resting EEG where a subject would sit relaxed with eyes either open or closed, without performing any specific mental activities. As is the case with ERPs, resting EEG has also been used for the investigation of possible EMF effects on the brain.

1.2.2.1. Spectral Content of EEG

A common derivative of the EEG is its spectral content. It has been observed that certain ranges of frequencies relate to certain cognitive states. These frequency ranges are usually defined as follows: delta (0.1-4 Hz), theta (4-8 Hz), alpha (8-12 Hz), beta (12-30 Hz) and gamma (30-100 Hz). Changes in the alpha frequency band during GSM handset like exposure have been the most consistently reported finding in literature. The alpha rhythm has been interpreted as cortical idling attenuated by mental effort and it has been shown to relate to attention, inhibitory processing, task complexity, and memory load [105]. The alpha rhythm can be driven simply by closing the eyes. Since it provides for a well defined EEG state (i.e. has a certain degree of inter and intra subject reliability [101]) it provides a good measure for cognitive changes. The remaining frequency bands have also been studied with relation to EMF induced effects but findings have not been as consistent.

1.2.2.2. Non Linear characteristics of EEG signals

In the context of electromagnetic field related investigations on the brain, conventional types of EEG analysis have commonly been employed, which generally concentrate on linear aspects of signals. The linear method of spectral analysis based on the Fourier transformation is most commonly used. However, analyzing only linear aspects of a signal can leave any potential non linear changes undetected. With evidence that EEG signals can exhibit non linear behavior [46], the question of whether those features of the signal change remains unknown. With the known difficulties, (refer to Chapter 2), that researchers are faced with when trying to detect effects using linear analysis, it becomes imperative to investigate this avenue of non linear EEG changes which has the potential of revealing new information.

Some examples of non linear methods of analysis are the Kolmogorov Smirnov entropy, the correlation dimension, fractal dimension, largest Lyaponov entropy, phase space plots and Hurst

exponent [127]. A method used successfully on EEG data is that of Approximate Entropy (ApEn). With this technique, the non-linear measure of complexity of the EEG can be calculated. In at least one case, an effect on the entropy of the EEG of rats has been shown under the influence of low frequency pulses [68]. However in that case the electromagnetic fields were of much higher intensity and of different frequencies to those emitted by mobile phone handset devices.

1.3. Research aims

The current thesis is designed to address the following research questions:

- Is GSM mobile phone radio frequency radiation capable of causing changes to the human resting EEG?
- If yes to the above, what is the role of the low frequency modulations of the radio frequency signal in observed results?
- Is GSM mobile phone ELF radiation capable of causing changes to the human resting EEG?
- What practical significance do these results carry for regular GSM mobile phone users?

1.4. Overview of the method

The thesis is divided into eight Chapters. In Chapter 1, an introduction to the research area and the necessary background knowledge is presented. In Chapter 2, a thorough literature review is presented and the research question is formulated in more detail. In Chapter 3, the design and results of a small sample study are presented. Weaknesses of the experimental method are identified and measures to address them before the execution of more experiments are outlined. In Chapter 4, the design and construction of an exposure device is presented that is to be used in the proposed experiments. Chapter 5 presents the design of the main study, incorporating those methodological

improvements that arose from Chapter 4. Chapter 6 presents the results, and Chapter 7 presents a series of discussions and interpretations of the results of the main study. Finally in Chapter 8 the outcomes of this research are discussed and assessed against those research aims that were outlined in Section 1.3. The implications of the findings are discussed and future research needs and directions are suggested.

1.5. Original contributions

The original contributions of this thesis are:

- Comparison of pulsed RF with continuous RF at identical instantaneous peak field intensities.
- Investigation of non linear features of brain signals during and shortly after GSM like electromagnetic field exposure.
- Investigation of the effects of ELF battery generated fields on brain activity.

1.6. Conclusion

This Chapter has introduced the broad research area and the key findings up to the time of writing. The basic necessary concepts that recur throughout the thesis have also been presented. These are not exhaustive but give the reader the opportunity to obtain a general picture of the research area. In addition the main form of the research questions have been given and the original contributions of the thesis were also listed. In the next Chapter a comprehensive literature review is presented. The review is aimed at providing a balanced view of all experimental outcomes relating to effects measured through the EEG and extracting qualitative attributes of research that appear to contribute to demonstration of effect or no effect at all. The conclusions of the review will be used in the design of any laboratory experiments to be performed.

2. Literature Review

It is not clear yet whether any health or biological effects arise from the exposure to the EM radiation emitted by GSM handset devices. Public concern about possible effects of mobile phones on health is still present, hence the need to address the uncertainty. The findings of the substantial amount of research that has been published to date, overall, can be characterized as inconclusive. This is partly attributed to the absence of a viable physical mechanism which would otherwise establish causality, and to the methodological limitations of the available human studies that could be contributing to the contradictory nature of results.

The rationale of reviewing the available literature is first to identify these methodological limitations and to specify appropriate modifications in protocol design in order to maximize the likelihood of obtaining error free and incontrovertible results. Secondly to identify outright gaps in the literature that can perhaps be addressed. Details of possible physiological mechanisms of interaction of EMF with human tissue are beyond the scope of this review and will not be discussed in any detailed form. The review is divided in three main sections. The first concentrates on possible biological effects arising from RF EMFs, the second on biological effects arising from ELF EMFs and the third on methods of analysis of the EEG.

In the RF and ELF sections, general research with endpoints that are not related to mobile phone use is presented, but the review on this is not exhaustive nor detailed. It serves the purpose of putting the more relevant literature into context. Then, an in depth focus is developed on the research with endpoints that relate to brain function, predominantly resting brain activity under

mobile phone EMFs and on brain activity during sleep. Other such attributes will be discussed to a lesser extent. This is followed by a discussion on the technical aspects of such research that need to be considered and from which methodological improvements can be extracted.

The third and final section of the review looks at some literature relating to non linear analysis methods of the EEG under EMF exposures as alternatives to those employed thus far. These methods are used to explore the sensitivity of the non-linear aspects of the EEG to the presence of the EMF radiation.

2.1. Research on Radio Frequency Bioeffects

With research into biological effects of RF radiation dating back at least as far as 1973, many sources of RF radiation have been assessed before the introduction of mobile telecommunications, [37]. These sources include radars, microwave diathermy equipment, welders, and broadcasting towers. The findings of these studies are relevant to this thesis since they constitute the basis for formulating exposure limits defined in guidelines, as well as being the basis for originally establishing the mechanisms of interaction of RF fields with biological organisms. In the next section a brief overview of the findings of this body of literature is considered. Following that, and with an understanding of the basis for current exposure limits, the relevant mobile phone related literature is reviewed.

2.1.1. Radio Frequency research with stressors other than mobile phones

The ICNIRP exposure guidelines, originally published in 1998, provide a basis for limiting exposure to RF fields based on findings of the then available literature [2]. The frequency range of interest here is between 100 kHz - 300 GHz. They draw conclusions from epidemiological studies covering cancer and reproductive outcomes, cellular and animal studies. The ICNIRP guidelines quote negative studies on cancer effects whose subjects were military personnel working in proximity to

radars, employees chronically exposed to low level microwave radiation, children chronically exposed to radiation from large microwave transmitters near their homes and in one study mobile phone users. The results were all negative but it was noted that in the case of mobile phone use it is still too early to observe an effect on cancer incidence or mortality. Some positive studies showed increase of cancer incidence, leukaemia and lymphoma among military personnel but results were difficult to interpret due to inadequate dosimetry and unclear sample sizes. Increase of leukaemia incidence in populations living near EMF transmitters has also been reported but the results are inconclusive. According to the ICNIRP guidelines, studies on reproductive outcomes suffer from very poor assessment of exposure and in many cases from very small sample sizes. They cover exposures of pregnant females to microwave diathermy (occupational and patient) and plastic welding equipment. No statistically significant effects on rates of abortion or foetal formation have been reported. However, an increased risk of miscarriage and birth defects has been reported. In volunteer studies it has been demonstrated that with exposures to high intensity fields in the range of 100 kHz to 10 MHz, the dominant biological effect changes from nerve and muscle stimulation to heating. Above 10 MHz the dominant mechanism of interaction is that of heating which results from energy absorption. Because it is known that 1-2 °C of core body temperature increase can have adverse effects on health (heat stroke and heat exhaustion in humans, in cases of animal studies alterations to neural and neuromuscular functions, increased blood brain barrier permeability etc) the aim of standards and guidelines is to limit this temperature increase to less than 1°C. At temperature increases below 1 °C thermoregulatory processes are able to maintain homeostasis, and therefore no adverse health effects from excessive temperature rise can result. Thermoregulatory studies on resting volunteers have shown that whole body exposures of less than 4 W/kg lead to increases in body temperature of less than 1°C. Animal studies have shown that exposure of rats and monkeys to SAR values of 1–3 W/kg resulted in decreased task performance. When absorbed electromagnetic energy results in temperature increases of 1–2 °C effects such as alterations of neural and neuromuscular functions,

increased blood brain barrier permeability, ocular impairment, stress associated changes in the immune system, haematological changes, reproductive changes, teratogenicity and changes in cell morphology, water and electrolyte content and membrane functions have been observed through cellular and animal studies.

2.1.2. Biological or health effects arising from mobile phone like EMF

In the context of non ionising EMF exposures the term *low-level* radiation refers to energies that are limited below the guidelines and are thus incapable of inducing any measurable temperature increase in tissues. Mobile phone radiation falls within the category of low-level radiation. The wide use of wireless telecommunications such as mobile phones, led to multiple investigations about possible effects arising from the radiation they emit. The findings of that earlier literature has been summarised by more than one groups of experts including the World Health Organization (WHO), ICNIRP and the Independent Expert Group on Mobile Phones (IEGMP) [2, 63, 118, 117].

A review by the WHO concluded that many effects have been reported at low level exposures, but it is the opinion of experts that no known health hazards were associated with these effects. On the other hand, biological effects have been identified that point towards a non-thermal mechanism of interaction, so replication and further study of these is necessary [117].

Similarly, in 2001, the Stewart report commissioned by the IEGMP concluded that the balance of evidence to date suggests that exposures to RF radiation below ICNIRP guidelines do not cause adverse health effects to the general population [63]. On the other hand, scientific evidence which suggests that there may be biological effects occurring at exposures below these guidelines does exist and its implications must be considered. The report also concludes that "it is not possible at present to say that exposure to RF radiation, even at levels below national guidelines, is totally without potential adverse health effects, and that the gaps in knowledge are sufficient to justify a precautionary approach."

2.1.3. Spontaneous Resting Electroencephalogram under GSM-like EMF

A substantial amount of research has been conducted that looks at brain function during and shortly after exposures to mobile phones. Indeed more research in this area has been called for by experts such as the IEGMP and the WHO. With results in the literature being somewhat divided, conclusive outcomes are yet to be made, and so more research is being conducted in accordance with the suggestions of experts [44]. Here we attempt to review the relevant literature with the aim of identifying those methodologies that correlate with positive results, identify gaps that could perhaps be addressed and importantly, identify the most reliable findings in literature.

Literature here is grouped according to important methodological attributes that appear to influence the outcome of studies. These are exposure duration, exposure monitoring period, sample size, blinding conditions, dosimetry, EMF frequency content, exposure distribution and interference issues.

2.1.3.1. Exposure duration

With investigations on resting EEG variables under EMF exposures dating as early as 1995, significant variations in experimental protocols are observed [116]. Despite these variations there is a finding, that of a power increase in the alpha band of the EEG (alpha band effect), which is demonstrated with some consistency across several studies. This has been reported for both during and after exposures, (Table 2.1). Other reports include findings such as decreased interhemispherical difference in alpha and delta activity, (see references [38] and [34] respectively). Additionally, effects on other EEG bands are also reported, (Table 2.1), but none are demonstrated with the same consistency as the alpha band effect. One of the experimental parameters seen to vary throughout protocols is that of exposure duration. Although in Table 2.1 a trend is observed by which studies with longer exposure durations show positive results more consistently than those of shorter durations, it is hard to deduce a clear correlation between duration and presence of effect. This is due to

the concurrent variation of other methodological characteristics between these studies which could equally contribute to the outcomes.

The first study to identify and address the issue of exposure duration was that of Croft et al. [34]. The authors employed a protocol suitable for testing the correlation between effect and duration of exposure. Indeed such a correlation is demonstrated whereby alpha band activity is reported to increase as a function of exposure duration under EMF exposure. The latter coupled with the trend that is demonstrated in Table 2.1 is good evidence that longer exposure duration increases the likelihood of detecting(demonstrating) an effect.

In a recent study, Kleinlogel et al. exposed 15 healthy volunteers to 30 minutes of GSM and Universal Mobile Telecommunications Service, (UMTS) signals. In that study no effect was detected under either exposure despite the extended exposure duration [48]. However as opposed to the majority of studies that record true resting EEG, here the authors employ a vigilance controlled EEG whereby the true resting EEG activity is interrupted every 20-40 seconds through the presentation of an auditory stimulus. It is possible that the auditory stimulus causes an interruption to the resting EEG that if large enough can mask any condition effect. On the other hand, the employed protocol can prove superior to a true resting EEG since the overall variability of vigilance is singificantly reduced. As the authors state, the employed protocol would result in lower variation within and between subjects but at the same time limits the scope of the study.

2.1.3.2. Exposure monitoring period

As highlighted by Croft et al. longer EEG monitoring allowing for a stronger averaging would result in improved signal to noise ratios [34]. Under this improvemement, a greater chance of detecting subtle effects arises in the otherwise highly variable and noisy EEG signal. In a recent literature review by Cook et al., the importance of post exposure monitoring periods is discussed in light of research outcomes where effects have been shown up to 30 minutes post exposure [26]. The authors

of this review suggest that failure to monitor EEG post exposure may lead to false interpretation of results. However, extended durations of EEG monitoring carry other confounding factors such as the increased variability in allertness that leads to increased variability of alpha band activity [95]. Since it is impossble to measure EEG activity indefinetely it would be correct for studies to limit conclusions to the duration of the respective monitoring period.

Table 2.1.: A summary of studies investigating the resting EEG activity under mobile phone radiation

Author	Exposure duration	Blinding / Sample Size	SAR & modulation content	Effect
Roschke & Mann 1997	3.5mins	Single / 34	• SAR = n/a • Mod -217 Hz, 12.5% DC • Localised Exposure (aerial 40cm away)	NONE - during exp
Hinrikus et al. 2004	1min X 5 times	Single / 20	• SAR = 0.35 W/kg • Mod -7 Hz, 50% DC (f_c = 450MHz) • Localised Exposure	NONE - during and after exp
Lebedeva et al. 2000	15mins	Single / 24	n/a	↑ global correlation dimension
Reiser et al., 1995	15	Single / 36	• SAR = n/a, 8W peak O/P • Mod- 217Hz ,12.5% DC • Localised exposure(aerial 40cm away)	α2↑ and β↑ - after exp
Hietanen et al., 2000	20	Single / 19	• SAR = n/a • Mod- 217Hz ,12.5% DC • Localised exposure(aerial 40cm away)	NONE - MISSING during exp
Croft et al., 2002	20	Single / 24	• SAR = n/a • Mod- n/a • Localised exposure (GSM handset)	α↑ and δ(hem diff)↓, during and after exp

D'Costa et a. 2003	5mins X 5 times	Single / 10	• SAR = n/a, 2W peak power O/P • Mod- 217 Hz • Homogenous exposure(patch antenna)	α↓ (hemispheric differential, during exp
Huber et al., 2002	30	Double / 15	• SAR = 1W/kg • Mod- 2, 8, 217, 1736 Hz (DTX-like) • Homogenous exposure(patch antenna)	α↑, after exp
Curcio et al., 2005	45	Double / 40	• SAR = 0.5 W/kg • Mod- 217Hz ,12.5% DC • Localised exposure	α↑, more during than after exp
Croft et al., 2007	30	Double / 120	• SAR = 0.674W/kg • Mod- 217Hz ,12.5% DC • Localised exposure (GSM handset)	α↑, during
Regel et al., 2007	30	Double / 24	• SAR = 1W/kg, • Mod- 2, 8, 217, 1736 Hz (similar to DTX) • Homogeneous exposure(patch antenna)	α↑, 30 mins after exp
Vechio et al., 2007	45	Double / 10	• SAR = n/a, • Mod- 217Hz ,12.5% DC • Localised exposure(rela handset, antenna 40cm away from head)	α2 ERCoh ↑at temporal areas & α2, α3 ERCoh ↓at frontal areas, after exp
Kleinlogel et al., 2008	30	Double / 15	• SAR = 1W/kg, • Mod- 2, 8, 217, 1736 Hz • Localised exposure(antenna placed over left ear)	NONE -during and after exp

2.1.3.3. Sample size

Where effects on the resting EEG have been observed, they have been of small effect size. Croft et al., reported an effect size ranging from 0.17 to 0.22 and in a later study a variance of 37% was

accounted for by the EMF factor [34, 35]. Curcio et al. reported a small effect size similar to that of Huber et al., (see reference [36] and [58] respectively). Similar effect sizes have also been reported with regards to reaction time measures under magnetic fields by Whittington et al., Cohens f effect size = 0.04 [139]. These suggests that effect sizes are small thus larger sample sizes are essential to obtain adequate statistical power (e.g. power of 60% or more). Discussions on the importance of sample size with regards to pulsed ELF and RF field exposure has also been presented in the review paper by Cook et al., and in more detail in the review by Valentini et al., (see references [26] and [133] respectively). With alpha band effect sizes now available through the various studies mentioned, adequate sample sizes can be estimated more accurately thus keeping the risk of type II errors at acceptably low levels. In the largest study yet on resting alpha reported by Croft et al., only 60% of subjects (n = 120) demonstrated the alpha band effect [35]. The authors proceed to speculate that this non homogeneity of effect could be related to individual differences between the participants [35]. Roschke and Mann investigated such possibility by testing for the existence of a bimodal distribution of data under the active radiation condition [121]. The failure to observe that however does not exclude the possibility since their exposure duration was considerably small, and no overall effect on alpha was observed. At the current state of knowledge replication of the alpha band effect with large sample sizes seems to be imperative if more confidence about the influence EMF on alpha activity is to be gained.

2.1.3.4. Blinding

Valentini et al. performed a comprehensive literature review in which they defined four criteria on which inclusion of literature is decided [133]. One of these four criteria is at least a single blind protocol, although a double blind protocol provides additional protection to experimental bias. As is evident through Table 2.1, the majority of studies reviewed here were single blind. Interestingly, all studies employing a double blind protocol demonstrated a statistically significant effect on the

alpha activity, (see Table 2.1).

2.1.3.5. Dosimetry

As is the case with any possible biological stressor it is imperative to quantify the exposure dose. Earlier literature defined minimum requirements for dosimetric assessment which extended beyond the simplistic peak SAR assessments that are used for compliance purposes [81, 82].

Kuster et al. define the replicability of exposure distribution as one of the requirements and proceed to say that the exposed tissues must be identical during the experimental risk evaluation to those exposed during the actual usage of the technology [2]. They define SAR distributions that should cover the entire cortex homogeniously, with significant absorptions reaching subcortical structures. This choice of exposure distribution appears to be deviating from the well known localized structure arising from standard mobile phone handsets [79, 124, 82]. Kuster et al. justify the choice of such a distribution by identifying that a typical exposure from mobile phones does not exist (different handset devices expose different brain areas) [82]. In addition, the relatively small anatomical variations of human heads can cause significant exposure variations between subjects for specific tissue regions due to the pronounced near field characteristics of the exposure [83]. These variations are considered too large by the authors to achieve reproducible exposures between subjects.

Interestingly, studies employing the uniform distribution delivered through large patch antennas, coming from the same research group, all demonstrated post exposure influences on the human alpha brain rhythm [58, 57, 59, 114]. Note that these studies did not monitor the EEG during exposure. On the contrary studies using realistic mobile phone-like antennas demonstrate an effect less consistently, see Table 2.1.

In line with the guidelines of Kuster et al. (see reference [82]), the recent study of Schmid et al. provided a detailed dosimetric assessment of the large patch antenna exposure system (homogeneous

exposure distribution) [124]. The authors performed a detailed uncertainty analyses in which they consider uncertainties due to deviations of the antenna structure from its nominal position with relation to the head, uncertainties in head size, uncertainties in dielectric properties of biological tissues, as well as uncertainties related to the delivered energy to the antenna. In addition, the effect of the EEG electrodes on the absorbed SAR was also investigated. With this complex uncertainty analysis a ~3 dB uncertainty was estimated. Note that this value is specific to the experimental setup under investigation. Other studies use exposure sources that produce more localised fields and thus more realistic than the aforementioned. As explained by Schmid et al., such studies should expect larger uncertainties since small variations in source positioning result in large contributions to exposure uncertainties [124]. From the above discussion stems the argument of trading off realistic exposure distributions with decreased dosimetric uncertainty. Although Schmid et al. remain supportive of homogeneous exposures so as to better define the dose (minimize uncertainty), they do state that such approach results in unrealistic exposures. The resulting exposures can be viewed as the equivalent to simultaneous multiple mobile phone exposures as opposed to the equivalent of a single mobile phone exposure. This deviation from realistic conditions results in overexposure of deeper brain structures. In addition, the field gradients that would otherwise be present under realistic expoosures are removed and therefore their influence cannot be assessed. On the other hand, by choosing to employ a real mobile phone exposure, apart from the inherent increased exposure uncertainty the fact that the exposure would only represent a subset of possible mobile phone exposures must also be considered.

In their recent topical review, Valentini et al., (see reference [133]), defined dosimetric assessment as one of the four inclusion criteria although their minimum requirements did not meet those set earlier by Kuster et al. [81, 82]. As a result their review contains literature that lacks SAR information. In these cases accurate dose cannot be extracted, but other information such as power density, frequency content, antenna size, distance from head, and power input can give rough

indications as to the exposure dose and perhaps sufficient confidence that exposure limits were not exceeded[1]. Particularly in cases where real mobile phone handsets were used, approximations of peak SAR values can be deduced from manufacturers data and so the possibility of over exposure in those cases is unlikely. Nevertheless the element of unknown exposure dose is a real problem for these studies.

Boutry et al. proceed a step further and identify the weakness in providing only the peak spatial SAR evaluation, determined based on the procedures defined in the ICNIRP Guidelines [18]. Since this procedure was defined for compliance purposes it is not surprising that it is not entirely suitable for the purposes of exposure assessment in such research. As identified by Boutry et al., the peak spatial SAR correlates poorly with the exposed brain regions and does not provide any information about the location of maximum absorption nor for the spatial distribution of exposure. Absolute dosimetric values for the specific brain tissues also remain unknown. Through suitable computational modelling, dosimetry for all relevant biological tissue can be reliably obtained. For an example see Huber et al. [57].

Since the modulation of the carrier directly affects the time averaged electromagnetic field, and time averaged electromagnetic field affects SAR, see Equation 1.1, it follows that the frequency content of the modulation is very important in SAR calculations. The next section looks at the frequency content of signals used, how they correlate with realistic GSM signals and what importance they might carry with respect to biological effect induction.

2.1.3.6. EMF Frequency content

The following excerpt from the IEGMP report clearly highlights the importance of modulation content of RF signals, [63]. *"On the basis of the current state of knowledge we recommend that priority be given to a number of areas of research related particularly to signals from handsets.*

[1]For the purposes of demostrating a low level effect it is sufficient to know that the SAR levels within the head are below the 2 W/kg limit

These should include the following:

- *effects on brain function,*
- *consequences of exposures to pulsed signals,*
- *improvements in dosimetry,*
- *the possible impact on health of subcellular and cellular changes induced by RF radiation"*

Because of the TDMA nature of the GSM signals (refer to Chapter 1 for details), low frequency modulating components are introduced in the spectrum. Their presence can have a direct influence on experimental outcomes through one or more of the following ways:

- First, if a biophysical process allows for the detection of these then clearly the low frequency content becomes important.
- Second, their presence directly affects SAR values.
- Third, the possibility of manipulating peak electric fields so as to achieve desired SAR values with the given modulation content introduces an extra variable that needs to be considered.
- Finally, signal demodulation can give rise to interference with bioinstrumentation equipment and directly influence the results of the experiment.

A discussion on these four points follows.

Absence of any modulations results in Continuous Wave (CW) exposures, while the presence of GSM-like modulation results in Pulse Modulated (PM) exposures. It has been suggested that the presence of modulations, and in particular, low frequency spectral content, might be important in order to induce biological effects [44]. A hypothetical mechanism that would allow for this to happen would be that of a biological demodulation process. Challis discusses the possibility of this in detail [24]. The conclusion is reached that such effect would be very unlikely at the carrier frequencies of

interest (around 1 GHz). Of course other mechanisms apart from that of demodulation could exist, although non has been convinsingly discussed.

Regardless of the absence of a viable theory for effect induction through PM RF, many positive studies have employed PM exposure schemes. Huber et al. investigated the significance of modulation in an experiment where rCBF and EEG were monitored after exposure to PM RF and CW RF [58]. Statistically significant changes were observed post PM RF (increased blood flow and increased alpha band EEG activity) but not under post CW RF. In a subsequent study by Huber et al., the effects of two PM RF signals on the rCBF were compared [59]. One exposure contained low frequency spectral components that were considerably lower than the other. It was shown that only the signal with the stronger low frequency components had a significant effect on rCBF. Although this result is not as strong as one comparing CW RF with PM RF it is still important. Further evidence of biological effects under PM and not CW RF is provided by a study by Regel et al., where again alpha band EEG increases were observed only under PM RF [114]. It is important to state that these three aformentioned studies utilised the same exposure setup (same antennae and signal characteristics resulting in homogeneous exposures), one that is not entirely representative of real GSM exposures. Therefore a degree of caution is warranted before generalizing these results to everyday mobile phone use.

Hinrikus et al. performed a study where exposure to a 450 MHz carrier with a 7 Hz on-off modulation produced no statistically significant results on the EEG spectra of 20 healthy volunteers [55]. In another study (n = 13) by the same group that used the same carrier frequency three different frequency modulations were tested [84]. Changes were observed in the EEG rhythms whose frequency was lower than that of the modulating frequency. Since the modulation frequencies were within the EEG spectrum and EEG recordings were performed during exposure, it is not clear whether interference issues could have influenced the result.

Bachmann et al. also investigated the effect of 7 Hz and 217 Hz modulation on the EEG power

spectral density (PSD) on 23 (for the 7 Hz modulation) and 19 volunteers (for the 217 Hz) [15]. They detected no significant results with the spectral analysis method but did detect some significant changes with a non linear analysis method (for more detail refer to Section 2.4). In these two studies it appears that statistical significance is not obtained on the whole sample, rather it is obtained on a per subject basis.

With all other things being equal, a modulated RF signal will always carry less energy than its unmodulated RF equivalent. As a consequence, a reduced SAR results from exposure to modulated RF fields. On the other hand, studies wishing to compare the effects of different modulation schemes tend to force SAR values to be equal. This approach ensures that potential differences in effects between exposures cannot be attributed to a thermal effect (SAR difference), simply because delivered energy would be identical between the two. However, for two RF signals that are modulated differently to have equal SARs, instantaneous peak electromagnetic fields must be unequal. So in effect, studies that compared DTX like PM RF with CW RF fields exposed subjects to electromagnetic fields of instantaneous peak that is 2.3 times greater during PM RF in comparison to CW RF. It is noted that if a real DTX structure was used the instantaneous peaks would vary by a factor of nearly 70 [58, 57, 59, 114]. A real DTX mode exposure would never reach a SAR dose of 2 W/kg. Therefore by selecting a DTX scheme RF exposure and setting the SAR dose to 2 W/kg, invariably the instantaneous electromagnetic field is elevated to unrealistic levels. However, such exposure does not violate any exposure guidelines.

Based on the discussion of the preceding paragraph, it is arguable that the observed effects appearing in the literature on brain activity of volunteers under PM RF, as opposed to CW RF, could be attributed to the differences in the instantaneous peak electromagnetic field rather than the pulsed nature of the fields.

If one can accept that thermal effects are not at play at energy levels equal to or less than 2 W/kg, as indicated by the studies of Huber et al. and Regel et al., then equating SAR values becomes

redundant [58, 57, 59, 114]. Instead the opportunity to equate instantaneous peak levels arises allowing us to determine if the effect is indeed related to the pulsed content. For such comparisons to be valid, SAR values must be kept at or below the levels used by Huber et al. [58]. Otherwise thermal effects would not be exluded.

2.1.3.7. Interference concerns

Since EEG recording equipment can be prone to noise, it is important to verify that the EM exposure source does not have any direct influence on the equipment. Pulsed RF fields can affect the amplifier circuitry through demodulation of either stray fields reaching the electronic components or currents induced on the EEG electrodes. If such effect takes place then it is possible to misinterpret this source of noise that is introduced in the EEG signals as a real EEG effect. Borbely et al., identified this problem in an early study and they minimised interference by placing the EEG amplifiers within a metallic casing and connecting individual electrodes to π-filters before connecting to the amplifier [17]. Schmid et al. used the same procedure to ensure that noise issues do not influence results [124]. It is noteworthy to mention that if the RF signal is not modulated with frequency components that are relatively close or within the EEG frequencies then it is most probable that noise will not be present. Studies that do use these modulations must take active steps to identify whether noise is present and if so to take measures such as those mentioned above to address the issue. It has also been shown that, under certain circumstances, the EEG electrodes can affect exposures by decreasing energy absorption [124]. Schmid et al. identify that effects on absorbed energy can be avoided by manipulating the orientation of the EEG electrode leads. However the specific arrangement is specific for the exposure setup against which this was assessed and does not necesserily transfer to handset like or monopole like exposures.

2.1.3.8. Effect location with respect to exposure location

Two trends dominate in terms of effect location of alpha band power increase. First is the trend of posterior ipsilateral effect localisation and second a global effect. Respectively these trends arise from localised and homogeneous exposures. Consistent with Curcio et al. (see reference [36]), Croft et al. hypothesised that the increase in alpha band activity would be greater in closer proximity to the exposure source [35]. Regel et al. highlight that the bilateral nature of effects reported by previous studies could be attributed to a sensitivity of the thalamus to the EMF exposure [114]. This therefore points towards an EMF exposure distribution specific effect and highlights the importance of replicating the spatial distribution expected from GSM-like exposures.

Sections 2.1.1 to 2.1.3 first reviewed some of the findings of the general research on effects on the human body arising from exposures to electromagnetic fields of various sources. Following that, a comprehensive review of the available literature on effects on the human resting EEG under GSM like electromagnetic exposure was presented. Several issues that are likely to have influenced results and may have contributed to the variable outcomes that are reported have been presented. These are exposure length, exposure distribution, dosimetry, low frequency modulation content, interference issues sample size and blinding. We have also identified elements in human studies that are necessary for results to be relevant to everyday mobile phone use. These are the frequency content and exposure distributions of the EMF stressor. The most consistent finding in the literature is that of increased posterior (and sometimes central) alpha energy during, and sometimes after cessation of exposure.

2.1.4. Sleep Electroencephalogram under GSM-like EMF

Apart from the resting EEG, sleep EEG has also been investigated under EMF exposure. The well defined nature of sleep architecture and sleep EEG serves as a good measure for assessing effects on the brain. A collection of sleep studies is reviewed next while a summary of these is given in Table 2.2. Mann and Roschke recruited 12 healthy participants for a single blind study where all night EEG recordings under EMF exposures were taken [98]. A signal with frequency content similar to that of a GSM phone (pulsed at 217 Hz with a duty cycle of 12.5%) was transmitted through an antenna situated 40 cm away from the subjects head. Although a power flux density value is given for the area of the participants brain no SAR calculations were available. Nevertheless exposures were kept below reference levels. They observed increases in alpha band power during REM sleep. In an attempt to replicate these findings under a more rigorous protocol, the same group of researchers recruited 24 participants in a single blind study [138]. The main improvement to methodologies was on the dosimetry. The exposure antenna was changed and a SAR level of 0.3 W/kg was reported. Since no effect was observed on the sleep EEG, the authors speculated that the failure to replicate their previous findings might be attributed to the difference in exposure. Although no dosimetric data was available from the first study, a comparison of power flux densities (0.2 W/m2 in the latter as opposed to 0.5 W/m2 in the former) would point to a comparatively elevated exposure in the first study, which could then justify the presence of the discrepancy. On the other hand, the results of the latter study would appear to be more credible from a statistical point of view, due to the larger sample size that they employed. To test the speculation that the failure to replicate results was due to an EMF dose difference, Wagner et al conducted another very similar study [137]. With a sample size of 20, the maximum permissible exposure levels were employed with the SAR reaching close to 2 W/kg. Once more the effects of their first study were not replicated. The authors point to the possibility of a window effect whereby the sleep EEG would be affected under certain SAR windows rather than the effect increasing monotonically with SAR. Such speculation remains to be

verified.

In another double blind sleep study by Borbely et al., 24 healthy participants were exposed to intermitted EMF (15 minutes on 15 off) throughout an entire night [17]. The exposure setup used resulted in homogeneous SAR levels of 1 W/kg in participants' heads [57]. They observed a non REM alpha power increase during the first 30 minutes of sleep. The same group conducted a double blind study which recruited 16 healthy participants [56]. They were exposed to 30 minutes of unilateral EMF (homogeneous in the exposed hemisphere), SAR = 1 W/kg, before night time sleep. Again, a non REM alpha power increase during the first 30 minutes of sleep was observed. The next study by the same group compared effects of 30 minutes exposure prior to sleep using two different exposure signals, one with no modulation at all and one with all GSM modulations [58]. The unmodulated signal had no effect on the sleep EEG whereas the modulated signal resulted once again in a non REM alpha power increase. Despite the fact that these studies and their results are closely related to mobile phone exposures, they are nevertheless different. The main point of distinction lies in the highly localised exposure distribution arising from real mobile phones as opposed to the one utilised in this series of studies, which is considerably more homogeneous.

Lebedeva et al. performed a sleep study where a distinct analysis method was considered [85]. Apart from normal sleep parameters and EEG spectral power, the non linear measure of correlation dimension D2 was calculated. With a sample size of 20, a decrease in correlation dimension was observed under the influence of the electromagnetic field. Unfortunately no information with regards to the EMF stressor is provided apart from it being a GSM standard mobile phone. As such no conclusions can be confidently drawn from this study.

Thus far, the largest sleep study was conducted by Loughran et al. who recruited 50 volunteers. In this experiment subjects were exposed to 30 minutes of GSM EMF radiation emitted by a Nokia 6110 handset that resulted in a SAR of 0.29 W/kg [90]. They observed an increase in the alpha frequency range during nonREM sleep. The effect started being significant 10 minutes into the

first non-REM episode. In this study, no Bonferroni adjustments were considered since the spectral analyses was hypothesis driven. The work of Loughran et al. can be considered as a replication of Huber et al's results, albeit with a more realistic localised exposure [56].

In a double blind study, Hinrichs et al. used a homogeneous all night exposure at a SAR level of 0.72 mW/kg [54]. This study varied from the rest (Table2.2) in that RF signals were set to simulate the GSM 1800 cellular system and as such used a 1800 MHz carrier signal as opposed to 900 MHz. Similar to the results of Wagner et al., no effect on the sleep EEG was observed under spectral analysis and correlation dimension analysis [138, 137].

Hung et al. conducted a small study with a unique protocol [60]. To investigate the effects of different modes of operation of GSM phones on sleep onset, they recruited 10 sleep-restricted participants which were exposed to 30 minutes of talk mode GSM signals (8 and 217 Hz modulations), listen mode GSM signals (2, 8 and 217 Hz) and standby GSM signals (132 Hz modulations) on different days. A 90 minute daytime sleep opportunity ensued where sleep onset latency was assessed. Significant delay in sleep onset only after the talk mode was observed. Changes in power spectral density in the 1 - 4 Hz range was also observed at frontal sites. They identify that their result is in agreement with that of Huber et al., (see reference [56]), who also recruited sleep-restricted participants and utilising similar signals to the listen mode employed here did not cause any significant change to sleep onset. They also identify that the presence of effect in talk mode as opposed to the listen mode is one that could be explained by the 9 times greater SAR value present in the talk mode exposure. This work does not report on alpha activity post exposure, a variable which showed significant increases in the Huber et al. study [56]. With the exposures in these two studies being of equal length and the SAR values being considerably different (0.015 W/kg in Hung et al and 2 W/kg in Huber et al.) useful comparisons could have been made on the alpha band effect. Comparisons of sleep onset effects with respect to varying SAR levels has been conducted by Regel et al., but no effect was demonstrated [114]. However a dose related effect on spindle frequencies

during non REM sleep was reported. Increase of fast (13.5 - 13.75 Hz) and slow (10.75 - 11.25 Hz) spindles was observed in active exposures when compared to sham. The increase was larger after exposure to the 5 W/kg SAR level and smaller after the 0.2 W/kg.

Finally the latest published work on sleep parameters under EMF exposure was that of Fritzer et al. [45]. Under a double blind protocol and with the same exposure setup as that of Borbely et al., (see reference [17]), 10 participants were exposed to 6 consecutive nights of homogenous EMF fields resulting in SAR levels of 1 W/kg. Since no effect was demonstrated on any of the monitored parameters, including sleep EEG, we may view this result as contradictory to that of Borbely et al. who observed an increase in alpha band power during the first 30 minutes of non REM sleep. However the distinction in sample sizes (24 in Borbely et al. and 10 in Fritzer et al.) would lend more confidence to the results of Borbely et al. The difference in exposure protocols, intermittent versus continuous, also needs to be considered before drawing conclusive comparisons.

Table 2.2.: A summary of studies monitoring the sleep EEG following RF exposures

Author	Exposure duration	Blinding / Sample Size	SAR & modulation content	Effect
Mann & Roschke 1996	8 hours	Single / 12	• SAR = n/a • Mod -217 Hz, 12.5% DC • Localized Exposure	α↑ during REM sleep @ Cz
Wagner et al., 1998	8 hours	Single / 24	• SAR = 0.3 W/kg • Mod -217 Hz, 12.5% DC • Localized Exposure	NONE
Wagner et al., 2000	8 hours	Single / 28	• SAR = 2 W/kg • Mod -217 Hz, 12.5% DC Localized • Exposure	NONE
Borbely et al., 1999	15mins on 15mins off for 8 hours	Double / 24	• SAR = 1 W/kg • Mod -2, 8, 217 & 1736 Hz, 87.5% DC • Homogeneous Exposure	non REM α↑ on first 30

Huber et al. 2000	30 minutes prior to sleep	Double / 16	• SAR = 1 W/kg • Mod -2, 8, 217 & 1736 Hz, 20.6% DC • Homogeneous within exposed hemisphere (a factor of 5 smaller in other hemisphere)	non REM α↑ (9.75-11.25 Hz & 12.25 - 13.25 Hz)
Huber et al. 2002	30 minutes prior to sleep	Double / 16	• SAR = 1 W/kg • Mod CW or -2, 8, 217 Hz, 20.6% DC • Unilateral Homogeneous within exposed hemisphere	non REM α↑ (12.25 - 13.25 Hz)
Lebedeva et al. 2001	n/a	n/a / 20	n/a	α↑ @ PzFz & D2↓
Loughran et al. 2005	30 minutes prior to sleep	Double / 50	• SAR = 0.29W/kg, • Mod-1736Hz 12.5% DC • Handset like localized exposure	non-REM α↑ with a 10 minute latency
Hinrichs et al. 2005	8 hours	Double / 14	• SAR = 0.072W/kg • Mod- mostly 1736Hz DC-n/a, f_c=1.8GHz • Base station like homogeneous head exposure	NONE
Hung et al., 2007	30 minutes	Single / 10	• Talk mode: SAR = 0.133W/kg, Mod- 8 & 217 Hz • Listen mode: SAR = 0.015W/kg Mod- 2, 8 & 217 Hz • Standby mode: SAR < 0.0001W/kg Mod- 1-32 Hz	talk mode increased sleep latency and 1-4 Hz frontal activity
Regel et al., 2007 (2)	30 minutes prior to sleep	Double / 15	• SAR = 0.2 & 5W/kg • Mod- 2, 8, 217, 1736Hz, 20.6% DC • Unilateral, homogeneous within exposed hemisphere	slow and fast spindle↑ (dose dependent) speed in 1-back task (dose dependent

Fritzer et al. 2007	6 8-hour exposures	Single / 10	• SAR = 1W/kg • Mod- 2, 8, 217, 1736Hz, 87.5% DC • Homogeneous head exposure	NONE

Apart from the sleep EEG, sleep studies have assessed the performance of other standard sleep parameters such as sleep latency, percentage of Rapid Eye Movement (REM) sleep, awakenings, sleep stages (I and II) duration etc. Although the majority of sleep studies did not detect any effects on sleep parameter1s, (see for example references [138, 137, 56, 85, 58, 54]), some did e.g. decrease of sleep latency, Waking After Sleep Onset (WASO) and decrease in REM sleep latency [60, 57, 97].

In conclusion 4 out of 12 sleep studies demonstrated no effect at all, 7 out of 10 showed some kind of alpha band power increase and 5 out of 10 demonstrated the same non-REM alpha band power increase during sleep. However, some of these studies used exposures that are not representative of mobile phone use (see Section 2.1.3) and therefore their outcomes should be related to mobile phone use with caution. Still, such results are extremely useful in identifying effects of RF radiation in general (neglecting the exposure distributions and other signal characteristics relating to GSM technology).

2.1.5. Miscellaneous brain related measures under GSM-like EMF

This section looks at literature that has investigated the effects of mobile phone-like radiation on the brain using some distinctive methods.

Intracortical EEG recording during mobile phone like exposure

Vorobyov et al., performed an experiment where 8 unanaesthetised rats with chronically implanted electrodes on the somatosensory cortex were exposed to a 945 MHz RF signal modulated at 4 Hz [136]. Intracortical recordings provide the opportunity to measure EEG signals directly from specific brain regions as opposed to the scalp EEG where readings represent the spatial addition of many different brain areas and is therefore smeared. With a free space field value of 0.2 W/m^2 and a signal averaging of 10 second long segments a hemispheric effect was detected in the 10.5 – 14 Hz band during first 10-20 seconds. This result is in line with the alpha effect reported repeatedly in human volunteer studies Table 2.1 and in particular with the result of D'Costa et al. [38]. The known similarities of the rat brain with the human brain add weight to this result and put it in context with human mobile phone related research. Interference issues in this study cannot be excluded so the result should be viewed with caution. Intracortical recordings are rarely reported in this field of study with at least one more case known [135]. Although such studies would need to be demonstrated on human volunteers, they are nevertheless capable of demonstrating an effect of low level radiation on biological tissue. Coupled with the difficulty of obtaining such data from human volunteers due to the invasive nature of the implantable electrodes, the significance of such studies becomes clear.

Inter-hemispheric synchronization of EEG rhythms

Vecchio et al. investigated the interhemispheric synchronization of cerebral rhythms under GSM-like radiation in a small sample size, double blind study that recruited 10 male volunteers [134]. A commercial GSM phone was used and was set to transmit at 2 W via a test card. No SAR information is given nor the model of the handset. Therefore the exposure dose remains unknown. Out of 19 electrodes recorded 8 were chosen to form the 4 pairs used to adequately investigate inter-hemispheric functional coupling. Using a three way ANOVA (electrode pair, frequency range and

condition) two statistically significant results were obtained. First, an increase in interhemispheric coherence at frontal sites in frequencies 8, 10 and 12 Hz and second a decrease in interhemispheric coherence at temporal sites in frequency bin 8 - 10 Hz. Once more this effect of increased coherence is observed in the alpha band thus being somewhat consistent with the power spectral increases in alpha band, Table 2.1.

Telemetric EEG for interference minimization

Kramarenko et al. used a telemetric EEG system to record noise free EEG during electromagnetic exposures (900 MHz with 217 Hz modulation) [80]. They recruited 10 young males and 10 children. Unfortunately this study provided no dosimetric data so the exposure dose remains unknown. The authors state that noise minimization is achieved with the telemetric system used but provide no information as to how this takes place. In fact, if signals are detected and digitized at the source near the head, which appears to be the case with the specific telemetric system, then the same interference issues applicable to any other non shielded amplification system would apply here. No statistical analysis is presented in this paper and the following results are cited: After a period of 1015 s the spectrum median frequency increased in areas close to antenna and after 2040 seconds, a slow wave activity (2.5 - 6.0 Hz) appeared in the contralateral frontal and temporal areas. The above results were applicable to the group of young males. Similar results were obtained for the group of children.

TMS

Recent studies have investigated the effects of mobile phone like radiation on brain excitability using Trans Cranial Magnetic Stimulation (TMS). Ferreri et al. exposed 15 male volunteers to GSM-like radiation for 45 minutes [42]. Subsequently, measures of Short Intracortical Inhibition (SICI) and Facilitation (ICF) time curves were obtained. It was observed that for the exposed hemisphere,

the SICI curve was reduced while the ICF curve was enhanced. In contrast, a similar study by InomataTerada et al. with a sample size of 10 and a GSM EMF exposure of 30 minutes showed no effect on SICI after exposure [123]. The authors state that even though no mild effects were detected, presence of such cannot be excluded due to the small sample size employed. Despite the limited quantity of studies utilizing TMS to investigate motor cortex function under EMF, from the above it appears that the contradictory nature of results found in other brain related outputs during EMF exposure (sleep and resting EEG, ERPs etc.) is also present in the TMS literature.

Regional Cerebral Blood Flow (rCBF)

Positron Emission Tomography (PET) scanning has also been used to map functional processes during or after EMF radiation. By means of PET scanning Huber et al. investigated the effects of GSM-like radiation on the rCBF [58]. After a 30 minute exposure rCBF of 13 healthy volunteers was assessed by using the average rCBF obtained from three PET scans (10 minutes apart each). They detected a significant increase in rCBF after EMF exposure in the dorsolateral prefrontal cortex of the exposed hemisphere.

Following that, Huber et al. conducted another PET study which differed from their first one only in that in addition to the GSM handset-like signal a GSM base station-like signal was also used as a separate exposure condition [59]. Consistent with their EEG findings, they observe that the handset like signal, containing low frequency components of higher intensity than the base station signal, caused more pronounced effects on cerebral rCBF. Their findings were consistent with those reported in their previous study in that the increased rCBF activity was observed in the exposed hemisphere and that again the prefrontal cortex was the affected area.

Haarala et al. performed a study with 14 participants in which rCBF was evaluated during active mobile phone exposure(as opposed to after exposure as was the case in the Huber study) while participants were performing visual memory tasks [49]. They report a bilateral effect associated

with the real exposure which is localized at the auditory cortex and did not correlate with the area of maximum EMF energy deposition. Although they state that this increase could be related to the mobile phone exposure, they also suggest that the observed effect may arise from auditory cues generated by the active phone. The results of Haarala et al. cannot be easily compared with those of Huber et al., (see reference [58, 59]), due to significant differences in exposure (SAR) distributions, the difference in rCBF monitoring time(during or after EMF exposure), and the EMF signal structure (see section 2.1.3.6). On the other hand, considering the replication of their results and the consistency with their EEG findings it appears that under the specific exposure conditions, which do differ from normal GSM exposure, rCBF is increased post EMF exposure.

2.1.6. Conclusions

This section started with a limited review of the general research investigating biological effects of electromagnetic radiation of various sources other than mobile phones. The aim of that was to provide the necessary frame in which the more relevant literature resides. Apart from the general literature, guidelines and standards defining exposure limits were introduced. Some of the relevant methods of assessing compliance of exposures with standards and guidelines were also discussed. Subsequently a detailed literature review on studies investigating the effects of mobile phone radiation on the human brain was developed and certain conclusions were drawn that would improve the quality and therefore the outcome of future research. These conclusions as will later be presented are to be incorporated in the design of studies that are described in this thesis.

2.2. Extremely Low Frequency Bioeffects

Mobile phones produce low frequency electromagnetic fields which are a by-product of the operation of the handset's electronics and battery. This source of exposure has only recently been taken into account so investigations on this matter are very limited. Even though the exposure intensity

expected should be much smaller than that coming from the RF source, the ELF components do need to be considered in relation to low-level, non established health and biological effects. In this section an overview of the findings relating to low frequency exposure of humans with stressors that do not include mobile phones are presented. These are relevant to mobile phone low frequency exposures because they form the basis on-which current ELF exposure standards are based on. The limited literature that relates to the specific mobile phone fields is presented next. An attempt to include all relevant publications is made, however, the bulk of this research is only concerned with characterizing the exposure with relation to the exposure limits thus virtually no investigations with human volunteers exist.

2.2.1. Extremely Low Frequency research with stressors other than mobile phones

The following section draws from the ICNIRP 2003 review on biological effects and health consequences arising from low frequency exposures [4]. The low frequency range is usually defined as that starting from close to DC up to 100 kHz. Apart from natural sources of radiation like the earth's magnetic fields and static charges from meteorological phenomena, many artificial sources of exposure exist in this frequency range. Static charges of the order of 10s to 100s of kV can build up from frictional forces such as walking on non conductive carpets. Any power generating system that uses DC current can potentially generate static fields, for example DC transmission lines or light rail systems. The biggest source of time varying electromagnetic fields present in the environment are related to the generation, transmission, and use of electricity. Typical frequencies are 50 and 60 Hz. Most devices using electricity usually produce some electromagnetic emissions. Some examples are television sets, refrigerator units, computers, hair dryers, telecommunication, and medical equipment etc. Most scientific research in this frequency range has concentrated on the effects of the exposures arising from overhead power lines. Studies extend from cellular to animal and human research, and epidemiological studies looking at either cancer effects or other short term effects. Hu-

man studies recruiting volunteers have studied various physiological and behavioral endpoints such as genotoxicity, immune and hematological systems, endocrine system, melatonin production, hormone production, cardiovascular function, perception of fields, effects on mood and other symptoms such as dermatological symptoms or headaches, and finally nervous system function.

The literature looking at nervous system function is of most interest in this thesis and therefore the relevant conclusions of the ICNIRP and the Repacholi and Greenbaum reviews on this matter are listed next [119, 4]. In general the human volunteer studies looking at the awake EEG under ELF fields suffer from the same limitations as those discussed in detail in Section 2.1.3. These include poor reproducibility of results, large variability in experimental conditions, variability in stressors, inadequate dosimetry, and often small sample sizes. The ICNIRP review concludes "...the studies analyzing effects on the power spectrum of different EEG frequency bands show a few inconsistent and in some cases contradictory results..."

It points out that the exposures used were comparable to those found in high exposure occupational environments and none used exposures at general environmental levels. Similar conclusions are drawn regarding sleep EEG measures, reaction times and cognitive and behavioral measures. The general conclusion of that review was that more studies are required to clarify these issues.

The more recent conclusions that are listed above are in line with the earlier findings of expert working groups which reported that "...the literature does not establish that health hazards are associated with exposure to low-level fields, including environmental levels.... However, reports of biological effects from low-level ELF field exposure..." were identified that need replication and further study for WHO to assess any possible health consequences [119].

As is the case for RF exposures, more research is recommended by experts to determine whether the biological effects demonstrated are indeed replicable and whether they lead to any health effects. In the next section the body of literature which characterizes the relevant fields and subsequently the results of some relating research with human participants is reviewed.

2.2.2. Mobile phone related Low Frequency research

The findings of technical studies delving into the characterization of ELF emissions from GSM handsets are listed here in chronological order. Extended technical details, conclusions, and considerations are discussed in Chapter 3. Linde and Mild performed the earliest assessment of these fields by measuring the current flow in the handsets' batteries as well as flux densities in the vicinity of the handsets [87]. They record a highest value of 1.8 mT (rms). Through current measurements they show the pulsed nature of the magnetic fields whose repetition rate corresponds to the 217 Hz main GSM modulating component (refer to Chapter 1 for more on TDMA characteristics and implications). Heath et al. concentrated more on the spectra of these emissions and identified the 2.1, 8.3 and 217 Hz components and harmonics. They also identify that the proximity of these frequency components to those observed in normal human EEG warrants investigations into possible effects on brain activity. Using a distinct approach Jokela et al. measured currents from battery packs of five different GSM handsets [72]. They then use the recorded current values in a numerical model consisting of a simplified human head, (represented by a sphere) and a loop structure through which the maximum recorded current level is established. Using two different methods of exposure assessment, they conclude that an exposure ratio of 27% of the permissible reference levels is the maximum observed. They also point out that even though reference levels can be seen to exceed guidelines, they are not valid exposure indicators in cases of near field exposures. Tuor et al. use a different approach to assess emissions from five GSM handsets. As opposed to Jokela et al., (see reference [72]), who measured currents from GSM battery packs, they measure the magnetic field directly and obtain the maximum value around the phone. Using those measurements they also produce a model source able to account for the observed field distribution. As in Jokela et al. the model source is a circular loop [72]. Different diameter values are found for the different handsets under investigation. As would be expected, none exceed the physical dimensions of the handset in question. They record a maximum field value of 75 μT which in some cases is shown to exceed

reference levels for certain 217 Hz harmonics. As indicated by Jokela et al. this violation does not signify over-exposure. Note also that the ICNIRP guidelines do allow for reference levels to be violated provided that basic restrictions are not [2]. Tuor et al. proceed a step further and suggest an exposure setup to assess the influence of these ELF fields on the brain. In that setup they recommend the use of large Helmholtz coils. These would deliver ELF energy homogeneously throughout the head. Considering the small dimensions of the current carrying loop that is identified to produce the equivalent of the GSM generated ELF fields, their choice of exposure is not able to reproduce the spatial characteristics of the field (the same concept discussed earlier in Section 2.1.3 with respect to RF fields also applies to ELF). Ilvonen et al. performed a study in which measurement of ELF fields was performed with suitable magnetic field detectors [64]. They collected data is used to create an equivalent source model which is then used to assess exposures numerically. The head model used in that investigation was inhomogeneous, containing various tissues (as opposed to the crude head approximation used by Jokela et al.).They selected the handset that exhibited the worst case exposure (as determined by the investigations of Jokela et al.) as their exposure device. Their findings suggested that exposures ranges are lower than those determined by Jokela et al., ranging from 3.6% to 4.1%. To verify the validity of their numerical modeling, they used two different numerical solving programs, one based on the Finite Element Method (FEM) and the other on the Finite Integration Technique (FIT). Good agreement between the two computational solutions was demonstrated. Straume et al., (see reference [128]), compared assessments of GSM ELF emissions based on frequency spectra from current measurements, as performed by Jokela et al., versus those based on magnetic flux density measurements as performed by Tuor et al. and Ilvonent et al. [64, 132]. They show that measurements based on frequency content of current measurements, leads to an overestimation of exposure of up to 2.2 times. They conclude that accurate exposure evaluation requires direct magnetic flux density measurements. Using improved numerical simulation methods, namely variable mesh sizes to better assess exposures close to the source, Jokela et

al. assessed exposures from three typical mobile phone usage positions [71]. In addition sources of uncertainty have also been taken into account in these simulations. Once more, results show that exposures are considerably lower than the basic restriction limit given in the ICNIRP guidelines.

To the best of the author's knowledge there are no peer reviewed published studies that investigate the effects of the low frequency fields emitted by GSM handsets on the human brain. However, some studies that have investigated the effects arising from the RF exposure have used real handsets for these assessments [32, 49, 36, 90, 93, 50, 35]. Interestingly, out of these studies those that looked at resting and sleep EEG have found statistically significant effects on the alpha frequency range. However, it would be premature and unjustified to conclude that this consistency can be attributed to the presence of the ELF since many other methodological factors are common amongst these studies. To the best of the author's knowledge the only attempt to assess effects from the ELF components of GSM handsets was that of Verschueren et al. [135]. In that study 10 subjects with temporal mesial lobe epilepsy were exposed to intermittent peaks of 2 Hz magnetic field at an intensity of 60 μT. Their findings are highly variable with observed increases and decreases in various bands. The authors suggest that these results might reflect variable individual responses to the stressor. Cook et al. exposed healthy volunteers to pulsed magnetic fields with spectral content ranging from 20 Hz to 18 kHz [30]. The fields were generated by large current carrying coils. The resemblance of this exposure to that of the GSM generated fields is limited only in the frequency content, as intensity and spatial distribution of fields varied significantly. With a sample size of 20, significant decreases in alpha activity after exposure were observed for both sham and real exposures. However, 1 minute after real exposure a significant increase in alpha activity is recorded in comparison to the sham condition. It is notable that these effects were observed in the same scalp regions as those reported by many studies employing the GSM related RF stressors. As summarized in Table 2.1, these are predominantly posterior regions. In a subsequent study by the same group utilising the same exposure protocol, EEG recordings were taken not only after exposure cessation

but also in the refractory periods (periods with zero field present) during exposure. A decrease in alpha activity 5 minutes after the start of the exposure was observed at posterior sites. No changes were observed post exposure and thus the result of their previous study was not replicated. They suggest that this discrepancy could be attributed to the different refractory periods employed between the two studies. From this limited amount of studies, no dominating trends can be seen. In at least one case the issue of individual variability in response to the fields has been raised; no further study investigating this possibility has been undertaken. It appears that it would be crucial to attempt to demonstrate an effect with a large sample size and subsequently replicate it in another study, employing identical protocols (exposure sources intensities durations EEG monitoring intervals etc), and perhaps using the same individuals, so as to assess the assumption of individual responses within populations. So in conclusion the effects of the GSM ELF generated fields on the human brain are yet to be assessed adequately so future studies towards this are essential. To avoid the variability observed in results relating to RF exposures, replication of results with identical protocols (as opposed to altering and re-adjusting protocols with every new study) can be very beneficial.

Even though experimental studies with human volunteers have not been performed under ELF exposures the technical aspects of these signals have been studied to a certain extent lately. These aspects include the field characterization and exposure levels expected from normal usage of GSM handsets.

2.2.3. Conclusions

No human studies have investigated the effects of GSM-like ELF fields on brain variables. An attempt to draw some conclusions that might be applicable to related exposures from the most relevant literature has been made. Although significant effects have been reported repeatedly, these effects have been somewhat inconsistent and therefore the overall results of this literature remain

inconclusive. There has been a suggestion that such fields might cause individual responses a fact that can be contributing to the inconclusive nature of results. In addition the relevant literature assessing ELF emissions from GSM handset has been reviewed briefly. This work originating from a few different groups using different evaluation techniques is in general consensus that observed fields cannot cause exposure that violate basic restrictions as defined by ICNIRP. In fact none were shown to exceed the 30% mark of limits. As detailed in these studies the fact that reference levels are exceeded does not signify overexposure of users. Model sources that can account for this ELF radiation have been developed by more than two independent groups, and all appear to agree that adequate modeling of these fields can be achieved with a simple current carrying loop structure whose diameter is comparable to that of the handsets' dimensions. These model sources can be used in experiments to expose human volunteers to ELF fields without the presence of the accompanying RF fields.

In the next two sections of this Chapter commonly used and alternative EEG analysis methods are discussed within the context of EMF related effects on the brain. Particular attention is drawn on the ApEn method, one that assesses the non linear property of complexity of any time series. The majority of studies that investigated the effects of mobile phone like radiation on the brain have used the linear measure of spectral power or spectral amplitude to quantify changes. This method is usually based on the Fourier transformation. Even though this is a well recognized method of analyzing EEG data whose output demonstrates common characteristics within and between individuals, it is true that it only provides limited information as to the characteristics of the recorded signal. Considering the difficulties in demonstrating an effect on spectral measures of the EEG under GSM like radiation (small effect size) with the current spectral measures, it may be beneficial to investigate alternative methods of analyzing EEG data. In the following two sections the basics of the linear method of FFT analysis and some of its drawbacks are introduced. Subsequently the available literature that used non linear measures to assess changes in EEG arising

from GSM like exposures is reviewed. Last, the non linear method of Approximate Entropy is introduced, which is considered suitable for use in the context of mobile phone related effects. Some of the literature that has used this method of analysis on EEG data is also presented.

2.3. Linear characteristics of the spontaneous EEG

Traditionally EEG analysis is performed on the linear aspects of the time series. Perhaps the most common method is that of spectral analysis based on the Fourier Transform that is often implemented by the Fast Fourier transform (FFT) algorithm. An FFT algorithm can decompose a time signal into a family of sinusoidal constituents of varying amplitudes and frequencies. The output of the FFT algorithm is called the frequency spectrum of the signal and contains amplitude spectral information as well as the relative phases of its constituents. Using the inverse FFT one can reconstruct the absolute original time series. When it comes to EEG data, the Fourier spectra obtained from a transformation represents collective rhythmic neural activity arising from many spatially separated sources under the recording site.

Under certain states of mental alertness, (e.g. sleepy, alert, thinking etc), "normal" EEG frequency spectra can be obtained from healthy populations. Different frequency ranges have been shown to carry clinical significance. For example, during a relaxed mental state, rhythmic activity around 10 Hz is observed and when alert higher 15 - 50 Hz activity is present. The spectral EEG analysis has proved as an indispensable tool to clinicians and researchers alike. It therefore comes as no surprise that when investigators decided to look at the possible effects of mobile phone radiation on the human brain, they did so by looking for abnormal patterns in the EEG spectra of healthy populations. Such an approach can be seen as the natural starting point but there is no obvious reason for one to expect such spectral specific changes in the EEG under EMF.

FFT analysis is not without its drawbacks. It requires signals to be stationary and periodic. When an FFT is performed on a discrete finite series of data points an assumption is made that

the observed pattern is repeated in time indefinitely thereby obtaining the periodicity required. However, this is generally not true since EEG signals change (they are non stationary) with time. Methods to minimize the errors that arise from such limitations are well known (e.g. windowing). The fact however remains that the non stationary aspects of signals remain unexplored under FFT analysis. In addition, evidence exist that EEG signals can behave as nonlinear oscillators and will therefore contain nonlinear features that would remain undetected with a FFT [46]. Various methods of studying non linear phenomena and time series have been developed. In the next section some literature that investigates non linear features of EEG signals is discussed. Particular attention is payed to investigations which relate to EMF effects on the EEG. Then a more focused review of the Approximate Entropy algorithm and its applications is developed.

2.4. Non linear characteristics of the spontaneous EEG

More recently the non linear measures of brain activity are becoming a popular EEG analysis tool. As Stam states in a review of non linear dynamical analysis of EEG and MEG "The application of nonlinear dynamics to electroencephalography has opened up a range of new perspectives for the study of normal and disturbed brain function and is developing toward a new interdisciplinary field of nonlinear brain dynamics" [127]. In addition as identified by Stam, the emergence of such new analysis tools that also include wavelet analysis artificial neural networks, etc, has resulted in renewed interest in EEG. These new avenues of exploration of EEG signals, have been employed in the detection of EMF related effects on the EEG only sporadically. As such, this avenue remains largely unexplored. Considering the difficulties that researchers are presented with when using spectral analysis methods to detect EMF related changes, the value of alternative analysis methods is evident.

2.4.1. General applications of non linear analysis on the EEG

Some of the areas of EEG analysis that have attracted interest in terms of non linear testing are listed next. The resting EEG has been shown to be a weak non linear structure but early evidence of low dimensional chaos was later refuted [107]. Weak non linear coupling between sites in multichannel EEG (see reference [19]), as well as increase of EEG dimensionality with age, (see reference [12]), have both been demonstrated during resting EEG states. In the field of sleep EEG, deep sleep stages were shown to exhibit lower complexity, (see reference [78]), and in stages I an II, non linear measures were more capable at discriminating between stages than the spectral measures [41]. In anesthesia non linear analysis methods were shown to correlate with anaesthetic depth. In particular one measure called the Bispectral Index (BSI) has been shown to be a reliable measure of anaesthetic depth [103]. The field of epilepsy has also attracted a lot of interest in this respect and researchers have particularly concentrated on the use of non linear analysis techniques in the detection and prediction of seizures, with the ultimate goal of administering preventative treatments [62]. In psychopharmacology, the administration of ethanol was shown to cause decreased non linearity in EEG, and the subjective feeling of intoxication also correlated with decrease EEG non linearity [40]. Correlation between emotional states and complexity has been shown in many cases and so is the case in patients with schizophrenia where a lower complexity than normal has been shown. A thorough review on the matter has been published by Stam [127].

2.4.2. Non linear EEG analysis under EMF exposures

Most peer reviewed literature, including some publications appearing in conference proceedings, in which detection of non linear changes in brain activity under RF radiation has been explored is discussed in the following paragraphs.

The earliest attempt to look at non linear features of brain activity under electromagnetic radiation was that of Lebedeva et al. [86]. Although that study lacked any quantitative or qualitative

information on exposure and basic experimental detail (blinding conditions, adaptation nights etc) the authors reported a statistically significant change in the correlation dimension, D2, of scalp locations Fz and Pz during an 8 hour sleep episode under electromagnetic exposure. It also demonstrated statistically significant changes in power spectral estimates during sleep under electromagnetic exposure.

The non linear measure of Higuchis fractal dimension was investigated in an experiment that incorporated microwave and photic stimulation [89]. With a very low SAR level of 0.0095 W/kg, derived from free space field measurements, they fail to find an effect on the fractal dimension. Increased fractal dimension was shown for the photic stimulation component but no statistical analysis is presented and for the majority of subjects no sham exposures were recorded. In a similar preliminary study, the same group reported a tendency towards increase of fractal dimension during photic and microwave stimulation [88]. Again no statistical analysis is presented.

In a series of two cross-over double blind studies by Bachmann et al., with sample sizes of 23 and 19, a non linear measure termed as Length Distribution of Low Variability Periods (LDLVP) was used [15, 96]. The results were compared with those derived from the conventional spectral analysis method, . The first study utilized a 450 MHz signal with a 7 Hz modulation and the second utilized a 217 Hz modulation. Cited free space power densities were identical for both studies even though modulation content was distinct. Although 9 scalp locations were recorded in the first experiment, only Fp1 or Fp2 were selected for analysis. This choice is based on the findings of Hinrikus et al., even though in that study no statistically significant result was shown [55]. Frontal channels, including Fp1 and Fp2, are prone to eye movement contamination which would contribute to the error variance. Nevertheless, using a custom statistical analysis approach they showed that 25% of subjects show a significant change in LDLVP values under the exposure condition in comparison to the Sham condition. Their statistical analysis is based on a measure calculated as the difference of LDLVP value before and during exposure, per subject, divided by the standard deviation of

Table 2.3.: A summary of the findings of studies that used non linear analysis methods as alternatives to the Fourier spectral method.

Author	Exposure Duration	Sample Size	SAR & Modulation Content	Effect Time Course	Effect
Lebedeva et al. 2000	8hrs	20	n/a	During	change in D2 and spectral power
Lipping et al. 2003	1min	8	SAR = 0.0095 W/kg 450MHz, 7 Hz, 100%DC	—	NONE
Liping et al. 2004	20sec	8	SAR = 0.0095W/kg 450MHz, 16 Hz, 100%DC	—	NONE
Bachmann et al. 2005a	1min on, 1 min off for 20 mins	23	SAR = 0.35W/kg Derived from free space power density 7Hz, 50%DC	During	LDLVP↑ in 5/23 LDLVP↓ in 1/23 PSD – no change
Bachmann et al. 2005b	1min on, 1 min off for 20 mins	19	SAR = 0.35W/kg Derived from free space power density 217Hz, 50%DC	During	LDLVP↑ in 1/19 LDLVP↓ in 1/19 PSD β↑ 4/19

these difference values across the 23 subjects. Corrections for multiple comparisons satisfying the Bonferroni criterion were made.

In the second study, only 10% of subjects (2/19) demonstrated a statistically significant change in LDLVP measures, with one subject demonstrating an increase and the other a decrease. The authors point out that the difference between the results in the two studies could be related to the modulating frequency. Also, in this study more statistical significance was demonstrated with the PSD method, although a direct comparison cannot be made since all channels were analysed for PSD as opposed to only Fp1 and Fp2 for LDLVP.

To the authors knowledge Jing et al. were the only researchers to investigate the effects of electromagnetic fields on EEG data, albeit on rats, using the ApEn method [68]. Sixteen rats fitted with implanted EEG electrodes were separated into two groups, exposed and sham. The exposure consisted of a train of 200 pulses, 200 kV/m, with a repetition rate of 0.5 Hz. The ApEn of the rats was assessed for several hours after exposure. It was found that 2 hours after exposure the ApEn of exposed rats significantly increase for 14 out of 16 channels. However, the authors mention that due to the implanted electrodes, and considering the strength of the pulses, it is possible that the distribution of exposure was modified, resulting in increased energy deposition in the vicinity of electrodes. It is also noted that in the context of mobile phone effects this result is not really relevant due to the orders of magnitude of difference in electric field values and frequencies that would be expected from mobile phone handsets (and base stations) and those used in this experiment.

It would be fair to say that the investigation of non linear aspects of EEG signals under EMF exposures is still at an early stage and most results are based on small sample sizes. It is clear that more research is required to identify whether non linear features of the EEG are affected under EMF exposures.

2.4.3. Review of general literature utilising the ApEn method for the analysis of EEG data

A variety of methods for calculating values for non linear properties of time series exist [127]. The Approximate Entropy, ApEn, is a non linear measure of complexity which was introduced in Chapter 1. With it, complexity measures of time series can be obtained. As opposed to other methods it can be employed on noisy data since it is *de facto* unaffected by noise through appropriate selection of the threshold parameter 'r' [112]. In addition, the algorithm performs well with small amounts of samples, as low as 70, a feature that does not characterize other methods such as the Kolmogorov Smirnof method [120], It is also robust to outliers [112]. As Stam states "... a strict interpretation

of nonlinear measures in terms of attractor dimensions, deterministic chaos and entropy as bits / second is almost never justified. However, the classic measures can still be used as 'tentative indices' of different brain states, and the newer measures often allow a less ambitious but more straightforward interpretation". Accordingly, for the purpose of comparing EEG data with and without the influence of the EMF stressor, the use of a non linear measure such as the ApEn seems appropriate for tentative comparisons. With other methods such as surrogate analysis, further information about the actual non linearity of EEG signals can be easily obtained. Since the solution of ApEn is based on the selection of two parameters, the embedding length 'm' and the threshold parameter 'r' (refer to appendix A.1), it is therefore imperative that fixed parameters are used for system comparison [120]. One should also be aware of the limitations of the ApEn algorithm which are the inherent biasing introduced in the algorithm by the inclusion of self comparisons, and in many cases the lack of relative consistency, when the 'm' and 'r' parameters are varied. Although not exhaustive the following review gives a good representation of the variety of applications and findings of the ApEn when it comes to EEG data.

Bhattacharya et al. compare linear and non linear methods, including ApEn, in distinguishing between 3 groups, control (healthy), seizure condition and mania condition, (n = 8 each) [16]. Using an ANOVA design it is shown that the EEG complexity of the seizure group is significantly less than the control group, whereas the mania group is found to be no different to the control. This effect is reported at 12 out of 16 electrode locations. The authors report that even though linear measures are found to be more useful to some extent, the usefulness of non linear measures such as the ApEn cannot be ruled out.

Abasolo et al. compared the EEG of 7 Alzheimer's Disease (AD) sufferers to that of 7 healthy individuals using the ApEn method [10]. Out of the 19 electrode positions (10/20 International system) used only one is chosen for analysis, P3. They find that complexity of EEG signals of healthy subjects is significantly higher than those of AD sufferers. In a subsequent study by the

same group the EEG background activity of 10 Alzheimer's disease patients and 8 control subjects was recorded [10]. The complexity of the data was analysed using the ApEn method. According to the authors, since non linear measures can be affected by linear changes in the signals, spectral analysis was also performed to determine whether detected changes in ApEn are influenced by the known linear change of diffuse slowing of the background activity, (see reference [100]) observed in Alzheimer's patients. For the Alzheimer group 14 out of 19 electrodes were found to have a decreased ApEn value but only two of those, P3 and P4, were significantly different. In addition the expected slowing of the EEG was indeed observed in the Delta band (T4, P4 and O2) and in the Alpha band (T3 and T4). The authors reach the conclusion that ApEn can be used as a complimentary method to the more conventional methods, although they stress the fact that their study is only a small sample size one and should be viewed as a pilot.

In many instances researchers choose one non linear method over another for use on collected data. This choice is based on identifying weaknesses of methods and selecting the one whose weaknesses would have the smallest impact on the type of data under investigation. A study comparing different parameters of complexity of sleep stages recruiting 8 participants has been performed by Acharya et al. [113]. The parameters studied were the correlation dimension, fractal dimension, largest Lyaponov entropy, ApEn, Hurst exponent, phase space plots and recurrence plots. The authors conclude that correlation dimension, fractal dimension, largest Lyaponov entropy, ApEn, Hurst exponent all decreased progressively from Stage 1 sleep to stage 4, and then decreased again during REM sleep. This study also had a small sample size so results should be treated with caution. No comparisons between the non linear methods used were discussed.

Similar results were obtained by Burioka et al., were in a small study recruiting 8 healthy volunteers, ApEn was able to distinguish with statistical significance between all sleep stages and awake resting eyes closed EEG [22]. However results were only present at 1 electrode out of the 6 recorded.

Burioka et al. looked at ApEn in a study that recruited 8 healthy and 8 epilepsy subjects. It

was found that during non epilepsy periods, ApEn of the healthy group was similar to that of the epilepsy group. During epilepsy periods, ApEn was found to decrease with statistical significance in the epilepsy group by 40%. Using the method of surrogate data analysis to assess the presence of absolute non linearity in the data, both groups failed to demonstrate significant non linear features as measured by ApEn. On the other hand, during epilepsy periods the epilepsy group did demonstrate statistically significant non linear features. So even though ApEn in healthy subjects is larger than in epilepsy subjects during epilepsy periods, non linearity in the healthy group was missing. The authors point out that ApEn could be used to determine pathological brain activity such as that occurring during absence epilepsy.

2.4.4. Conclusions

A brief introduction of linear and non linear analysis methods for time series as related to EEG signals has been developed. It is seen that linear methods are widely used especially in EMF research, however, some recent attempts to look at non linear aspects under EMF have been developed. In this review particular attention has been drawn on the ApEn method which has demonstrated usefulness in various condition diagnosis through EEG signals.

2.5. Chapter Conclusions

The findings of the literature that investigates biological effects of radio frequency electromagnetic fields have been briefly summarized. For intensities exceeding those defined by guidelines, biological and health effects are well established and documented [4, 6]. At the current state of knowledge there are no established biological effects that could arise from exposure to intensities below guidelines. However the widespread use of mobile phones and the implications that could arise from any potential side effects has led researchers to investigate rigorously the possibility of effects. These

investigations led to multiple outcomes, none of which have been reliably classified as health effects. In Section 2.1.3 the literature that has investigated effects of the GSM RF radiation on brain activity using the spontaneous EEG has been reviewed. The predominant trend in the results of this body of literature is that of inconsistency (see Tables 2.1, 2.2 and 2.3). Even though statistically significant changes in the EEG are demonstrated they are almost never replicated. However one result that does stand out as being relatively consistent, is that of increased alpha band EEG activity at posterior sites during, and sometimes after exposure to GSM-like radiation. The effect is statistically small and may vary between individuals, facts that might be contributing to the difficulty in detecting it. As it stands, this effect does not seem to have any health impact on users. However, more investigations are required to establish that with more certainty. Weaknesses of thus far performed human studies have been discussed with the major ones being related to dosimetry and small sample sizes. Gaps in the influence of modulation of signals on the resting EEG, especially during exposure have been identified. Future studies should concentrate on replicating the alpha band increase effect under realistic exposures, in large sample size studies (as suggested by Cook et al. and Valentini et al. [26, 133]) with detailed dosimetric information, and should also be designed to assess the influence of modulation characteristics on observed effects [18, 124]. The findings of literature investigating the effects of ELF radiation of various sources on the human body and in particular on the human brain, is also inconclusive with poor reproducibility of results, large variability in experimental conditions, variability in stressors, inadequate dosimetry and sometimes small sample sizes. The ICNIRP review concludes that more studies are required, especially at low-level general public exposure levels, to clarify these issues. Unfortunately studies investigating the effect of the GSM-like ELF radiation on the brain have yet to be performed. The fields however, have been characterized adequately by various research groups, and exposures levels arising from these sources are well below the guidelines [72, 132, 64]. Still, their potential influence on users needs to be addressed. With the majority of studies investigating the EEG under GSM

electromagnetic stressors using linear methods of analysis a gap, is identified in the analysis of the non linear features of the EEG signals. Therefore such analyses need to be performed and can be considered as supplementary to the well established linear methods of analysis.

3. Small Sample Size Study

This chapter[1] presents a small sample size study that was undertaken to identify and compare effects on brain activity arising from two kinds of RF radiation, continuous (CW) and pulsed (PM). Specific aspects of the exposure have been designed in a manner that renders results applicable to actual mobile phone usage. The protocol is designed to detect acute effects on the EEG manifesting during or shortly after exposure. The study addresses the question of whether signal modulation matters when it comes to possible bio-effects. In addition, it serves as a test platform for the statistically stronger large sample size study that is presented in Chapters 5-7. Such a test platform is critical since it allows for validation and improvement of the experimental design. Aspects that might need to be improved upon include the suitability of the overall protocol, exposure device, physiological data acquisition hardware, selected physiological measures and methods of data analysis. The chapter is structured as follows: The underlying rational for the experiment is outlined and connected to literature. Subsequently the experimental design is outlined and then analysis and results are presented followed by discussions. Finally methodological gaps are identified and the precautions developed to address them before the conduct of additional experiments are discussed.

[1]The majority of this work has been published by Perentos et al. in the Australasian Physical & Engineering Sciences in Medicine Journal, see reference [110].

3.1. Introduction

Numerous studies have been published looking at different indices relating to brain function under GSM electromagnetic exposures. These include event related potentials and performance tasks, sleep variables and resting electroencephalogram variables [58, 52, 90]. On reviewing these studies, it can be observed that results are highly variable [51, 29]. Studies that attempt to replicate results often fail, (see for example [52, 50], with at least one exception [36, 35]). Part of the variance between studies arises due to the variable experimental conditions employed. These include exposure duration, post exposure monitoring periods and statistical analysis methods. Therefore, the need to thoroughly investigate these effects remains.

One of the most consistent findings reported across several independent studies is that of increased resting EEG alpha band activity under EMF exposure [58, 36, 35]. The consistency observed across these studies could be partly attributed to some common methodologies employed such as accurate dosimetry, the extended duration of exposure and the duration of EEG recording. The significance of the last two factors is discussed comprehensively elsewhere [34]. On the contrary, studies that investigated resting EEG but did not show an effect of EMF exposure on alpha band activity, have tended to employ small exposure durations, for example Roschke and Mann who used exposure periods shorter than 3.5 minutes [99].

Another important experimental condition which varies between studies is that of the characteristics of the electromagnetic exposure. Of particular importance are the SAR distributions in the head and the spectral content of the stressor due to the type of modulation employed. At frequencies greater than 100 kHz, SAR is defined as the rate at which electromagnetic energy is absorbed per unit mass of biological tissue. It is the main metric for assessing exposure compliance of devices such as GSM mobile phone handsets.

With respect to SAR distributions, Curcio et al. and Croft et al. utilized real GSM handsets with monopole antennas as opposed to Huber et al. who used a non-handset based patch antenna.

In another publication by Huber et al. [36, 35, 58]. Huber et al. have shown that using a patch antenna, such as the one used in Huber et al. [58], results in a SAR variation within the exposed hemisphere of approximately 12.5 dB (between the exposed surface and the farthest side to the exposed hemisphere), with some areas deep in the brain exposed to SARs of at least 5 dB [57]. However, it has been shown that the variation of SAR in the head due to exposure from monopole antennas operating at 900 MHz is much greater, reaching 24 dB [79]. Thus it is evident that a more homogeneous exposure is produced under the patch antenna relative to the localized nature of the exposure resulting from a monopole antenna. Huber et al. argue that the SAR observed from the patch antenna they used would be representative of a real mobile phone exposure [58]. However, as discussed above, this is not the case, and in particular, some parts of the mid-brain are exposed to much higher SARs (by a factor of up to 80) than would occur from any commercially available mobile phone.

Absence of any modulations results in CW exposures, while the presence of GSM-like modulation results in PM exposures. It has been suggested that the presence of modulations, and in particular, low frequency spectral content, might be important in order to induce biological effects [44]. Consistent with this, recent positive studies have all employed PM exposure schemes. We should note that the nature of pulse modulation and spectral content amongst some of these studies did differ. For example Huber et al. utilized a signal with the same frequency components as the DTX mode spectrum of the GSM handset (2, 8, 217 and 1736Hz) while Curcio et al. and Croft et al. made use of the main 217 and 1736 Hz pulse modulation frequencies. In addition, in Croft et al. the pure Extremely Low Frequency (ELF) exposures (217 and 1736Hz) were also present due to real handset battery operation [58, 109, 36, 35].

Huber et al. tested the importance of modulation characteristics by comparing effects on the EEG arising after exposure to PM RF (DTX like spectrum) with those arising after CW RF exposure [58]. Effects were observed on alpha band activity after PM RF exposure but not after CW RF.

They concluded that modulation characteristics are critical in inducing the alpha band activity increase after mobile phone exposure. However, as discussed above, since the exposure distribution used differed from that of a real mobile phone, the question remains of whether such an effect would be observed under an exposure that more closely resembles that of a mobile phone, or whether Huber et al's findings are specific to their exposure setup.

Hence, the main purpose of the present study was to attempt to replicate the findings of Huber et al. (CW RF vs PM RF) using a monopole antenna as the exposure source, thereby allowing us to test whether the spectral content is indeed significant under more realistic exposures, and making the findings of Huber et al., if replicated, more generalizable to real mobile phone handsets and thus everyday exposures.

Here, we also explored the usefulness of a non-linear analysis method of the EEG. The most conventional way of analyzing resting EEG signals is the Fourier transform, which is a linear method of signal analysis in the frequency domain. On the other hand, evidence exist that EEG can behave as a non-linear oscillator, and therefore a non-linear signal analysis method may be appropriate [46]. One such method is the Approximate Entropy (ApEn) with which the non-linear measure of complexity of the EEG can be calculated. This may provide new information regarding the interaction of RF with the EEG that would otherwise remain undetected with conventional linear analyses methods.

For example, the regularly occurring pulsing of the incident radiation could introduce more regularity in the EEG time series and therefore decrease the complexity of the resting EEG, much like the case of auditory or visual entrainment [9, 20]. In at least one case, an effect on the entropy of the EEG of rats has been shown under the influence of low frequency pulses; although in that case the electromagnetic fields were of much higher intensity and of different frequencies to those investigated here [68].

3.2. Materials and Methods

3.2.1. Subjects

Twelve healthy volunteers (6 males and 6 females) aged between 19 and 32 (Mean = 26.5, SD = 3.29) were recruited. Participants were informed about the details of the experiment and written informed consent was obtained. The design of the study was approved by the RMIT University Human Research Ethics Committee.

3.2.2. Protocol

Participants attended a 2 hour recording session in which RF exposure occurred for two 15-minute intervals (15 minutes for CW and 15 for PM RF), a sufficient time to allow for a cumulative effect to take place, (see reference [34]), as well as there being a 15-minute Sham exposure, (Sham). Resting EEG was monitored throughout the experiment while subjects were seated comfortably with eyes closed.

The exposure protocol, depicted in Figure 5.3, comprised twelve 7 ½ minute periods, four periods for each exposure condition (one pre exposure, two during exposure, one post exposure period). Subjects were instructed to remain as still as possible and keep their eyes closed throughout the duration of recordings. One minute breaks were allocated between each 7½ minute period in which subjects were instructed to open their eyes and stretch; the latter aimed at reducing subject fatigue and irritation from being confined for long periods. Although a fully counterbalanced double blind cross over design was applied, the study was analysed as single blind. This was necessary since ELF artifacts were present 'during' exposure, most likely originating from the PM RF signal demodulation in the EEG amplifiers, which were sometimes visible in the EEG recordings. For the same reason, only the pre and post exposure periods are analysed here.

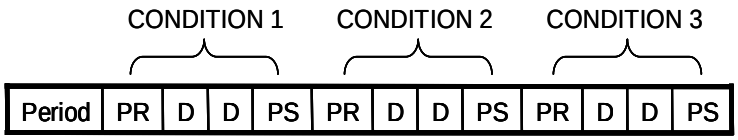

Figure 3.1.: Experimental protocol of the small sample size study. PR: pre-exposure, D: during exposure, PS: post exposure. Conditions 1, 2 and 3 are Sham, PM RF and CW RF randomly assigned. Each period lasts for 7½ minutes. For all subjects, after each PS period, there was a 1 minute break.

3.2.3. Data Acquisition

Participants were fitted with a Compumedics Neuroscan 19 Channel Tin Quick EEG Cap employing the standard 10/20 international electrode positioning system (excluding Fz, Cz and Pz), referenced to linked mastoid electrodes. Data were recorded using the MINDSET, MS-1000, 16-channel EEG amplifier (fixed gain of 32768) . Signals were sampled at a rate of 256 samples per second and band pass filtered with two, fourth-order Sallen-Key active filters, 48 dB roll-off per octave and a 3dB pass band between 1.5 Hz - 34 Hz. Impedances were below 12 kΩ at the start of the recording. Recordings took place inside a electromagnetically shielded room, see Figure 3.2, with the RF generator and amplifier situated outside the shielded room. Apart from the subject under test, another person, responsible for monitoring the physiological recording equipment, was present in the shielded room. Physiological recording equipment and modulation circuitry were also inside the room.

3.2.4. RF exposure

Dummy Handset

The exposure device used, depicted Figure 3.3, was a model handset consisting of a metallic casing acting as the ground and a monopole antenna. This constitutes a crude approximation of a commercial GSM handset. Detailed description of the handset can be obtained elsewhere [38, 102].

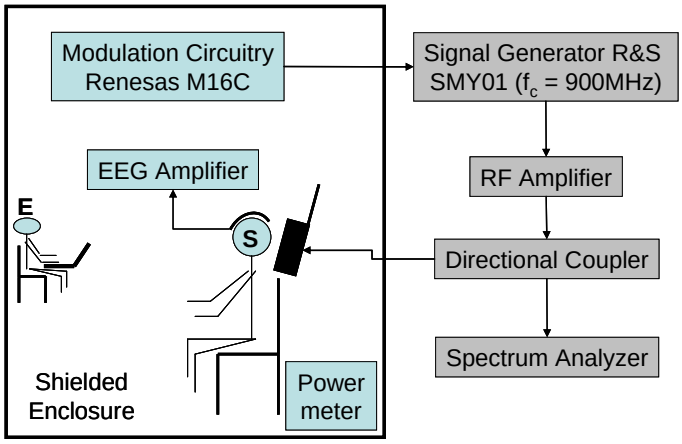

Figure 3.2.: A depiction of the experimental setup. The experiment takes place in a high frequency shielded enclosure in which the participant and the experimenter are found. RF measurement and generating equipment (excluding an RF power meter) are situated outside the enclosure thereby minimizing EM emissions. Physiological recording equipment are found within the enclosure.

The main advantage of using such a model handset instead of a real one is that it does not produce thermal and auditory queues during operation, as is the case with real GSM handsets, which could compromise the blinding of the experiments. The handset device was placed according to the standard 'touch' ear to mouth position [5]. A left hemisphere exposure was used for all subjects.

Exposure characteristics

Two different signals were used. The first was an unmodulated RF signal at 900 MHz containing no low frequency content (CW RF), and the second was a pulse modulated 900 MHz signal containing all components found in the signal emitted by GSM handsets which are operating in the DTX mode, (PM RF). These components arise from the frame structure of the GSM signal and include 2, 8, 217 and 1736 Hz plus harmonics [109]. Input levels to the model handset were set to simulate the 2 W peak signal of a commercial GSM mobile phone handset operating at 900 MHz. For compliance purposes, dosimetric evaluation of this handset was performed at a commercial facility in Melbourne

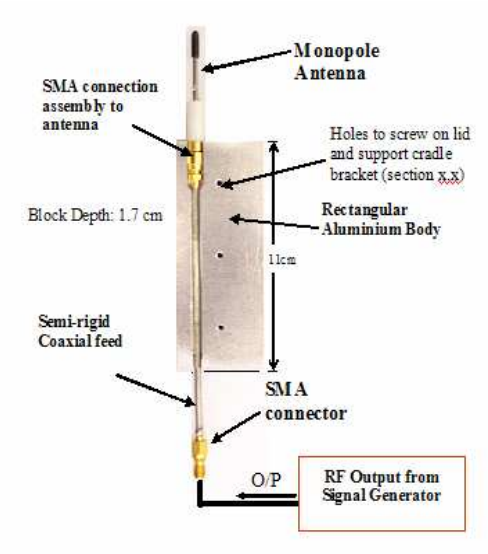

Figure 3.3.: The exposure device is shown with the back cover removed to reveal components which are clearly marked.

Australia (EMC technologies). With a peak input power of 276 mW, a 10g averaged Peak SAR of 1.56 W/kg is achieved at the base of the handset's antenna which corresponds to the left ear region of the SAM phantom.

3.2.5. Data analysis

For the spectral analysis, data were epoched into 2 second segments and analysed in the Matlab environment, using EEGLAB [39]. Epochs were baseline corrected over the entire epoch. Segments containing data greater than +/-60 μV were automatically rejected. On average 67% of the data were retained. To obtain relevant EEG bands, processed epoched time series were passed through a Fourier transform (Hamming window) with a window size of 2 seconds with no overlap. Subsequently, the following EEG bands were extracted: δ (2 - 4 Hz), ϑ (4.5 - 7), α (7.5 – 13) and β (13.5 - 32). For each band, the maximum spectral power (POWER) is calculated. For the ApEn

analysis, 8 artifact free (rejection criteria as above) consecutive seconds for each 7 minute period were retained and subsequently analysed in the Matlab environment.

Two Statistical Analyses were performed with SPSS statistical package version 11.5:

Fourier analysis

The first analysis involved measures of Fourier Power Spectra of recorded EEG time series. It was based on the comparison of recordings collected before and after the real exposures, a difference value, with that collected before and after the sham exposure (again expressed as a difference value). For each channel the difference value is obtained by subtracting the 'after' radiation power spectra from the 'before' radiation power spectra. A positive result would indicate an increase in the relevant amplitude level, and a negative would indicate a decrease. Electrodes were grouped (by averaging) in pairs in order to reduce the amount of statistical comparisons. Electrode groups were: Left Prefrontal (LPF = mean (Fp1, F7)), Right Prefrontal (RPF = mean (Fp2, F8), Left Frontal (LF = mean (F3, T3)), Right Frontal (RF = mean (F4, T4)), Left Central (LC = mean (C3 & T5)), Right Central (RC = mean (C4, T6), Left Posterior (LP = mean (P3, O1)) and Right Posterior (mean = (P4, O2)). Statistical significance was tested with Repeated Measures Analyses of Variance (RM-ANOVA) for each of the four predefined EEG bands. Each RM-ANOVA consisted of three within subjects factors; Exposure Source (SRC: Sham, PM RF and CW RF), Laterality (LAT: Left and Right hemisphere) and Sagittality (SAG: Prefrontal, Frontal, Central, Posterior). Where significance was observed, appropriate post hoc tests were conducted with Bonferroni corrections.

ApEn analysis and theory

Non linear analysis The second method of analysis was based on ApEn measures, a statistical measure of complexity that can be applied to any kind of finite time series with a minimum data length of 50 samples. It has been used on the analysis of human EEG data in relation to Alzheimer's

disease [10], epilepsy [74] , hypobaric hypoxia [108] and sleep [21, 22].

Theoretical background ApEn represents the mean probability that temporal sections (of length m) of a time series which are 'close' to each other (where 'close' is any distance smaller that a threshold distance r), will remain close for the temporal sections of incremental length m+1. The mathematical realization of the algorithm is presented in Appendix A.1.

ApEn data analysis The ApEn measures were calculated using Kaplan et al.'s implementation in the Matlab environment [75]. Although it was developed and used for Heart Rate Variability, its use extends for any kind of information series.

Data was first passed through artifact rejection based on the same criteria as the ones used for the Fourier analysis. A data length of 2048 consecutive points, free of artifacts, equivalent to 8 seconds, was retained for each 7 ½ minute period and was then submitted for ApEn analysis. Consistent with Pincus, we choose an embedding dimension, 'm', equal to 2 and a filter factor, 'r', equal to 0.2 times the standard deviation of each 8 second interval [111]. To verify the correct performance of the algorithm i.e. increasing ApEn value with corresponding increase in mathematical function complexity we submitted functions of increasing complexity through it. Increasing ApEn values were obtained which demonstrates the efficacy of the algorithm, (see Figure 3.4). A One-Way Repeated Measures Analysis of Variance (RM-ANOVA) was performed on the difference values ('after' minus 'before', 2 channel averages for each brain region as defined in the FFT analysis) of ApEn measures obtained using the same within factors that were used for the Fourier Spectral analysis (SRC, LAT, SAG).

Non linearity Test To demonstrate that recorded EEG time series contain non-linear features, a non-linearity test which is based on surrogate analysis was performed. The original time series was recreated in the form of surrogate data using the Amplitude Adjusted Fourier Transform Method

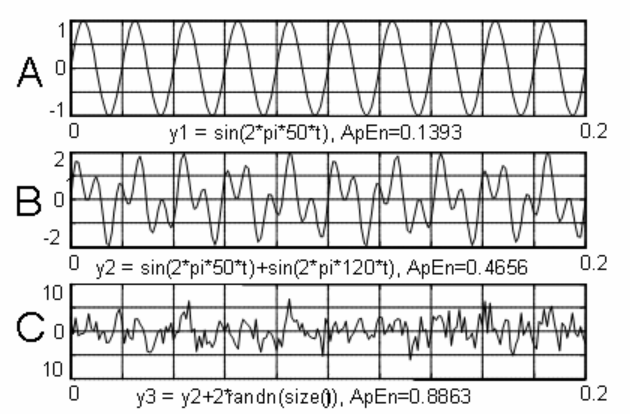

Figure 3.4.: Three different functions of increasing complexity are submitted through the ApEn algorithm (A: simple sinusoidal, B: two different frequency sinusoids algebraically added and C: function B but embedded in noise). The increasing ApEn value, from A to C, reflects the relative increase in signal complexity.

(AAFT). This method calculates and retains the Fourier amplitude spectra of the original time series, randomizes the phase information, and finally performs an inverse Fourier transform to create a Surrogate series. This ensured that surrogates are restricted in terms of linear properties of the original data, but were otherwise random, see Figure 3.5 and 3.6. Ten surrogates were created for each 8 seconds of data and the respective ApEn was calculated. It is noted that a complexity analysis can be performed on the data without evidence of non-linearity but any differences between real and surrogate data would not necessarily insinuate the presence on non linearity.

A t-test was performed on each real data series against its ten surrogates. With 9 degrees of freedom and a significance level of 0.05, a critical value of t=2.26 was obtained.

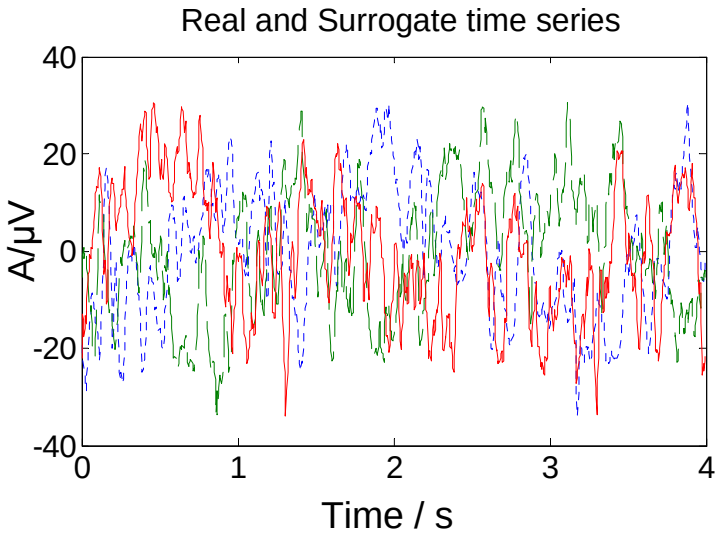

Figure 3.5.: Four seconds of real (dotted blue line) and surrogate data (solid red and green lines) are depicted here. It is evident that in the time domain signals are different.

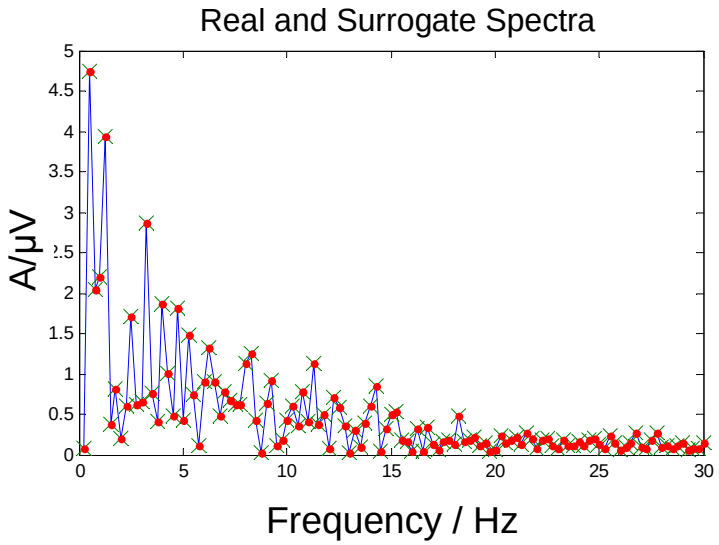

Figure 3.6.: Real (dotted blue line) and Surrogate data (red dots and green crosses) have identical spectra even though their time domain equivalent signals were different.

3.3. Results

3.3.1. Fourier Power Spectra

For the main factor SRC, significance was observed in the delta band ($p = 0.034$) only. Post hoc tests for the factor SRC in the delta band showed that neither Sham compared to PM RF ($p=0.502$), nor Sham compared to CW RF ($p=0.087$), reached the Bonferroni-corrected significance level (alpha = 0.002). For each EEG band, no significant effects or interactions were obtained for SRC with SAG, LAT, or SAG by LAT, see Table 3.3.1. Mean power spectra are shown in Figure 3.7 and topographies of grand mean spectral powers for before and after exposure periods are shown in Figure 3.8.

Band	Factor or Factor Interaction	Significance (p)
Delta	SRC	0.038*
	SAG*SRC	0.363
	LAT*SRC	0.238
	LAT*SAG*SRC	0.608
Theta	SRC	0.557
	SAG*SRC	0.809
	LAT*SRC	0.213
	LAT*SAG*SRC	0.746
Alpha	SRC	0.435
	SAG*SRC	0.149
	LAT*SRC	0.103
	LAT*SAG*SRC	0.366
Beta	SRC	0.700
	SAG*SRC	0.549
	LAT*SRC	0.917
	LAT*SAG*SRC	0.447

Table 3.1.: A Summary of the RM-ANOVA results of the small sample size study. The factor SRC for the delta band is the only one that reached significance but post hoc contrasts did not reveal any statistically significant differences at the Bonferroni-corrected alpha level.

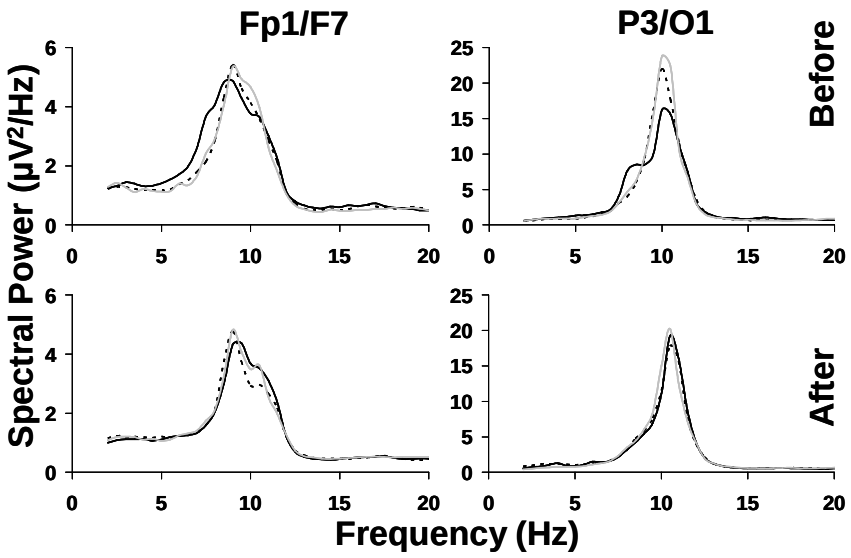

Figure 3.7.: Grand mean, n=12, EEG spectral power before (top) and after exposure (bottom) are shown at frontal and occipital regions ipsilateral to exposure. Sham exposure; solid black line, PM RF exposure; dashed black line and CW RF exposure; solid grey line.Despite the large difference between active and sham exposures at occipital sites, these were not statistical significant. The large variance that is observed in the sample can explain the absence of effect.

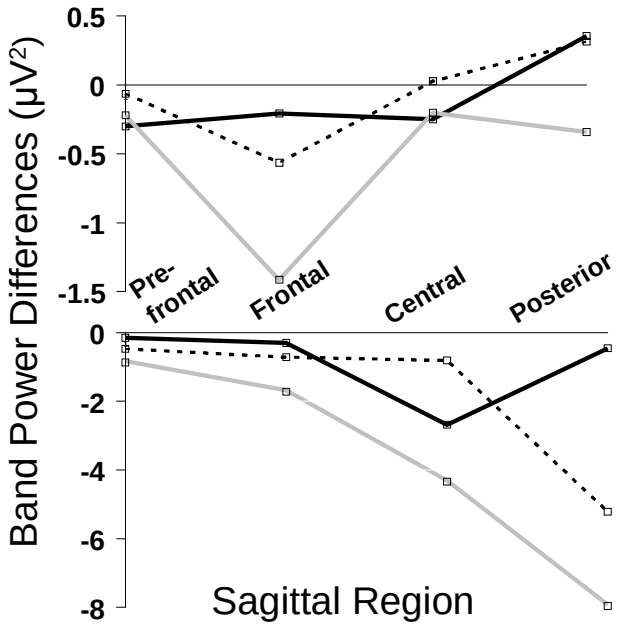

Figure 3.8.: Band Power differences, ('after' minus 'before'), on the y-axis for Sagittal values on the x-axis for Sham (solid black line), PM RF (dashed black line) and CW (solid grey line) conditions. Top graph for delta band and bottom for alpha band, both for left hemisphere (ipsilateral to exposure).

3.3.2. ApEn analysis

Non linearity tests based on the method of surrogate analysis showed that in total 80% of cases contained statistically significant non linear features. One subject specifically showed no evidence of non-linearity in all of its recorded intervals, accounting for the bulk of the data that failed the surrogate test. No significant difference was obtained for any of the factors or their interactions, see Table 3.2. Mean ApEn values are shown in Figure 3.9.

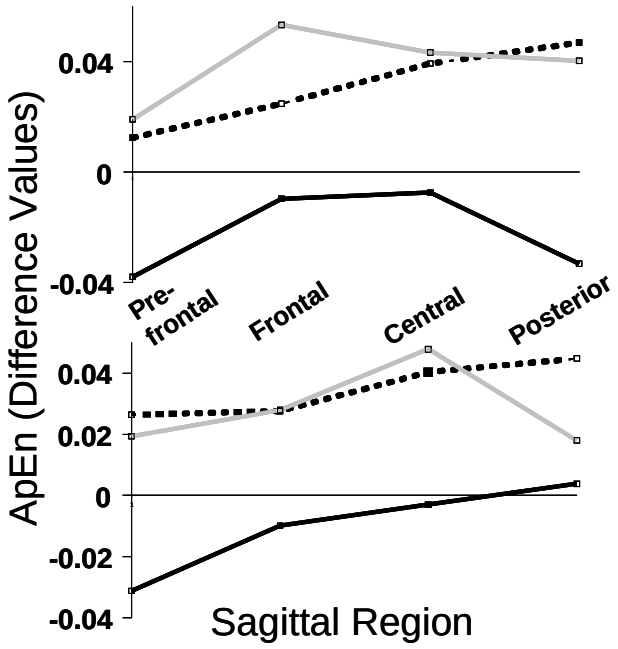

Figure 3.9.: Means of ApEn difference values on the y-axis with Sagittal regions on the x-axis. Sham (solid black line), PM RF (dashed black line) and CW (solid grey line), Top panel: Ipsi-lateral to exposure and Bottom panel: contra-lateral to exposure.

Table 3.2.: 'p' values for the various factors and factor interactions of the ApEn analysis. None reached or approached significance

Factor or Factor Interaction	Significance (p)
SRC	0.581
LAT*SRC	0.952
SAG*SRC	0.412
LAT*SAG*SRC	0.461

3.4. Discussion

This study was performed with two aims. The first was to compare the possible effects arising from CW RF versus PM RF in an attempt to reproduce the results reported by Huber et al. [58], but using a radiation exposure distribution more closely resembling that of a GSM mobile phone handset. The secondary aim was to investigate the usefulness of a non-linear analysis method, the ApEn.

We failed to replicate the reported alpha band activity increases during resting wakefulness under PM RF monopole exposure with the conventional Fourier analysis method. The only significant factor was SRC ($p = 0.034$) for the delta band, but post-hoc tests did not reveal any statistically significant changes at the Bonferroni-corrected significance level. Delta band changes have been previously reported on at least one occasion [34]. The ApEn method did not reveal any statistically significant differences in the EEG with relation to the exposure condition.

The use of the ApEn analysis method provided the opportunity to investigate the non-linear features of the recorded EEG data and any correlation with the RF exposure. It is difficult to determine whether this represents a lack of advantage of the ApEn measure over FFT, or whether differences between the methods may have been masked by the lack of any significant effect. For instance, it is possible that the effect sizes for both methods were too small to be detected with the current sample size, with larger sample sizes required to clarify this issue. Three factors are identified

which may have contributed to the inconsistency between findings in the present study and those reported in Huber et al. [58]. Firstly, the difference in SAR distributions between the two antennas could have been a contributing factor. The patch antenna source used by Huber et al., covers exposures for all possible mobile phone locations relative to the brain simultaneously (equivalent to superimposing exposures from more than one handset) [58]. The homogeneity of exposure results in overexposure of areas deep in the brain, which could possibly be more vulnerable to external stressors such as RF and thus result in an enhanced effect. In support of the above, the effect in Huber et al. [58] was shown with a smaller sample size, n= 15, than the effect reported by Curcio et al. and Croft et al.(sample sizes of 20 and 120 respectively), with the latter researchers employing a realistic exposure which would produce a lower exposure in deep brain regions [36, 35]. In addition, Curcio et al. and Croft et al. report effects during radiation but not after, as opposed to Huber et al. who report a post exposure effect larger than the during exposure effect of Croft et al. and Curcio et al. It may be speculated that the patch antenna exposure of Huber et al. produced an effect that lasted longer than the effect from the monopole exposure.

Secondly, the exposure duration herein was 15 minutes as opposed to Huber et al. who used 30 minutes. More time would allow for a cumulative process, if one exists, to enhance the effect under the longer exposure, thus justifying the observed effect under the Huber et al. protocol as opposed to the protocol used here. On the other hand effects have been previously demonstrated with exposure lengths of 15 minutes and smaller , (see references [116, 38]), a fact that makes the above argument a less likely explanation for the observed discrepancy. A third factor is that of possible carry-over effects since exposures took place in the same day. This may have increased error variance and reduced the chance of identifying a real effect.

Finally, when comparing the results of Curcio et al., and Croft et al., with those of Huber et al., we observe that the former two made use of the 217 Hz modulation and 1736 Hz only, whereas latter made use of a DTX like spectrum (2, 8, 217, 1736 Hz) [58, 36, 34, 35]. Thus if the 2 and 8Hz

components contributed to the increase in alpha, this would be another factor that could account for the larger effect size observed by Huber et al. [58].

Based on the assumption that the effect expected from a monopole antenna would be of a smaller effect size in comparison to that from a large patch antenna, and given that the small sample size of the present study has limited interpretation, we will now conduct a study with a substantially larger sample size in order to compare CW and PM RFs, with exposure distributions resembling those from real mobile phones. In conclusion, this study failed to replicate the findings of Huber et al. [58]. Possible reasons for this have been identified, with the main reason argued to be the difference between the homogeneous exposure of Huber et al. and the monopole exposure of the present study. That is, although in homogeneous exposures (e.g. patch antenna source) the modulation content has been shown to be important in affecting the resting EEG, the same may not be true for more realistic exposures such as the dipole source used here. In addition, the exploration of a non linear feature of complexity of the EEG did not produce greater clarification of this issue.

3.5. Limitations and Future improvements

As stated in the introduction of this Chapter the main function of this small sample size study is to identify methodological flaws and limitations. These can subsequently be addressed before recruiting large sample sizes thereby avoiding unnecessary wastage of resources. In this section we discuss the identified limitations and their implications. In conjunction corresponding improvements to experimental methodology are presented.

3.5.1. EOG correction

There are two methods with which eye movement artifact can be accounted for in EEG recordings. First is the method of EOG rejection where data consisting of large amplitude artifacts are excluded from analysis. Second is the method where voltages generated by eye movement are recorded;

subsequently portions of those recorded values are subtracted from the EEG thereby minimizing data rejection. In the present study, EOG was recorded by a single channel placed under the eye (VEOL) which was used for rejection purposes (note that EOG channels are not essential for eye movement rejection but more accurate results can be achieved with them). Although eye movement rejection is an acceptable method of dealing with eye movement artifacts, correction is considered a more robust method [33]. There are three ways with which artifact rejection can negatively influence the experimental outcome. First, even after artifact rejection some eye movement contribution, mainly the one under the threshold voltage of rejection remains in the data. In the already noisy environment of the EEG and considering that the purported effect under investigation is particularly small, it is obvious that any extra noise contribution could add enough to variability to prevent detection of effect. With EOG correction this source of noise contribution is minimized. Second if recordings suffer from excessive eye movement artifact, which can be quite common, rejection can leave too few epochs from which to extract meaningful spectral averages. In addition, when such averages arising from much smaller sample populations are compared to those from recordings with typical amount of epochs, then the difference between the two again would introduce bias to the data set. Finally, under certain circumstances, rejection can lead to biased sampling due to the link between cognition and eye movement [13]. For example, if a cognitive process has an impact on eye movement parameters and is also affected by radiation exposure, then the radiation related effect will remain undetected upon eye movement-artifact rejection. Due to the reasons stated above it is concluded that EOG correction as opposed to rejection would be a better approach to dealing with eye artifacts in these experiments.

3.5.2. Noise susceptibility of EEG recording hardware

In this small sample size study, two issues arise due to the susceptibility of the EEG amplifiers to the GSM-like electromagnetic fields. These are prevention of double blinding and EEG signal

contamination

The main component of any EEG recording system is its amplifiers. These detect and amplify voltage differences between two electrodes. In this specific case the MINDSET MS-1000 uses an amplification of 90 dB. Such large amplification is required for detection of the small amplitude brain signals when recorded at the scalp. Any noise within the amplification range of frequencies will also be amplified. As a result, the recorded signal will be contaminated. The exposure source, in this case a mobile phone handset, transmits electromagnetic fields that are of pulsed nature. The RF fields are pulse modulated with the DTX components which happen to overlap with parts of the EEG spectrum (refer to Chapter 1 and 2). As a result brain signals during PM RF but not during CW RF exposure were contaminated rendering EEG data unusable, see Figure 3.10. To obtain reliable data during PM RF exposures suitable measures need to be taken to shield the EEG equipment.

If the PM RF noise is visible in the EEG recording, as was the case in this study, then double blind conditions cannot be enforced since the experimenter would be aware of the status of the exposure (for the importance of double blinding refer to Chapter 2). Suitable methods of addressing this source of noise were discussed in Chapter 2. Further discussions and shielding demonstrations are presented in Chapter 5.

3.5.3. Sample size

This study purposefully recruited only a small sample size study for reasons stated in the introduction of this chapter. Since studies have generally shown that effect sizes are small it is crucial to employ large sample sizes to obtain more meaningful statistics.

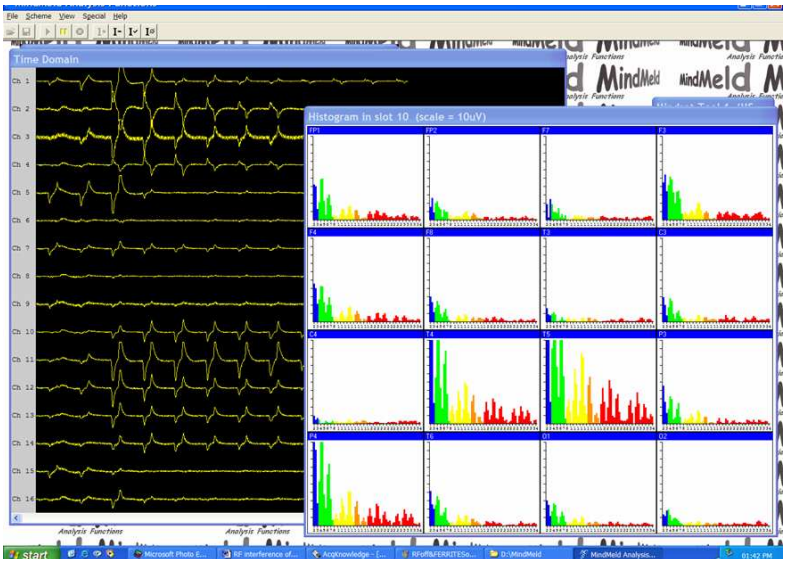

Figure 3.10.: The influence of RF generated noise on the MINDSET EEG amplifier is visible in most channels. Apart from rendering the recorded data unusable the double blind nature of the experiment is inevitably broken.

3.5.4. Verification of radiation emission from handset

To verify presence of radiation emission, a test sequence at the start of each experimental session was used. In this, the signal generator and amplifier system were set to transmit and their performance was monitored through a spectrum analyzer, Figure 3.2. With this method we can be fairly sure that transmission is indeed taking place provided that the handset device is attached correctly to the output of the amplifier and that no mechanical damage has occurred on any of the cables between the time of running the test sequence to the actual start of the experiment.

As an improvement to this methodology, and to avoid the latter possibility, another approach is suggested below that allows testing the actual transmission of electromagnetic energy from the handset itself. This would be a two step process where first,the test sequence is run as described above where the correct amplifier output is verified. Following that and while the test sequence is running we use a Diode Detector connected to CRO system to detect the RF signal and verify its presence visually. The exact position under which the mobile phone handset is placed during the experiment can be replicated in this test sequence thereby ensuring that for the actual experimental arrangement radiation emission indeed takes place. Performing the same procedure at the end of the experimental session provides with sufficient confidence that the nominated exposure occurred during the experiment.

3.6. Conclusion

In conclusion, this study failed to replicate the findings of Huber et al. [58]. Possible reasons for this have been identified, with the main one argued to be the difference between the homogeneous exposure of Huber et al. and the monopole exposure of the present study. That is, although in homogeneous exposures (e.g. patch antenna source) the modulation content has been shown to be important in affecting the resting EEG, the same may not be true for more realistic exposures such

as the dipole source used here. In addition, the exploration of a non linear feature of complexity of the EEG did not produce greater clarification of this issue. Due to the small sample size employed, the results should be viewed with caution. Therefore an extended, larger sample size study is suggested. In addition, methodological improvements for any future studies have been extracted from this study which will now serve as a precursor on which future ones will be based. These are management of EOG artifacts, noise susceptibility of EEG recording hardware, sample size and verification of exposure with sufficient confidence.

The next chapter describes a large sample size study that employed 72 participants. The implementation of the improvements that were suggested in this Chapter are also described.

4. Exposure Device - Modeling and Construction

4.1. Introduction - The need for a new exposure device

The principal aims of this thesis is to determine whether GSM-specific EMF radiation is capable of causing any measure able change in the human resting EEG. To achieve this objective, the possible stressor to be applied , RF or ELF, must be as closely related to real GSM exposures as possible. To this extend, a set of exposure criteria were defined in Chapter 2 (applicable to both RF and ELF), which if implemented can render the outcomes of studies directly applicable to GSM mobile phone use. First the intensity of the electromagnetic stressor must be such that it represents adequately the real exposures. Since exposures in the head and neck area are also limited by the exposure standards the maximum allowed intensity as found in those standards can be used. For the head and neck area at RF frequencies a maximum exposure of 2 W/kg is specified and is the one to be used here. Second the spatial distribution of the electromagnetic stressor must also be representative of real mobile phone exposures. It must therefore be highly localized and within the exposures hemisphere only. Third, the frequency content of the exposure must also be carefully selected since specific modulations of RF signal has been linked with changes in brain function. Although real handsets satisfy these criteria, they do not allow for selective RF or ELF exposures since one generates the other. As such, real handsets cannot be used for the exclusive assessment of the RF or the exclusive assessment of the ELF radiation. In addition, real handsets can produce auditory or thermal cues that can give away the status of operation and influence the outcome of experiments. There are

examples in literature where RF GSM-specific exposure setups have been suggested but no such examples exist for ELF exposures[1]. Therefore the need for a new exposure device arises, one that must satisfy the predefined criteria but also allow for RF and/or ELF exposures to occur selectively.

The predefined criteria can be easily employed for RF exposures since the RF radiation characteristics are well understood. The same however does not apply to ELF exposures. Although recently characterized to some extend, they have yet to be used in any human biological experiments. As such, suitable exposure setups are currently unavailable. To design one, first the nature and characteristics of the radiation need to be defined.

This chapter covers the experimental procedures and results for the characterization of this ELF field, producing an equivalent model for it, and verifying the performance of the model experimentally. The design and construction of the new exposure device, implementing the equivalent model is also presented. This device is capable of producing the RF and ELF components of GSM handset emissions, replicating them according to the criteria defined in Chapter 2. The two radiation sources can emit simultaneously or independently. Finally input power levels to the handset, for which desired exposures are achieved for both RF and ELF, are determined and validated through computational models. A short literature survey precedes the experimental procedures and results, in which existing exposure setups as well as any other relevant data regarding exposures are discussed.

4.2. Literature survey

4.2.1. ELF emissions from GSM handsets

The articles reviewed in this section attribute the generated magnetic fields to the varying current flow within the handset. This concept originates from Faradays Law, $\nabla \times E = -\frac{\delta B}{\delta t}$, which states

[1] An exception exists in the study of Tuor et al.[132], but that setup does not satisfy the exposure criteria defined in here.

that a changing electric field, (that is the current flow inside the handset), induces a changing magnetic field.

Linde et al. reported crude measurements of GSM-emitted ELF fields [87]. They measured the frequency spectrum between 40 and 800 Hz using a commercial magnetic flux density meter. Peak magnetic field values were approximated through current values that were simultaneously recorded across the battery terminal of phones. The maximum rms value recorded was 1.8 μT which was then scaled according to the rms to peak current ratio to give a peak field of 5.2 μT. As these values are recorded at a certain distance away from the handset, it is expected that field values would be much higher at distances closer to the handset, however such assessment was not performed.

In a more detailed technical report by Tuor et al., different methodologies were used to measure ELF components [92]. An equivalent source was proposed, and extrapolated maximum field values were contrasted with the ICNIRP guidelines [2]. The low frequency components, down to 8.3 Hz, were also identified. A model radiation source is also proposed as an equivalent source that can account for this radiation. Extrapolated peak values range from 25 to 75 μT and in most cases, 4 out of 5 investigated handsets, some of the harmonics exceeded the relevant ICNIRP guideline limits [2]. Despite proposing an equivalent source for the ELF radiation, an exposure device that employs a different field distribution is suggested for use in ELF experiments. This is a Helmholtz coil setup capable of more homogeneous fields as opposed to the highly localized ones that are associated with GSM handsets. Using this setup, the field gradients are removed from the exposure, and therefore their influence cannot be assessed. In addition, deeper brain structures are exposed to higher field intensities than those expected from GSM handsets. Therefore the exposure setup proposed by Tuor et al. does not fulfill the criteria defined here. The Helmholtz coil setup is perhaps more suitable in radiation specific (generic) investigations as opposed to source specific (GSM handset-like) investigations.

In a study attempting to obtain the ICNIRP exposure ratios resulting from GSM-ELF exposures,

through means of computational models, Jokela et al. used a circular current carrying loop to model the exposure source [72]. A loop of a 30 mm radius is chosen as the exposure source in this computational model. The choice of radius is clearly important, as is highlighted by the results of Jokela et al., since it affects the amount of exposed tissue[2]. The current values applied to the loop model were those determined from the measurement of five real GSM handsets. A maximum ICNIRP ratio of 28% is reported whereas the equivalent IEEE ratio is reported to be ten to twenty times smaller. The results of Jokela et al. clearly support that even though the magnetic field at close proximity to the equivalent loop source (5 - 25 mm) might be considerably higher than the ICNIRP reference levels , basic restriction levels are not violated.

The exposure ratios reported by Jokela et al., (see reference [72]), are found to be overestimated by a latter study [64]. The basic restriction ICNIRP ratio in this paper was estimated between 0.036 - 0.041. The authors attribute the difference to the simplistic head model that was used by Jokela et al., as opposed to the anatomically realistic model of human brain [64]. The authors chose to use the GSM handset that displayed maximum fields in the Jokela et al. study therefore addressing a 'worst case' scenario.

The cited works looked at exposure levels from the perspective of the limits define in standards [2]. Since they are found to comply, there is sufficient confidence that none of the established mechanisms of interaction with biological tissue are applicable to GSM-like ELF exposures since limits in the relevant standards are set specifically to guard against these. However, the need to investigate for possible low-level effects remains. The aforementioned studies are of great value to such investigations because the characterizations of fields are indispensable in the design of dosimetrically accurate ELF exposure setups. The ELF measurements reported in this Chapter build on the results of the studies that have been introduced above.

[2]The ICNIRP guidelines, see reference [2], require the current to be averaged over surfaces of 1 cm^2 a fact that will also lead to increased dependency of exposure ratios to the radius of the loop. Note also that the possible loop radii for different handsets are confined to the dimensions of GSM handsets. Therefore the selection of 30 mm radius can most likely be considered as representing the larger GSM handsets rather that average ones.

In the following section, some aspects of GSM-like RF exposures that are relevant to the design of the new exposure device are discussed.

4.2.2. RF emissions from GSM handsets

Both technical aspects, (see references [81, 82]), as well as the biological effects of RF exposure have been covered extensively in literature [51, 29, 26, 133]. Studies have been conducted where the influence of GSM like radiation on a variety of human physiological variables (resting EEG, event related EEG, skin impedance, heart variability etc) was investigated (see Chapter 2).

Earlier studies exposed human volunteers using GSM handsets that were operating in normal GSM networks, (for example see [34]). Such practice is not sufficient since exposure levels remain largely uncharacterized. With unknown intensity of the possible stressor, a relationship between exposure dose and effect cannot be reliably established. At the extreme, it could be argued that the radiation levels exceeded those defined in the ICNIRP guidelines, and therefore observed effects could be irrelevant, and may be attributed to the already established thermal interaction mechanism. Other studies have utilized software controlled GSM handsets enabling constant exposures throughout experiments, and providing dosimetric estimates, (for examples see [36, 50, 35]).

Although software controlled handsets eliminate the uncertainty with regards to exposure dose, they pose as a confounding factor with regards to blinding, where neither the experimenter, not the subject should be aware of the experimental conditions. Assuming that the screen and speaker of the phone have been deactivated, GSM handsets can still produce thermal or auditory cues, arising from the operation of the battery and the electronics, which can give away the status of operation. Under these circumstances double blind conditions might be compromised because either the subject or the experimenter are now aware of the GSM phone's state [50].

To address this, D'Costa et al. created a model handset that can simulate the radiation of a GSM phone [38]. The confounding factors of thermal or auditory cues are removed since no electronics

are part of the handset. Radiation power levels can be controlled by varying the input power. The specific handset however carries a monopole antenna which is not representative of newer GSM handset antennas. Current models of GSM handsets carry internal mobile phone antennas which are mainly PIFA, patch antennas, printed monopoles and dipoles [76].

Other researchers have avoided the use of GSM handsets as well. Some examples are the studies of Huber et al. (see references [58, 57, 59]), and the more recent studies of Regel et al., (see references [115, 114]), which have opted the use of large planar antennas. Even though the confounding factors of auditory and thermal cues are eliminated, as discussed in Chapter 2, the SAR distributions obtained by such exposures vary considerably when compared to those from real GSM handsets so are not representative of real exposures.

To address the blinding concerns, and produce exposures that are representative of current GSM handsets, patch internal antennas such as those found in newer GSM handsets are considered for the design of the exposure device presented here. In the next Section the construction and characterization of the ELF and RF sources are presented. But first requirements for the model handset are defined.

The proposed handset must:

- Replicate ELF exposures in terms of intensity, spatial distribution, and frequency content.
- Replicate RF exposures in terms of intensity, spatial distribution, and frequency content.
- Allow for RF and ELF exposures to take place simultaneously or independently, thereby providing with more flexibility with regards to the endpoint that is to be examined (e.g. is it one of the exposure sources that are producing observed biological effects or is it the combination of the two?).
- Allow for operation under double blind conditions

- Resemble real GSM handsets in its physical appearance so as to preserve ecological validity.

4.3. Simulation of GSM ELF magnetic fields

The reason for characterizing the ELF emissions of GSM handsets, as stated previously in Section 4.1, is to develop an equivalent source model that can reproduce the ELF emissions. Here we present experiments designed to characterize the frequency spectrum, time domain characteristics, and spatial distribution of ELF emissions. These data are used in the modeling of the source. We hypothesize here that the magnetic field radiator structure of GSM handsets can be approximated by simple loop antennas. Small loop antennas are also used for detection of the magnetic fields in question. Measurements that verify this assumption, as well as results that achieve the above two objectives are presented[3].

4.3.1. Materials, Theory and Methods

4.3.1.1. Materials

A software controlled Nokia 6110 handset was used to obtain ELF magnetic field measurements. It was set to transmit at the maximum permissible power level of 2 W (RMS peak). Magnetic fields around the mobile phone handset were measured with two purpose built, single axis, shielded loop probes (The necessity for two Probes is explained in the Theory and Methods section). Probe 1 was a small diameter loop, (34 mm), providing good spatial resolution of the 217 Hz main spectral component. The time domain characteristics of the pulse were measured with a larger diameter, (127 mm), loop probe, Probe 2, having a flat frequency response from 20 Hz to 70 kHz, (+/-1 dB). A balanced amplifier (INA 118, Burr-Brown with voltage gain set to 30 dB) was used for amplification of voltages across Probes 1 and 2. To minimize RF interference, coaxial cables were

[3]Large parts of this work has been published by Perentos et al. in the Australasian Physical & Engineering Sciences in Medicine Journal, see reference [104].

oriented orthogonally to the mobile phone's monopole antenna, cable sheaths were ferrite loaded and the amplifier system was shielded and grounded. Except as noted, the output of the loop-amplifier system was fed to a Spectrum Analyzer, (Tektronix DSA 8566B, freq range 20 Hz – 2 GHz). To obtain components below 20 Hz, another Spectrum Analyzer was used with an operating frequency from DC to 100 kHz, (HP Agilent DSA 3562A).

4.3.1.2. Theory and methods

Response of an electrically small magnetic field loop probe Faraday's law of induction states that the line integral of the electric field around a closed loop is equal to the negative of the rate of change of the magnetic flux through the area enclosed by the loop.

$$\oint_l E \cdot ds = -\frac{d}{dt} \int_S B \cdot dS \tag{4.1}$$

The same field acting on a loop composed of a perfectly conducting thin wire and opened at an end will produce a frequency dependent open circuit voltage given by (assuming $e^{-j\omega t}$ time convention):

$$V_{OC} = -j\omega \int_S B \cdot dS \tag{4.2}$$

V_{OC} = the open circuit voltage (V)

B = component of the magnetic flux density normal to the plane of the loop (T)

S =πr^2 , the area enclosed by the wire loop, where r is the loop radius (m^2)

ω = angular frequency (rad. s^{-1}).

Provided that the field is uniform within the area enclosed by the wire loop, the voltage developed across it can be given by

$$V_{OC} = -j\omega B_n S \tag{4.3}$$

where B_n represents the field component of B that is normal to the plane of the loop. It is evident from Equation 4.3 that for a sinusoidally varying magnetic field of a known angular frequency ω, the open ended voltage measured across the wire loop is directly proportional to the normal component of the magnetic flux that intersects the loop. The relationship defined by Equation 4.3 applies to single frequency sinusoidal fields.

To allow for broadband field characterization using loop probes the impedance of the sensor/amplifier system needs to be manipulated in such a way so as to establish a constant response throughout the frequency range of interest. This constant response, preserving the relative amplitudes and phases of individual spectral components, allows the time domain characteristics of a pulsed magnetic field to be measured. A constant frequency response can be achieved by placing a load at the terminals of the loop which is purely resistive and sufficiently small [126]. To determine the appropriate loading impedance, consider the equivalent circuit of the electrically small loop probe shown in Figure 4.1. The output voltage is given by:

$$V_{out} = V_{OC} \frac{Z_{load}}{Z_{loop} + Z_{load}} \tag{4.4}$$

For $Z_{load} = R_{load}\, and\, Z_{loop} = 2\pi f L_{loop} + R_{loop}$

$$V_{out} = \frac{j\omega BSR_{load}}{j\omega L_{loop} + R_{loop} + R_{load}} \tag{4.5}$$

For frequencies where

$$j2\pi f L_{loop}| \gg R_{load} + R_{loop} \tag{4.6}$$

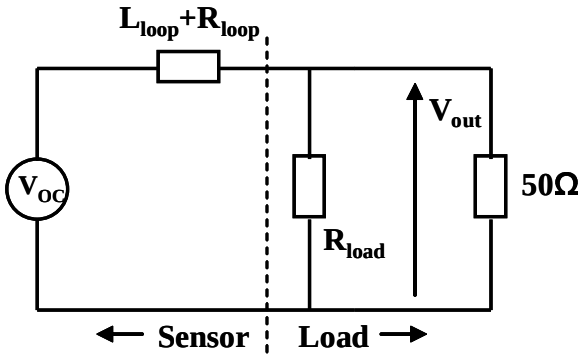

Figure 4.1.: Equivalent circuit of an electrically small loop probe terminated with a load impedance Z_{load}. The loop consists of an inductance L_{loop} and resistance R_{loop}.

the expression for the output voltage reduces to

$$V_{out} = \frac{BSR_{load}}{L_{loop}} \tag{4.7}$$

The frequency dependency is thus eliminated. The region over which the response of the probe is flat (independent of frequency) extends from $f_{co} = (R_{load} + R_{loop})/2\pi L_{loop}$ to an upper frequency f_{up} where the probe may no longer be electrically small, or 'its response is influenced by parasitic components (e.g. inter-winding capacitance for a multi-turn loop). For Probe 2, a flat frequency response was achieved from $f_{co} = 20$ Hz to $f_{up} = 70$ kHz with a +/-1 dB variation.

Measurement method To achieve accurate measurements of magnetic fields with a loop probe, Equation 4.3 needs to be satisfied. This is physically achieved by keeping the probe dimensions small enough so as to detect homogeneous fields. However, according to Equation 4.3, V_{OC} depends on the surface area of the loop probe. As such a small probe would produce a small voltage response and since higher harmonics of the broadband pulse will be small, the small signal to noise ratio would not be sufficient to reliably detect them. It becomes evident that a reliable measurement of broadband fields that are spatially confined in small areas cannot be achieved with a single probe.

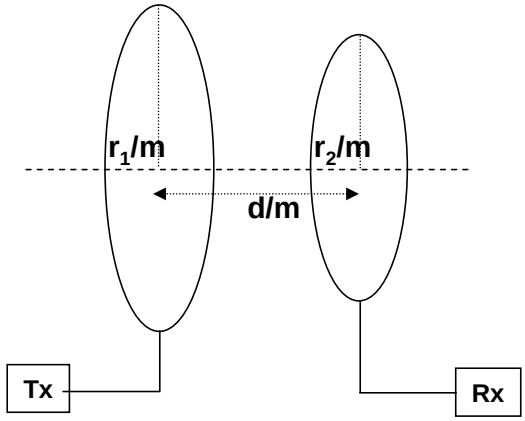

Figure 4.2.: The ELF calibration setup. The two loops are separated by distance 'd' and are positioned in a coaxial configuration. This is also equivalent to the setup for the detection of the mobile phone handset magnetic field, where Tx would reside inside the handset.

The problem can be resolved by combining readings from two probes, where the first, Probe 1, is optimized for spatial resolution and the second, Probe 2, for broadband signal pickup. Data from the two probes are used in conjunction as follows: With the amplified output of Probe 1 fed into the Spectrum Analyzer, the real magnetic field value of the strongest 217 Hz spectral component of the broadband pulse can be reliably obtained with minimal spatial averaging error. The flat frequency response of Probe 2 provides the relative amplitudes (but not absolute) of the majority of the frequency components that make up the broadband pulse. A scaling factor can be established from which the Probe 2 reading of the 217 Hz component can be converted to a real amplitude value based on the known 217 Hz spatial peak value that has been measured using Probe 1. This scaling factor will also be applicable for all the frequency components recorded by Probe 2 owing to its flat frequency response. The broadband pulse can then be scaled according to this factor to give the true pulse peak.

Probe calibration Probe 1 was calibrated according to the standard field method where the loop probe to be calibrated, (Rx), was placed in a coaxial configuration, Figure 4.3.1.2, with the Tx loop, which transmitted a field of known intensity [47]. Using Equation 4.8 for a spatially averaged field in the plane of the receive loop, we calibrated its response to a 217 Hz sinusoidal signal, and determined an antenna factor, which is the ratio of the magnitude of the average 217 Hz magnetic field $|\mathrm{H}_{av}|$ to the measured voltage in the receive loop probe. As errors in magnetic field measurements arise because a loop probe measures the spatial average of a magnetic field, (see reference [65]), the 'true' field at the center of the loop for a coaxial arrangement can be estimated using Equation 4.8 by setting $r_2 = 0$.

$$|H_{av}| = \left[1 + \frac{15}{8}\left(\frac{r_1 r_2}{R_o^2}\right)^2 + \frac{315}{64}\left(\frac{r_1 r_2}{R_o^2}\right)^4\right]\sqrt{1+\beta^2 R_o^2} \tag{4.8}$$

where , I = transmitting loop current, rms (A)

r_1 = radius of transmitting loop, (m)

r_2 = radius of receiving loop, (m)

d = axial spacing between loops, (m)

β = wavelength constant and

$R_o = \sqrt{d^2 + r_1^2 + r_2^2}$

Since Probe 2 is only used to obtain time domain pulse characteristics (or relative spectral data), no absolute amplitude calibration was necessary. Instead, it was designed to have a flat frequency response within the frequency of interest so as to meet the conditions for Equation 4.6, i.e. small loop resistive impedance and a small load resistive impedance. Its frequency response was assessed with a setup that included a signal generator, set to generate 217 Hz pulses with rise time exceeding that of GSM handset pulses, connected to one end of a single turn loop (r = 150 mm). The other end of the single turn loop was terminated in a Cathode Ray Oscilloscope (CRO) which acted as a current measurement probe and as a 50 Ω termination load. The time domain characteristics of the

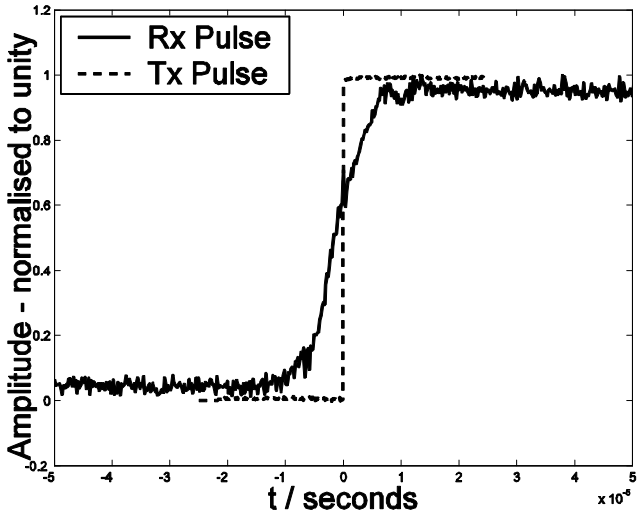

Figure 4.3.: Probe 2 is immersed in a pulsed field with rise time of 25 ns which is considerably higher than that of GSM pulses, rt $>$ 10 µs. The pulse is picked up as with minimal spectral distortion (rt = 5 µs). As the probe response exceeds any reported GSM-ELF handset rise times it is considered adequate for broadband pulse characterization, [72, 132, 64].

generated field, which are directly proportional to the loop current, were measured across the input of the CRO and compared to those picked up by Probe 2 – amplifier system. It is shown, Figure 4.3, that Probe 2 can pick up pulses with frequency content exceeding those of GSM handsets (20 Hz to 70 kHz), with virtually no loss of spectral-amplitude information.

ELF field pattern (polar coordinates) To substantiate the hypothesis that the ELF source of the mobile phone handset can be approximated by a current carrying loop, the magnetic field pattern of the mobile phone in polar coordinates was measured and compared with that of an ideal current carrying loop. The measurement was performed using Probe 2 at the fixed distance of 160 mm from the center of the handset.

Determination of Equivalent Source To calculate the characteristics of this transmitting loop, Equation 4.8 was used where r_1 defines its radius, d its distance from the receive loop (Probe 1),

I the current flowing in it, and r_2 the radius of Probe 1. In this case, the axial spacing d is made up of variable a, the distance of the loop source below the surface of the phone and b the distance of the loop probe from the surface of the phone (i.e. d=a+b). This approach is necessary since, to determine the position of the theoretical loop source, distance d needs to be adjusted in order to obtain a best fit between the measured spatial decay, and the theoretical decay of the model source. Since distance b is a real, measurable one, it cannot be adjusted, therefore, the variable a is introduced to perform this function.

From here on we refer to a, r1 and I as the fit coefficients. These are used to determine the equivalent source characteristics that would produce a match between the field that would be emitted by the theoretical equivalent source and the one that has been measured experimentally.

With the phone transmitting at full power, local maximums of magnetic field are observed on the front and back surfaces of the handset. From those points, measurements of magnetic field versus distance were then recorded along the 'x' direction, (see Figure 4.4).

Assessment of Discontinuous Transmission Mode (DTX) The below 217 Hz components, transmitted during DTX mode of operation of GSM handsets, were detected using the same Nokia 6110 handset, but this time operating in a real GSM network under forced DTX conditions. To obtain an indication of the percentage of ICNIRP guidelines present for frequency components overlapping with those of the human EEG, an assessment using the Weighted Peak Method (as outlined in an ICNIRP statement [1]) was performed in Matlab^{TM} (Mathworks) using the pulse characteristics defined in Table 4.3. First, the pulse with characteristics described in Table 4.3 was realized in Matlab^{TM} (Mathworks). A series of DTX frames was reconstructed, and was filtered with a first order high-pass filter (f_c = 800 Hz) so as to obtain the weighted peak equivalent [1]. The Fourier spectra of the time series were then calculated.

4.3.2. Results

A detailed uncertainty analysis for this experimental setup was performed. Uncertainties were calculated for all likely contributing factors, and were subsequently standardized and listed in Table B.1. The total expanded uncertainty in the pulse peak measurement was ±10.7% with a confidence level (CI) of 95%.

4.3.2.1. Evidence of a loop source

Measurements of the radial field component, Figure 4.5, were recorded for the φ (rotation around the z–axis with the origin as the center point) and ϑ (rotation around the y–axis with the origin as the center point) angles, as shown in in Figure 4.4. The observed radiation pattern is consistent with one of a circular loop since at points along the axis of the loop source, field values are at a maximum whereas at points perpendicular to the axis of the loop source values drop to a minimum, (20 dB difference). It is also clear that the back side of the handset, 180^o, has a higher peak value than the front at 0^o, which implies that the equivalent loop source that best describes the handset's ELF fields would reside within the handset and would be closer to the battery component at the back.

4.3.2.2. Fit coefficients for equivalent source

After adjustment of the fit coefficients the equivalent source field decay is matched with the field decay observed through measurement. These fit coefficients now represent the equivalent source characteristics. Measured and 'calculated' values are shown in Figure 4.6 and the fit coefficients used are shown in Table 4.1.

Based on these fit coefficients we conclude that we can replicate the spatial decay characteristics of the field with a circular current carrying loop whose properties are listed in Table 4.1.

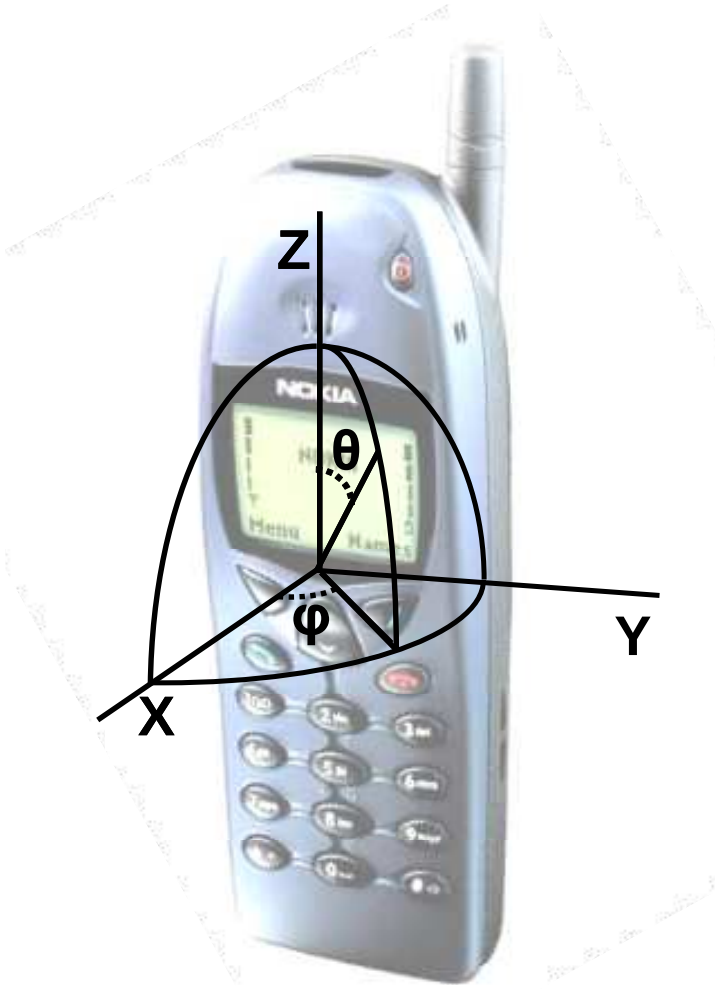

Figure 4.4.: Geometry for radial component as well as field decay measurement from the local maximum, represented by the origin of the coordinate axis, on the front face on a line parallel to the 'x' axis.

Table 4.1.: Model fit coefficients for front and back sides of the measured handset.

Side/Fit Coefficient	a = d - b / (mm)	r / mm	I / (mA)
Front Side	39	9	176
Back Side	19.5	9	681

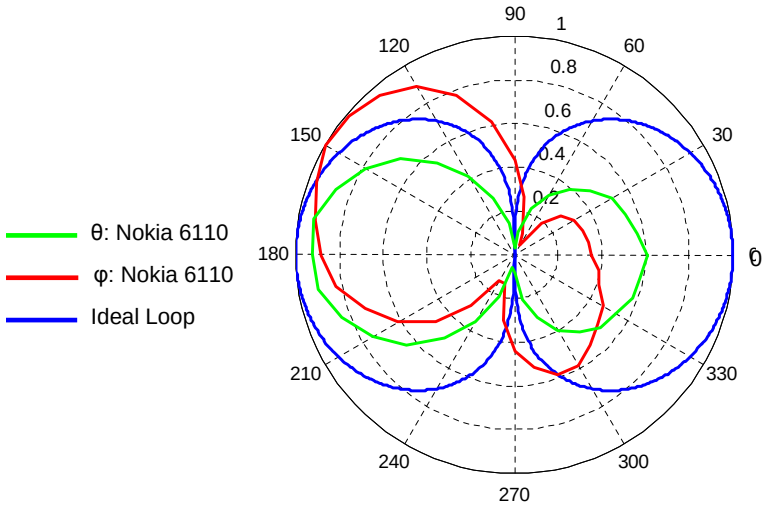

Figure 4.5.: Normalized radial field values in degrees measured for the Nokia 6110 handset . Both ϑ and φ patterns are in agreement with the 9 mm diameter ideal loop. The discrepancy in front to back amplitudes and the deviation of the peak field points from 0^o and 180^o suggest that the equivalent source that best describes the handset's ELF fields would be offset within the handset to be closer to the battery component at the back, and rotated slightly off parallel with respect to the handset's back and front surfaces.

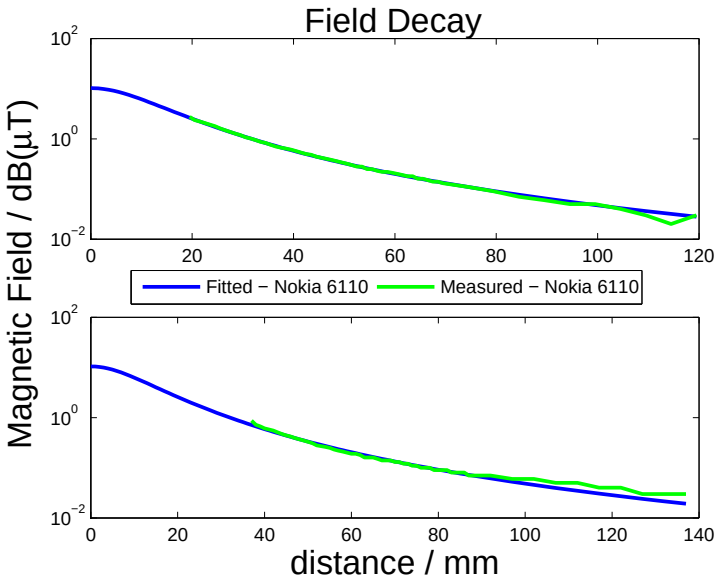

Figure 4.6.: ELF field decay depiction. Top Panel; Front face of Nokia 6110 and Bottom Panel; Back face. Measured values for the 217 Hz component (green line), are shown against the calculated values (blue line) which were extrapolated from the maximum field value at the corresponding surface of the phone using r_1, a and I adjusted to match measured values.

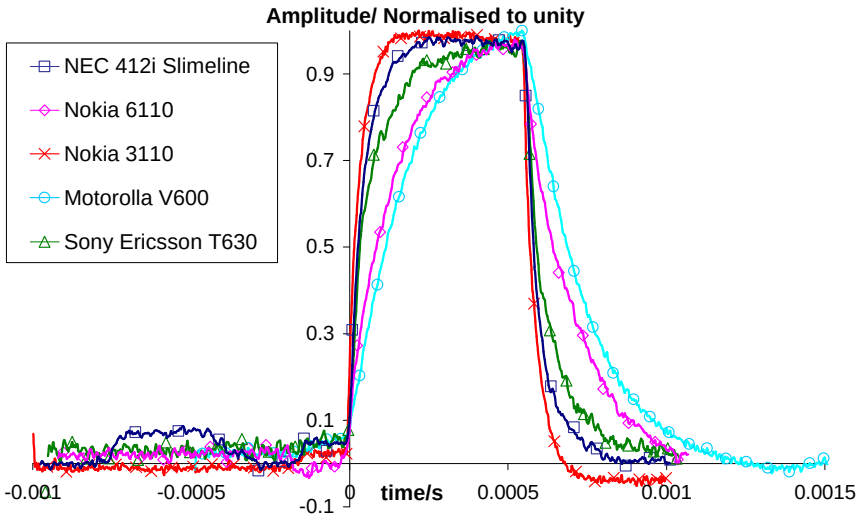

Figure 4.7.: Normalized pulsed ELF magnetic fields. A range of different rise and fall times is observed with pulse width ranging in the vicinity of 576µs.

4.3.2.3. Time domain characteristics of pulsed ELF fields

Since time domain characteristics reflect the frequency content of the pulse which has a direct impact on exposure, see reference [2]), it is important that the equivalent source replicate them as well. Using Probe 2, time domain characteristics were obtained for the Nokia 6110 handset. In addition, the time domain characteristics of pulses from four other handsets were measured. Results are shown in Figure 4.7. Pulses were normalized to peak amplitude of unity allowing for comparison of their time domain characteristics.

Different handsets produce different pulse characteristics, as shown in Table 4.2. This observation has been reported previously [132].

4.3.2.4. Peak fields observed

Using Probe 2, results show that the overall pulse peak is 4.2 times greater than the 217 Hz component. After correcting for spatial averaging (refer to Section 4.3.1) the maximum pulse peak

Table 4.2.: Pulse characteristics for five GSM phones of various brands

Handset Model	Rise Time (μs)	Fall Time (μs)	Pulse Width (μs)
NEC 412i Slimline	128	124	556
Nokia 6110	300	564	576
Nokia 3110	72.3	74	562
Motorola V600	340	384	568
Sony Ericsson T630	150	112	641

Table 4.3.: Proposed equivalent ELF source characteristics

Equivalent Source Characteristics	Value
Loop Radius	9 mm
Loop Distance below phone surface	10 mm
Peak Current in loop	681 mA
Pulse Rise and Fall Times	100 μs[a]
Pulse Peak at handset surface	25 μT[b]

[a] A pulse rise time equivalent to 75% of the maximum observed among the five handsets is chosen

[b] A 25 μT pulse peak amplitude is chosen which is 10% above the highest measured. This accounts for the possibility that other handsets that have not been measured could exceed the maximum observed in the five handset sample.

field at the surface of the Nokia 6110 handset was calculated to be 7.02 μT at the front and 44.4 μT at the back. It was found that the Nokia 3110 handset exhibited the maximum front side fields out of the five phones measured at an amplitude of 22.4 μT. This value is only an approximation since fit coefficients of the Nokia 6110 were used. It is expected that fit coefficients would vary among the two handsets. In another investigation3 the front surface pulse amplitude for the same handset was found to be 19.3 μT giving us sufficient confidence that our approximation is reasonable. Combining the results from the measurements listed above pertaining to equivalent source characteristics, time domain characteristics and peak field values we present the recommended resultant exposure source in Table 4.3.

4.3.2.5. Exposure Levels[4]

Preliminary results through numerical simulations show that absolute peak currents generated within participants' heads from exposure to the field defined in Table 4.3, do not exceed 100 μA/m2 or 1% of ICNIRP exposure limits. Compliance of exposure with the ICNIRP limits is also suggested indirectly through the work of Jokela et al. where fields three times as large were assessed against ICNIRP basic restrictions and were shown to only reach 28% of the limit [72]. As such, there is sufficiently confident that the recommended field is compliant with exposure guidelines. The below 217 Hz Discontinuous Transmission Mode (DTX) components were detected using the same Nokia 6110 handset, but this time operating in a real GSM network under forced DTX conditions. Measurements, shown in Figure 4.9, verify the presence of the 2.1 Hz and 8.3 Hz components associated with the DTX GSM frame structure [109]. As previously mentioned, it has been speculated that these frequency components could be important with regards to biological effect induction due to the frequency overlap with human brain rhythms, even though their presence implies that the overall levels of radiation are significantly reduced since they arise from missing GSM pulses. Frequency components in the range of 0.1 Hz to 40 Hz are found to be at most about 6% of the relevant ICNIRP reference levels, see Figure 4.8, which range from 125 μT to 40 mT for the given frequency range [2]. This calculation is based on the pulse characteristics detailed in Table 4.3 and the weighted peak method of calculation [1]. Further details analysis and ELF exposure modeling results are presented in Section 4.5.2.

4.3.3. Discussion

The measurements of the ELF magnetic field emitted by a Nokia 6110 handset were presented and an extrapolated maximum value of 44.4 μT (+/- 10.7%, 95 CI) was observed on the back surface of the phone and a maximum of 7.02 μT on the front. Additionally we measured the time domain pulse

[4]For the complete ELF exposure assessment see Section 4.5.2.

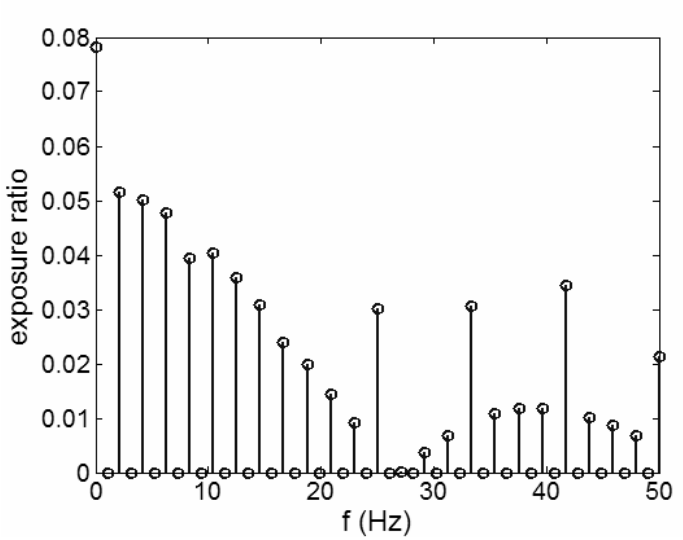

Figure 4.8.: The ratios of ICNIRP reference levels, determined using the weighted peak method, for the DTX components in the range of overlap with normal human brain rhythms are plotted. All components are below 6%.

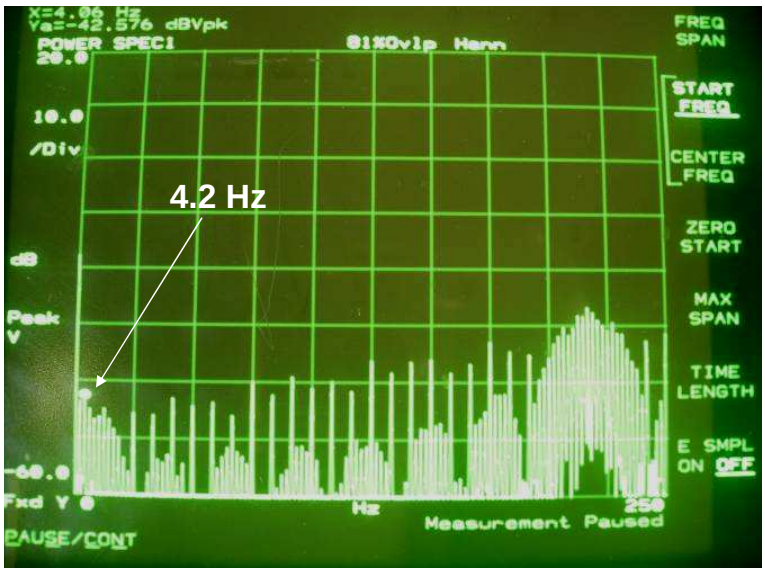

Figure 4.9.: The 2.1 and 8.3 Hz components and their associated harmonics as recorded with Probe 2 using a network operated Nokia 6110 are depicted, with DTX conditions enforced by silencing the microphone of the handset under measurement and maintaining continuous incoming noise. The 4.2 Hz 1st harmonic of 2.1 Hz and the main 217 Hz frequency components are marked.

characteristics of four other commercial phones. Through approximation we deduced a worst case front pulse peak of 22.4 μT. It was shown that the emitted field can be sufficiently approximated by a circular current carrying loop centered at a specific point beneath the surface of the handset. For a Nokia 6110 handset this loop has a radius equal to 9 mm. We have also detected and measured the 2.1 and 8.3 Hz components and their harmonics in pure ELF range. Some studies have suggested using a uniform field exposure utilizing Helmholtz coils, [132]. Although such a setup might maximize the chance of detecting an effect (by minimizing inter subject variability to the exposure condition that can arise from the inevitable variations in source positioning) its results would not be directly applicable to mobile phone exposure since the spatial distribution of the field does not correspond to that of any real mobile phone exposure. In addition a Helmholtz coil setup of the suggested dimensions [132] would result in overexposure of deeper brain structures. Since it is our intention to replicate mobile phone fields as closely as possible, we therefore suggest the use of the equivalent source presented in this work as a more appropriate one if results are to be directly applicable to GSM handset usage. With regards to modulation of fields and their relation to biological effect induction, no definite link has been demonstrated. No mechanism has been established for such purported effects and studies with human volunteers have not shown consistently that modulation does matter [44] (with the exception of some research where a certain degree of replication was possible [58, 114]). Mobile phone handsets produce exposure to ELF and RF fields. Quite possibly, these fields might require different mechanisms if they are to interact with the human brain at intensities below those defined in the ICNIRP guidelines. Using the model developed here, we propose the construction of a model handset to be used in human volunteer studies capable of both RF (modulated or unmodulated) and ELF exposures to test the influence of these fields on the human EEG. For results to be applicable to GSM mobile phone use the model handset will replicate the fields in all three aspects: Intensity, field distribution and frequency content.

In conclusion, Section 4.3 presents the experimental measurements that lead to the development of an equivalent source model to replicate the battery related fields of GSM mobile phone handsets. Peak fields at the front of 5 commercial GSM phones were assessed and a maximum of 22.4 μT was observed. With a worst case scenario pulse of 25 μT amplitude we are sufficiently confident that the ICNIRP basic restrictions are not violated (verification of this is presented in Section 4.5.1). Using these results we recommend simulating the GSM-like ELF fields with a loop of 9 mm radius carrying enough current to produce peak fields of 25 μT at the outer surface of the exposure device. The recommended exposure source will be incorporated in a model handset which will deliver this battery related field to human volunteers in future controlled experiments.

4.4. Model handset design, specifications and performance

This Section presents the design, construction, and performance of the model handset for both RF and ELF radiating elements. The ELF source characterization measurements that were presented in Section 4.3 are not necessary for the RF exposure component since the RF radiating source is one that is chosen, therefore no theoretical model needs to be defined. Instead a suitable RF antenna needs to be selected so as to best replicate GSM-like fields.

4.4.1. RF radiating component

D'Costa et al. have used a model handset in human volunteer exposures which consisted of a monopole antenna as the radiating element [38]. Although a very simple structure and thus easy to construct and assess, an antenna that would be closer to newer mobile phone antennas is preferred here. This choice renders the results of the study relevant to the use of current GSM devices. The choice of antenna was also based on the degree of complexity of construction and the availability of information describing performance and design specifications.

The majority of current GSM phones utilize various designs of internal antennas. There are two

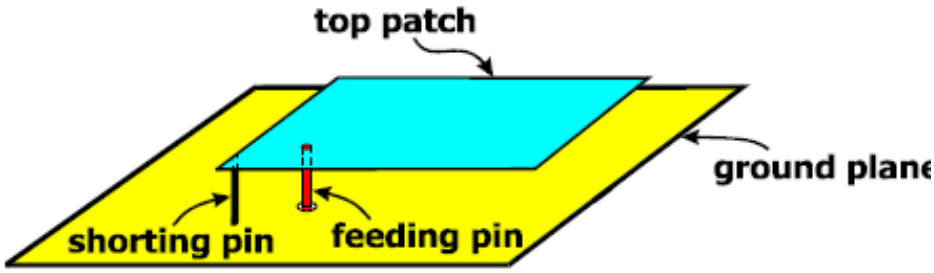

Figure 4.10.: Basic PIFA structure.A conducting sheet is suspended at a critical distance above a ground plane. The antenna is shorted to the ground plane at a critical distance from the feeding pin.

main reasons for this selection. The firs, is that internal antennas are not as vulnerable to damage as external ones. The second, is that the majority of handsets are at least dual band, with some of them being tri or quad band, and therefore require more complex radiating structures that can combine good radiating properties in as many frequency bands. Some internal antenna structures that are currently used are the printed monopole or dipole, patch antennas and the planar inverted F-type (PIFA) antennas.

A design by Kivekas et al. that is a simple version of a PIFA antenna operating at 900 MHz was chosen [76]. The specific structure has also been characterized in terms of SAR performance against crude head and hand models as well as other important antenna parameters [76, 106]. With the available information to backup the design and the indications as to its radiating performance and the impact of various of its parameters on SAR, the antenna selection is justified.

The basic PIFA structure is depicted in Figure 4.10 and the selected antenna in Figure 4.11.

The meandering of the antenna presented by Kivekas et al. improves the bandwidth efficiency and minimizes the distance between the ground plane and the patch antenna making the whole structure more compact [76]. The ground plane was printed on a dielectric substrate (Fiber-Glass,

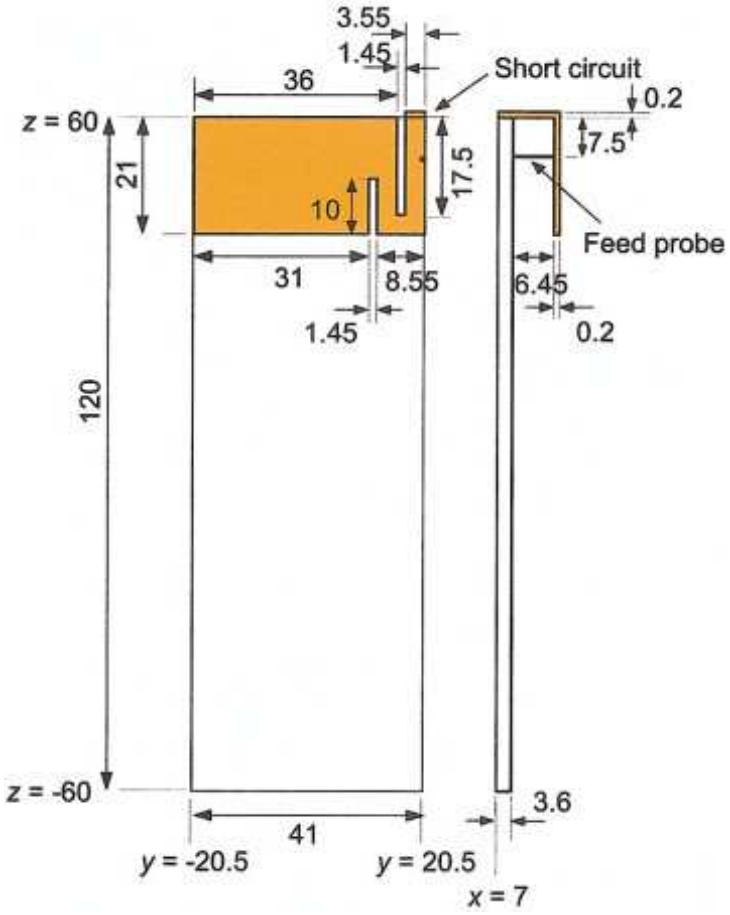

Figure 4.11.: The Kivekas et al. PIFA antenna. The relative simplicity of this design allows for easy physical construction.

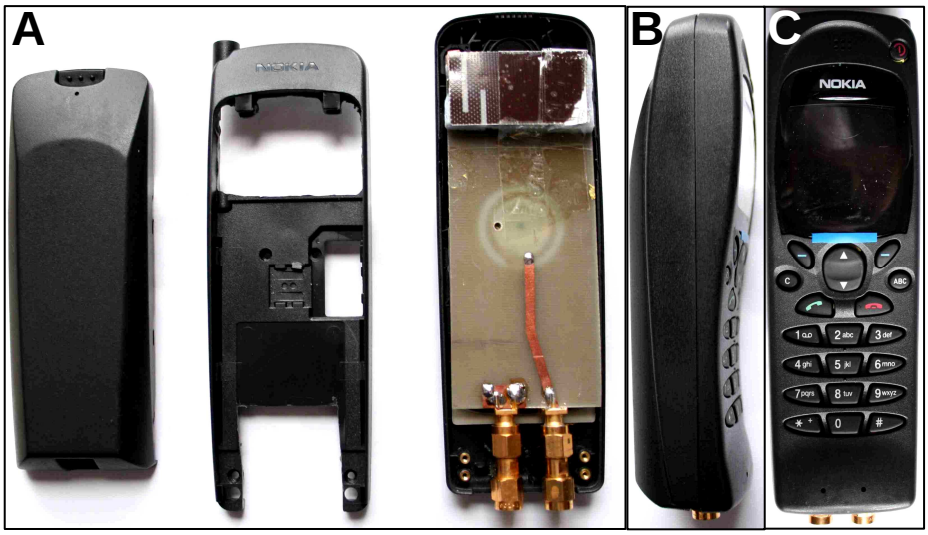

Figure 4.12.: The constructed exposure device is depicted here. A) The antenna elements are fitted within a Nokia 6110 housing and B) When closed the exposure device resembles a real mobile phone.

FR-4, $\epsilon_r = 3.8$, thickness = 1.6 mm). This deviation form the original design required the distance of the PIFA structure from the ground plane to be modified to 6.5 mm. To better support the suspended antenna, a 6.5 mm thick polystyrene slice was inserted between the patch and the ground plane. The length of the ground plane was reduced to 100 mm so as to fit in a GSM handset casing. Finally the feeding point of the antenna was moved to the bottom edge of the structure via the addition of a coaxial feedline. All modifications where performed for design purposes, (e.g. convenient length, height, position of feeding point and rigidity), and not radiating performance. A prototype was constructed, Figure 4.12, and its performance was assessed in terms of radiation pattern and return loss.

Free space radiation pattern The radiation patterns was measured in an anechoic chamber and is shown in Figure 4.13. At 180^o , the handset side that is closest to the users head, are close to minimum. This implies that SAR values would also be at a minimum at that side. However, the

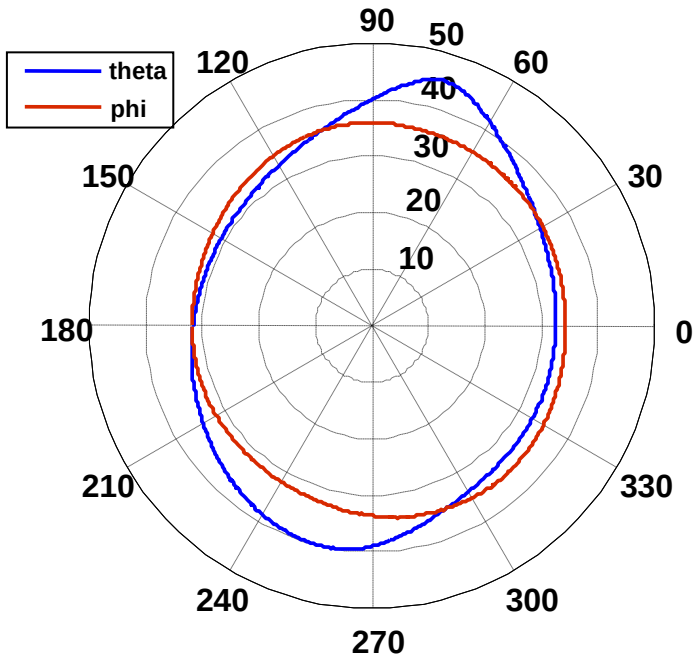

Figure 4.13.: The RF radiation pattern as measured in free space in an anechoic chamber. The pattern suggests that on the side closest to the users head, 180^o, the radiation pattern is at a minimum

influence of the dielectric volume of the head needs to be considered before reaching such conclusions about the SAR performance of the handset.

4.4.1.1. Return loss

The return loss of the antenna demonstrates adequate radiating properties at 900 MHz, Figure 4.14.

4.4.1.2. Input Impedance

The input impedance of the handset was measured with a network analyzer (Wiltron 360B) and was found to be $41.8 + 13.8j\,\Omega$ when held against the head, and $33.7 + 13.7j\,\Omega$ in free space. Both measurements were taken with the antenna inside the casing.

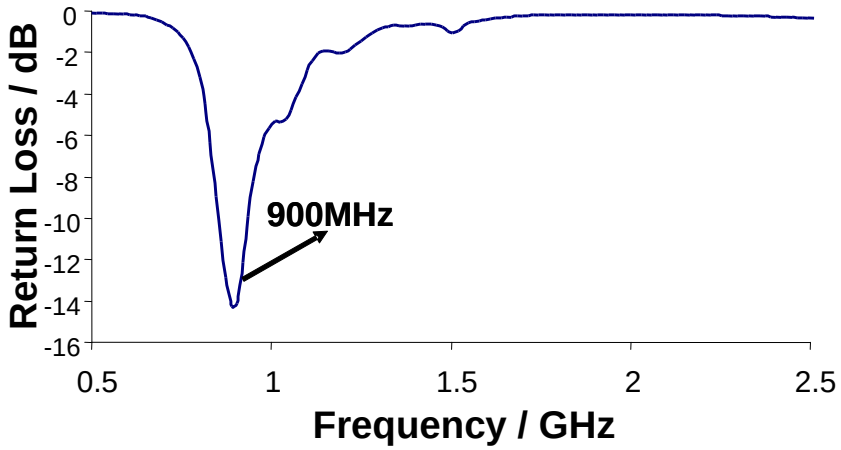

Figure 4.14.: The return loss of a constructed antenna adapted from the Kivekas et al. design [76]. Good radiating properties are demonstrated at 900 MHz.

4.4.2. ELF radiating component

The developed ELF model of Table 4.3 was implemented in the model handset. The loop structure was engraved on the ground plane as shown in Figure 4.15. To verify the performance of this implementation, the same procedure that was used for the measurement of the Nokia 6110 ELF radiation pattern was followed here. An extra turn was added to the engraved loop, allowing for a twofold decrease of required current, while maintaining the target field level.

4.4.2.1. Radial performance

The radiation pattern, (measurement geometry defined in Figure 4.4), is in agreement with the ideal loop as well as with the Nokia 6110, see Figure 4.16. As explained, the discrepancy of the back to front peak values on the Nokia 6110 measurement are associated with the discrepancy between the relative position of the hypothetical loop inside the handset in relation to the center of rotation. This does not appear on the constructed loop measurement because the loop position is centered with respect to the axis of rotation.

Figure 4.15.: The loop structure engraved on the ground plane of the PIFA antenna is depicted. One extra turn is added to the ELF loop thereby minimize the required current value by a factor of two. The added coaxial line is also visible. This enables the feeding point to be conveniently placed at the bottom end of the ground plane.

Coaxial field decay As seen in Figure 4.17 the coaxial field decay is in good agreement with the one predicted by the model as well as the real measurement obtained for the Nokia 6110 handset.

The pulse input to the ELF loop had rise and fall times of 100 µs which is close to 75% of the maximum pulse rise time observed, Table 4.3. The amplitude was chosen to be 25 µT, slightly higher than the maximum field value observed for the front surface of the five handsets that were studied. With these signal specifications none of the spectral components exceed reference levels, see Figure 4.18.

4.4.3. Complete exposure setup

The exposure setup is divided into two modules, the RF and ELF. Before exposure commencement a testing software routine allows to verify the transmission of both RF and ELF modules. The RF transmission is verified via a diode detector which is connected to a CRO as illustrated in Figure 4.19. In addition, a measurement of the input power to the handset ensures the correct exposure

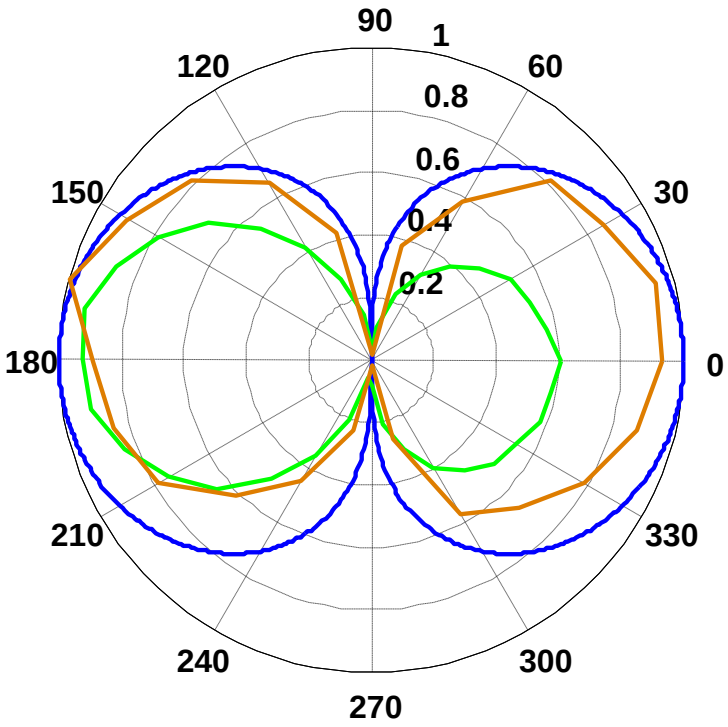

Figure 4.16.: The radiation pattern of the constructed model loop source (orange) is in good agreement with that of the real Nokia 6110 handset (green). The absence of back to front discrepancy is due to the centered position of the model loop during measurement as opposed to the unknown position of the real ELF source within the Nokia 6110 handset. The radiation pattern of an ideal loop is also shown for comparison.

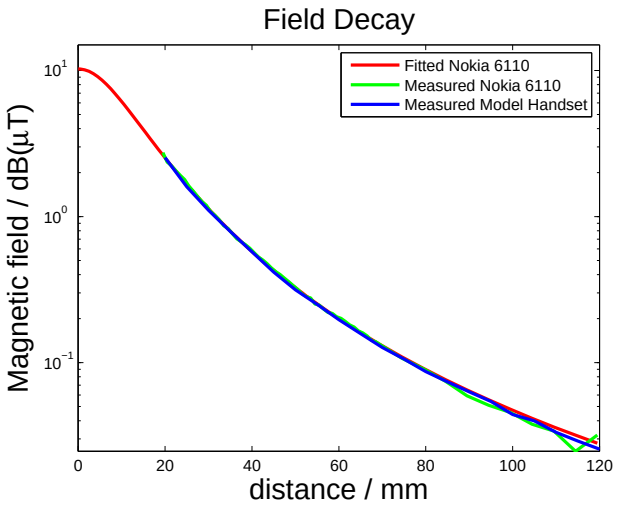

Figure 4.17.: A good match is observed between the measured Nokia 6110 radiation pattern and the constructed loop source. This is achieved through the fitting coefficients defined in Table 4.1 which are also used to produce the fitted Nokia 6110 curve shown here.

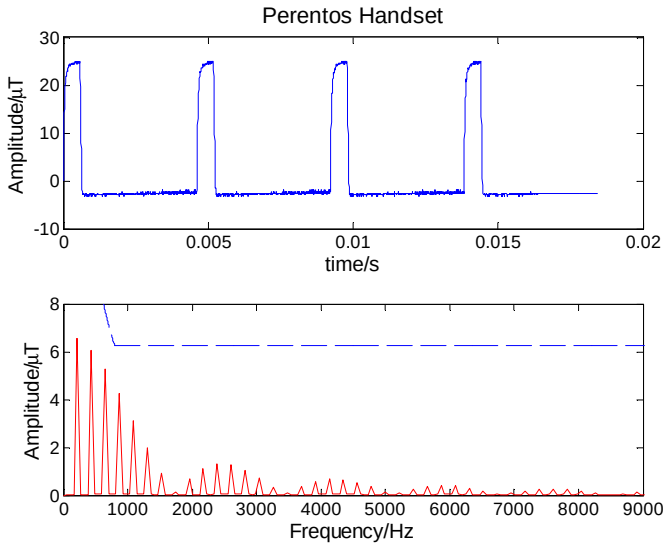

Figure 4.18.: Time (top panel) and frequency (bottom panel) characteristics of recorded ELF fields for the model handset. Bottom panel-Blue dashed line; ICNIRP reference peak reference levels and Bottom panel-Red dashed line; Spectral peak amplitude data of the GSM pulse train.

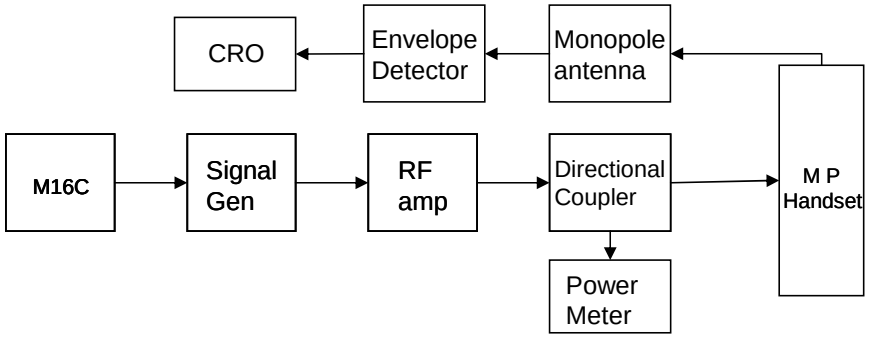

Figure 4.19.: A depiction of the RF exposure setup. The setup allows for reliable measurement of input power levels as well as the presence of EM fields before commencement of experiments.

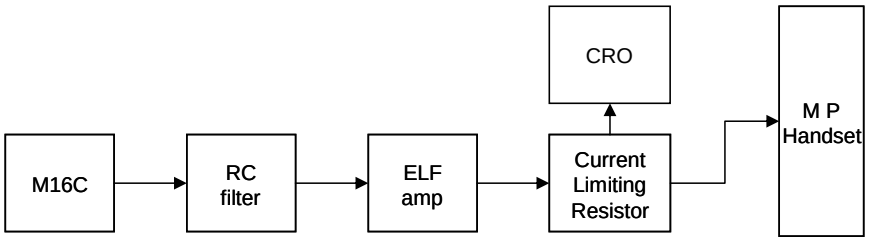

Figure 4.20.: A depiction of the ELF exposure setup. The setup allows for reliable measurement of input current to the ELF loop before commencement of experiments.

levels. Power limiting attenuators placed between the RF amplifier and the directional coupler ensure that overexposure cannot occur. The ELF exposure is confirmed by measuring the voltage drop across the current limiting resistor which is attached to the transmitting loop, see Figure 4.20.

Current through the engraved loop was adjusted to produce a field intensity level of 25 μT at the front surface of the handset. Figure 4.20 illustrates the final ELF exposure setup used. The rms voltage across the current limiting resistor as measured using a CRO allows for continuous exposure level monitoring.

4.4.3.1. Handset casing

To preserve ecological validity the radiating elements were fitted inside a Nokia 6110 housing, Figure 4.12. All metallic coatings and components were removed from the casing so as to minimize impact on radiation patterns and unwanted shielding effects.

4.5. Computational modeling: RF and ELF absorption

Exposure assessment was performed for both RF and ELF exposures. RF exposures were evaluated based on SAR measurements obtained through physical measurements as well as through computational modeling. ELF exposures were assessed through computational models only.

4.5.1. RF absorption

4.5.1.1. Peak spatial-average SAR - physical measurement

The SAR performance of the handset was evaluated at an accredited commercial facility (EMC technologies). It was performed on the complete handset (radiating element and casing), thus mimicking performance under real conditions of use. The standard ear to mouth positioning was used on a SAM [6] right section human head phantom, filled with tissue equivalent liquid (ς = 0.979801 S/m, ϵ_r = 42.1673; ρ = 1000 kg/m^3). An input power of 743 mW corresponded to a 10 gram peak spatial-average SAR of 2.1 W/kg, Figure 4.21. The power level was later scaled down so as to achieve a SAR of 1.95 W/kg thus ensuring compliance with the ICNIRP guidelines [2]. Based on power drift measurements, the uncertainty on the measured value was 17.63%

4.5.1.2. Computation validation of peak SAR and SAR distribution

Computational modeling of the RF exposure was undertaken for two reasons. Firstly, to validate the peak spatial-average SAR obtained through the physical measurement. Secondly to obtain

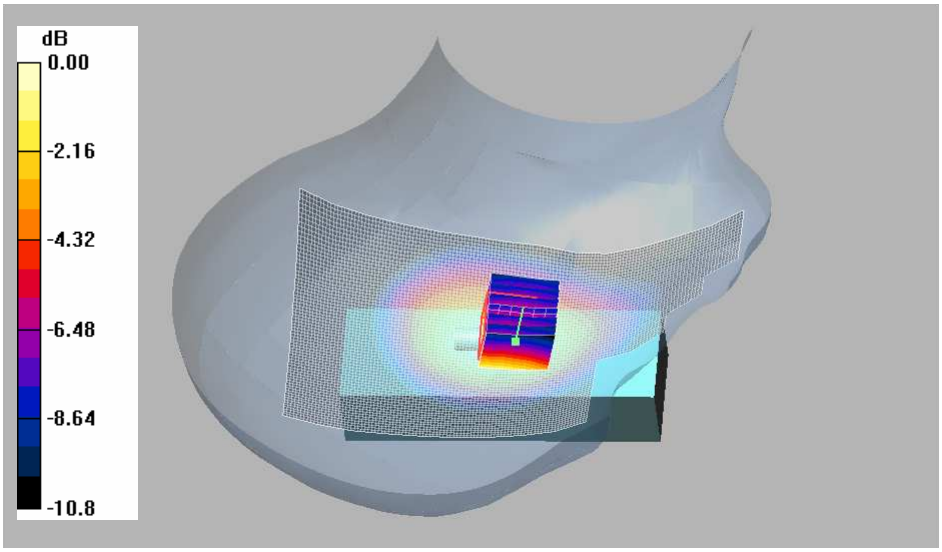

Figure 4.21.: The 10 gram peak spatial-average SAR volume cube is shown here as obtained through the physical measurement. As expected due to the strong coupling of the antenna to the ground plane, the peak spatial-average SAR is roughly midway along the longest dimension of the ground plane.

information regarding the exposure distribution within the head volume since it remains unknown through the physical measurement.

Model construction Computational modeling were performed using the FEKO^{TM} electromagnetic simulation environment. A realization of the IEEE SAM phantom, [6], without the enclosing perspex shell was used as the head model. The head model was set to the dielectric tissue properties that were used during the physical measurement ($\sigma = 0.979801\ m\Omega/m$,$\epsilon_r = 42.1673$; $\rho = 1000$ kg/m3). The phantom was meshed at 10 mm satisfying the FEKO^{TM} software condition that defines a maximum mesh size of $\lambda/10$. At 898 MHz, $10\,mm \simeq \lambda/30$. The antenna structure was constructed according to the specifications defined in Section 4.4.1. Additionally to simulate the effective ground length, that is modified by the presence of the SMA connectors, two metal planes were added at the bottom end of the ground plane with equivalent length and width. The antenna was enclosed in a dielectric case which acted as a crude approximation of the real handset housing. The position

of the antenna and ground element within the casing was adjusted so as to compensate for the irregular shape of the casing.

Since the model is only an approximation of the real handset and the overall measurement geometry, the obtained SAR value can only be an approximation. For this reason slight adjustments to the geometry (position of the antenna within the housing and the position of the antenna and ground relative to the head) were performed in order to get a best match with the physical peak spatial-average SAR measurement and at the same time obtain a sensitivity of SAR to these geometrical adjustments. If a small sensitivity is observed that is centered around the nominal SAR value then the model is considered to represent the physical measurement scenario adequately. A range of SAR values is presented which is shown to be in the vicinity of the physical measurement. The amount of variation observed on the SAR through these series of simulations is also compared to the uncertainty estimate that is provided with the physical SAR measurement. It is also shown that with additional structural detail of the handset housing (the antenna its self is adequately modeled), better SAR approximations can be obtained.

To account for the omission of the coaxial feedline (see Figure 4.15), the input power to the FEKO model handset was adjusted based on the difference in input impedances through the use of Equation 4.9which represents the power that is dissipated in the antenna load.

$$P = \frac{|\ V_0^+\ |^2}{2Z_0}[1- |\ \Gamma\ |^2] \tag{4.9}$$

where

P = the dissipated power in the load

V_0^+= incident voltage

Z_0= line impedance and

Γ= reflection coefficient with $\Gamma = \frac{Z_L - Z_0}{Z_L + Z_0}$ and $Z_L$is the input impedance of the handset.

Table 4.4 lists the properties of the real and FEKO model handset as well as the appropriate

Table 4.4.: Adjustment of input power in FEKO model so as to achieve equivalence with the real handset.

	Real Handset	FEKO Model Handset
Input Impedance	$41.8 + 13.8j$	$62.4 + 41.9j$
Γ	0.17	0.36
Forward Power	1.34 W	1.20 W
Input Power Adjustment Ratio	—-	10%
Voltage Source (rms)	11.74 V	12.41 V (adjusted)
SAR	1.95 W/kg	1.98 W/kg[a]

[a]The quoted SAR value is not an absolute one, rather it is indicative of the validity of the physical measurement.

scaling used to achieve the desired input power to SAR level ratio.

Results A best fit to the real measurement was obtained for an antenna distance away from the casing of 12 mm and an angle deviation of 8^o away from the plane of the casing's front face.

SAR sensitivity to mesh size To establish whether the model output (measured by SAR) is sufficiently stable, progressively smaller meshing sizes (handset only) were implemented for identical geometries. It is shown that a meshing of 10 mm is adequately given that a SAR reduction of less than 2% is observed when the mesh is reduced from 10 mm to 8 mm.

SAR sensitivity to the distance of the antenna's ground plane from the casing Due to the irregular shape of the real handset casing the distance 'd' (see Figure 4.23) of the antenna ground plane with respect to the casing varies between 10 to 12 mm. Through a series of simulations a sensitivity of SAR to variable 'd' was obtained (1 mm intervals, from 10 to 13 mm) and was found to be 18% for the 10 gram peak spatial-average SAR (see Figure4.24).

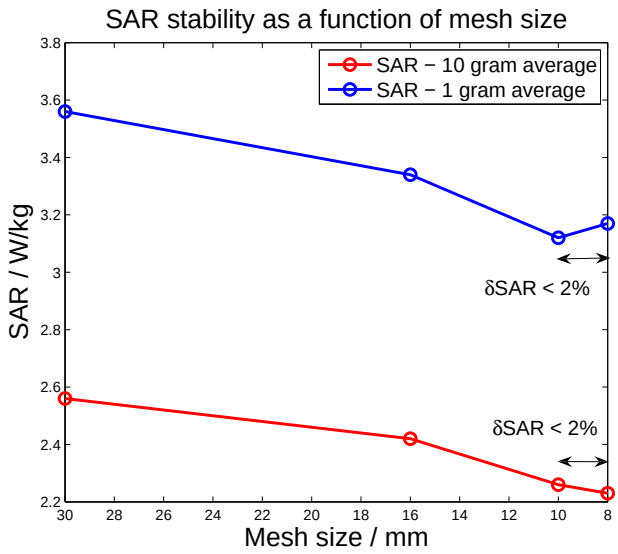

Figure 4.22.: A graph of the variation of SAR with mesh size. Small variations are observed at mesh sizes less than the recommended $\lambda/10$. However the reduction obtained from 10 mm to 8 mm is less than 2% and as such the a mesh size of 10mm is deemed as adequate.

SAR sensitivity to sagittal handset displacement Owing to the non exact positioning of the model phone in comparison to the actual physical measurement, a sensitivity analysis is performed for sagittal displacements around the point of measurement (the sagittal plane is the one that contains the common point in space where the handset housing touches the SAM phantom). The antenna and casing are displaced according to the arrangement shown in Figure 4.25, thus producing a SAR deviation of 5% (see Table 4.5 for absolute values).

Considering the sensitivity of SAR to the model geometry (less than 30%), the agreement between the physical and computational results is good.

Therefore, the model is considered to replicate the real measurement scenario adequately, albeit with inherent uncertainty, and as such representative SAR distributions in the head volume can be reliably obtained.

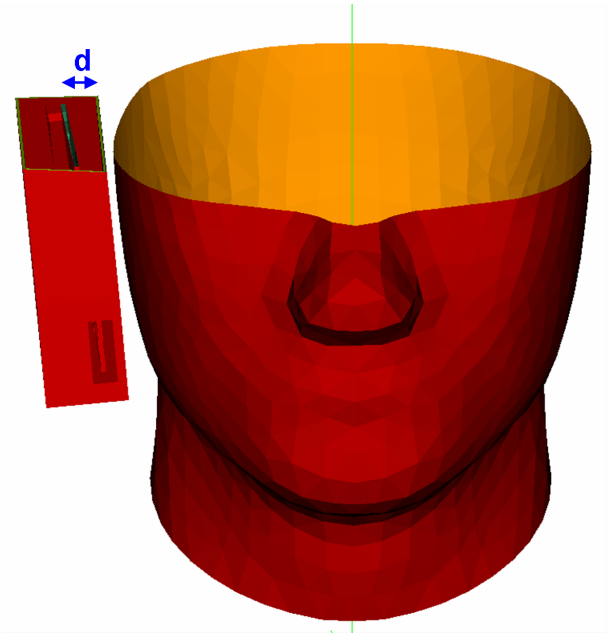

Figure 4.23.: Value 'd' represents the distance between the handset housing and the antenna ground plane. Since this distance varies due to the irregular shape of the real Nokia 6110 housing, the sensitivity of SAR to variable 'd' was assessed.

Table 4.5.: 10 mm displacements of the handset unit in the U and V directions produces small variations in the 10 and 1 gram peak spatial SAR. All values are for 12mm antenna displacement within the handset

	SAR 10 g (1 g) / W/kg	
Displacement	+10 mm	−10 mm
U	2.08 (2.88)	1.87 (2.56)
V	2.02 (2.82)	1.91 (2.58)
None	1.98 (2.72)	

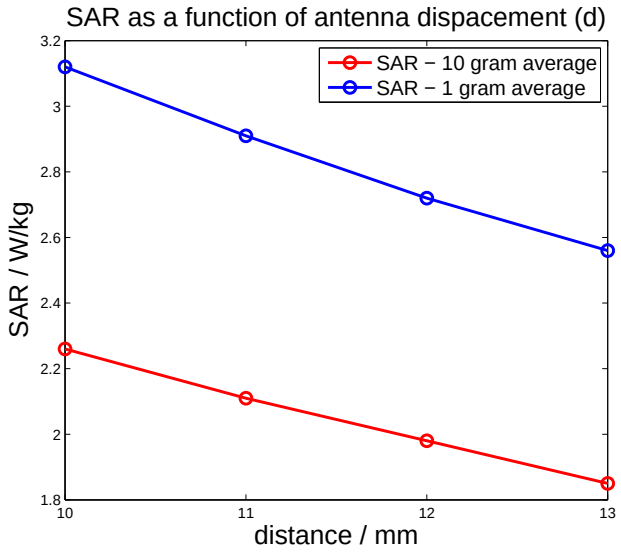

Figure 4.24.: SAR variation as a function of antenna displacement is depicted here. It lies in the vicinity of 18% for the range of 10 to 13 mm. With the nominal input power the desired SAR lies within this range of values of 'd'.

4.5.1.3. SAR distribution in the head volume

The SAR evaluation required for compliance purposes, that is, a single value representing the 10 gram peak spatial-average SAR, does not provide any information regarding the distribution of exposure inside the head volume. This issue was discussed by Boutry et al. [18] who identify that the spatial peak SAR correlates poorly with the exposed brain regions and does not provide any information about the location of maximum absorption. The spatial peak-average SAR evaluation contains no information regarding the distribution of exposure in the remaining brain. This knowledge is essential in identifying correlations of EEG effects and exposure levels.

The distribution of SAR in various head slices, as extracted from the FEKO model, is presented next. It is noted that the analysis presented in this section is extracted from the FEKO simulation using the homogeneous SAM phantom. Therefore the dielectric properties of different brain tissues are not accounted for. This is a limitation of the reported SAR distribution despite which a good

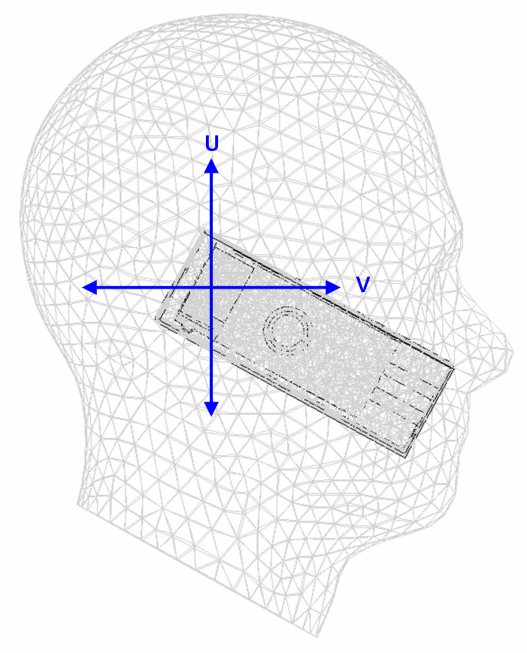

Figure 4.25.: A SAR sensitivity analysis was performed for sagittal plane displacements ±10mm for both U and V directions.

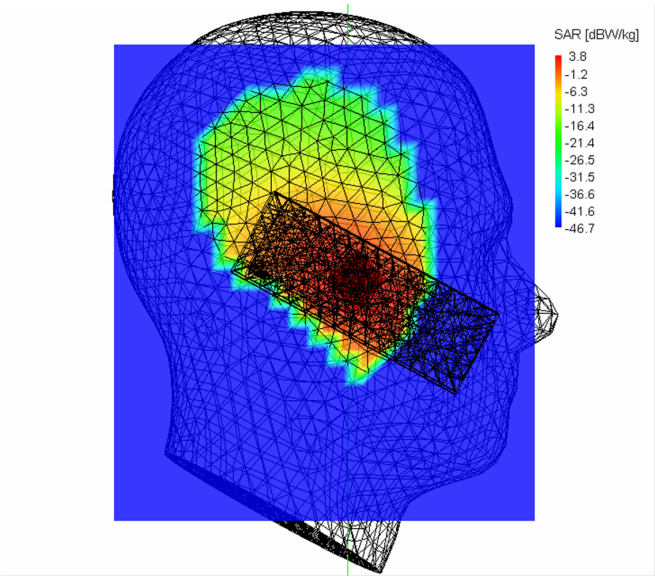

Figure 4.26.: Sagittal slice crossing the 10g peak-average SAR cube. The slice is just below the surface of the head.

approximation of distributions in the head volume can be obtained.

As expected, the SAR distribution within the head volume is highly localized (see Figures 4.26, 4.27, 4.28 and 4.29). The maximum exposure occurs close to the surface of the head, near the handset. The exposure close to the mid brain falls below 0.5 W/kg. Half way within the exposed hemisphere, Figure 4.29, the SAR value peaks at around 0.5 W/kg. The results demonstrate that the desired localized exposure is achieved using the constructed handset. Relative to the exposure source, the variation within the contralateral brain region is always well below 0.5 W/kg.

4.5.2. ELF absorption

The assessment of ELF exposures was performed first through comparison to reference levels, and subsequently through comparison to basic restriction levels.

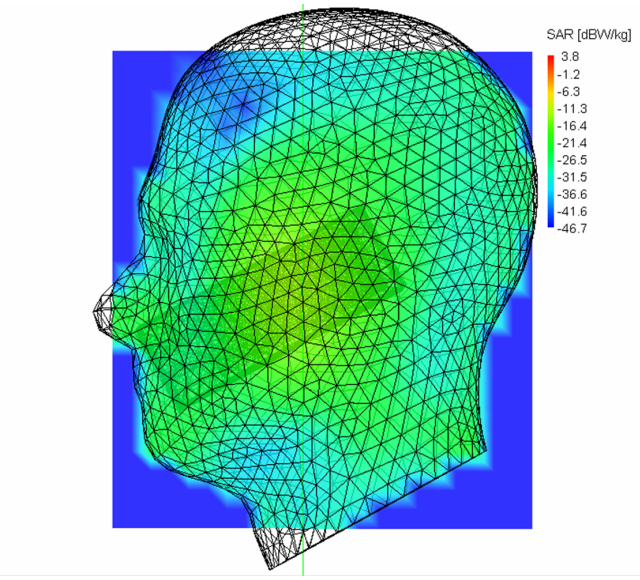

Figure 4.27.: The midline sagittal slice.At this depth the exposure drops to at least -11dB[W/kg]. Exposures in the left hemisphere will be well below this SAR value.

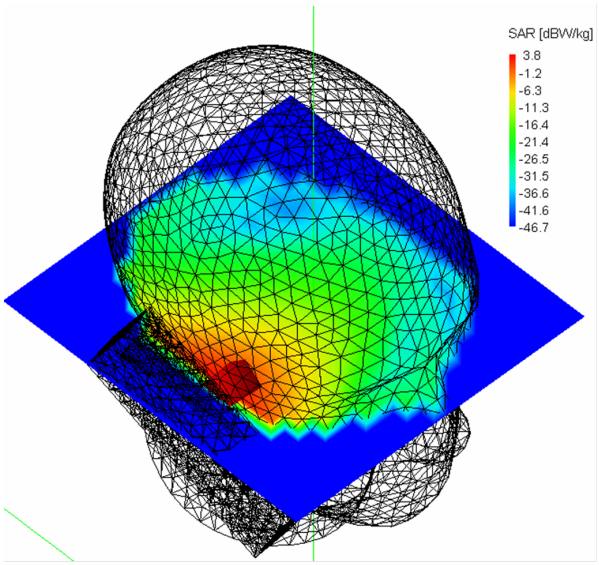

Figure 4.28.: An axial slice in the vicinity of the 10g peak average SAR cube. The localized nature of the exposure can be clearly seen.

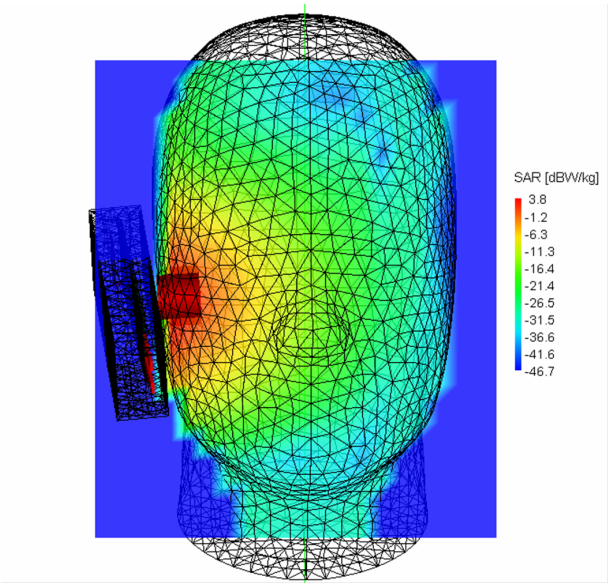

Figure 4.29.: A coronal slice in the vicinity of the 10g peak average SAR cube. The peak spatial-average cube resides roughly at the height of the cheekbone.

4.5.2.1. Comparison to Reference Levels

Background, methods, and materials To demonstrated compliance to the ICNIRP limits for a device that produces sinusoidal ELF fields, it is possible to measure its magnetic field levels in free space and compare them with the reference levels defined in the ICNIRP standard [2]. The ICNIRP also defines a special procedure with which pulsed ELF fields are to be assessed. The distinction is made since pulsed fields contain spectral components extending higher than the basic pulse repetition frequency and as such, these components need to be incorporated in the determination of exposure levels. The ICNIRP [2] originally defined the Multiple Frequency Rule (MFR) for this application, which is given by

$$R = \sum_{j=1Hz}^{100kHz} \frac{B_j}{B_{i,j}} \leq 1 \tag{4.10}$$

where

B_j = the magnetic flux density at frequency j

$B_{i,j}$ = the magnetic flux density reference level at frequency j

However, when this approach is applied to broad-band pulsed fields, it leads to overestimation of exposure because an explicit assumption is built into the equation, by which all frequency components are considered to be in phase, and are therefore additive without adjustment. For broad-band fields, this assumption is not valid. An ICNIRP statement defines an approach that produces more realistic exposure ratios [1] for such scenarios. This approach, termed as the Weighted Peak Method, takes into account the phase of individual frequency components before summation, as detailed by the following equation

$$R = \left| \sum_{j=1Hz}^{100kHz} \frac{B_j}{B_{i,j}} \cdot cos(2\pi f_j t + \theta_j + \phi_j) \right| \leq 1 \tag{4.11}$$

where

θ_j is the phase of the jth component and

$\phi(f) = 0$ when $f < f_c$ or $\phi(f) = -\frac{\pi}{2}$ when $f > f_c$ and

$f_c = 800$ Hz

The Weighted Peak Method [1] was used to assess the field produced by the pulse and model source combination defined in Table 4.3. The high pass filter ($f_c = 800$ Hz) approximation was used since the pulse is limited in terms of spectrum to frequencies well below 100 kHz [1]. The evaluation takes place with field values corresponding to the surface of the model handset, where a maximum of $25\mu T$ can be reached, thereby representing the maximum exposure achievable. It is noted that this peak value is spatially confined within a small vicinity around the source (in the order of a few millimeters) so exposures further away will be significantly smaller.

The ELF waveform (input to the handset see Figure 4.20, pulse characteristics as shown in Figure 4.18) was recorded on an oscilloscope with a sampling period of $4\,\mu s$, providing useful spectral information up to 125 kHz. The recorded pulse representing the exposure signal was imported in

Table 4.6.: Exposure Ratios based on the Weighted Peak Method

Waveform	Percentage of Reference Levels
217 Hz pulse DC of 12.5%	174%
DTX pulse frame	175%
2.1 Hz DTX component	<6%
8.3 Hz DTX component or worst harmonic	<8%

the Matlab^{TM} environment (The Mathworks, Inc., Natick, MA) where a time series of several signal periods (12.5% Duty Cycle) was constructed. In addition a time series of several DTX multi-frames was also constructed. Both were normalized to a peak value of 25 μT and were then submitted through the Weighted Peak Calculation Algorithm.

Results The results are summarized in Table 4.6. In addition the time domain effect of the Weighted Peak Method, which is in effect a high pass filter with $f_c = 800$ Hz, on the basic GSM pulse is shown in Figure 4.30. The Spectral content of the DTX pulse is also presented in Figure 4.31.

Since the ICNIRP reference levels are violated, Table 4.6, an evaluation against basic restriction levels is necessary so to ensure compliance with the ICNIRP standard. The next Section presents such dosimetric al evaluation based on computational modeling.

4.5.2.2. Comparison to Basic Restriction Levels

Background, methods, and materials ICNIRP provide with several different methods for the evaluation of compliance with the basic restriction levels. These are the MFR, the Weighted Peak Method, and the equivalent frequency method. The one chosen here was the equivalent frequency.

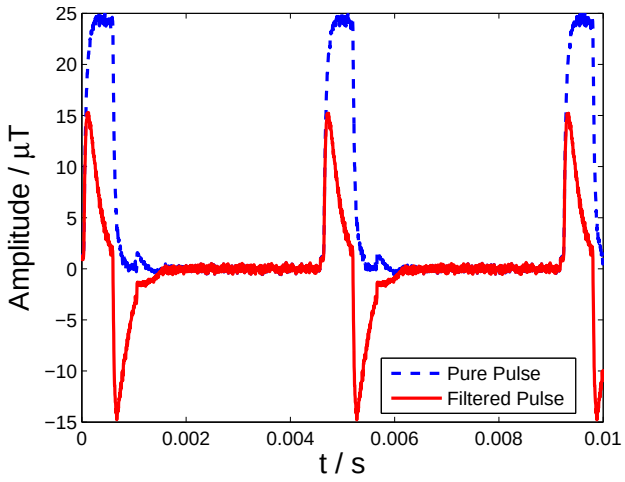

Figure 4.30.: The original pulse is shown, along with the one filtered to provide the percentage of reference levels. The exposure level is calculated as the ratio of the filtered pulse to the corresponding peak reference level at the cut-off frequency of 800 Hz which is 8.84 μT.

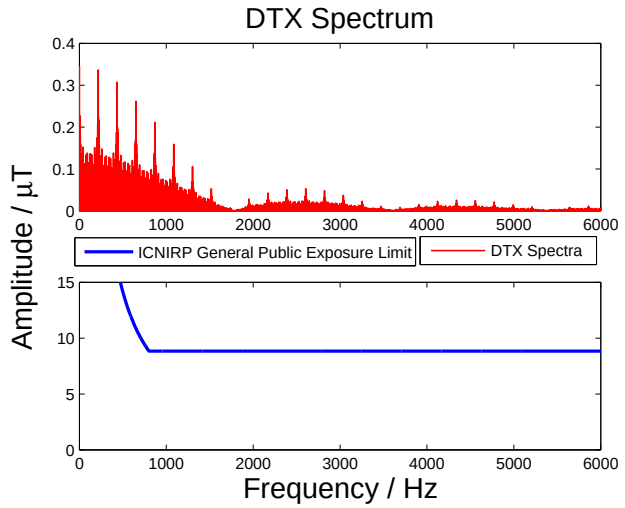

Figure 4.31.: The spectrum of the DTX pulse is shown; top panel, along with reference limit of the ICNIRP levels in the same frequency range. Individual frequency components of the DTX multiframe are well below the reference levels. However, according to the Weighted Peak Method, the ICNIRP reference levels are exceeded.

Table 4.7.: Dielectric properties of tissues at 868 Hz, and corresponding tissue thicknesses.

Tissue	Conductivity σ (S/m)	Thickness (mm)
Wet Skin	0.00051627	2
Cortical Bone	0.060261	6
Cerebral Spinal Fluid	2	1
White Matter	0.094115	88

With this, pulses of duration t_p, are evaluated against basic restrictions at the frequency determined by $f = 1/2t_p$. Jokela et al. have shown that the use of this method leads to an increase in basic restriction value of 2.6, a factor that can be easily accounted for [70].

Reported measurements were obtained using the low frequency solver of the CST software (CST Studio Suite^{TM}). CST is a general purpose electromagnetic simulator that is based on the Finite Integration Technique. A multi-layered simplified human head model was used and a current carrying loop, with dimensions and current flow same as those defined in Table 4.3, served as the excitation source. The current source was positioned at a distance of 10 mm from the surface of the side of the head. The model was constructed from simple geometric shapes and contained tissues with properties as defined in Table 4.7. Since the conductivity and permittivity values of tissues at 868 Hz fulfill the relationship $\sigma \gg \omega\epsilon$, quasi static conditions were assumed. This allowed for a simplified computational solution using the Magneto-Quasi-Static (MQS) solver. The MQS solution ignores displacement current since its contribution to the overall current, at the frequency of interest, is negligible.

Current Density - cross-sectional averaging algorithm In order to determine induced currents in biological tissues the ICNIRP guidelines define that currents need to be averaged over a cross sectional area of 1 cm^2. This cross-sectional area must lie on the plane that has the current direction as a normal [2]. In addition the ARPANSA standard defines this cross-sectional area to be a circle whose center is the point-current for which averaging is to occur. To obtain the averaged current

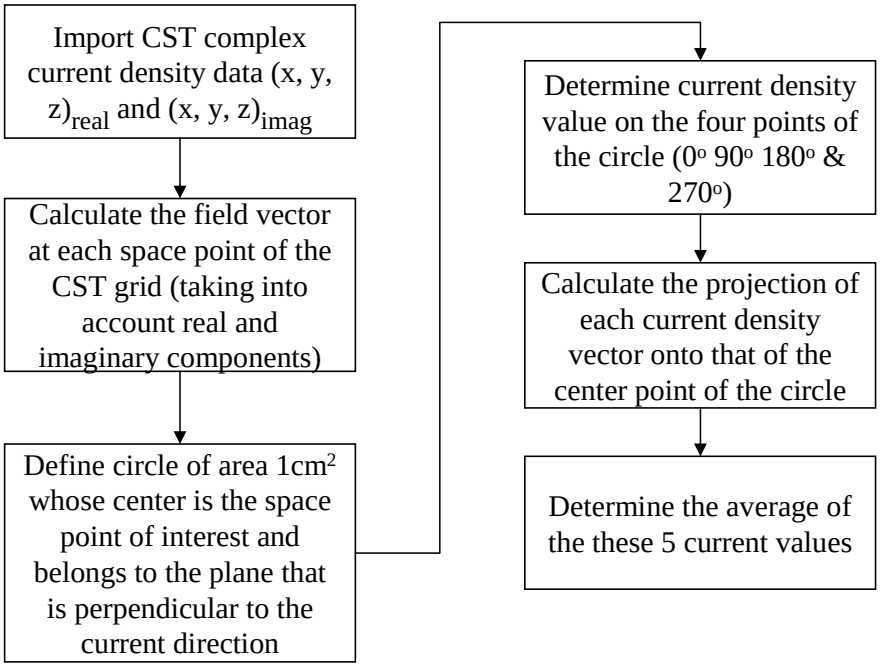

Figure 4.32.: Current Density Averaging algorithm. CST^{TM} provides a current vector output for each grid point point in the simulation. A parametric equation defining the circle of interest (in 3 dimensional coordinates) is created. Subsequently, four equidistant points on this circle are selected and their respective vector current values are averaged along with the center point. The resulting value is the peak spatial average current density which is then compared to the basic restriction level at 217 Hz.

density, the current values extracted through the CST simulation, were processed in Matlab^{TM} according the algorithm shown in Figure 4.32.

Results The results are summarized in Table 4.8. With the crude head model used it is shown that the ELF exposure setup that is recommended in this Chapter reaches 1% of the ICNIRP basic restriction level. As expected, the maximum current density is observed in the CSF which carries the largest conductivity value.

Model limitations First, there are instances in which the cross-sectional surface-averaging algorithm does not cover the full 1cm^2 surface area due to the proximity of the measuring point to the

Table 4.8.: Current Density values and corresponding exposure ratios in comparison to the ICNIRP Basic Restriction Levels as obtained with a tetrahedral meshing. Both absolute and spatially averaged current density peaks are well below the restriction levels ($2^{mA}/_{m^2}$ at 217 Hz).

	Current density (at 217 Hz)	Percentage of general public exposure limit (at 8 Hz)
Absolute Peak	0.397 $^{mA}/_{m^2}$	20%
Spatially Averaged Peak (cross-section of 1cm^2)	$7.77^{\mu A}/_{m^2}$	<1%

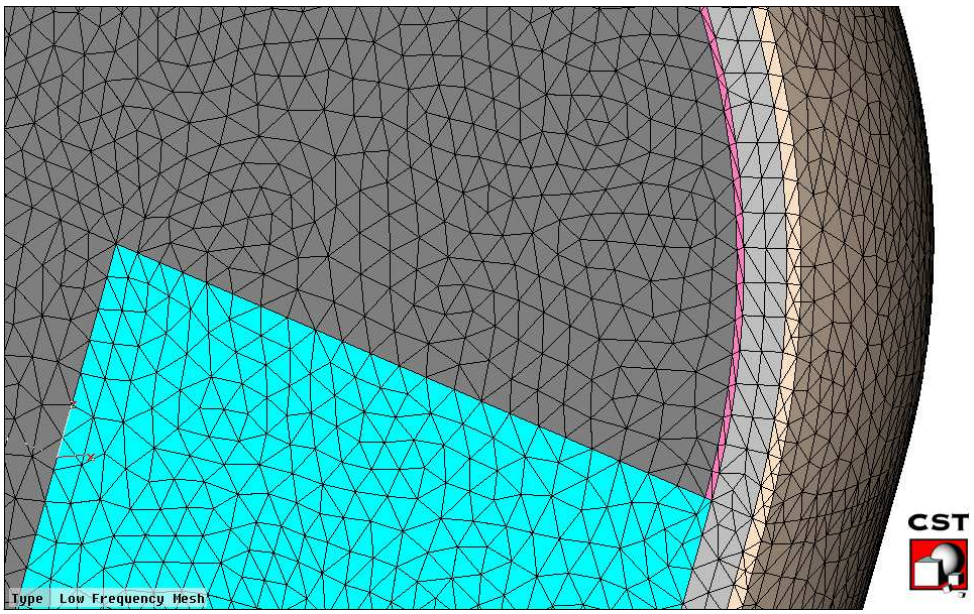

Figure 4.33.: A view of the meshing of the head volume. Dark Grey; Brain Matter, Blue; Average Head, Light Grey; Cortical Bone, Light Brown; Skin and Purple; CSF

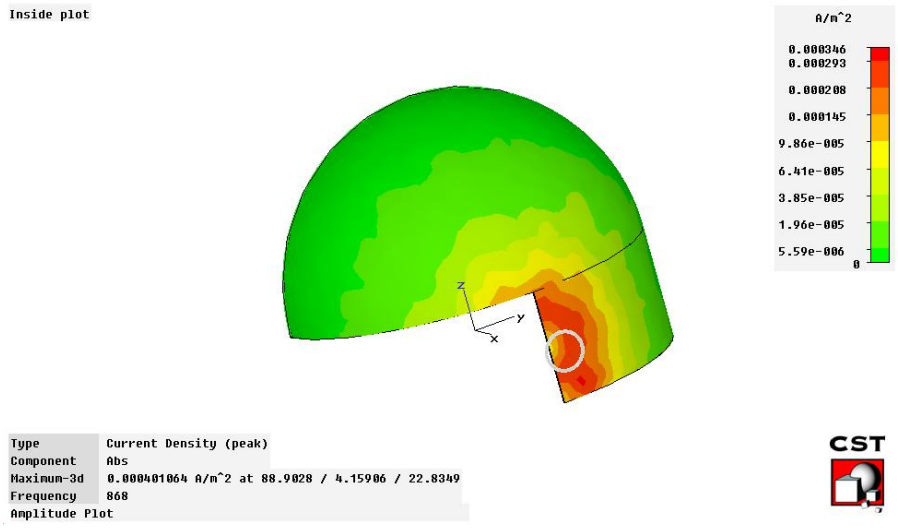

Figure 4.34.: A 3-dimensional view of the CSF structure showing the distribution of currents within it.

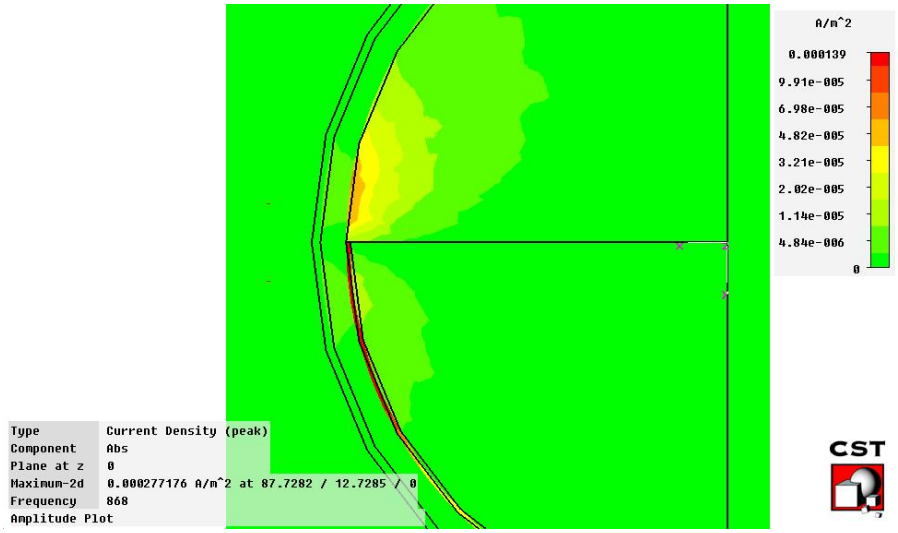

Figure 4.35.: An axial slice of the head model at the height of the center of the loop source. The current crowding within the CSF causes the current density with it to reach the maximum levels in the head.

outer boundary of the head volume (skin-air boundary). There might also be instances in which an averaging surface cannot be extracted at all. For these cases, no compensating measures were taken, however the reduced set of measurement points was taken into account before averaging. This shortcoming is unlikely to lead to an underestimation of induced current density because, as can be seen in results (Figure 4.35), peak current density values are observed in the CSF, which is at least the length of the radius of the averaging circle away from skin-air boundary, and therefore the averaging area around the peak current densities will remain unaffected. Second, the limited model detail in terms of the tissue detail can affect the results especially if tissue structures other than the CSF exist which can have the analogous effect of current crowding due to the higher conductivity. Although this is possible, the proximity of the CSF to the radiating loop is such that maximum fields will indeed appear within it as opposed to further away within the brain (the tissue detail between the CSF and skin is adequate).

4.6. Chapter conclusions

Two main issues were addressed in this Chapter. First, the modeling of ELF fields arising from GSM handsets has been presented. An equivalent source has been recommended which can simulate the observed fields in controlled experiments. It was concluded that a small current carrying loop can simulate fields adequately. Second, an exposure device for use in human volunteer experiments was designed and constructed. The device incorporated the developed ELF exposure model along with an RF exposure component representative of current GSM mobile phones. Both exposure sources were dosimetrically assessed and the results of physical and computational modeling were presented. Input levels to the two exposure modules, that will produce the desired exposure levels were recorded. The presented exposure setups (ELF and RF), as incorporated in the model handset, along with the determined input levels were used in the large sample size study that is described in Chapters 5 and 6 and 7.

5. Main Study - Design

This Chapter introduces the design of the main study of this thesis. The principal characteristics of this human volunteer study are its large sample size, and the mobile phone specific exposures in both RF and ELF domains. The Chapter includes:

- Rational leading to the specific experimental design
- Presentation of methodological improvements that arose from the small sample size human volunteer study described in Chapter 3
- Protocol
- Detailed experimental setup and
- Rational for methodologies of data analysis

5.1. Rational for experimental design

The investigations into short term effects on human brain activity under mobile phone radiation are ongoing and for good reason. The literature has thus far been inconclusive, although some trends have been demonstrated (see Chapter 2). The main trend is that of increased alpha band activity both during and shortly after exposure, (up to one hour), to PM RF fields. The effect is usually observed in brain regions closest to the exposure source [35]. However, there are issues that prevent direct comparison between studies which relate to the experimental protocols. These encompass duration and type of exposures, durations of EEG monitoring, methods of analysis and statistical

strength of results. There are some main experimental design characteristics that are increasingly recognized as essential for the results of studies to carry more weight. These have been outlined by several sources including a recent literature review by Valentini et al., human volunteers studies such as the one presented in Chapter 3, the study of Curcio et al. and Croft et al. [36, 133, 35]. As some recent studies have incorporated most or all necessary methodological characteristics in their design, the observed alpha band increase effect gains more weight, and it becomes harder to dismiss as a random fluctuation of the EEG. Despite the fact that a few studies demonstrated this increase only a subset of those, the more recent ones, have incorporated these methodological improvements [35, 36]. Currently there is insufficient evidence to conclude beyond doubt that the alpha band increase observed in some studies is a real effect. For this reason replication studies are necessary.

It has been argued that modulation of RF fields is a necessary signal characteristic to elicit alpha band power increase in the resting EEG. Accordingly, the present study was primarily designed to test the hypothesis that PM RF but not CW RF radiation can increase the resting brain alpha activity. Huber et al., performed such an investigation in a small study that employed 15 participants [58]. In that study, the authors matched SAR levels between the two exposures so as to ensure that differences in observed effects between the two cannot be attributed to any thermal mechanisms. It follows that in those experiments, to achieve identical SARs between two exposures that differ in the time domain, different instantaneous peak field levels needed to be employed. So, inherent in their exposures were the differences between the PM RF and CW RF instantaneous peak fields. Under the PM RF exposure, a resting alpha band power increase was observed. A subsequent study by the same group did observe an alpha increase but in a different time interval [**?**]. However, through their experimental design it cannot be clear whether the observed effect under the PM RF signal is due to the presence of the pulsing or due to the increased instantaneous peak RF exposure. One can proceed through a new exposure protocol to determine whether these two exposures, PM and CW RF, if set to identical instantaneous peak field values, produce a similar outcome and thereby

determine if the observed effect can be attributed to the peak RF field instead of the pulsed nature. This was the approach followed in the present study.

In addition, the protocol was expanded to incorporate an ELF exposure component which replicates exposures that accompany typical GSM mobile phone handsets. As detailed in Chapter 4, these pulsed ELF fields originate from the operation of the battery/electronics of GSM handsets. Since they are of ELF form, and even though they contain the same frequency components as their RF modulated counterpart, it is possible that if they interact with resting brain activity, they do so through a different mechanism. These field components are only comparable to RF exposures in terms of their time domain characteristics, that is identical time domain structure. They are otherwise different, and exposure wise, cannot be compared due to the difference in established mechanisms of interaction between the two frequency ranges, whereby the RF radiation induces tissue heating, and ELF fields induce current flow inside tissue.

PM RF and ELF exposures were set to contain all time structure components found in the Discontinuous Transmission (DTX) mode. The approach followed by Huber et al. of modifying the time structure of the DTX mode by adding extra time slots so as to minimize the instantaneous peak field difference between CW and PM RF was not employed here [58]. To the contrary, the time structure of the DTX mode was employed as would be found in handsets operating GSM network. This makes results more applicable to real mobile phone use. This concept also extends into the spatial field characteristics that were used by Huber et al., where homogeneous unlike mobile phone exposures were opted for, as opposed to the mobile phone-like, highly localized exposures employed here. Of course this decision is not without its drawbacks whereby the inter-subject variability in exposure is significantly higher than that of the Huber et al. setup. However this discount in dose accuracy establishes the mobile phone related outcome that is the basic characteristic of this study. Discussions and comparisons between handset based and homogeneous based exposures were reported by Schmid et al. [124].

In the design of such human volunteer studies the selection of single day versus multiple day protocol is a crucial one. Each approach carries specific advantages and disadvantages. In a multiple day protocol one needs to consider the week-to-week variability of the resting EEG which, if large enough, could potentially mask radiation related changes [122]. With equal importance, due to the finite resources available, one needs to consider the subsequent limitations imposed on the interpretation of results arising from a reduced size study. For the specific study, a four-fold increase in experimental sessions (in comparison to the single day protocol) would be required, a factor which will inevitably have an impact of reduction on the recruited sample size. The major positive element of a multiple day protocol is the reduced chance of carry over effects, through sufficient time separation, typically employed as a week between sessions. Typically, however, in multiple day protocols abstinence from mobile phone use is only monitored during the last few hours before the experiment. So the washout period is in the order of a few hours and not days as is implied by the weekly separation of experiments. Nevertheless the multiple day protocol is superior to the single day proposed here, since washout periods can be in the order of hours versus minutes respectively.

In a single day protocol, one needs to consider the magnitude and time course of carry over effects, and the impact of other compromises that need to be made, such as extended testing time, in order to accommodate for multiple exposures in a limited time frame. Carry-over effects of length comparable to that of the duration of the protocol can be a problem. Literature has shown mixed results to this extend where carry over effects have, (see references [58, **?**], and have not, (see reference [35]), been observed. The bulk of carry-over effects can be accounted for by condition counterbalancing. In addition statistical methods can also aid to further reduce the variability of measures that do not relate to the experimental condition, which among others include carry-over effects.

It is desirable to maximize the exposure duration so as to allow for sufficient signal to noise ratios as well as cumulative effects to occur [34]. If a similar protocol to that of the small sample study

is employed here the experiment will span two hours, while exposures will span 14 minutes. It is desirable to expand the exposure periods to 20 minutes. However, since two hours of experimental time is already long, subject fatigue will introduce notable variability in the resting EEG [94]. For this reason, It is not considered as a good choice to expand the experimental time even further. Instead, baseline and post exposure periods can be reduced to 5 minutes from 7 minutes and the extra time can be used to expand exposure intervals from 14 minutes to 20. This way, experimental time and subject fatigue are kept the same, while exposure intervals are maximized.

None of the disadvantages associated with the single day protocol are considered big enough to prevent detection of subtle spectral EEG effects. On the contrary, the increased sample size that can be achieved through a single day protocol, provides a considerable advantage that addresses a large gap in literature. Based on these discussions the single day protocol is considered a better option and is thus selected for this study.

In short the main requirements of this study are that it must:

- Be able to detect changes in the frequency spectra of the EEG relating to the experimental condition
- Be able to compare PM RF with CW RF whose instantaneous peak field levels are identical
- Incorporate an ELF exposure component that has identical time domain characteristics to those of the PM RF component, and
- Recruit a large sample size, a characteristic that is achieved through the implementation of a single day protocol

In the next Section some important methodological improvements to the design of this study, as identified through the execution of the pilot study, are presented.

5.2. Improvement to methodology

In Chapter 3 methodological limitations to the experimental design were identified and appropriate recommendations for the improvement of protocols were presented. This section features the steps taken to avoid the identified limitations i the present study by implementing those recommendations.

5.2.1. Minimizing EEG variance through EOG correction

In Section 3.5.1, three possible ways with which EOG artifacts can influence the outcome of these experiments have been listed. It was recommended that an EOG correction, instead of rejection approach, would be superior. With the migration of the study to a 64 channel amplifier as well as a larger amplification range, it becomes feasible to implement EOG correction. Standard automated algorithms are available with which to perform the EOG correction without introducing any bias through human intervention. An example of this is the RAAA method, which was selected for this study [33].

5.2.2. Addressing the noise susceptibility of the EEG recording hardware

The noise susceptibility to pulsed RF fields of the Mindset^{TM}-MS1000 EEG amplifier system has been demonstrated and discussed in Chapter 3. Since the main study is to be migrated to a Neuroscan Synamps^{2TM} system it remains to determine whether a similar effect is observed in the new equipment. Experimental design and results to address this are presented next.

5.2.2.1. Experimental setup

To assess this source of noise it would be preferable to do so in the absence of any real EEG voltages, which for the purposes of this investigation will act as a source of noise that can obscure the outcome. Instead, a conducting volume (with permittivity and conductivity values close to those of a real head) can be used to simulate the real head volume. In addition to further approximate the real

case scenario, it would be desirable to electrically connect the EEG electrodes to the surface of the phantom. The latter cannot be achieved with a plastic phantom. A watermelon provides with a good solution for this application since it can approximate the volume conducting properties of real head due to its high water content, ($e_{r-water} = 87$, $e_{r-Brain\,Grey\,Matter} = 83$, $e_{r-Brain\,White\,Matter} = 59$, see also reference [67]), and in addition electrical connection of the electrodes can be achieved allowing for the simulation of electrode impedance values.

Setup Three electrodes (ground, reference and active electrode) were connected to a water melon (from here on the watermelon is referred to as the dummy head). To simulate the electrical properties of the connections, electrode impedances were kept below 10 kΩ, using standard methods such as the application of conducting gel. The RF emitting device was placed first close to the dummy head (within 10 cm away from the active electrode) and second, in the proximity of the Synamps^{2TM} headbox unit. A DTX like pulse modulated RF signal was used for the experiment. The signal had the same structure as the one used during actual human exposures, however the signal amplitude was increased two-fold in order to maximize any noise induction and increase the probability of detecting it. Three minute spectral averages of dummy-EEG time series were produced for each of RF, ELF, and Sham radiation conditions The same signal processing procedures as those performed on the real EEG data of human participants were employed here, excluding the EOG artifact correction routine.

5.2.2.2. Results

The results clearly demonstrate that during the presence of the RF source the EEG spectra are significantly distorted, see Figure 5.1. Additionally the double blinding design of the study can be violated, since the experimenter can be in a position to visualize the presence of the noise and therefore deduce the condition of exposure.

Despite the in-band nature of the ELF exposure field with the EEG, no noise was detected. It

is likely that this is attributed to the low level and highly localized field intensity emitted by the designed ELF source.

Shielding specifications and construction

After demonstrating the susceptibility of the Synamps^{2TM} system to pulsed modulated RF fields, appropriate measures need to be taken to prevent it. To shield against the RF interference, an Electromagnetic Interference Interference, (EMI) shielding box needs to be constructed. It must be capable of reducing high frequency interference to a minimum while permitting unattenuated ELF current flow (at least up to 100 Hz). The box, was constructed out of two folded aluminum sheets, (box and lid). Any joints within each of these pieces was covered with adhesive copper layers after the removal of the outer oxidized layer of aluminum. To ensure that leakage does not take place through the gap between the box and the lid, EMI gasket was fitted on the entire perimeter of the lid. To prevent RF currents from penetrating the box through the EEG electrode leads, each lead was fed through the shielded box via an individual π-section filter. The selected filters, (TUSONIX 4209-053), at least 65 dB of attenuation at 900 MHz. To avoid leakage through any gaps at the feed through points for the π-filters, a second enclosure was incorporated, see Figure 5.2, which covered the collection of π-filters. In addition, the cable connecting the Synamps^{2TM} head box to the amplifier unit also needs to be shielded. As this cable is only carrying digitized signals, there is no concern for noise susceptibility of outgoing signals. However, RF currents can be conducted to the inside of the box and for this reason the cable needs to be shielded. This is achieved via ferrite loading of the cable on the inside and outside of the shielded box, and in addition, enclosing the cable on the outside of the box with a copper mesh that is grounded to the shielded box. As for the Synamps^{2TM} amplifier boxes, they are adequately shielded as is, sufficiently far from the EMF sources, and once more, the digitized nature of signals is an added assurance that RF noise cannot affect them.

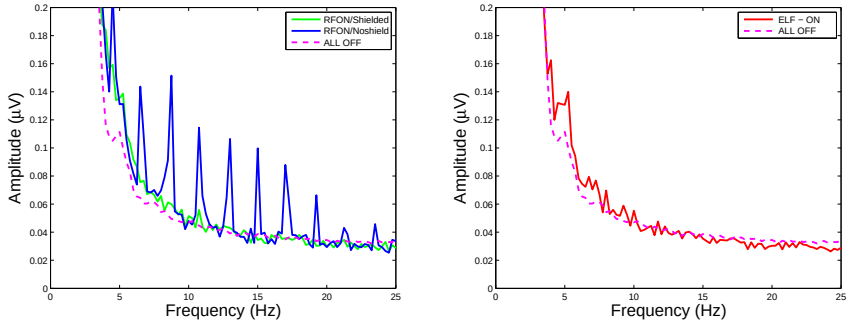

(a) (b)

Figure 5.1.: Spectral output from the EEG amplifier are shown as obtained from the three minute recordings. RFON/shielded; Recording in the presence of RF radiation and shielding box, RFON/NoShield; Recording in the presence of RF radiation without the shielding box, ALL OFF; Recording in the absence of radiation and with the presence of the shielding box and ELF ON; Recording in the presence of ELF radiation and shielding box. Noise susceptibility is detected only during the presence of the RF EMF but when shielding was introduced the noise source was no longer detectable. The smoother curve of the ALL OFF period arises due to the longer recording interval (30 minutes as opposed to 3) which improves the signal to noise ratio.

Figure 5.1, demonstrates the effect of shielding on the recorded signal in the presence of the PM RF and ELF EMFs. The clearly distinct peaks under the PM RF radiation that occur in the absence of the shielding box, are significantly suppressed with the introduction of the shielding box. Although some leakage may be observed in the lower spectrum (< 7 Hz), the possibility of this occurring in the real experiment is remote because the radiation levels would be at least half of those used for this experimental investigation.

5.2.3. Maximizing exposure duration

In the pilot study presented in Chapter 3, exposure durations were set at 14 minutes. In this study, the exposure periods are increased to 20 minutes but at the same time the total experimental time is kept the same (30 minutes total per condition). This is achieved by shortening the baseline and post

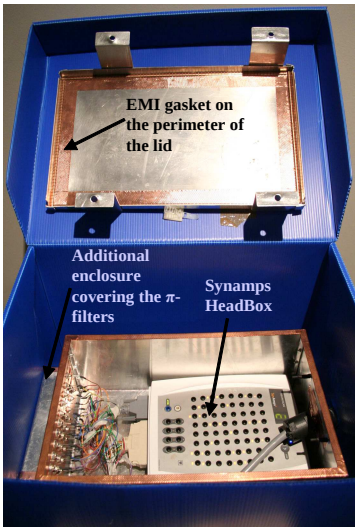

Figure 5.2.: The shielded box is shown opened with the lid at the top of the picture and the box below it. The EMI gasket which ensures adequate contact between the lid and box is also marked (two clamps ensure sufficient pressure between the lid and the box). The additional enclosure for the π-filters is also marked and so is the Synamps^{2TM} headbox.

exposure monitoring periods. These modifications render the protocol more suitable for detection of acute as well as cumulative effects of radiation.

5.3. Protocol

Following multiple evidences, coming from independent laboratories, of alpha band power increase during and after exposure, see Table 2.1, the protocol of this study focuses on detecting such effects. In contrast to most studies where event related potentials and performance tasks were incorporated in parallel to the resting EEG monitoring, this study steers away from such measures since the predominant trend in those indices is that they remain unaffected under RF exposures. Instead, a long interval (greater than 5 minutes) of true resting EEG can be recorded.

To accommodate for a large sample size, (n $>$ 60), a single day protocol was selected. Figure 5.3 shows the experimental protocol. There are four experimental sessions and each lasts for 30 minutes.

During each session, the first 5 minutes serve as the baseline, the next 20 have an active or a Sham exposure present, and the last 5 minutes serve as a post exposure monitoring period. In each interval participants received one of four conditions, Sham, CW RF, PM RF and ELF electromagnetic exposures. The order of exposure was randomly assigned in a fully counter balanced double blind cross-over design. With four experimental conditions 24 sequences of exposure are generated (see Appendix C.1). In these sequences each condition occurs equally as a first, second, third, and fourth exposure. A 4 minute break was allocated between half hour intervals where participants were asked to complete an AD-ACL questionnaire and were then allowed to stretch and drink water. Electrophysiological readings were recorded continuously while participants were seated comfortably with eyes open. Although the characteristic alpha peak is suppressed during eyes open when compared with eyes closed, due to the length of recording intervals the eyes open condition will help avoid large fluctuations in alertness. A second reason reason for employing an eyes open protocol, arises from the expectation that alpha activity may increase. By employing an eyes open protocol, alpha activity has room to increase without potentially reaching any ceiling effect. Half way through each thirty minute exposure, participants were asked if they felt comfortable. In addition if any signs of drowsiness were observed through the EEG recording, (since no visual contact was allowed between subject and experimenter), the participant was addressed and reminded to keep their eyes open.

The compromise of a single day protocol was identified as the possibility of carry-over effects from one condition to any of the subsequent ones. Some evidence exists in support of the alpha band EEG increase 30, but not 0 or 60 minutes post exposure, (see reference [**?**]), immediately after exposure, (see reference [58]), shortly after, (see reference [36]), and no spectral changes in the first 10 minutes post exposure, (see reference [35]). No clear trend arises from the results of these studies regarding the time course of the effect after exposure cessation. Therefore, it is unclear whether carry over effects will compromise the outcome of the study. The advantages, however, that arise

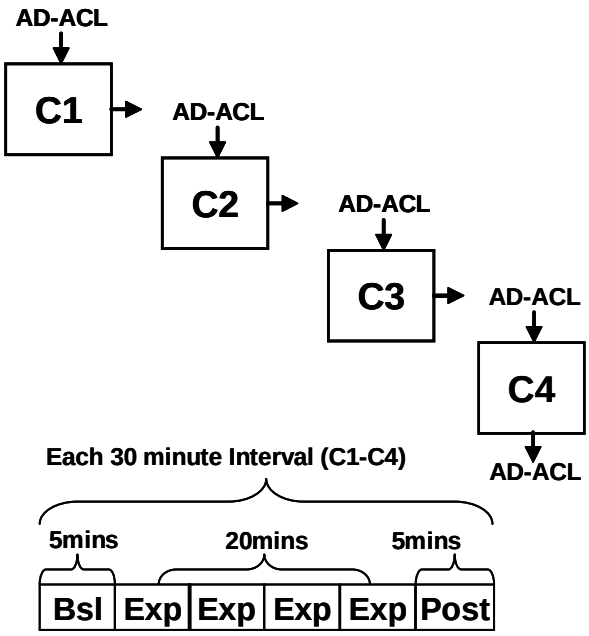

Figure 5.3.: The protocol. Each Condition (C1-C4) is randomly assigned to one of four exposure conditions CW-RF, PM-RF, ELF and Sham and lasts for 20 minutes. Before and after each condition an AD-ACL questionnaire is administered.

from the employment of a single day protocol outweigh the potential disadvantage of a carry over effect. The implementation of the moving baseline partly guards against those carry-over effects that extend through out the duration of the subsequent experimental interval, but has little effect on those carry-over effects that are transient within the duration of the subsequent experimental interval.[1]. An additional strong point of the moving baseline protocol is that it also guards against drifts in arousal which can have an impact on the EEG spectrum during the 2 hours of experiment. More detail on the issue of carry-over effects is found in Section 5.5.

5.4. Experimental setup

5.4.1. Participants

Seventy two healthy volunteers (35 female and 37 male) participated in the study. The mean age of the sample was 24.5 years and the standard deviation was 5.4 years. Participants were instructed to abstain from alcohol consumption within the 24 hours before the experiment, and abstain from mobile phone use and caffeine consumption within the six hours before the experiment. The Human Research Ethics Committees of RMIT and Swinburne Universities approved the study protocol. Written informed consent, see Appendix C.2, was obtained from all participants prior to any experimental procedures. A monetary reimbursement was made available to participants who concluded the experiment. Participants were informed that they were free to withdraw from the study at any stage.

5.4.2. Questionnaires

After signing the informed consent form participants were required to complete a screening questionnaire, see Section C.2, before the start of the experiment, Appendix C.2. The AD/ACL was also

[1] "Experimental interval": refers to the collection of baseline exposure interval and post exposure interval which make up the complete half hour interval.

administered five times throughout the experiment, at the start, in between the half hour intervals, and at the end. It was used to obtain indications of participant's activation/deactivation levels, see Appendix C.4 .

5.4.3. Double Blinding

Exposure sequences were controlled through a software programmable microcontroller (M16C). To facilitate double blinding, twelve versions of coded exposures were created in which the exposure sequences were mixed up and recorded, Table C.1. The corresponding software implementations of these twelve different exposures sequences were then created and passed to a person unassociated with the experiments. That person performed a random selection of one code realization which was then recorded and uploaded on the microcontroller. Validation of microcontroller operation was performed by a fourth person, again unassociated with the experiments, before acquiring any experimental data. As such, the sequences remained unknown to the experimenter until after data collection and analysis completion, where a successful verification of exposure sequences was again conducted.

5.4.4. Data Acquisition

Participants were fitted with a Compumedics Neuroscan 19 Channel Tin QuickCap employing the standard 10/20 international electrode positioning system. Reference levels were recorded from unlinked mastoids, (M1 and M2). The vertical and horizontal components of the EOG were also recorded. Data were recorded through the Synamps^{2TM} system with a sampling frequency of 250 Hz. Electrode impedances were kept below 5 kΩ at the start of the experiment. Recordings took place in an electromagnetically semi-shielded room. Apart from the subject under test the experimenter was present in the same room but no visual contact with the subject was possible.

5.4.5. Electromagnetic exposure characteristics

Exposures were delivered through the specially constructed model handset which was described in Chapter 4.

The handset was placed according to the standard ear to mouth position, on the right hemisphere. The speaker and antenna were located over the auditory canal. The phone was held in place with a specially constructed cradle, Figure 5.4 (see also Boutry et al. [18]). Additionally, another not radiating handset was placed on the left side of the head so as to avoid lateralization of participants' attention. Handsets were of the same appearance and weight.

CW RF exposures were set at a SAR level of 1.95 W/kg, just under the maximum permissible level of 2 W/kg. Peak RF fields during PM RF were kept equal to those of the CW RF exposure. The location of the peak averaged SAR inside the SAM phantom was presented in Section 4.5.1. The PM RF exposure, as measured by SAR, drops to 3% (0.06 W/kg) in comparison to the CW RF. This is a direct result of the time structure of the DTX mode where most time slots are switched off. Since we are interested in non-thermal effects, this arrangement allows to test the importance of the pulsing by keeping the peak field levels identical[2]. This arrangement builds on the findings of Huber et al. who concluded that the difference in effects between PM and CW RF are not due to a thermal effect, but rather an effect of the pulsing itself [58]. However, since their fields were not identical in terms of the instantaneous peak, the question remains as to whether this is purely an effect of the pulsing, or a threshold effect revealing a sensitivity of the EEG to the peak field levels, rather than the time structure of the field.

The ELF exposures were based on the exposure model that was presented in Chapter 4. Signal inputs to the loop structure were set as those defined in Table 4.3. The peak spatial averaged current density assessment was presented in Section 4.5.2 and was found to be less than 1% of the

[2]It can be argued that since SAR levels are different between the two exposures, the potential demonstration of an effect during the CW RF exposure could be attributed to a thermal phenomenon. However non thermal, as opposed to thermal, have been demonstrated for SAR values greater that the ones to be used here, [114]. As such there is sufficient confidence that thermal effects will not occur with the planned exposures.

Figure 5.4.: A depiction of the mobile phone head cradle which can support two mobile phone devices in the standard ear to mouth position. Here only one device is shown.

permitted maximum (see Table 4.8). It was also noted that the maximum occurred within the CSF.

5.5. Data analysis

5.5.1. Activation-Deactivation Adjective Checklist

The AD-ACL questionnaire was administered between half hour intervals, at the start of the experiment and at the end. Scoring was calculated through summation of the 4 sub-scales (activation: Energy, Tension and deactivation: Tiredness and Calmness) as described by Thayer [129]. Difference scores were calculated to reflect the change of activation/deactivation from the start of the experimental interval to the end, (the index was calculated as "after interval minus before interval" so that a positive value would represent an increase in activation). Four variables were formed, one for each exposure, and the differences between each of the active exposures in comparison to the Sham were assessed with Wilcoxon Signed Ranks tests as data could not be normalized.

5.5.2. Rational

Two sets of statistical analyses were considered. The first was a hypothesis driven one where specific findings reported in literature were addressed, that is, whether the alpha band of the EEG changes under EMF exposure and that the change would be larger at scalp sites closer to the exposure source. According to literature the expectation is that the effect would be apparent in pulsed modulated RF signals and pulsed ELF signals but not in continuous RF signals [58, 115, **?**, 114]. Double sided tests were implemented for both RF and ELF exposures. Owing to the hypothesis driven nature of these investigations no multiple comparison corrections were considered and so the statistical criterion for significance was kept at the $\alpha = 0.05$ level.

To obtain more information about the dataset, a set of exploratory analyses was planned. First analyses of the spectral estimates of the remaining EEG bands were considered. Second, changes in the signal complexity were assessed using the ApEn method. It is possible that non linear properties of the EEG can be altered under the presence of EMF and such changes would remain undetected under spectral analysis. Considering that the observed effect size in EEG spectral measures for the detection of acute radiation exposure effects is small (no more than 10% of spectral variation in the alpha band has been attributed to the exposure condition, see for example the study of Curcio et al. [36]), it is worthwhile exploring alternative methods of analysis. The non linear measure of ApEn was proposed as such an alternative and used in the small sample study that was presented in Chapter 3 (see also Appendix A.1 and Perentos et al. [110] for more details). Although no statistically significant changes of ApEn were observed, the method's appropriateness was not discounted due to the simultaneous absence of effect on the spectral content of the resting EEG. Under the same rational, the ApEn was used in the study reported here. The largest sample size employed here, provides with the opportunity to more thoroughly investigate whether this method provides with any supplemental or new information to the largely studied spectral estimates. More stringent statistical criteria were implemented on these exploratory investigations and these are

detailed in Section 5.5.4.

5.5.3. Data processing routines

Unless indicated otherwise EEG data were analysed with the EDIT 5.5.2 software (Scan 4.3, Compumedics^{TM}). It was observed that channels with large artifact can occur in cases where the channel impedance is less than 5 $k\Omega$. To ensure that such channels did not interfere with the analysis routine, in addition to the impedance criterion, channels containing large amplitude, continuous artifact were excluded from the analysis through visual inspection. This manual step was necessary to ensure that the automated algorithm which will reject epochs with voltages greater than ± 200 μV does not do so based on a single channel that is contaminated by continuous artifact as this would result in the loss of useful data. A flowchart of the data analysis procedure is shown in Figure 5.5. Data were subsequently re-referenced to the numerical average of the left and right mastoids (channels M1 and M2 respectively) and submitted through the RAAA automated artifact reduction routine [32]. EOG-corrected data were epoched in 4 second intervals, spline-fitted to 1024 samples and the mean was removed using DC correction as implemented by the baseline removal function of the EDIT 5.5.2 software (Scan 4.3, Compumedics^{TM}). Epochs which included data of voltages greater than ± 200 μV were considered to contain artifacts and were automatically rejected. Epochs were then grouped into six 5-minute intervals (pre, during 1, during 2, during 3, during 4, and post exposure).

At this stage, depending on the endpoint that is being examined, (amplitude spectra or signal regularity), data was either submitted through an FFT algorithm or the Approximate Entropy analysis routine respectively.

Spectral data Spectral estimates were obtained (10% cosine window, no overlap) for each 5-minute interval. Through those, average amplitudes of the nominal EEG bands were obtained. These were Delta (0 - 3.74), Theta (3.99 - 7.74 Hz), Alpha (7.99 - 12.73 Hz) and Beta (12.99 - 25.32 Hz).

Frequency resolution was 0.25 Hz.

ApEn data ApEn was calculated from the same 4 second intervals that were used to calculate spectral averages thereby maintaining consistency between data sets. The average ApEn of the collection of 4-second epochs in each 5-minute interval was calculated for all exposure conditions. To increase the signal to noise ratio and to decrease the amount of statistical comparisons, electrodes were grouped by averaging before analysis as follows: Left Frontal (LF = mean (Fp1, F3, F7)), Mid Frontal (Fz), Right Frontal (RF = mean (Fp2, F4, F8), Left Central (LC = mean (C3, T7)), Mid Central (Cz), Right Central (RC = mean (C4, T8), Left Posterior (LP = mean (P3, P7, O1)) Mid Posterior (Pz), and Right Posterior(RP = mean (P4, P8, O2). The flowchart presented in Figure 5.6 shows the detailed steps followed for the ApEn analysis. For the ApEn analysis multiple comparison corrections were taken into consideration due to the exploratory nature of the investigation (see Table 5.2 and Section 5.5.4.2).

Surrogate Data To demonstrate that the recorded EEG time series contained non linear features, a test which is based on surrogate analysis was employed. Using the Amplitude Adjusted Fourier Transform Method (AAFT), 10 surrogates data series were created for each 4 seconds epoch [130, 131]. This method calculates and retains the Fourier amplitude spectra of the original time series, but randomizes the phase information, and finally performs an inverse Fourier transform to create a surrogate series. This ensured that surrogates are restricted in terms of linear properties of the original data, but were otherwise random, see Figures 3.5 and 3.6. It is noted that a complexity analysis can be performed on data without evidence of non-linearity, but any differences between real and surrogate data would not necessarily insinuate the presence or variable degree of non-linearity. A t-test was performed on each real data series against its ten surrogates. With 9 degrees of freedom and a significance level of 0.05, a critical value of t=2.26 was obtained. Epochs with t-values exceeding the critical value were considered as containing non linear features.

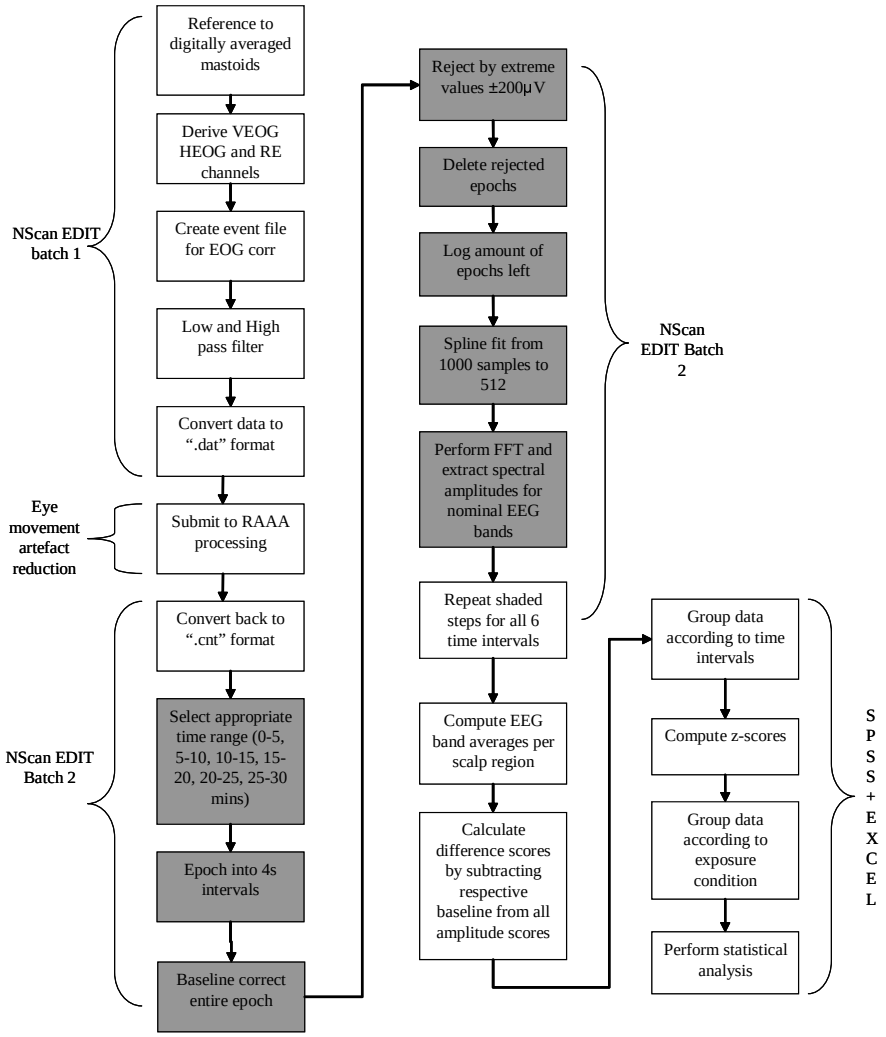

Figure 5.5.: The spectral analysis procedure is depicted here. The processing is predominantly automated excluding the first step and all steps involving the SPSS software. In the first step channels that are contaminated with continuous low amplitude artifact are replaced with an adjacent channel in order to ensure that low amplitude continuous artifact does not interfere with subsequent processing. Next the first of two automated batch routines (EDIT software) is executed, followed by the RAAA routine for eye movement reduction (implemented in Matlab^{TM}). The second EDIT batch routine follows which produces the final EEG spectral bands for each individual electrode. Data are then standardized using SPSS and are then ready for the statistical analysis..

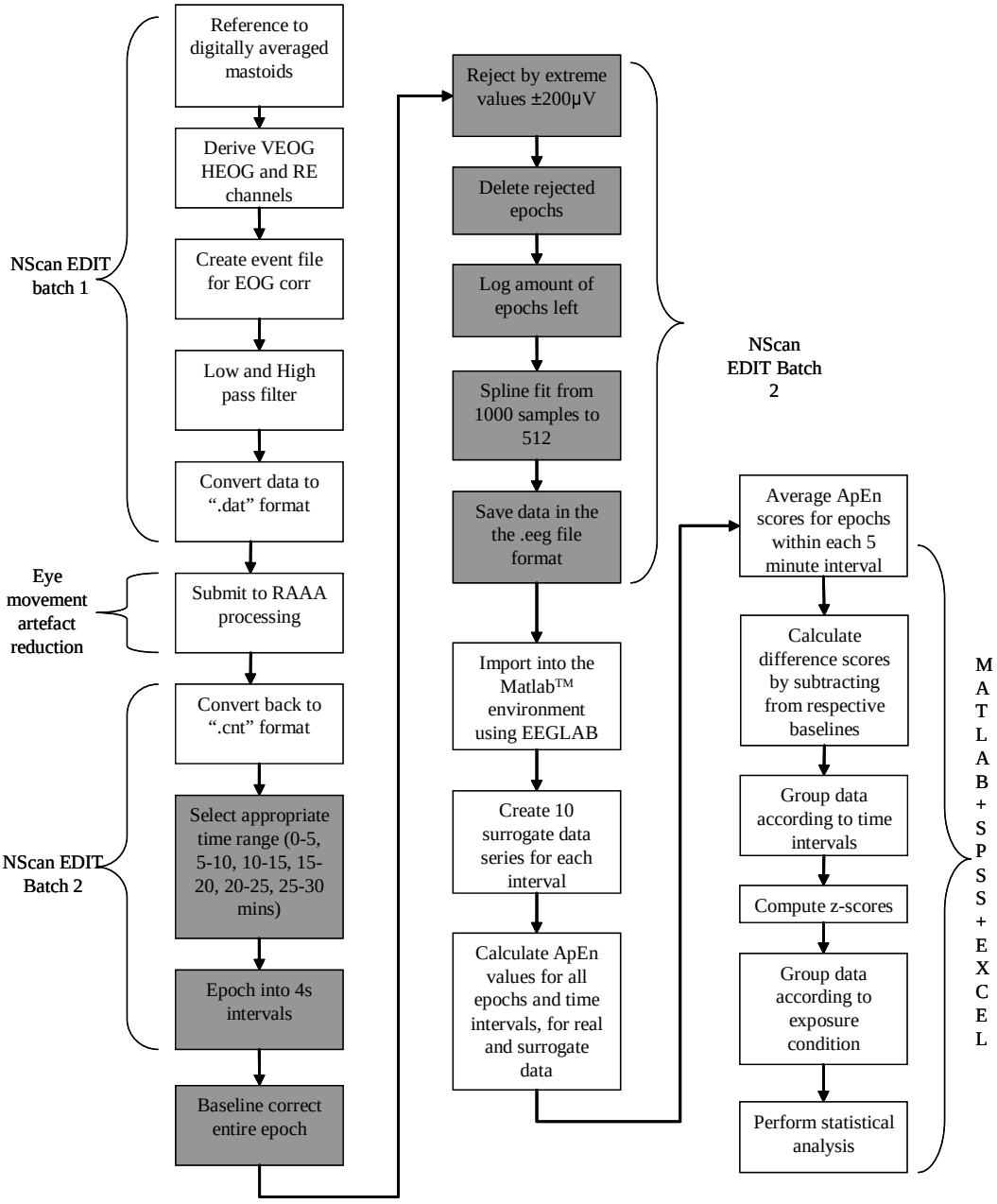

Figure 5.6.: The ApEn analysis procedure is depicted here. The processing is predominantly automated excluding the first step and all steps involving the SPSS software. The analysis is identical to that of spectral estimates up to the point that is marked as (A).Subsequently automated Matlab^{TM} scripts create surrogate data and calculate the ApEn values. Data are then standardized using SPSS and are then ready for the statistical analysis..

5.5.4. Statistical analysis

5.5.4.1. Spectral estimates

The statistical analysis was based on difference values (during exposure minus baseline and post exposure minus baseline), computed from the average spectral amplitude data of EEG bands, of pre exposure intervals to during, and post exposure intervals. Electrodes were grouped by averaging to reduce noise and the amount of statistical comparisons.

To remove any effects associated with the duration of experiment, data were grouped according to time intervals irrespective of exposure condition, (i.e. 1st 30 minutes 2nd, 3rd, and 4th), and corresponding z-scores were calculated for each interval. As such data of the complete sample per experimental interval had identical means of 0 and standard deviations of 1. As a significant amount of dependent variables failed normality tests and could not be normalized, non parametric statistical procedures were implemented. Significance was tested through Wilcoxon Signed Rank tests and where appropriate treatment effects were calculated with the Hodges-Lehmann estimate [91]. Since this non parametric procedure has limited flexibility in comparison to the alternative[3] parametric approach of RM-ANOVA, new variables were calculated to test specific a *priori* and exploratory hypotheses.

Hypothesis driven tests To test for main effects of exposure condition, difference values of alpha band activity over all during exposure intervals and all scalp regions were averaged so as to reflect a global alpha band change. Individual contrasts were then performed for each active exposure condition against the Sham. The same averaging procedure was employed for periods after cessation exposure. To test for the interaction of exposure condition with laterality (with respect to exposure) all alpha band difference levels (all time intervals and all sagittal regions) were grouped according

[3] A precise non-parametric equivalent to the RM-One-Way-ANOVA is the Friedman Test. However, in this design the interest lies in the specific contrasts between the active exposures and the Sham exposure, therefore the omnibus design is not necessary.

Table 5.1.: Electrodes are grouped according to location. This grouping allows for a reduced set of statistical comparisons and an improved signal to noise ratio of spectra.

		Laterality		
		Left	Midline	Right
Sagittality	Frontal	LF (Fp1, F3, F7)	MF (Fz)	RF (Fp2, F4, F8)
	Central	LC (C3, T7)	MC (Cz)	RC (C4, T8)
	Posterior	LP (P3, P7, O1)	MP (Pz)	RP (P4, P8, O2)

to laterality. Subsequently ipsilateral to contralateral differences were calculated for each exposure condition resulting in a total of four variables. The interaction of exposure condition with the ipsi/contra differences at central scalp derivations was also tested. Since the planned contrasts are designed to test the previous findings in literature of alpha band change during and after exposure in proximity to the exposure device, no multiple comparison corrections were performed on the obtained significance levels. Table 5.2 lists these planned comparisons analytically.

Exploratory tests In addition to the hypothesis driven tests described in the previous paragraph, the identical statistical analyses were implemented on the three remaining EEG bands (delta, theta and beta), see Table 5.2. The interaction of exposure condition with sagittality (frontal versus posterior) was also investigated for all four EEG bands. Owing to the exploratory nature of these statistical analyses, adjusted Bonferroni corrections were applied to significance values. To correct for multiple comparisons the Dubey/Armitage & Parmar method (D/AP) as outlined in Sankoh et al. was followed [8]. This is a variation of the Bonferroni method where the correlation of variables is considered when determining the adjusted rejection criterion. Compared to the Bonferroni correction, the D/AP method improves the chance of detecting statistically significant changes while maintain the Type II error at acceptable levels. With an overall correlation value of 0.1 and a total of 78 tests the comparison-wise significance criterion was lowered to 0.0009 thus retaining an experiment-wise error rate of 0.05.

Table 5.2.: The collection of the planned statistical comparisons, hypothesis and exploratory driven, and the number of contrasts per factor or factor interaction. C; Exposure Condition, dL; distal Laterality (Frontal and Posterior Right versus Frontal and Posterior Left), pL; proximal laterality (Central Right versus Central Left), L; Laterality (Frontal, Central and Posterior), S; Sagittality, χ; no comparisons performed.

	Factor or Factor interaction	Hypothesis Driven Tests [a]	Exploratory Tests [b]
Spectral	C	Alpha band (6)	Delta, Theta & Beta bands (18)
	C x dL (ipsi vs contra)	Alpha band (6)	Delta, Theta & Beta bands (18)
	C x S (posterior vs frontal and posterior vs central)	χ	Delta, Theta, Alpha & Beta bands (24)
	C x pL (ipsi vs contra)	Alpha band (6)	Delta, Theta & Beta bands (18)
Total comparisons		18	78
Significance Criterion		0.05	0.0009
Non Linear	C	χ	$\surd$ (6)
	C x L (ipsi vs contra)	χ	$\surd$ (6)
	C x S (posterior vs frontal and posterior vs central)	χ	$\surd$ (12)
Total comparisons		χ	24
Significance Criterion		χ	0.0028

[a] The significance criterion is kept at 0.05 for the hypothesis driven tests.

[b] Using the D/AP method the significance criterion is lowered to 0.0009 for all exploratory tests.

5.5.4.2. Signal complexity - ApEn measures

The statistical analysis was based on difference values computed from the average spectral amplitude data of EEG bands pre exposure to those during, and post exposure. Electrodes were grouped by averaging to reduce noise and the amount of statistical comparisons. Electrode groups were listed in Table 5.1.

To remove any effects associated with the duration of experiment, data were grouped according to time intervals irrespective of exposure condition (i.e. 1st 30 minutes 2nd, 3rd, and 4th) and corresponding z-scores were calculated for each interval. As such data of the complete sample per experimental interval have identical means of 0 and standard deviations of 1. Subsequently, statistical significance was tested with Repeated Measures Analysis of Variance (RM-ANOVA).

Significance was tested for main effects of exposure condition, the interaction of exposure condition with laterality and the interaction of exposure condition with sagittality. Since these planned contrasts were exploratory the D/AP method was implemented to account for multiple comparisons. With a correlation level of 0.094 between ApEn variables the significance criterion was lowered to 0.0028 so as to retain an experiment wise error rate of 0.05, see Table 5.2.

5.5.5. Testing the performance of the automated routines

A test was implemented that allowed to check whether the automated routines performed as expected. This was achieved by comparing the final output of the automated routine with the output of a manual routine. Following a random selection of a final SPSS reading (subject, exposure period, 5 minute sub-interval, scalp location and EEG band) the original raw EEG amplitude-time data was retrieved from storage. A simplified manual analysis procedure was implemented that excluded digital re referencing, the eye artifact reduction routine and automated extreme value rejection. Instead, a crude manual rejection of large artifact was performed and spectral averages were calculated with the manual execution of EDIT commands. With the direction of change replicated using

this largely independent procedure, there is increased confidence regarding the performance of the automated data routines (outlined in Figures 5.5 and 5.6).

5.6. Conclusion

This Chapter has presented the rational for the design, the experimental setup, and the data analysis planning of the study. The design of the study is optimized to accommodate for the detection of acute effects of PM RF, CW RF, and ELF radiation (during exposure, or shortly after cessation) while maintaining a sample size that is significantly larger than the majority of relevant[4] studies. The data analysis was separated into hypothesis driven, implemented to test the specific finding reported in literature of changes in alpha band activity during and shortly after exposure, and exploratory, implemented to investigate changes in the remaining classical EEG bands and the non-linear features of EEG. Statistical significance criteria were more stringent for the exploratory analysis in comparison to the hypothesis driven analysis.

[4]Relevant studies are considered those that investigated the effect of mobile phone-like radiation on the brain during waking or sleep. The three largest studies have recruited 40 [36], 50 [90] and 120 [50, 35]participants. With a sample size of 72, this study is the second largest.

6. Main Study - Results

This Chapter presents the results of the main study. First the sample characteristics are outlined and questionnaire results are presented. The second section presents the results of the hypothesis-driven investigation, that is whether the alpha band resting-EEG activity is changed under GSM-like RF GSM-like ELF. The third section presents the results of the exploratory analysis which include the extended analyses of the remaining EEG bands, (delta theta and beta) and the non linear analysis using the ApEn method. Results are subdivided further into those during exposure, and those post exposure. For a detailed description of planned statistical comparisons refer to Table 5.2.

6.1. Sample characteristics, questionnaire responses and miscellaneous data trends

In total 75 subjects were recruited out of which 72 completed all experimental procedures. The results presented here are based on the recordings of those 72 (35 female) participants with a mean age of 24.5 years and a standard deviation of 5.4 years.

Participants' data were screened after processing to ensure that a sufficient amount of epochs per five minute experimental interval, more than 15 (equivalent to 1 minute), had survived. The average amount of epochs throughout the sample was found to be 52 with a standard deviation of 9. There were no instances of less than 15 epochs per five minute interval so none of the subjects were excluded from the analysis.

Table 6.1.: The results of the AD/ACL questionnaires. No significant differences were observed between any of the active exposure groups in comparison to the Sham exposure.

	PMRF-Sham	CWRF-Sham	ELF-Sham
Z(71)	-1.091	-0.048	-0.738
p	0.275	0.962	0.461

6.1.1. Activation-Deactivation Adjective Checklist

The AD-ACL questionnaire revealed no statistical changes in subject activation and deactivation levels associated with any of the active exposure conditions in comparison to the Sham condition. Results are presented in Table 6.1.

6.1.2. Data time trends

A general increase in the means of the EEG band amplitudes was observed throughout the 2 hour interval, see Figure 6.1. The source of this trend is not immediately clear but could be attributed to either an increase in white noise mediated by an increased amplifier temperature, or a real brain activity.

An experimental procedure was implemented to assess whether the observed trend is a by-product of the Synamps^{2TM} amplifier unit. This was achieved by repeating the experimental protocol in the absence of any real EEG data. To simulate the volume condition properties and impedances of a real head with the absence of EEG voltages a watermelon was used as a dummy head. In addition to the 'real' experimental procedure, background ELF noise measurements at the vicinity of the dummy head were recorded. A total of three 2-hour experiments were performed and the results are shown in Figure 6.2.

A trend opposite and much smaller than the one required to explain the increase in the real human data was observed, whereby the background noise amplitude spectra are seen to reduce as a function of time. The reduction is of the order of 0.05 μV as opposed to the increased in the

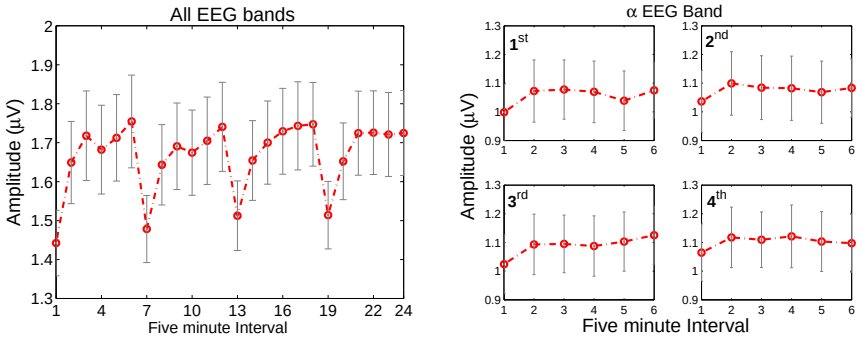

(a) (b)

Figure 6.1.: Data time trends (independent of exposure condition). In total, there was 4 thirty minute intervals amounting to 24 five-minute intervals. On average there was a tendency of spectral amplitudes to increase throughout the duration of the experiment.(a) full spectrum, (b) alpha band, 1^{st}; First 30 minute interval, 2^{nd}; Second 30 minute interval, 3^{rd}; Third 30 minute interval and 4^{th}; Fourth 30 minute interval

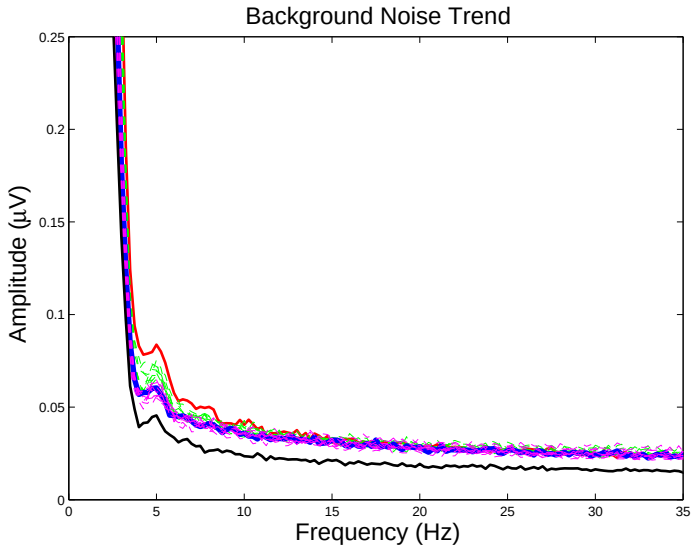

Figure 6.2.: Spectral averages of three 2-hour experiments. Each curve represents a 5-minute spectral average. A decreasing noise trend as a function of time is observed. Red line; 1^{st} 5-minute interval, Green lines; 2-11^{th} intervals, Blue line; 12^{th} interval, Purple lines; 13-23^{rd} and Black line; 24^{th} interval.

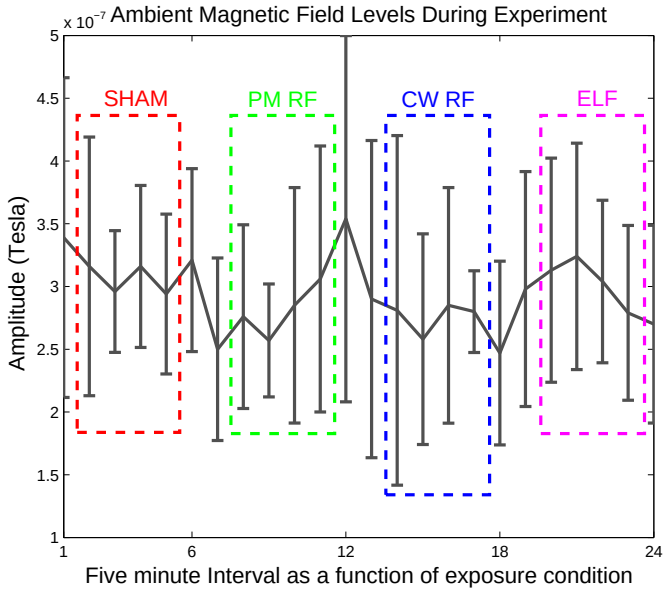

Figure 6.3.: Ambient magnetic field levels during experiment. No changes are evident with respect to exposure condition.

real human data which ranges from 1 to 3 μV. Based on these observations it seems likely that the spectral increases observed throughout the recording are a real EEG effect as opposed to an artifact related to the experimental setup.

Ambient Magnetic Fields The ambient magnetic fields in the vicinity of the participants were also measured during the experiment described above and the results are shown in Figure 6.3. Magnetic fields are very similar for all experimental intervals, so these ambient fields are not expected to influence the experiment.

6.2. Hypothesis-driven investigation (EEG alpha band changes)

6.2.1. During exposure

6.2.1.1. PM RF exposure

Under The PM RF exposure the tendency of the alpha band activity to increase was significantly lower in comparison to the Sham condition, ($Z(71) = -2.003$; $p = 0.045$; $\theta = -0.169$)[1]. Exposure condition did not interact with neither distal nor proximal laterality. Raw amplitude averages for all lateralities are shown in Table 6.2. Spectral averages by scalp region before and during Sham exposure are shown in Figure 6.4, and in Figure 6.5 for the PM RF exposure.

Table 6.2.: Alpha band means and standard deviations, $\mu(\sigma)$, before (PRE) and during (DUR) exposure. Values are expressed as raw amplitudes.

EEG	Sham		PM RF		CW RF		ELF	
Derivation	PRE	DUR	PRE	DUR	PRE	DUR	PRE	DUR
Contralateral	0.90	0.97	0.95	0.98	0.94	0.98	0.92	0.98
	(.04)	(.05)	(.05)	(.05)	(.04)	(.05)	(.05)	(.05)
Midline	1.15	1.26	1.23	1.27	1.21	1.27	1.19	1.26
	(.06)	(.06)	(.07)	(.99)	(.06)	(.99)	(.06)	(.07)
Ipsilateral	0.90	0.98	0.95	0.99	0.95	0.99	0.93	0.99
	(.04)	(.05)	(.05)	(.05)	(.04)	(.05)	(.05)	(.05)
Global	0.99	1.07	1.04	1.09	1.03	1.07	1.01	1.08
	(.05)	(.05)	(.06)	(0.05)	(.05)	(.05)	(.05)	(.05)

6.2.1.2. CW RF exposure

During CW RF exposure there were no significant changes in comparison to the Sham exposure. However, there were trend level interactions between exposure condition and distal laterality ($Z(71) = -1.734$; $p = 0.082$; $\theta = -0.393$, ipsi/contra difference) and between exposure condition and proximal laterality, ($Z(71) = -1.745$; $p = 0.081$; $\theta = -0.318$), both representing decreases in

[1]The symbol θ represents the Hodges-Lehman estimate of treatment effect, [91]. It does not represent the effect size since it corresponds to a treatment effect on ranks and not the actual medians of the populations.

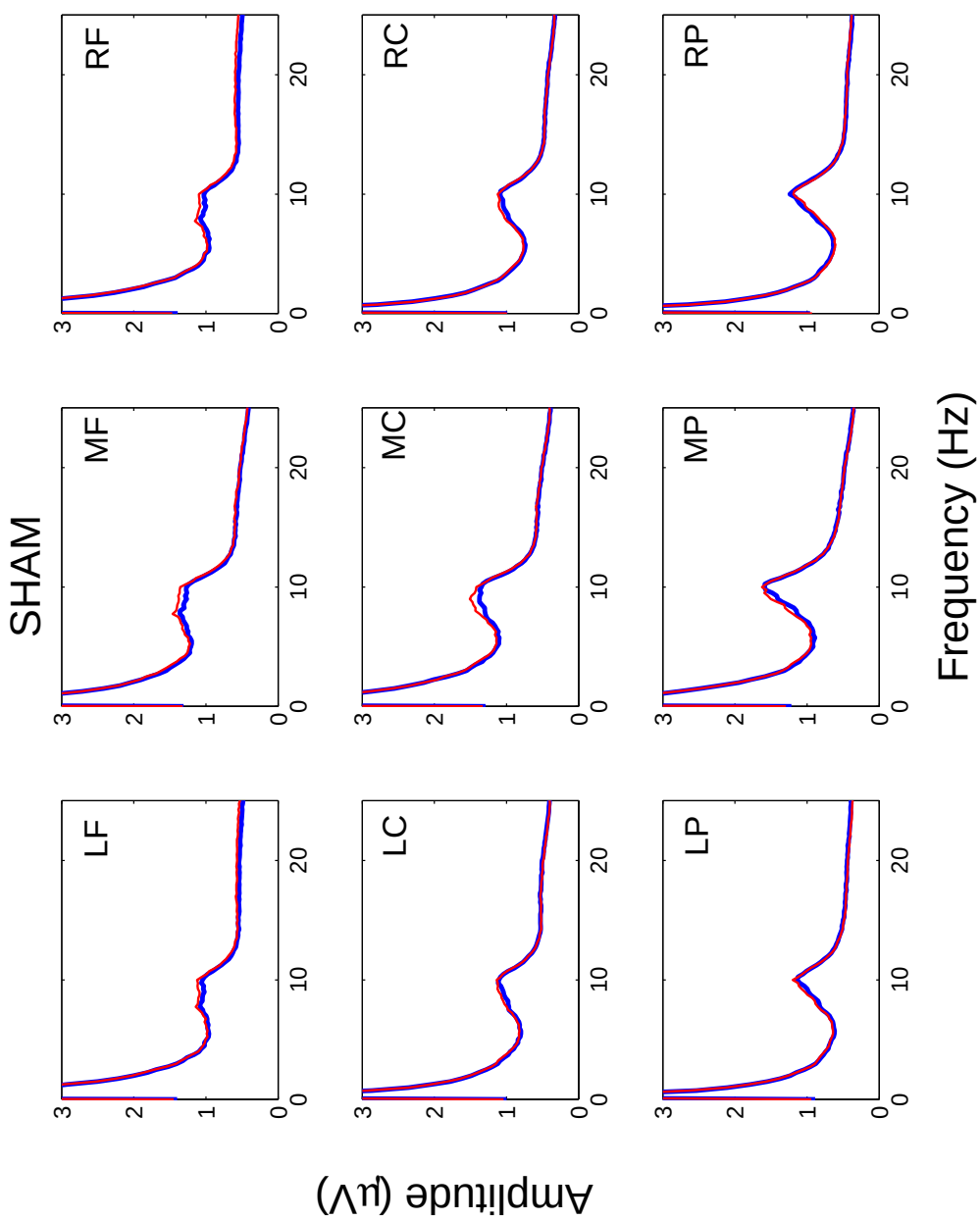

Figure 6.4.: Raw amplitude spectra before (blue line) and during (red line) Sham exposure are displayed for each of the nine scalp regions (LF; Left Frontal, MF; Mid Frontal, RF; Right Frontal, LC; Left Central, MC, Mid Central, RC; Right Central, LP; Left Posterior, MP; Mid Posterior, RP; Right Posterior).

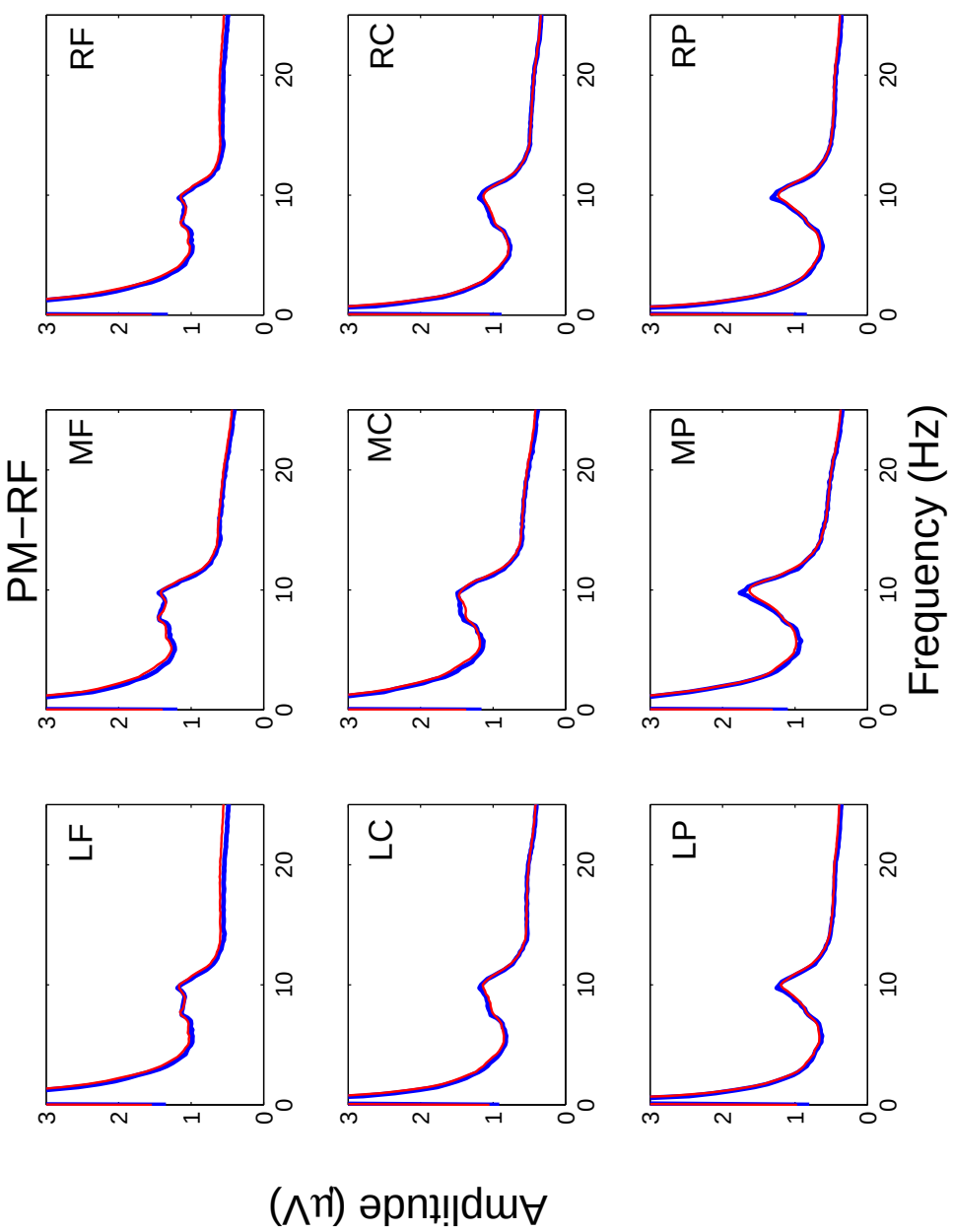

Figure 6.5.: Raw amplitude spectra before (blue line) and during (red line) PM RF exposure are displayed for each of the nine scalp regions (LF; Left Frontal, MF; Mid Frontal, RF; Right Frontal, LC; Left Central, MC, Mid Central, RC; Right Central, LP; Left Posterior, MP; Mid Posterior, RP; Right Posterior).

the ipsilateral alpha activity in comparison to Sham. Raw amplitude averages for all lateralities are shown in Table 6.2. Spectral averages by scalp region before and during CW RF exposure are shown in Figure 6.6.

6.2.1.3. ELF exposure

During ELF exposure there was a statistically significant interaction of exposure condition with proximal laterality ($Z(71) = -2.2781$; $p = 0.023$; $\theta = -0.383$, $ipsi/contra\,difference$) representing a decreased alpha activity. No statistically significant changes were observed for the interaction of exposure condition with distal laterality. Raw amplitude averages for all lateralities are shown in Table 6.2. Spectral averages by scalp region before and during ELF exposure are shown in Figure 6.7. Difference amplitude spectra are shown in Figures 6.8 and 6.9 for all exposure conditions.

6.2.2. After exposure

6.2.2.1. PM RF, CW RF and ELF exposures

No statistical changes were observed for any of the active exposure conditions in comparison to the Sham condition for neither the main factor of exposure condition nor the interaction of exposure condition with distal or proximal laterality. Raw amplitude averages for all exposure conditions and lateralities are shown in Table 6.3. Spectral averages by scalp region are shown in Figures 6.10 to 6.13 for all exposure conditions..

6.3. Exploratory investigation

The exploratory analysis incorporates the spectral and the non linear analysis based on the ApEn. The planned statistical contrasts are outlined in Table 5.2.

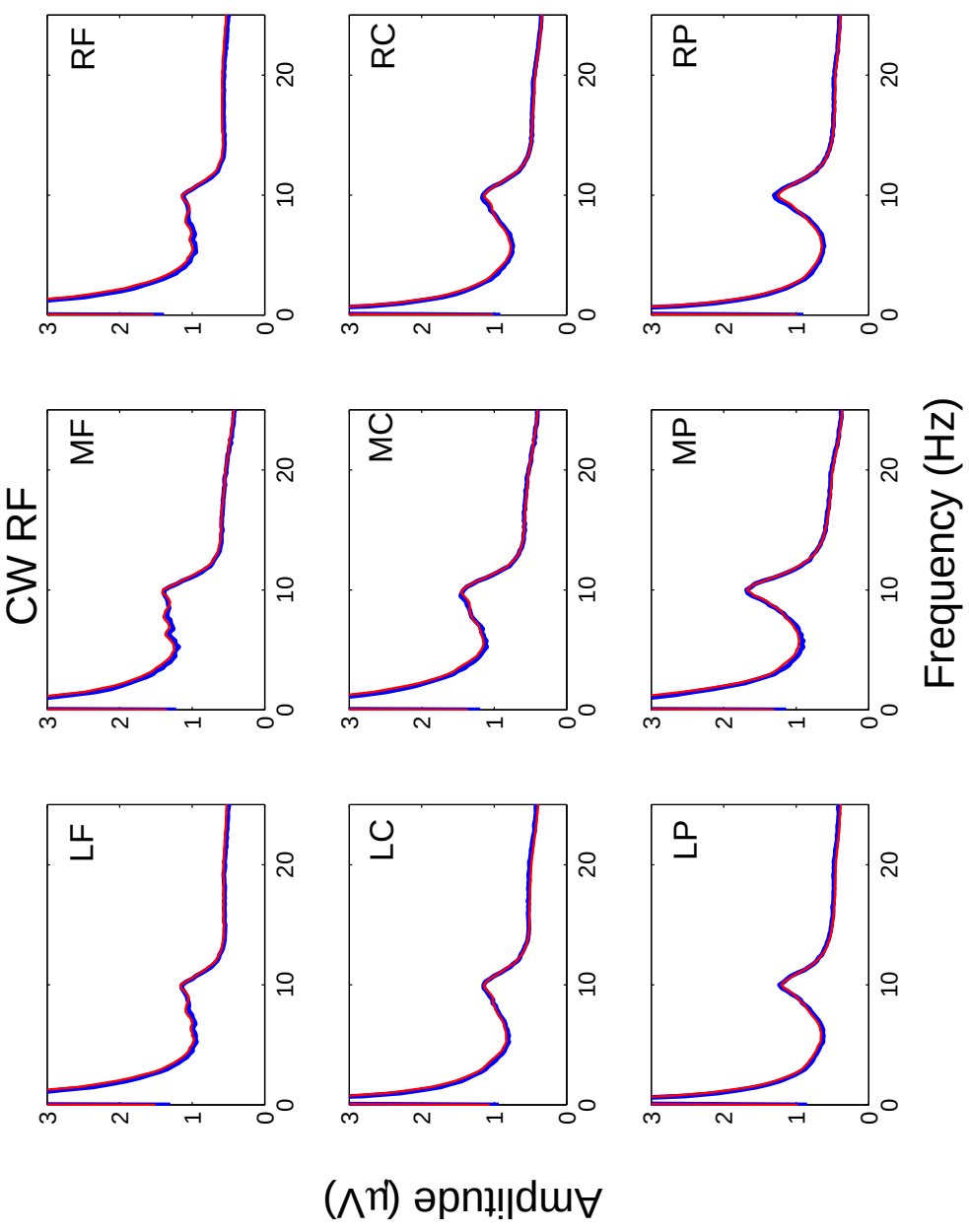

Figure 6.6.: Raw amplitude spectra before (blue line) and during (red line) CW RF exposure are displayed for each of the nine scalp regions (LF; Left Frontal, MF; Mid Frontal, RF; Right Frontal, LC; Left Central, MC, Mid Central, RC; Right Central, LP; Left Posterior, MP; Mid Posterior, RP; Right Posterior).

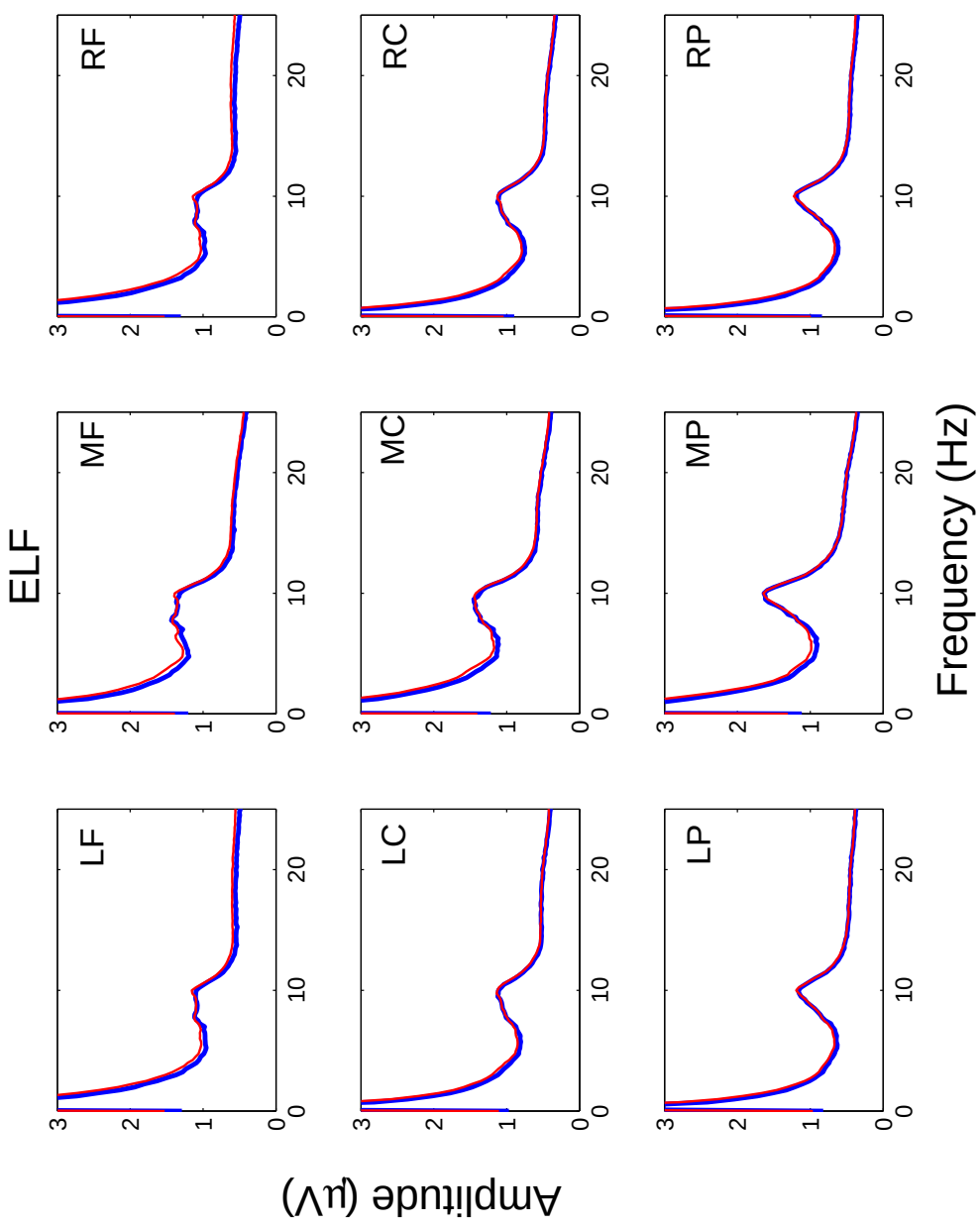

Figure 6.7.: Raw amplitude spectra before (blue line) and during (red line) ELF exposure are displayed for each of the nine scalp regions (LF; Left Frontal, MF; Mid Frontal, RF; Right Frontal, LC; Left Central, MC, Mid Central, RC; Right Central, LP; Left Posterior, MP; Mid Posterior, RP; Right Posterior).

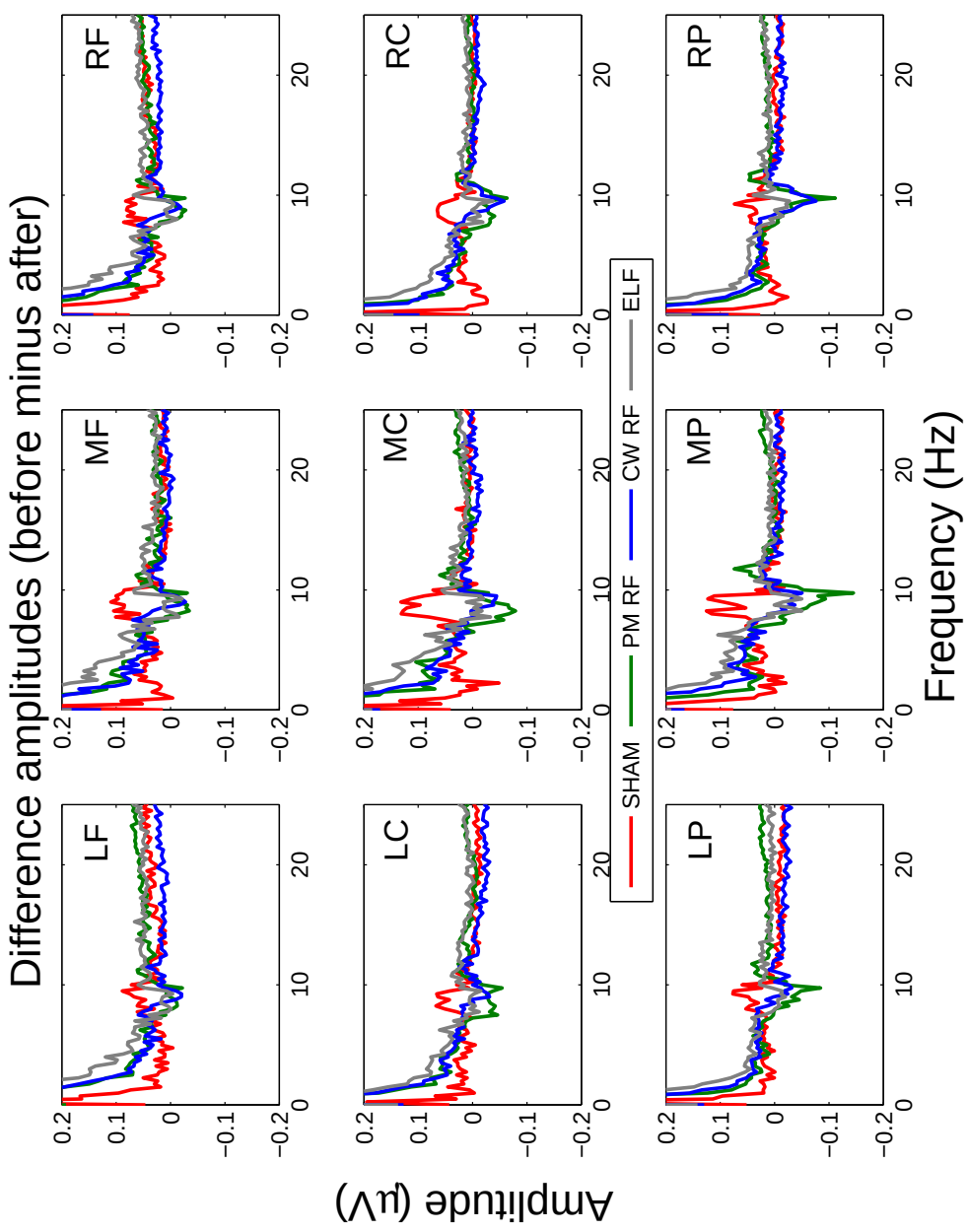

Figure 6.8.: Amplitude differences (during minus before exposure) are plotted for each exposure condition and at each scalp region separately. A general increase in the alpha band (8 -13 Hz) can be observed during the Sham exposure as opposed to the general decrease that is observed during all active exposures. (LF; Left Frontal, MF; Mid Frontal, RF; Right Frontal, LC; Left Central, MC, Mid Central, RC; Right Central, LP; Left Posterior, MP; Mid Posterior, RP; Right Posterior)

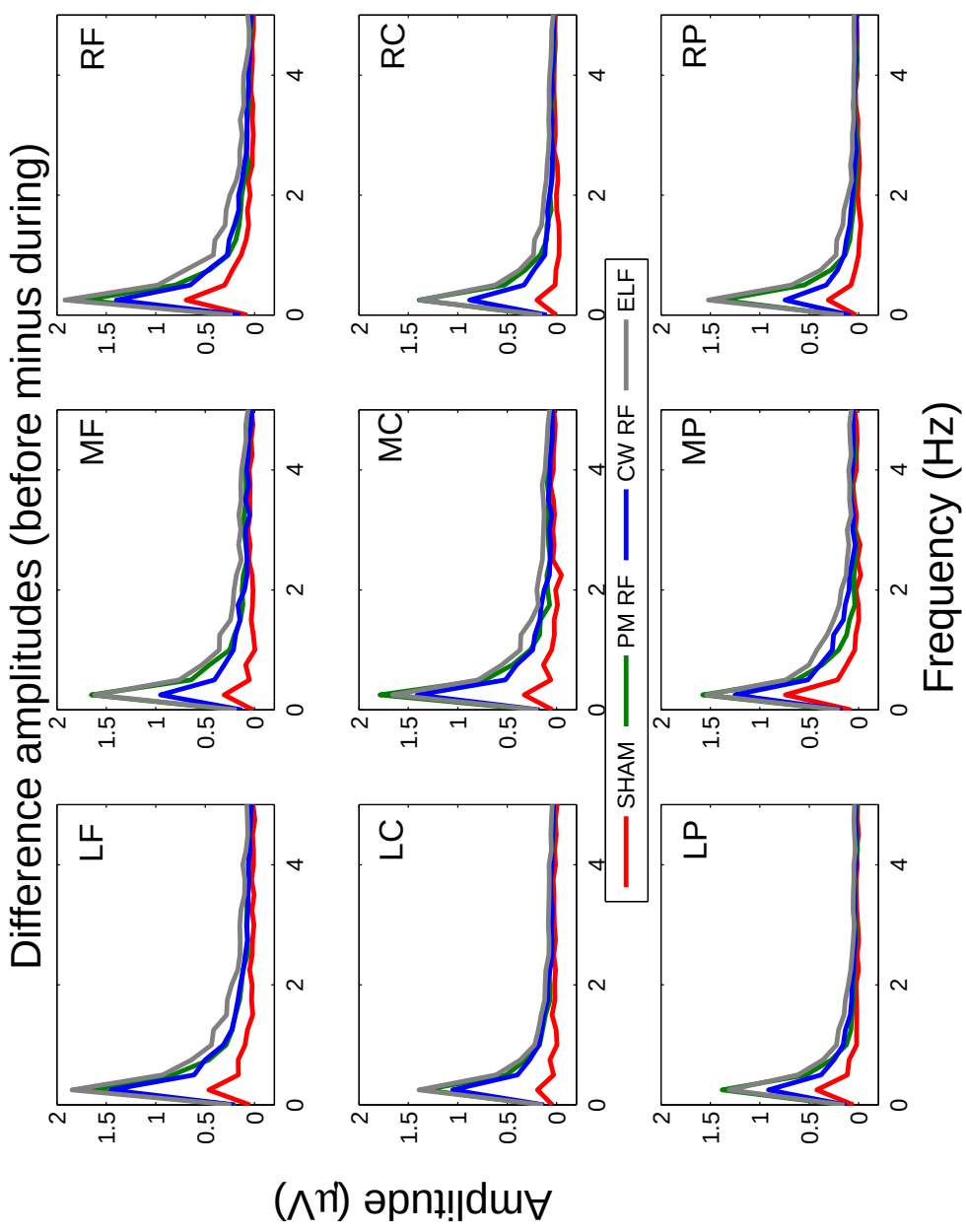

Figure 6.9.: Amplitude differences (during minus before exposure) are plotted for each exposure condition and at each scalp region separately. A larger increase in the slow waves, (up to 2 Hz), can be observed during all active exposure conditions in comparison to Sham. (LF; Left Frontal, MF; Mid Frontal, RF; Right Frontal, LC; Left Central, MC, Mid Central, RC; Right Central, LP; Left Posterior, MP; Mid Posterior, RP; Right Posterior)

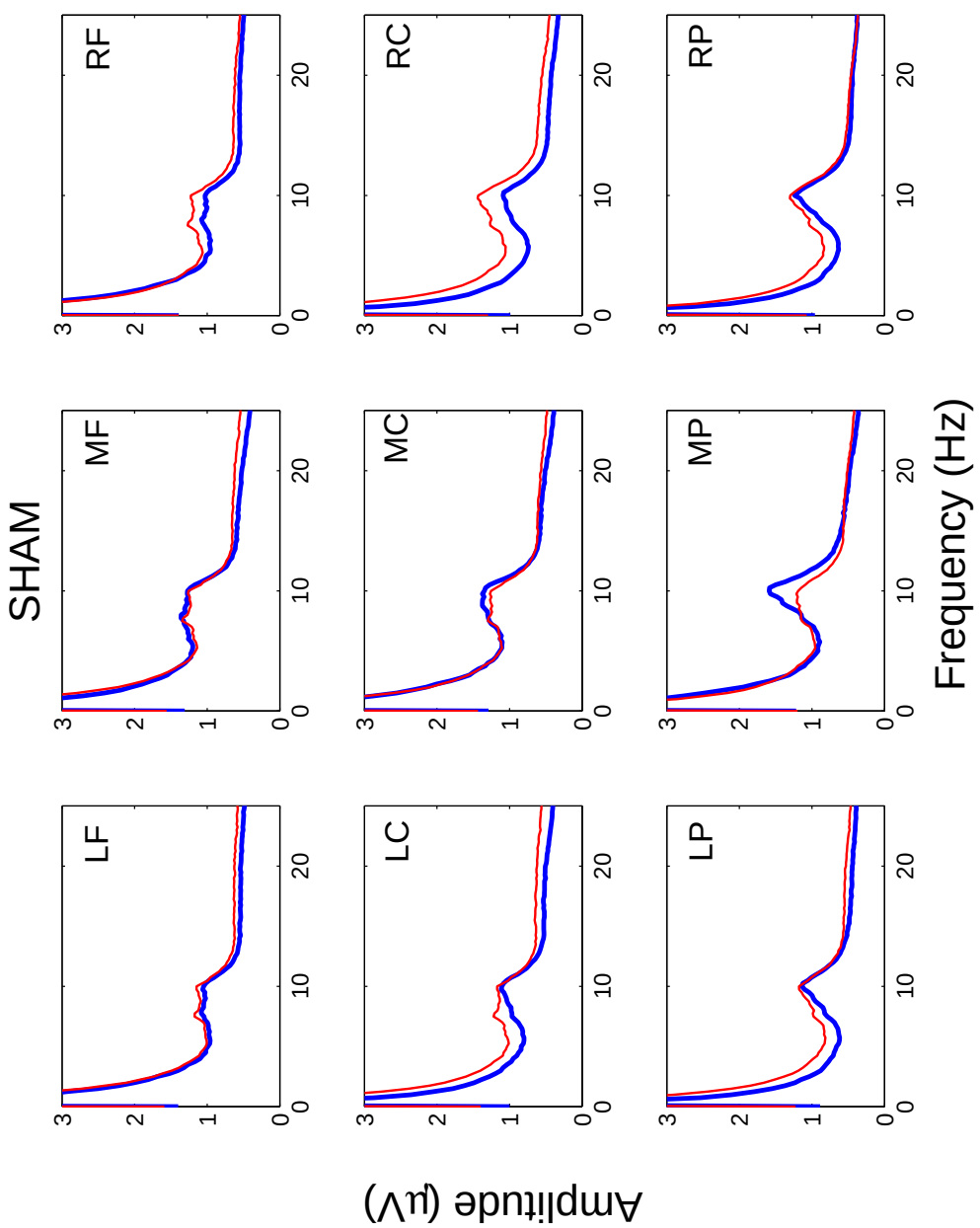

Figure 6.10.: Raw amplitude spectra before (blue line) and after (red line) Sham exposure are displayed for each of the nine scalp regions (LF; Left Frontal, MF; Mid Frontal, RF; Right Frontal, LC; Left Central, MC, Mid Central, RC; Right Central, LP; Left Posterior, MP; Mid Posterior, RP; Right Posterior).

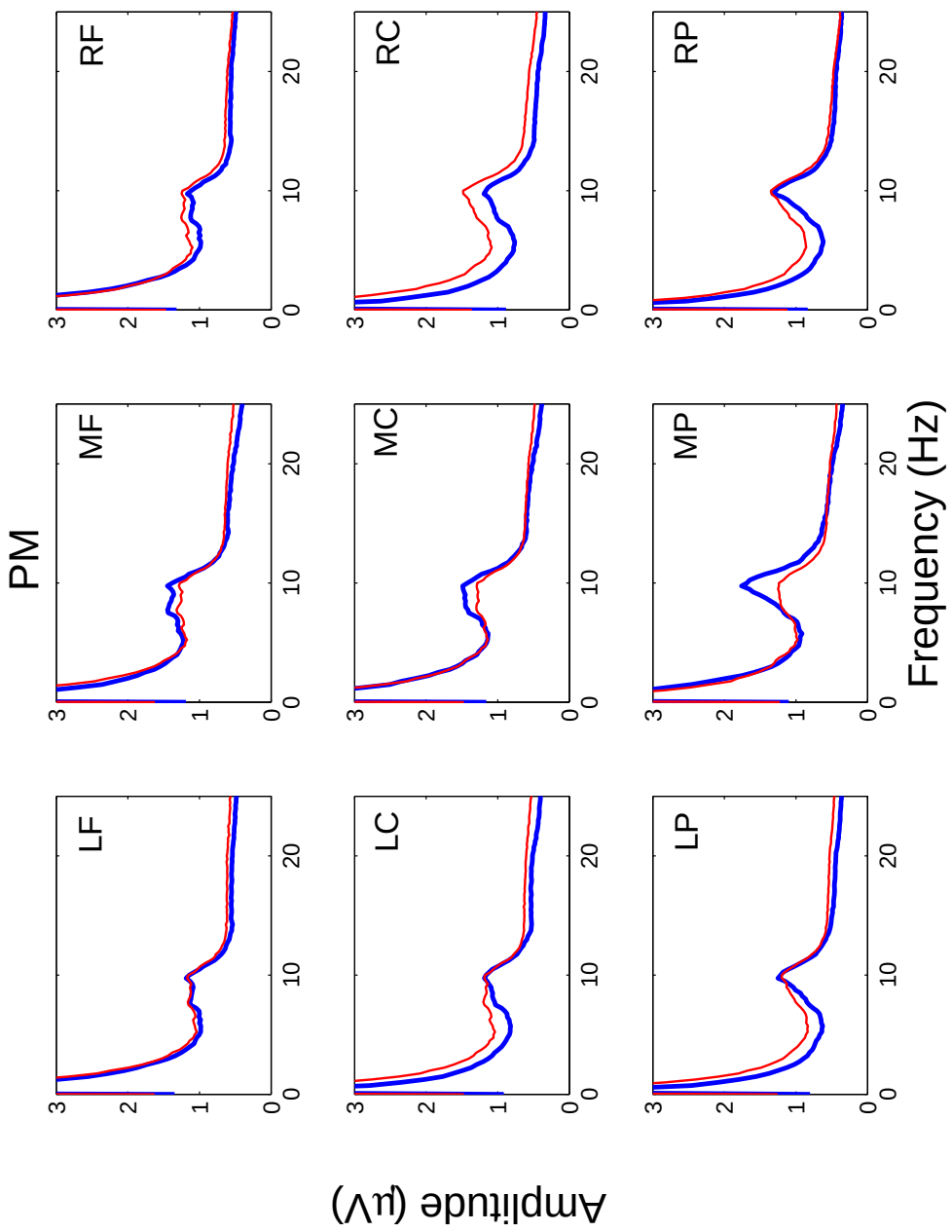

Figure 6.11.: Raw amplitude spectra before (blue line) and after (red line) PM RF exposure are displayed for each of the nine scalp regions (LF; Left Frontal, MF; Mid Frontal, RF; Right Frontal, LC; Left Central, MC, Mid Central, RC; Right Central, LP; Left Posterior, MP; Mid Posterior, RP; Right Posterior).

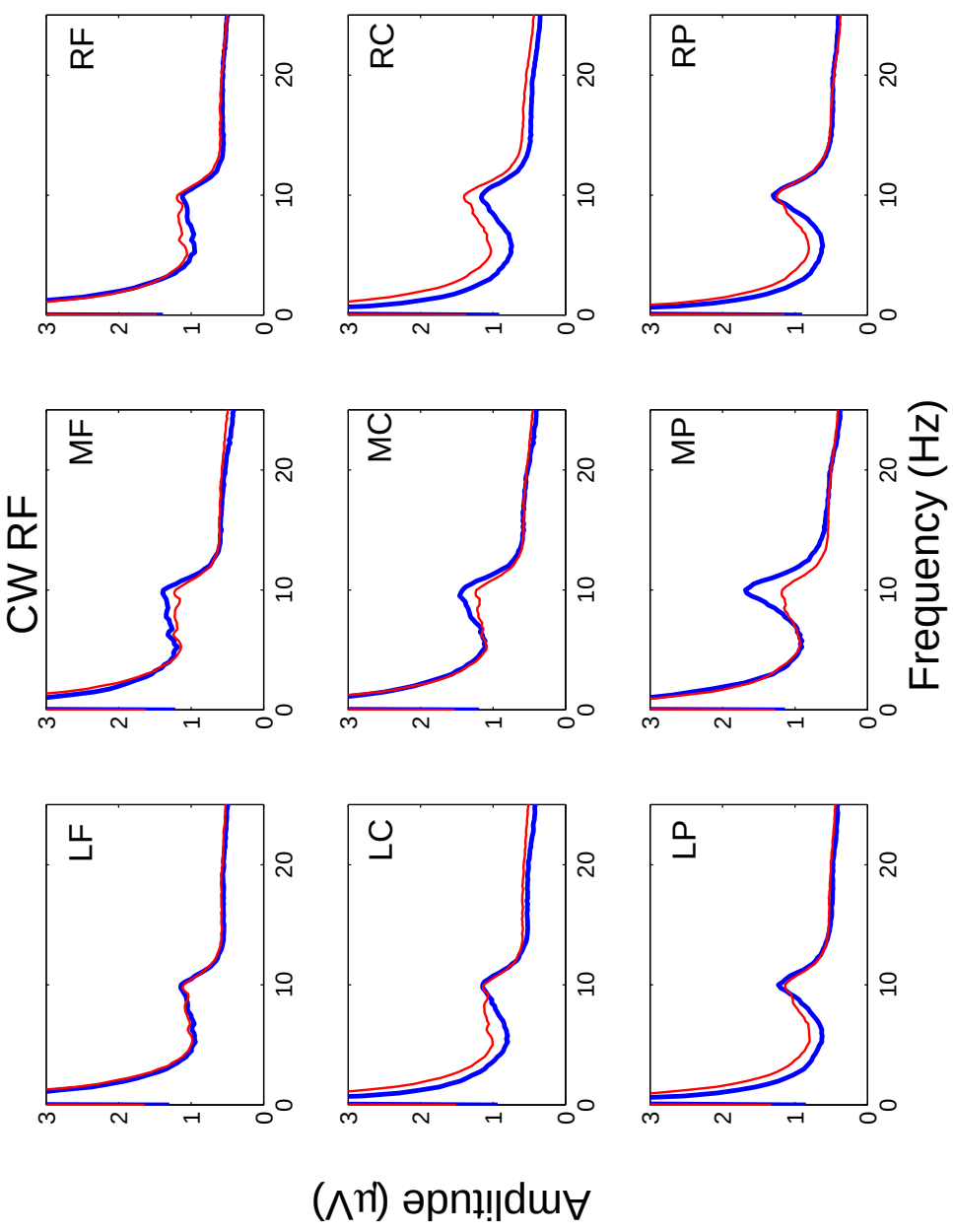

Figure 6.12.: Raw amplitude spectra before (blue line) and after (red line) PM RF exposure are displayed for each of the nine scalp regions (LF; Left Frontal, MF; Mid Frontal, RF; Right Frontal, LC; Left Central, MC, Mid Central, RC; Right Central, LP; Left Posterior, MP; Mid Posterior, RP; Right Posterior).

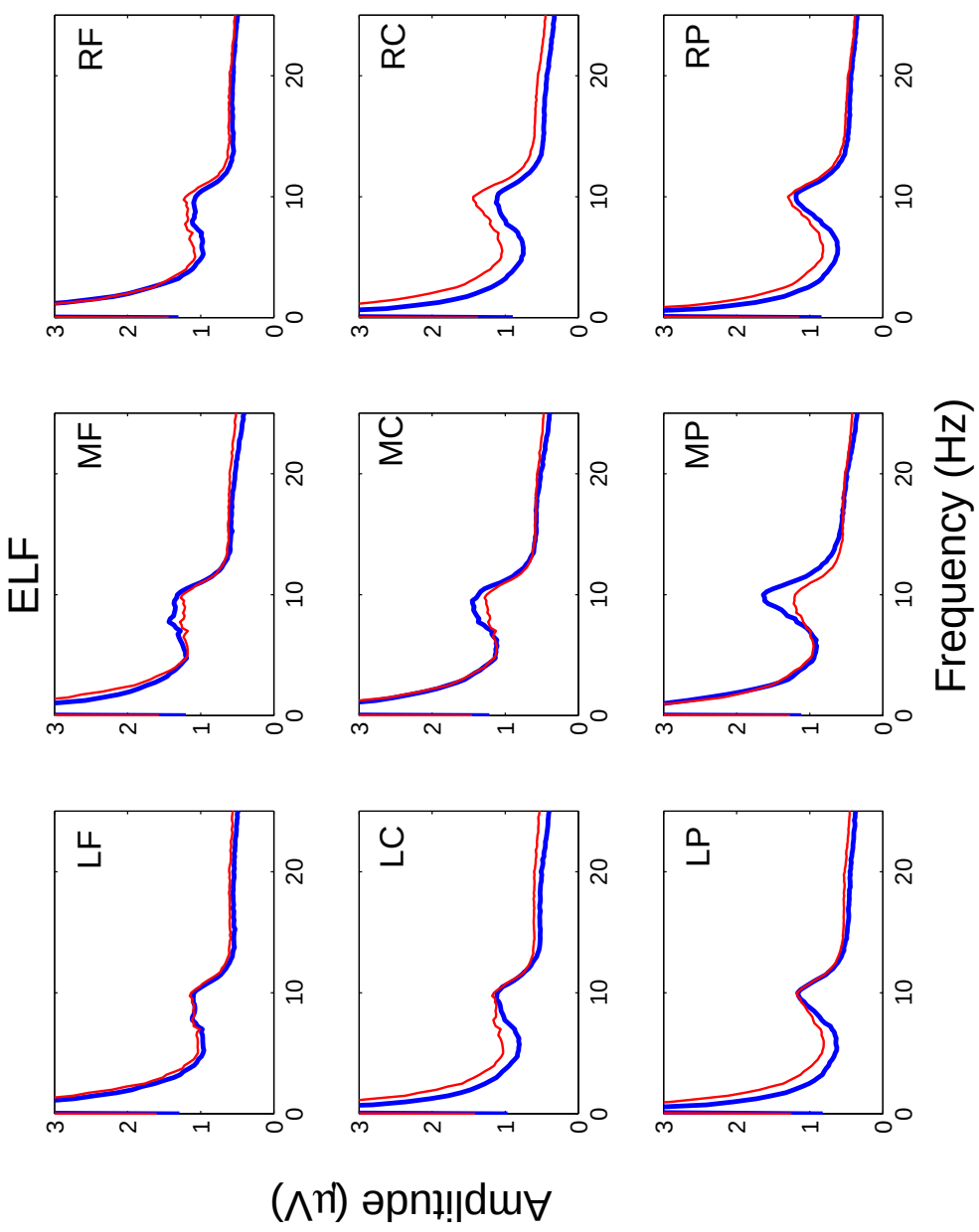

Figure 6.13.: Raw amplitude spectra before (blue line) and after (red line) CW RF exposure are displayed for each of the nine scalp regions (LF; Left Frontal, MF; Mid Frontal, RF; Right Frontal, LC; Left Central, MC, Mid Central, RC; Right Central, LP; Left Posterior, MP; Mid Posterior, RP; Right Posterior).

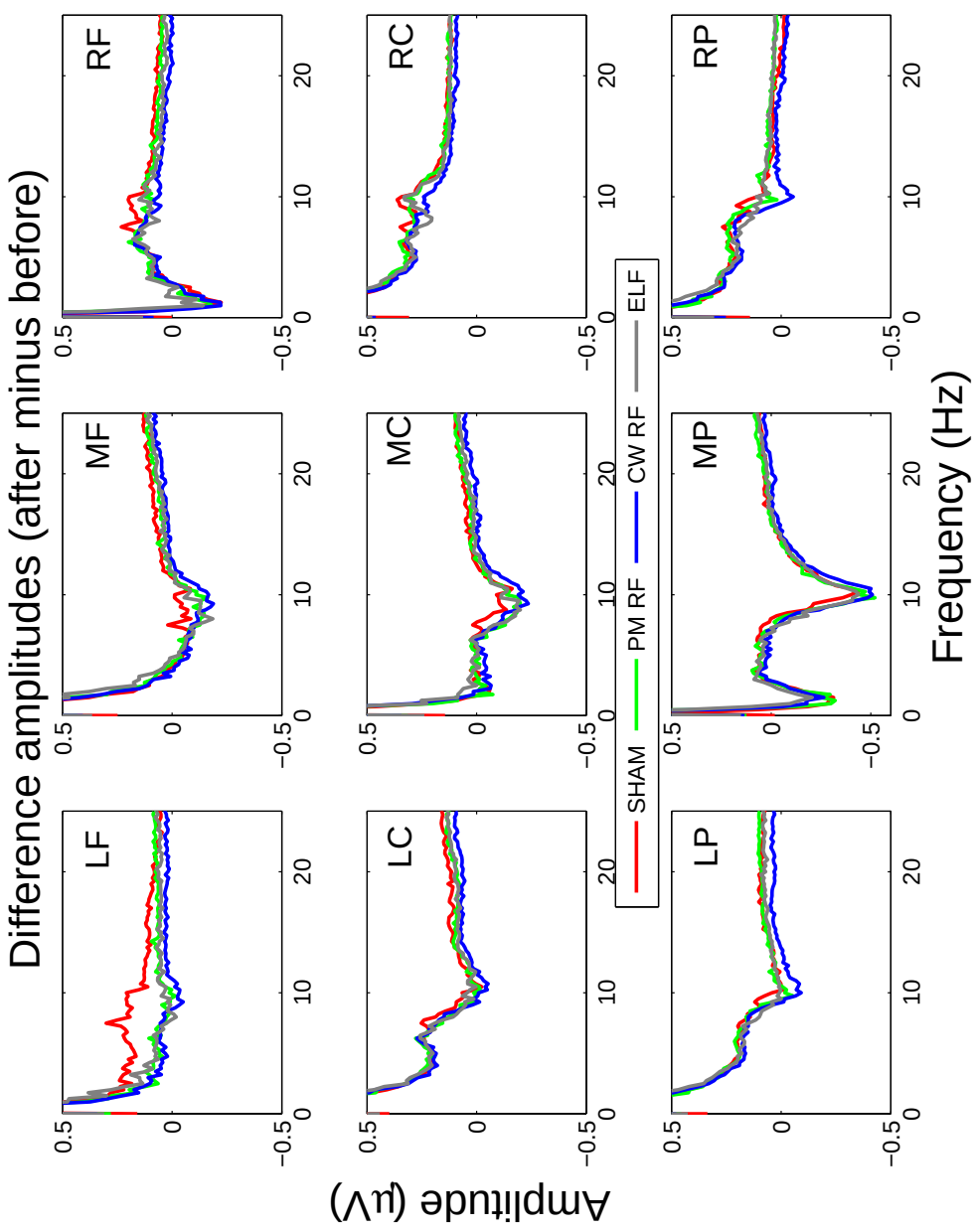

Figure 6.14.: Amplitude differences (after minus before exposure) are plotted for each exposure condition and at each scalp region separately. (LF; Left Frontal, MF; Mid Frontal, RF; Right Frontal, LC; Left Central, MC, Mid Central, RC; Right Central, LP; Left Posterior, MP; Mid Posterior, RP; Right Posterior)

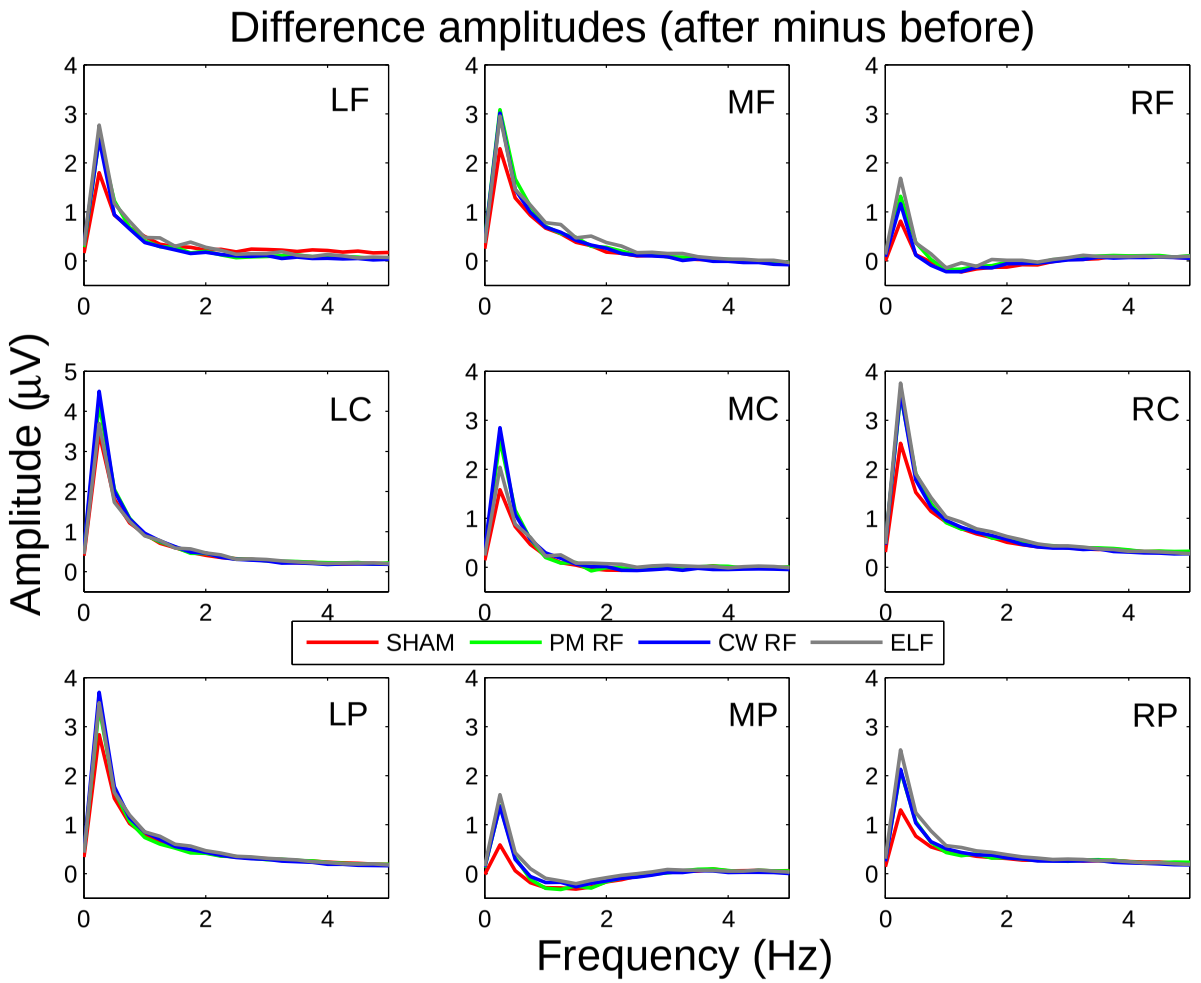

Figure 6.15.: Amplitude differences (after minus before exposure) are plotted for each exposure condition and at each scalp region separately. The Sham condition scored less than all the active exposures. (LF; Left Frontal, MF; Mid Frontal, RF; Right Frontal, LC; Left Central, MC, Mid Central, RC; Right Central, LP; Left Posterior, MP; Mid Posterior, RP; Right Posterior)

Table 6.3.: Means and standard deviations, $\mu(\sigma)$, per sagittal regions before (PRE) and after (POST) exposure. Values are expressed as raw amplitudes.

	Sham		PM RF		CW RF		ELF	
Sagittality	PRE	POST	PRE	POST	PRE	POST	PRE	POST
Contralateral	0.90 (.04)	0.99 (.05)	0.95 (.05)	1.01 (.05)	0.94 (.04)	0.95 (0.04)	0.92 (.05)	0.97 (.04)
Midline	1.15 (.06)	1.28 (.07)	1.23 (.07)	1.32 (.07)	1.21 (.06)	1.24 (.06)	1.19 (.06)	1.26 (.06)
Ipsilateral	0.90 (.04)	0.99 (.05)	0.95 (.05)	1.02 (.05)	0.95 (.04)	0.97 (.04)	0.93 (.05)	0.99 (.04)
Global	0.99 (.05)	1.07 (.05)	1.04 (.06)	1.09 (0.05)	1.03 (.05)	1.07 (.05)	1.01 (.05)	1.08 (.05)

6.3.1. Spectral analysis

6.3.1.1. During exposure

Delta band

PM RF No statistically significant changes were observed under the PM RF exposure in comparison to the Sham condition for neither the main factor of exposure condition nor the interaction of exposure condition with distal or proximal laterality or sagittality.

CW RF Under The CW RF exposure there was a trend level tendency of the alpha band activity to increase less than the Sham condition, ($Z(71) = -1.762$; $p = 0.079$; $\theta = 0.121$). There were no significant interactions between distal or proximal laterality, or sagittality with the exposure condition.

ELF No statistically significant changes were observed under the ELF exposure in comparison to the Sham for neither the main factor of exposure condition, nor the interaction of exposure condition with distal or proximal laterality or sagittality. Raw amplitude averages for all four EEG bands and conditions are shown in Tables 6.4 and 6.5.

Table 6.4.: Global means and standard deviation, $\mu\,(\sigma)$, for each band, exposure condition and time interval separately (PRE; before exposure, DUR; during exposure, POST; after exposure). Values are expressed as raw amplitudes.

EEG band	Sham			PM RF			CW RF			ELF		
	PRE	DUR	POST	PRE	DUR	POST	PRE	DUR	POST	PRE	DUR	POST
delta	2.46	2.88	2.97	2.43	2.90	3.00	2.43	2.87	3.04	2.39	2.94	3.03
	(.08)	(.10)	(.09)	(.08)	(.10)	(.09)	(.08)	(.09)	(.10)	(.07)	(.10)	(.103)
theta	0.93	0.98	1.01	0.96	0.99	1.03	0.93	0.98	0.98	0.94	0.99	0.99
	(.04)	(.04)	(.04)	(.03)	(.03)	(.04)	(.03)	(.03)	(.03)	(.04)	(.03)	(.04)
alpha	0.99	1.07	1.09	1.04	1.09	1.12	1.03	1.07	1.05	1.01	1.08	1.07
	(.05)	(.05)	(.05)	(.06)	(.05)	(.05)	(.05)	(.05)	(.05)	(.05)	(.05)	(.06)
beta	1.53	1.75	1.79	1.51	1.76	1.81	1.52	1.78	1.83	1.49	1.78	1.83
	(.05)	(.05)	(.05)	(.04)	(.05)	(.05)	(.04)	(.05)	(.06)	(.04)	(.06)	(.06)

Table 6.5.: Global means and standard deviation, $\mu\,(\sigma)$, for each band, exposure condition and and 5 minute intervals of the 'during' exposure period separately (1^{st}; first 5 minute sub-interval, 1^{st}; first 5 minute sub-interval, 1^{st}; first 5 minute sub-interval, 1^{st}; first 5 minute sub-interval,). Values are expressed as raw amplitudes.

	Sham				PM RF				CW RF				ELF			
Interval	1^{st}	2^{nd}	3^{rd}	4^{th}	1^{st}	2^{nd}	3^{rd}	4^{th}	1^{st}	2^{nd}	3^{rd}	4^{th}	1^{st}	2^{nd}	3^{rd}	4^{th}
	2.74	2.94	2.94	2.88	2.82	2.90	2.94	2.96	2.82	2.87	2.84	2.97	2.77	3.00	2.94	3.05
delta	(.087)	(.11)	(.11)	(.09)	(.09)	(.09)	(.09)	(.09)	(.09)	(.09)	(.09)	(.09)	(.09)	(.11)	(0.10)	(.10)
	0.96	0.98	0.99	0.99	0.98	1.01	0.99	1.01	0.98	0.98	0.98	0.98	0.97	1.02	0.99	1.01
theta	(.03)	(.03)	(.04)	(.04)	(.03)	(.04)	(.03)	(.03)	(.03)	(.03)	(.03)	(.03)	(.03)	(.04)	(.03)	(.04)
	1.07	1.06	1.07	1.06	1.08	1.10	1.08	1.08	1.08	1.07	1.08	1.06	1.09	1.09	1.06	1.06
alpha	(.05)	(.05)	(.05)	(.05)	(.05)	(.06)	(.06)	(.05)	(.06)	(.05)	(.05)	(.05)	(.06)	(.05)	(.05)	(.05)
	1.67	1.78	1.78	1.75	1.72	1.76	1.78	1.79	1.72	1.74	1.73	1.80	1.69	1.81	1.78	1.84
beta	(.05)	(.06)	(.06)	(.05)	(.05)	(.05)	(.05)	(.05)	(.05)	(.05)	(.05)	(.05)	(.05)	(.06)	(.06)	(.06)

Theta band

PM RF During PM RF exposure a trend level difference was observed for the interaction of exposure condition with distal laterality ($Z(71) = -2.643$; $p = 0.009$; $\theta = -0.630$, $ipsi/contra\,difference$). There were no significant effects for either the main factor of exposure condition, nor the interaction of exposure condition with proximal laterality or sagittality. Table 6.6 lists the amplitude data for all exposure conditions for both during and after exposure as a function of Sagittal region.

CW RF No statistically significant changes were observed under the CW RF exposure in comparison to the Sham condition for neither the main factor of exposure condition, nor the interaction of exposure condition with distal or proximal laterality or sagittality.

ELF During ELF exposure a trend level interaction between exposure condition and distal laterality was observed ($Z(71) = -2.475$; $p = 0.013$; $\theta = -0.688\,ipsi/contra\,difference$). No other changes were observed for the main factor of exposure condition, nor the interaction of exposure condition with sagittality or proximal laterality.

Alpha band The remaining investigation for the alpha band is that of the interaction of exposure condition by sagittality for which no statistically significant differences were observed for any of CW RF, PM RF or ELF exposure conditions.

Beta band

PM RF No statistically significant changes were observed under the PM RF exposure in comparison to the Sham for neither the main factor of exposure condition, nor the interaction of exposure condition with distal or proximal laterality or sagittality.

Table 6.6.: Means and standard deviation, $\mu\,(\sigma)$, for each band, exposure condition and sagittal region separately (PRE; before exposure, DUR; during exposure, POST; after exposure). Values are expressed as raw amplitude data.

		Sham			PM RF			CW RF			ELF		
Band	Sagittality	PRE	DUR	POST	PRE	DUR	POST	PRE	DUR	POST	PRE	DUR	POST
Delta	Frontal	2.84	3.34	3.49	2.84	3.40	3.54	2.80	3.32	3.49	2.76	3.42	3.50
		(.09)	(.11)	(.11)	(.10)	(.11)	(.11	(.09)	(.10)	(.12)	(.08)	(.12)	(.11)
	Central	2.35	2.71	2.79	2.30	2.73	2.80	2.30	2.70	2.85	2.29	2.79	2.86
		(.07)	(.09)	(.09)	(.07)	(.09)	(.09)	(.07)	(.08)	(.10)	(.06)	(.10)	(.10)
	Posterior	2.21	2.58	2.64	2.17	2.59	2.67	2.20	2.60	2.77	2.12	2.62	2.72
		(.09)	(.10)	(.09)	(.07)	(.10)	(.10)	(.08)	(.10)	(.11)	(.06)	(.10)	(.11)
Theta	Frontal	1.06	1.12	1.14	1.10	1.15	1.18	1.06	1.12	1.13	1.07	1.15	1.15
		(.04)	(.04)	(.04)	(.04)	(.04)	(.04)	(.03)	(.03)	(.03)	(.04)	(.04)	(.04)
	Central	0.94	0.99	1.02	0.98	1.00	1.04	0.94	0.98	0.98	0.95	1.00	1.00
		(.04)	(.04)	(.04)	(.04)	(.04)	(.04)	(.04)	(.03)	(.03)	(.04)	(.04)	(.04)
	Posterior	0.79	0.83	0.86	0.81	0.84	0.88	0.79	0.83	0.83	0.79	0.85	0.84
		(.03)	(.03)	(.03)	(.03)	(.03)	(.03)	(.03)	(.03)	(.03)	(.03)	(.03)	(.03)
Alpha	Frontal	0.95	1.05	1.08	1.01	1.08	1.10	1.00	1.06	1.04	0.98	1.07	1.07
		(.04)	(.05)	(.05)	(.05)	(.05)	(.05)	(.05)	(.05)	(.04)	(.05)	(.05)	(.05)
	Central	0.98	1.06	1.08	1.03	1.08	1.11	1.02	1.05	1.04	1.01	1.07	1.06
		(.04)	(.05)	(.05)	(.05)	(.05)	(.05)	(.05)	(.05)	(.04)	(.05)	(.05)	(.05)
	Posterior	1.03	1.09	1.11	1.08	1.11	1.15	1.08	1.11	1.09	1.05	1.10	1.09
		(.06)	(.06)	(.06)	(.07)	(.06)	(.06)	(.06)	(.06)	(.05)	(.06)	(.06)	(.06)
Beta	Frontal	2.57	2.99	3.09	2.53	3.02	3.11	2.53	2.98	3.14	2.50	3.06	3.15
		(.08)	(.10)	(.09)	(.08)	(.09)	(.09)	(.07)	(.09)	(.10)	(.07)	(.11)	(.11)
	Central	1.19	1.35	1.37	1.19	1.35	1.39	1.19	1.35	1.40	1.17	1.37	1.40
		(.04)	(.04)	(.04)	(.03)	(.04)	(.04)	(.04)	(.05)	(.05)	(.03)	(.04)	(.05)
	Posterior	0.82	0.91	0.92	0.80	0.92	0.93	0.83	0.92	0.96	0.80	0.91	0.94
		(.03)	(.03)	(.03)	(.02)	(.03)	(.03)	(.03)	(.03)	(.03)	(.02)	(.03)	(.03)

CW RF During CW RF exposure a trend level difference was observed for the factor interaction of exposure condition with sagittality (posterior versus frontal, $Z(71) = -2.059$; $p = 0.039$; $\theta = -0.441$). No significant differences were observed for the main factor of exposure condition, nor the interaction of exposure condition with distal or proximal laterality.

ELF During ELF exposure there was a trend level decrease of beta activity in comparison to the Sham exposure, ($Z(71) = -2.233$; $p = 0.026$; $\theta = 0.309$). There were no statistically significant changes observed for any of the interaction of exposure condition with sagittality, nor distal or proximal laterality.

6.3.1.2. After exposure

Raw band averages for each exposure condition, time intervals (pre, during and post exposure) and laterality are displayed in Table 6.7.

Delta, Theta and Beta bands

PM RF, CW RF and ELF With the exception of a trend level interaction of exposure condition with distal laterality in the theta band during PM RF ($Z(71) = -1.633$; $p = 0.099$; $\theta = -0.07\, ipsi/contra\, difference$), there were no statistically significant changes under the PM RF, CW RF or ELF exposures in comparison to Sham for neither the main factor of exposure condition, nor the nor the interaction of exposure condition with distal or proximal laterality, or sagittality.

Alpha band

PM RF After cessation of PM RF exposure a trend level interaction of the exposure condition with sagittality was observed, $Z(71) = -2.043$; $p = 0.041$; $\theta = 0.119$), whereby posterior alpha

activity was higher than the frontal activity in comparison to Sham exposure. There were no other significant differences observed after PM RF exposure cessation.

CW RF and ELF After cessation of exposure no statistically significant changes were observed under the CW RF or ELF exposures in comparison to the Sham condition for neither the main factor of exposure condition, nor the interaction of exposure condition with distal or proximal laterality or sagittality.

6.3.2. Non linear: ApEn - results

6.3.2.1. Presence of non linearity in data

In total, 69% of data passed the surrogate test, suggesting that an equal proportion of data contained non linear features at a 95% probability. No pattern in the presence of non linearity was observed with respect to EEG derivation (~69% of Posterior data, ~68% of Central data and ~70% of Frontal data).

6.3.2.2. During exposure

For all factor or factor interactions, the significance criterion (a = 0.0043) was determined through the D/AP method using the overall correlation between variables, r = 0.094, and the amount of planned contrasts, a total of 15. Raw ApEn values for all time intervals are shown in Tables 6.9, 6.8 and 6.10 for each lateral region, sagittal region and individual scalp region respectively. During all active exposures, (PM RF, CW RF and ELF), there were no significant differences in comparison to the Sham exposure for neither the main factor of exposure condition nor the interaction of exposure condition with sagittality or laterality. This was true at both the adjusted, ($\alpha = 0.0043$) and unadjusted, ($\alpha = 0.05$), significance level.

Table 6.7.: Means and standard deviations $\mu\,(\sigma)$, for each band, exposure condition, time interval (PRE; before exposure, DUR; during exposure, POST; after exposure) and lateral scalp region separately (ipsilateral midline and contralateral).Values are expressed as raw amplitudes.

		Sham			PM RF			CW RF			ELF		
Band	Laterality	PRE	DUR	POST	PRE	DUR	POST	PRE	DUR	POST	PRE	DUR	POST
Delta	Contra	2.24	2.63	2.73	2.24	2.68	2.77	2.21	2.63	2.77	2.19	2.70	2.79
		(.08)	(.10)	(.09)	(.08)	(.09)	(.09)	(.08)	(.09)	(.10)	(.06)	(.10)	(.10)
	Midline	2.75	3.17	3.26	2.70	3.19	3.29	2.71	3.17	3.32	2.67	3.25	3.33
		(.09)	(.11)	(.10)	(.09)	(.10)	(.10)	(.08)	(.10)	(.11)	(.07)	(.12)	(.11)
	Ipsi	2.39	2.83	2.93	2.37	2.84	2.95	2.38	2.82	3.02	2.31	2.87	2.96
		(.08)	(.10)	(.09)	(.08)	(.10)	(.10)	(.08)	(.09)	(.11)	(.07)	(.10)	(.11)
Theta	Contra	0.83	0.86	0.89	0.85	0.88	0.91	0.82	0.86	0.86	0.83	0.88	0.88
		(.03)	(.03)	(.03)	(.03)	(.03)	(.03)	(.03)	(.03)	(.02)	(.03)	(.03)	(.03)
	Midline	1.11	1.18	1.21	1.16	1.19	1.25	1.12	1.17	1.18	1.12	1.20	1.19
		(.05)	(.05)	(.05)	(.05)	(.04)	(.04)	(.04)	(.04)	(.04)	(.04)	(.04)	(.04)
	Ipsi	0.85	0.90	0.92	0.88	0.91	0.94	0.85	0.90	0.90	0.86	0.92	0.92
		(.03)	(.03)	(.03)	(.03)	(.03)	(.03)	(.03)	(.03)	(.03)	(.03)	(.03)	(.03)
Alpha	Contra	0.90	0.97	0.99	0.95	0.98	1.01	0.94	0.98	0.95	0.92	0.98	0.97
		(.04)	(.05)	(.05)	(.05)	(.05)	(.05)	(.04)	(.05)	(0.04)	(.05)	(.05)	(.04)
	Midline	1.15	1.26	1.28	1.23	1.27	1.32	1.21	1.27	1.24	1.19	1.26	1.26
		(.06)	(.06)	(.07)	(.07)	(.99)	(.07)	(.06)	(.99)	(.06)	(.06)	(.07)	(.06)
	Ipsi	0.90	0.98	0.99	0.95	0.99	1.02	0.95	0.99	0.97	0.93	0.99	0.99
		(.04)	(.05)	(.05)	(.05)	(.05)	(.05)	(.04)	(.05)	(.04)	(.05)	(.05)	(.04)
Beta	Contra	1.38	1.59	1.65	1.37	1.61	1.66	1.38	1.58	1.67	1.34	1.62	1.66
		(.04)	(.05)	(.05)	(.04)	(.05)	(.05)	(.04)	(.05)	(.05)	(.04)	(.05)	(.05)
	Midline	1.98	2.27	2.32	1.95	2.29	2.35	1.96	2.29	2.38	1.93	2.33	2.39
		(.06)	(.08)	(.07)	(.06)	(.07)	(.07)	(.06)	(.08)	(.08)	(.06)	(.08)	(.08)
	Ipsi	1.22	1.38	1.42	1.20	1.39	1.42	1.22	1.38	1.45	1.18	1.40	1.44
		(.04)	(.04)	(.04)	(.03)	(.04)	(.04)	(.03)	(.04)	(.04)	(.03)	(.04)	(.05)

6.3.2.3. After exposure

No significant changes were observed following cessation of all active exposures, (PM RF, CW RF and ELF), in comparison to the Sham exposure for neither the main factor exposure condition nor the interaction of exposure condition with laterality or sagittality.

6.3.3. Conclusion

The results of a same-day protocol study have been reported in this Chapter. With a relatively large sample size, (n = 72), and exposures that replicate mobile phone use at maximum levels during DTX mode, (SAR $\approx$ 0.06 W/kg), we were unable to detect the alpha band increase that has been previously reported in literature. On the contrary, a statistically significant decrease of global alpha activity was observed during PM RF exposure. Additionally an effect of decreased alpha activity was also observed during the ELF and CW RF exposures that were statistically significant at sites ipsilateral to the exposure source. Changes in the remaining EEG bands (delta ,theta and beta) have also been reported. The statistically significant changes that were observed in the alpha band seem to be a result of a decreased baseline value during the Sham exposure, see Figure 6.16 for a clear representation of this effect.

As such changes during and after Sham exposure were larger that any changes during or after the active exposures. Therefore the accurate description of the observed effect is that the baseline of the active exposures was the one that was mostly affected. Of course such an interpretation is meaningless since the effect of the radiation can only be present during or after and not before its appearance. Owing to the single day protocol that was employed it is imperative to examine whether the baseline suppression during Sham exposure was the result of a carry-over effect. The latter is addressed in the next Chapter along with other possible interpretations of this outcome. Additionally the investigation on the signal regularity during and after the active exposures in comparison to the Sham exposure revealed no significant changes implying that signal complexity

Table 6.8.: ApEn means and standard deviation, $\mu\,(\sigma)$, for each band, exposure condition, sagittality and time interval separately (PRE; before exposure, DUR; during exposure, POST; after exposure). Values are expressed as raw amplitudes.

	Sham			PM RF			CW RF			ELF		
Sagittality	PRE	DUR	POST	PRE	DUR	POST	PRE	DUR	POST	PRE	DUR	POST
Frontal	1.03	1.02	1.00	1.02	1.01	0.99	1.01	1.01	1.00	1.02	1.01	1.00
	(.02)	(.02)	(.02)	(.02)	(.02)	(.02)	(.02)	(.02)	(.02)	(.02)	(.02)	(.02)
Central	1.05	1.05	1.03	1.04	1.04	1.03	1.05	1.05	1.04	1.06	1.05	1.04
	(.02)	(.02)	(.02)	(.02)	(.02)	(.02)	(.02)	(.02)	(.02)	(.02)	(.02)	(.02)
Posterior	1.10	1.10	1.09	1.10	1.10	1.09	1.12	1.11	1.11	1.12	1.11	1.10
	(.02)	(.02)	(.02)	(.02)	(.02)	(.02)	(.02)	(.02)	(.02)	(.02)	(.02)	(.02)

Table 6.9.: ApEn means and standard deviations, $\mu\,(\sigma)$, for each band, exposure condition, laterality and time interval separately (PRE; before exposure, DUR; during exposure, POST; after exposure). Values are expressed as raw amplitudes.

	Sham			PM RF			CW RF			ELF		
Laterality	PRE	DUR	POST	PRE	DUR	POST	PRE	DUR	POST	PRE	DUR	POST
Contra	1.13	1.13	1.11	1.12	1.12	1.11	1.13	1.13	1.12	1.13	1.12	1.12
	(.02)	(.02)	(.02)	(.02)	(.02)	(.02)	(.02)	(.02)	(.02)	(.02)	(.02)	(.02)
Midline	0.94	0.94	0.92	0.94	0.93	0.92	0.94	0.94	0.94	0.95	0.94	0.94
	(.02)	(.02)	(.02)	(.02)	(.02)	(.02)	(.02)	(.02)	(.02)	(.02)	(.02)	(.02)
Ipsi	1.11	1.10	1.09	1.09	1.10	1.08	1.10	1.10	1.09	1.12	1.11	1.09
	(.02)	(.02)	(.02)	(.02)	(.02)	(.02)	(.02)	(.02)	(.02)	(.02)	(.02)	(.02)

Table 6.10.: ApEn means and standard deviation, $\mu\,(\sigma)$, for each band, exposure condition, laterality, sagittality and time interval separately (PRE; before exposure, DUR; during exposure, POST; after exposure). Values are expressed as raw amplitudes.

		Sham			PM RF			CW RF			ELF		
Sagittality	Laterality	PRE	DUR	POST	PRE	DUR	POST	PRE	DUR	POST	PRE	DUR	POST
Frontal	Contra	1.09	1.08	1.06	1.09	1.08	1.07	1.08	1.08	1.07	1.09	1.07	1.06
		(.02)	(.02)	(.02)	(.02)	(.02)	(.02)	(.02)	(.02)	(.02)	(.02)	(.02)	(.02)
	Midline	0.94	0.94	0.92	0.94	0.93	0.92	0.94	0.94	0.93	0.94	0.94	0.93
		(.02)	(.02)	(.02)	(.02)	(.02)	(.02)	(.02)	(.02)	(.02)	(.02)	(.02)	(.02)
	Ipsi	1.04	1.03	1.01	1.03	1.02	1.00	1.02	1.02	1.01	1.03	1.02	1.01
		(.02)	(.02)	(.02)	(.02)	(.02)	(.02)	(.02)	(.02)	(.02)	(.02)	(.02)	(.02)
Central	Contra	1.12	1.12	1.10	1.11	1.11	1.10	1.12	1.12	1.11	1.12	1.11	1.11
		(.02)	(.02)	(.02)	(.02)	(.02)	(.02)	(.02)	(.02)	(.02)	(.02)	(.02)	(.02)
	Midline	0.91	0.91	0.89	0.91	0.90	0.89	0.91	0.91	0.90	0.91	0.91	0.91
		(.02)	(.02)	(.02)	(.02)	(.02)	(.02)	(.02)	(.02)	(.02)	(.02)	(.02)	(.02)
	Ipsi	1.13	1.13	1.11	1.11	1.12	1.10	1.12	1.12	1.11	1.14	1.13	1.11
		(.02)	(.02)	(.02)	(.02)	(.02)	(.02)	(.02)	(.02)	(.02)	(.02)	(.02)	(.02)
Posterior	Contra	1.18	1.18	1.17	1.17	1.18	1.17	1.20	1.19	1.19	1.19	1.19	1.18
		(.02)	(.02)	(.02)	(.02)	(.02)	(.02)	(.02)	(.02)	(.02)	(.02)	(.02)	(.02)
	Midline	0.96	0.97	0.96	0.97	0.97	0.96	0.98	0.98	0.98	0.99	0.98	0.98
		(.02)	(.02)	(.02)	(.02)	(.02)	(.02)	(.02)	(.02)	(.02)	(.02)	(.02)	(.03)
	Ipsi	1.16	1.16	1.15	1.15	1.15	1.14	1.17	1.16	1.16	1.17	1.17	1.15
		(.02)	(.02)	(.02)	(.02)	(.02)	(.02)	(.02)	(.02)	(.02)	(.02)	(.02)	(.02)

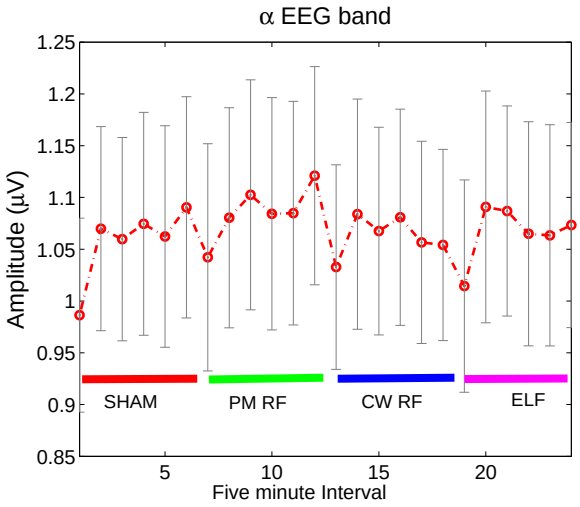

Figure 6.16.: In this figure it can be seen that the alpha band amplitude during the baseline of the Sham exposure is the lowest intervals throughout the experiment. The remaining 5 minute intervals display a variation in amplitude that is always below the variation that is observed between the baseline Sham and any other 5 minute interval. This deviation from the mean is what gives rise to the statistically significant effects that have been observed.

or regularity as measured by the comparative measure of the ApEn remain unchanged.

Table 6.11.: Collective spectral and non linear analysis results. ↓↓; statistically significant decrease, ↑↑; statistically significant increase ↓; trend level decrease, ↑; trend level increase ($\alpha \leq 0.1$ for hypothesis and $\alpha \leq 0.05$ for exploratory tests). θ; Hodges-Lehman estimate of treatment effect, E; Main effect of exposure condition, E x dL; Interaction of exposure condition with distal laterality, E x pL; Interaction of exposure condition with proximal laterality, E x dL; Interaction of exposure condition with sagittality, E x L; Interaction of exposure condition with laterality. All comparisons containing the factor laterality refer to the ipsi versus contra comparison.

Summary of results	Band	E	E x dL	E x S	E x pL
Spectral	delta	-	-	-	-
-PM RF	theta	-	↓↓ $\theta = -.630$	-	-
During	alpha	↓↓ $\theta = -.169$	-	-	-
Exposure	beta	-	-	-	-
Spectral	delta	↑ $\theta = .0121$	-	-	-
-CW RF	theta	-	-	-	-
During	alpha	-	↓ $\theta = -.393$	-	↓ $\theta = -.318$
Exposure	beta	-	-	↓ $\theta = -.441$	-
Spectral	delta	-	-	↓ $\theta = -.229$	-
-ELF	theta	-	↓ $\theta = -.688$	-	-
During	alpha	-	-	-	↓↓ $\theta =$
Exposure					$-.383$
	beta	↓ $\theta = -.309$	-	-	-
Spectral	delta	-	-	-	-
-PM RF	theta	-	↓ $\theta = -.007$	-	-
After	alpha	-	-	↑ $\theta = .119$	-
Exposure	beta	-	-	-	-
Spectral	delta	-	-	-	-
-CW RF	theta	-	-	-	-
After	alpha	-	-	-	-
Exposure	beta	-	-	-	-
Spectral	delta	-	-	-	-
-CW RF	theta	-	-	-	-
After	alpha	-	-	-	-
Exposure	beta	-	-	-	-

ApEn	E	E x L	E x S	
During PM RF	-	-	-	n/a
During CW RF	-	-	-	n/a
During ELF	-	-	-	n/a
After PM RF	-	-	-	n/a
After CW RF	-	-	-	n/a
After ELF	-	-	-	n/a

7. Discussions

In this Chapter the findings that were reported in Chapter 6 are contrasted with those of previous relevant studies. Possible interpretations of the results are presented which cover both the possibility of a real radiation induced effect as well as alternatives. Where appropriate, additional analyses and experiments are presented that either support or refute the proposed interpretations. Since these additional analyses and experiments were not planned *a priori*, they are completely described in the present Chapter. Lastly, this Chapter discusses the limitations of the main study.

7.1. Contrast with previous findings and interpretation of results

Studies investigating changes on the resting EEG both during and shortly after exposure to RF and ELF radiation have been reviewed in Chapter 2 and the respective results were summarized in Table 2.1. Here, those findings are contrasted with those reported in Chapter 6.

7.1.1. Spectral analysis - During Exposure

From Table 2.1 it is seen that where changes were observed in the alpha band of the resting EEG they were mostly positive in direction, that is leading to increases of alpha band amplitude or power. Additionally, the changes were observed mostly under pulse modulated exposures. The modulations used varied between laboratories. For example Huber et al. and Regel et al. employed SAR values of 1 W/kg with all DTX components, and the studies of Curcio et al. and Croft et al.

employed SARs of 0.5 and 0.674 W/kg with the 217 Hz modulation only, (see references [58, **?**] and [34, 36] respectively). The former two studies also had a common exposure distribution that was considerably more homogeneous within the exposed hemisphere as opposed to the later two studies that employed the more realistic localized distributions.

The studies of Huber et al. and Regel et al. did not obtain 'during exposure' EEG recordings and so cannot be compared with the 'during exposure' results of the present study. On the other hand the studies of Curcio et al. and Croft et al. did record EEG during exposures and their findings of alpha increase were not replicated in the current study. Several differences may have contributed to these different results. These are the DTX modulation content and the far lower SAR values, (0.06 W/kg equivalent to a decrease of 12.5 dB), that were employed here versus the single frequency (217 Hz) modulation and the SAR value of about 0.5 W/kg.

Despite the prevalence of the increased alpha activity under EMF there are exceptions as seen in the study of D'Costa et al., where a decrease was observed during PM RF [38]. That change corresponded to a laterality effect since data was based on bipolar recordings. Additionally the phone was placed at the back of the head and presumably, the exposure would have been similar in both hemispheres. For these reasons a direct comparison between the two studies cannot be drawn, but nevertheless the changes were in the same direction.

In regards to the CW RF exposure no comparisons are available for those periods during the exposure since the only previous studies that did employ CW RF measured the EEG after exposure cessation only [58, **?**]. However the results presented in Chapter 3, the small sample size study, do agree with the current finding of no statistically significant effect. It is also notable that the SAR levels of these studies were both set at 1.95 W/kg. Finally, the presence of trend level changes during CW RF exposure cannot be neglected particularly since those become important when considering alternative interpretations of the observations, as discussed in Section 7.3.

Despite the considerable differences between the present ELF exposure and those of Cook et

al. the results of these studies are the most relevant in literature [30, 28, 27]. These differences include at least the highly localized exposure employed here versus the homogeneous exposure, and the roughly 10 dB ($25\mu T$ used here versus $\pm 200\mu T$) difference in peak magnetic field between the present study and those of Cook et al. In their last two studies, (2005 and 2008), the EEG activity within the refractory intervals of the exposure period corresponding to a 'during exposure' recording were monitored. A decrease in alpha activity in the first study and an increase in the second study (employing identical exposure signals) were observed, but also a statistically significant decrease under a modified exposure signal. In the current study a decreased alpha activity was observed which was statistically significant at sites ipsilateral to exposure. It is seen that these results are partly in agreement and partly in disagreement with the present findings, so no reliable direction of change can be deduced.

7.1.2. Spectral analysis - After Exposure

In the present study no effects were detected after cessation of CW RF exposure. Trend level changes in alpha activity were observed after PM RF exposure where the posterior/frontal difference score was higher for the active in comparison to the Sham condition.

The absence of statistically significant results is inconsistent with the findings of Croft et al. where hemispherical differences were observed (contralateral alpha decrease) post PM RF exposure, the findings of Curcio et al. where the alpha increase effect was larger during exposure but was also present in the 7 minutes post exposure and the findings of Huber et al. where again an increase in alpha activity was observed [36, 35]. However the presence of a trend level increase in posterior alpha after PM RF exposure cannot be overlooked. It provides at least a weak support to the general trend of alpha increase post exposure as seen across some of these studies.

Since Huber et al. employed the DTX mode exposure signal as did the present study, the differences in results are discussed in an attempt to identify the potential sources of the disagreement.

These differences are the duty cycle of the DTX signal leading to different SAR levels, the instantaneous peak field levels and the SAR distribution. Even though both studies employed DTX like signal structures containing the 2, 8, 217 and 1736 Hz modulation components Huber et al., Regel et al. and Kleinlogel et al., employed a signal structure that deviates from the real DTX mode [58, 59, 115, 114, **?**, 48]. Inherently, during the DTX mode SAR levels drop well below those of talk mode, (217 Hz and 1736 Hz modulations only), due to the absence of extra time slots, see Figure 1.3. In order to elevate the SAR level during the DTX mode exposure condition to the same as the CW RF exposure condition while maintaining a convenient peak to average signal ratio, the authors of those studies introduced extra time slots in the signal. This gives rise to two important differences between the two DTX-like exposures. In the latter studies instantaneous peak field levels in the head are estimated to be approximately 2.3 times higher than the present study (peak field ratio of 4.8 versus 2.1) and SAR levels are substantially different, (1 W/kg versus 0.06 W/kg)[1]. Additionally there are the differences in exposure distributions where those studies employed a homogeneous exposure but the present study employed a localized one. Since Huber et al. have already shown that a CW RF signal of the same SAR level as a PM RF one does not cause any changes in the resting EEG, differences cannot be attributed to the SAR level alone. At the same time, the present study used PM RF signals and did not detect statistically significant changes. It may be argued that for effects to arise under PM RF radiation a sufficient SAR level as well as crest factors are required. This point finds support in the studies of Curcio et al. and Croft et al. since those employed higher SAR levels, (0.5 and 0.674 W/kg), as well as higher crest factors, (4 and 5.36 respectively), than the present study. However the fact that a SAR level of 2 W/kg cannot occur under DTX conditions should be considered before attempting to relate the results of those studies to real mobile phone use under DTX conditions, see references [58, 59, 115, 114, **?**, 48].

[1] Assuming the same modulation content, the crest factor of the signal would be directly dependent on the instantaneous peak field levels. However, when comparing the collection of studies employing the DTX mode as described by Huber et al. with the present study it is observed that both SAR as well as instantaneous peak field levels differ.

In strict statistical terms the present results are consistent with those of Roschke and Mann, Hinrikus et al., Hietanen et al., the results presented in Chapter 3, the results of Regel et al., and the results of Kleinlogel et al. [121, 53, 55, 110, **?**, 48]. Consistent with Huber et al. no statistically significant changes were observed under the CW RF exposure, even though the SAR level in the present study was twice as high. This finding reinforces the notion that CW RF exposure does not cause changes in the resting EEG.

No changes in the alpha band activity were observed after the ELF exposure and this finding is in disagreement with the results of Cook et al. (2004) were alpha increases were observed one minute after the exposure condition. The current results are in agreement with the subsequent findings of the 2005 and 2008 studies of Cook et al. where no changes were observed post exposure in the alpha band of the resting EEG [30, 28, 26].

7.1.3. Possibility of dose-response relationship

The present study employed a SAR of 0.06 W/kg whereas other studies that demonstrated alpha increases employed SAR values ranging from 0.5 to 1 W/kg. Despite the fact that all studies employed low frequency modulations the effects were in different directions. This distinction may be interpreted as a dose response relationship. However an appropriate protocol would need to be employed to identify whether this statement carries any validity. There has been at least one occasion where dose-response relationships were demonstrated during stage 2 sleep [114]. However that study employed SARs of 0.5 W/kg and 5 W/kg under which only increases (larger for the 5 W/kg exposure) of sleep spindles were detected.

7.1.4. Possibility of non-specific response

One interpretation that can account for the different direction of changes under the active radiation is one that is based on a non-specific response to the potential stressor. A non-specific response

can arise through a secondary process, that is the exposure may cause a change in brain function, (primary effect), which in turn produces the measured response (secondary response i.e. non-specific effect). If this is the case, it may be so that the observed effect varies with respect to the cognitive state of participants (e.g. the secondary process arises only when participants are performing a specific task or are in a particular state of alertness). Due to the extended periods of resting EEG monitoring, the cognitive state in the present experiment should be expected to differ from most of the studies summarized in Table 2.1 which incorporated various performance related tasks. This distinction could have given rise to the opposite direction of changes that were observed.

ApEn analysis- Regularity In Chapter 3 a rational for the use of a non linear measure in the detection of EMF induced changes on the EEG was developed. One of the motivations was to attempt to demonstrate an effect more reliably than what has been the case with spectral analysis. Through the results t was concluded that there was difficulty in determine whether the lack of any significant effects represented a lack of advantage of the ApEn measure over FFT, or whether differences between the methods may have been masked by the lack of any significant effect, see Section 3.4. A comparison with the spectral results introduced in Chapter 6, it appears that the spectral analysis was more powerful than the ApEn method since a range of changes were observed under the former whereas no changes were observed under the latter, see Table 6.11. The ineffectiveness of ApEn in the present study to detect any changes cannot be taken as indicative of absence of non linear effects. It is merely indicative of the insensitivity to changes of the chosen numerical method in combination with the input parameters. The likeliness of detecting EMF induced changes under other non linear constructs cannot be excluded. In support of the above several studies have indeed detected changes in non linear features of resting EEG signals. Some of those were listed in Table 2.3.

7.2. Sources of variability in data and their potential influence on the experimental outcome.

Here several sources of error variance are identified and their potential influence on the results of the current study is discussed. These include the temperature levels in the experimental room in combination with their impact on the input noise of the amplification unit and the stability of subjects' arousal levels.

7.2.1. Temperature variation in the experimental environment

Electronic amplification systems, including the Synamps^{2TM} system, are susceptible to thermal noise[2] [69]. Temperature variations within the experimental environment may have an impact on the input noise of the amplifier. Such noise becomes important in the current experiment due to the purportedly small magnitude of the effect, which thus far has been reported to be $\approx 0.1\mu V$. To assess this noise level the Synamps^{2TM} unit was subjected to a temperature variation of 23.8 - 33.0 ^oC using an electric heater. This temperature variation represents a worst case scenario. The experimental setup was kept the same as that during the real experiment with the main difference being the use of a dummy head instead of a human participant. This way any brain activity was removed from the experiment and therefore recordings represent noise measurements only. Three electrodes were used for this assessment which were connected to a watermelon that acted as the dummy head. Electrode impedances were kept below 5 $k\Omega$ at the start of the experiment through the application of conductive gel. Three 20-minute recordings were obtained at 23.8, 25.6 and 33 ^oC approximately. Data were then analyzed using the EDIT 5.5.2 software (Scan 4.3, Compumedics^{TM}). Data were epoched into 4 second intervals, the mean of each epoch was removed so as to remove ant DC components before spectral analysis, subsequently spline fitted to 1024 samples, and were finally

[2]The Synamps user's guide defines an operating temperature range of 15 - 30 ^oC . Note that this source of noise is one that partly remains after common mode rejection

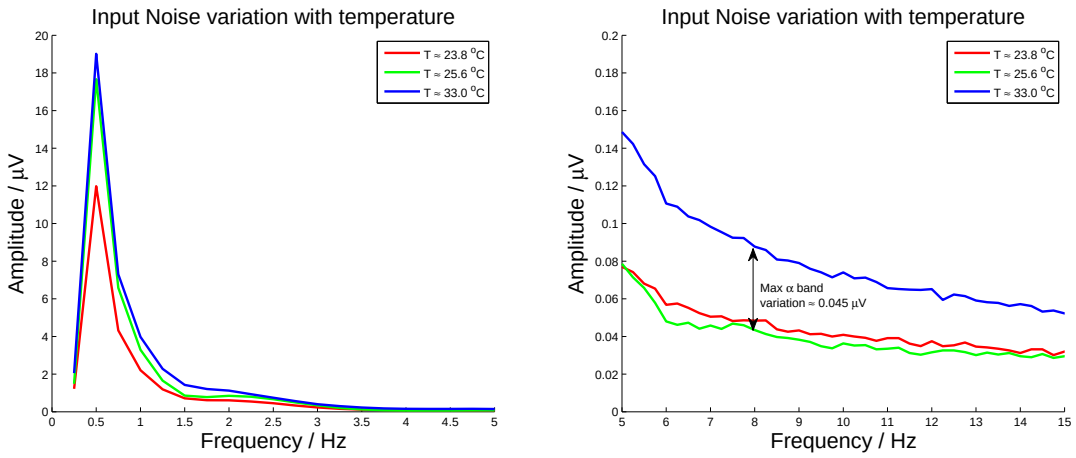

(a) (b)

Figure 7.1.: (a) Thermal Noise variation in the lower EEG spectrum; and (b) in the alpha band range. Maximum variation is $0.045\mu V$ which is roughly half of the EMF induced alpha band effect.

submitted through the FFT algorithm, (10% cosine window, no overlap).

It was observed that noise fluctuation was considerably large in the delta EEG band, see Figure 7.1a, and dropped to below 0.2 μV once in the alpha band range. In fact the worst case variation within the alpha band was $\approx 0.05\,\mu V$, see Figure 7.1b,. This magnitude is indeed comparable to the treatment effect of the current study $\approx 0.03\,\mu V$, see Figure 6.8. It is therefore possible that this noise source may obscure the radiation induced effect.

7.2.2. Stability of subjects' arousal levels

The focus of the present study was on alpha band activity changes in relation to the exposure condition. Since alpha activity is known to change along with psychological/cognitive states any such variation within the duration of the experiment will contribute to the error variance.

Oken et al. identify a variety of factors that contribute to alertness levels [14]. These include motivation and drowsiness, factors which may readily change within the duration of a 30 minute

experiment. Shaw identifies that arousal is an important confounding factor in any study of alpha, (see reference [125]), and being a subject in an EEG experiment is particularly prone to induce drowsiness (see Cantero et al. [66]). As discussed by Knott, to achieve stable levels of vigilance recordings of 5 minute duration are recommended. More recent work by McEvoy et al. has shown high reliability in a within session test-retest regime during a resting state which was slightly lower than the task related equivalent [101]. However in that study a one hour rest between the test-retest interval is administered and for this reason those results may not be representative of the 2 hour, largely continuous recording of the present study. An indirect contribution to the alpha activity error variance may be introduced by the temperature fluctuations in the experimental environment through introduced changes in arousal, although no supporting literature has been identified that can support this speculation.

Based on the above evidence it would be accurate to state that in EEG records arising from extended duration sessions, the error variance attributed to fluctuations in vigilance would be greater than that which is observed in records of shorter duration. However if such a comparison is to be drawn for the current study the state of the eyes, that is open or closed, during recordings should be taken into consideration.

Studies show that in same day test-retest regimes the stability of the resting EEG (approximately 4 minute interval) is greater under eyes closed than in eyes open conditions [31, 43, 101]. Therefore the present study may have suffered from an increased error variance due to this extra variable. At the same time the eyes open condition serves as guard against the large fluctuations in vigilance that can occur under extended recording periods (more than 5 minutes). Therefore in conclusion a decreased reliability is introduced in the data due to the eyes open condition but counteracting that is the decreased probability of large fluctuations in vigilance. In addition, the eyes open condition allows the experimenter to intervene when drowsiness is detected through slowing of eye artifact thus considerably preventing vigilance lapses.

Other implications arise due to the implementation of the eyes open condition particularly in the interpretation of the outcome. A discussion on these follows.

It is well known that when compared to the eyes closed condition eyes open resting alpha activity is lower [125]. The majority of the resting EEG studies reviewed in Chapter 2, see Table 2.1, employed the eyes closed condition as opposed to the present study which employed the eyes open condition. Two possible implications arising from this distinction have been identified.

First, it is possible that since the alpha activity is less under eyes open condition a floor effect may be observed whereby alpha activity cannot decrease as much as it would under the eyes closed condition thereby resulting in a much weaker effect. The expectation however was that alpha activity will increase under the influence of the radiation. This increase could be easily accommodated in the eyes open condition since alpha activity will be suppressed and alpha resources would not be fully engaged. Second, any induced effect on alpha activity may be dependent on a cognitive state that relates to the state of the eyes. This possibility, although remote, can potentially explain the opposite direction in changes observed here with respect to some of the reviewed studies that were summarized in Table 2.1). However, such explanation would be in disagreement with the findings of Croft et al. who employed an eyes open protocol and detected alpha band increases [34, 35].

The present study examined only resting EEG activity in an attempt to focus on the most common finding in literature, that of increased alpha activity. However, a portion of studies that demonstrated the resting alpha activity increase made use of event related potentials as well as performance tasks. This distinction may have had an impact on the fluctuation levels of alertness. First, according to McEvoy et al. and Fingelkurts et al., task performance imposes a more uniform level of alertness and mentation, thus has a stabilizing effect on the EEG [101, 43]. Second the introduction of performance tasks between resting EEG periods, interrupts the alertness variation and results in EEG records that are limited to the initial state of the resting EEG which displays a more stable vigilance profile, (see Figure 3 in reference [77]). It is therefor possible that the exclusion

of performance tasks from the protocol has caused vigilance fluctuations to be larger that those of other studies. In the current study, subject vigilance was monitored manually through observation of eye movements. If eye movements slowed down the participants were reminded to keep their eyes open and remain awake. A more structured approach has been followed by Kleinlogel et al. who introduce random auditory cues during EEG recordings to which participants had to respond by pressing a button as quickly as possible. Due to this distinction Kleinlogel et al. define their recordings as vigilance controlled EEG as opposed to resting EEG. This approach could be a more suitable one for the purposes of this investigation where the interest lies on the resting EEG only.

The present Section has identified some sources of error variance and it has been observed through measurement that the inherent noise of the amplifier unit is comparable in amplitude, within the alpha band of the EEG, with the purported effect reported here and elsewhere, see Table 2.1. In addition it is possible that fluctuations in temperature can lead to additional variance that can further obscure the radiation induced effect. It was also concluded that the eyes open condition was superior for the specific protocol. Some difficulties were also identified in terms of contrasting results with previous studies again due to the eyes open state of the recording. Finally the possible implications of the absence of any performance tasks on the resting EEG have been discussed.

7.3. Alternative interpretations of results

When observing Figure 6.16 it was seen that the baseline of Sham exposure scored lower that any other baseline and in fact any other time interval throughout the experiment. It appears that this score is at least contributing to the observed suppression of EEG activity during the active exposures. Table 6.11 summarized these statistically significant changes which in the majority were one directional thus favoring the above speculative statement. For this reason it is important to investigate whether this observation arises from some artifact. Several artefactual possibilities have been identified that may have been the source or partly contributed to this decrease of alpha

amplitude in the baseline of the Sham exposure. They are discussed next.

7.3.1. Regression to the mean

It is possible that the observation is partly the result of a chance effect whereby the baseline of the Sham condition scored at a lowest extreme of the actual alpha band distribution. With the diminished possibility of repeatedly scoring at the same extremity, the family of the following 5-minute averages regresses toward the true mean. Thus the change in alpha band activity (from baseline to subsequent intervals) appears to be larger than real. So despite the trend whereby in all four half hour experimental intervals spectral amplitudes change towards the positive direction with respect to time, the abnormally low baseline score, followed by a a collection of measurements that regressed toward the mean, is translated as an elevated increase with time in comparison to the other exposure conditions. Although such a possibility is real, it is rather remote since the baseline of the Sham condition is correlated positively with the subsequent exposure intervals, ($r>0.9$).

7.3.2. Contamination of Sham from preceding exposures

It is possible that the lower baseline score may arise due to a carry-over effect. In 75% of the sample the Sham condition occurred after a combination of active exposure(s). It is possible that a change in alpha due to a preceding exposure outlasted the time constraints of that experimental interval and as a result contaminated the Sham baseline which immediately followed. Such effect can be manifested by either a direct suppression of the alpha activity that outlasted that half hour interval, or by a rebound effect where a preceding active exposure condition caused an increase in alpha activity, and after exposure cessation the alpha activity was reduced to lower than average[3]. For such contamination to influence the results, the effect must be constrained within the baseline

[3]If such effect did indeed occur then it is also a strong indication of a real effect. Therefore the occurrence of carry-over effects does not undermine the validity of the experimental outcome so long as the source of carry-over is identified.

period and not extend in the subsequent intervals.

Some approaches that can reveal more information to this effect are discussed below.

1. If the baseline Sham suppression was a result of a carry-over effect, then the group that received Sham as the first exposure should not suffer from such a reduction. A comparison of the Sham baselines grouped according to which time interval they occurred can reveal whether such contamination did indeed occur.

2. A further subdivision and comparison of the sample into groups where Sham was preceded by specific exposures can potentially reveal which of those caused the reduction and whether specific time separations (that is immediately preceding, second precedence or third precedence to Sham) were exclusively responsible for the observed effect.

To investigate the first point the sample was split into four groups, a between subjects arrangement, according to the position at which Sham exposure occurred, that is first, second, third or fourth. The four means are calculated and compared. If a carry-over effect is indeed present the expectation is that groups that received Sham exposure first should score higher that those that were preceded by active exposures.

From the collection of means and medians($\mu(median)$ First; -.138 (-.420), Second; -.145 (-.187), Third; -.059 (-.075)and Fourth; -.024 (-.365)) it is clear that this speculation is not supported. In fact the opposite is occurring whereby the baseline of the Sham exposure in those cases where the condition is preceded by nothing registers the lowest average alpha.

The splitting of the sample as outlined above has an inherent bias in that each group mean and median is formed by scores of the same experimental time intervals. Considering the increasing trend of alpha activity throughout the experiment, see Figure 6.1, there is a bias in the 'Sham first' group to score lower. It should be noted that standardization of the data would have removed most of this bias but possibly not all.

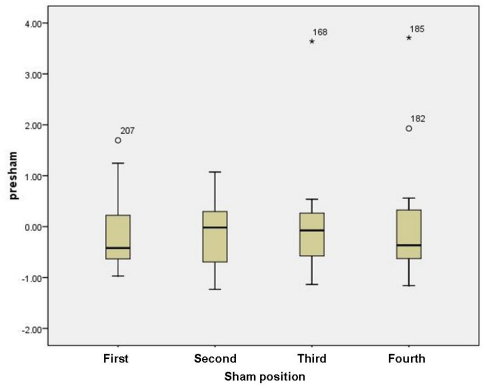

Figure 7.2.: Box plot of the Sham baselines split according to which interval they were presented.

The second, approach involving a division of the sample based on which exposure condition precedes the Sham, might suffer less from this potential bias and thus be more sensitive to detecting any carry-over effect. The probability of observing a decreased Sham baseline can be enhanced if the sub-sample that received Sham first is removed from this comparison.

A grouping selection is made based on previous findings. There exists at least one case in literature where extended post exposure monitoring periods were implemented, see reference [**?**], and in that study with 24 participants Regel et al. observed changes in the alpha band activity of the EEG that extended into a six minute interval separated in time with respect to the end of RF exposure (either PM or CW) by 60 minutes. Taking this observation as a precedence for carry-over effects at 60 minute intervals after exposure warrants the investigation of a similar effect in the current sample.

Sham exposure conditions were grouped according to what exposure took place 60 minutes before the baseline. Since Regel et al. observed decreases after both PM RF and CW RF exposures, Sham cases preceded by either exposure are grouped together and are compared with the remaining cases. The above selection and subdivision of the sample brings the sample size to 54 participants.

Once more, the observed means and medians in both baseline and during exposure intervals do

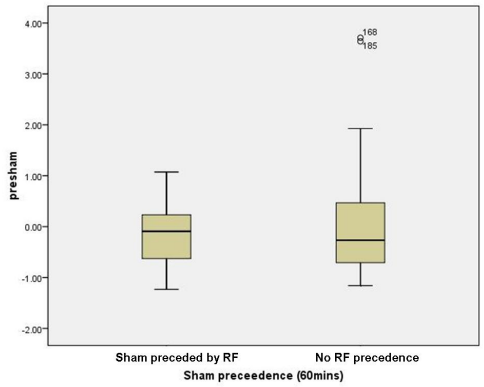

Figure 7.3.: Box plot of the Sham baselines divided according to whether they were immediately preceded by either a PM or CW RF exposures or not. Cases where Sham occurred first were excluded from this comparison. First group contains 30 cases and the second 24.

not indicate any carry-over effects.. In cases where Sham was not preceded by one hour by PM RF or CW RF the standardized mean and median where -0.162 and -0.322 but in the group with precedence the mean and median were 0.106 and -0.268.

Further, the baseline of the Sham condition was split according to whether it was preceded by a PM RF or not. Additionally cases where Sham occurred first were not included in this analysis for the same reasons that were discussed above. No difference is observed between these two distributions with means and medians of -0.0454 and -0.0757 when there was no PM RF preceding the Sham condition, and -0.0628 and -0.1692 when they were preceded (see also Figure 7.4 for full distributions).

It is possible to identify the necessary order of magnitude of the potential carry-over effect in order for it to be large enough to give rise to statistically significant changes. When observing the Table C.1 in a Appendix C, it can be seen that in 18 out of 24 cases, Sham exposure is preceded by an active exposure. On the contrary active exposures are preceded by other active exposures in 12 out of 24 cases. Assuming that carry-over effects are produced equally by all active exposures, we can conclude that the Sham condition will suffer larger carry-over effects than the active conditions.

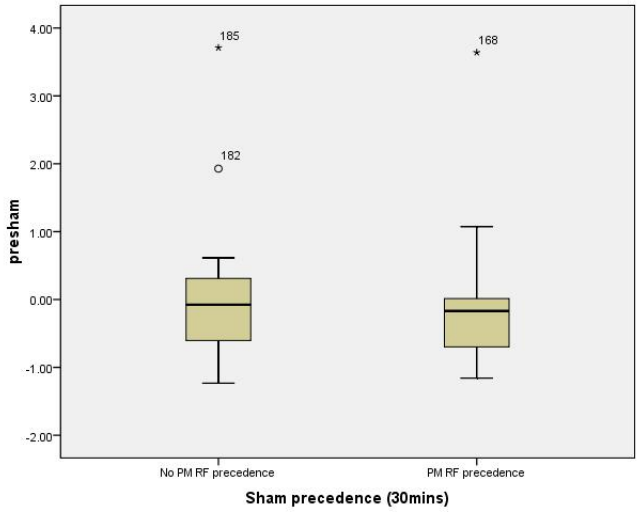

Figure 7.4.: Box plot of the Sham baselines divided according to whether they were preceded by a PM RF exposure or not. Cases where Sham occurred first were excluded from this comparison. First group contains 36 cases and the second 18.

Since the observation in the current data set was that of a decreased baseline, it follows that the carry-over effect must be negative. Assuming that the electromagnetic field effect has an amplitude of unity, through calculation it is observed that the carry over effect will have to be 6 times grater than the electromagnetic field effect, in the opposite direction (rebound effect) and must attenuate greatly by the time the during Sham exposure period begins. Current evidence does not support the existence of such a large effect which amounts to 0.6 μV. As mentioned repeatedly in this thesis, reported effects range in the vicinity of 0.1 μV, (see Section 2.1.3.3).

7.3.3. Direct comparison of exposure intervals (exclusion of baselines)

As revealed by the analysis presented in Section 7.3.2, a carry-over effect was not the source of the low baseline score that was observed under the Sham condition. No systematic experimental bias has been detected (see Section 6.1.2) that would justify this scoring and it was deduced that the possibility of a regression to the mean occurrence was remote. In Table 7.1 the statistical significance

Table 7.1.: Wilcoxon signed rank tests between the baseline of the Sham condition versus the active exposure baselines for the factor exposure condition and the factor interaction of exposure condition by laterality (ipsi/contra contrast).

Band		PM RF_{BSL}vs $Sham_{BSL}$	CW RF_{BSL}vs $Sham_{BSL}$	ELF_{BSL}vs $Sham_{BSL}$
delta - global	Z	-.713	-1.111	-1.106
	p	.476	.267	.269
delta - ipsi/contra	Z	-.168	-.045	-1.437
	p	.866	.964	.151
theta - global	Z	-1.975	-.735	-1.218
	p	**.048,** $\theta = .062$	.462	.223
theta - ipsi/contra	Z	-.281	-.499	-.572
	p	.779	.617	.576
alpha - global	Z	-2.301	-1.661	-.982
	p	**.021,** $\theta = .077$	**.097,** $\theta = .064$	.326
alpha - ipsi/contra	Z	-1.470	-2.553	-1.891
	p	.141	**.011,** $\theta = .028$	**.059,** $\theta = .020$
beta - global	Z	-.256	-.410	-.893
	p	.798	.682	0.372
beta - ipsi/contra	Z	-.241	-1.077	-.690
	p	.809	.281	.490

of baseline differences is assessed and it is seen that some of these correspond to the changes that were reported in Chapter 6. It is thus possible that at least some of the baseline differences gave rise to the observed statistical differences relating to exposure condition as listed in Table 6.11.

An alternative approach to the analysis that was presented in Chapter 6 would be to remove the baseline conditions from the statistical analysis and instead compare the exposure intervals and the post exposure intervals directly (in the form of 'raw' standardized values as opposed to difference values subtracted from a pre exposure baseline). Such data treatment would be consistent with studies in this field were baseline measures were not taken but exposure/Sham periods were compared directly in different or same day per exposure protocols [121, 53, 34, 30, 36, 28, 35, 27]. There is additional benefit from this data treatment in that the the time interval between exposures is increased to 14 minutes from 9 minutes thereby allowing for any transient undetected carry-over

effects to subside. This treatment however is expected to reduce the overall sensitivity of the method since an increased error variance will be present due to inter-individual differences in raw data. This is the case since a subtraction from the baseline serves as a normalization of individuals' data.

The results of the baseline free data analysis are presented next. No multiple comparison corrections were considered for these statistical tests. For this reason a conservative approach in the interpretation is warranted. Statistical significance was tested for the factor of exposure condition, and the factor interactions of exposure condition by laterality and exposure condition by sagittality using Wilcoxon signed rank tests.

7.3.3.1. During exposure

PM RF exposure During PM RF there was a trend level significance for the exposure condition factor, ($Z(71) = -1.767$; $p = 0.077$; $\theta = .046$), representing an increase in theta activity. Additionally there was a significant interaction of exposure condition with laterality, ($Z(71) = -3.025$; $p = 0.002$; $\theta = -.027$ ipsilateral versus contralateral), representing a decrease in ipsilateral theta activity during PM RF exposure. No other significant differences were observed.

CW RF exposure There were no statistically significant differences observed for any factor or factor interactions during CW RF exposure.

ELF exposure A statistically significant change was detected during the ELF exposure, ($Z(71) = -2.104$; $p = 0.035$; $\theta = .071$), representing an increase in theta activity. Additionally there was a significant interaction of exposure condition with laterality, ($Z(71) = -2.542$; $p = 0.011$; $\theta = -.093$, ipsilateral versus contralateral), representing an increase in ipsilateral delta activity during ELF exposure. No other significant differences were observed.

7.3.3.2. After exposure cessation

PM RF exposure A trend level change was detected post PM RF exposure, ($Z(71) = -2.116$; $p = 0.034$; $\theta = -.075$), representing a decrease in delta activity. No other significant differences were observed.

CW RF exposure There was a trend level interaction of exposure condition with sagittality post CW RF exposure, ($Z(71) = -2.020$; $p = 0.043$; $\theta = .085$), representing an increase in delta activity. Additionally the same interaction was observed in the alpha band activity, ($Z(71) = -2.020$; $p = 0.023$; $\theta = -.054$) , again representing an increase in activity. No other significant differences were observed.

ELF exposure There was a statistically significant interaction of exposure condition with sagittality post ELF exposure, ($Z(71) = -2.070$; $p = 0.038$; $\theta = -.060$), representing a decrease in theta activity.

Out of a total of 72 comparisons there was a total of 8 statistically significant results out of which only one reproduced the result in the analysis of Chapter 6. That is the result of statistically significant decrease of ipsilateral theta activity during the PM RF exposure.

The alternative analysis that was presented in this Section can be considered as a more robust alternative since the possibly large shift in alertness, as would be interpreted by the steep rise in alpha from the baseline to the subsequent intervals, will not be adding to the error variance of the data. Equally important if any undetected carry-over effects were present within the baselines that source of error variance would also be removed.

7.4. Limitations

The protocol employed in the main study described in Chapters 5 to 7 was optimized for detection of acute effects on the resting EEG from EMF radiation with exposure characteristics replicating as closely as possible the GSM radiation characteristics in terms of absolute SAR values, SAR distributions in the head volume and modulation content. These characteristics allowed for results to be as closely related to mobile phone use as possible. However there are certain trade offs associated with the selected design/protocol which are listed in Table 7.2.

DC correction through mean removal is standard practice in resting EEG analysis. However, additional processing can be performed that can further improve the quality of the data particularly at the lower end of the spectrum. One such technique is linear detrending which can be performed on epoched data. As this technique is not commonly employed, for purposes of consistency and direct comparison of results, it was omitted in the presented studies.

To obtain an indication of possible impacts of detrending on the data, linear detrending was employed on three random subjects. The results shown in Figures 7.5 and 7.6 clearly demonstrate the effect on the lower spectrum of the delta EEG band. Below 1 Hz frequency content is suppressed. Provided that this low frequency content does not arise from real EEG activity but from artificial amplifier noise such as low frequency drift an improvement in signal to noise ratio can be achieved. However before employing such analysis technique further investigations need to be performed to ensure that no EEG activity is removed from the data.

7.5. Conclusion

In this Chapter the results of the main study were put within the context of the previous studies in literature. The current results suggest that resting alpha activity decreases under radiation exposure. This finding is rather uncommon since the majority of literature reports no changes at all

Table 7.2.: A detail account of the limitations imposed by the selected main study protocol and the corresponding perceived benefits.

Protocol Characteristic	Benefit	Imposed Limitation
Single day protocol	Allows for large sample size (literature lacks large studies)	The increased possibility of carry-over effects due to the decreased washout period
Extended exposure duration	Allows for cumulative effects to prevail	Risking increases in error variance from large variations in alpha
DTX mode	Allows to test the relevance of induced effects with signal pulsing	Reduced SAR
CW and PM RF identical instantaneous exposures	Potential effect not attributed to instantaneous peak field differences	Low SAR during PM RF exposure
RF shielding of Synamps^{2TM}	Allows for EEG records during PM RF exposure to be taken	Remote possibility of increased input noise to the Synamps^{2TM} unit through elevated temperature
Localized SAR	Allows for close relevance of outcome to real mobile phone use	Increased exposure uncertainty (with respect to distribution and intensity)
"Only resting EEG" protocol	Allows to test for the most common finding in literature (changes in resting alpha)	Absence of cognitive tasks increases the variability of the alpha rhythm
Eyes open protocol	Avoids large fluctuations in alertness	Suppresses the alpha rhythm considerably

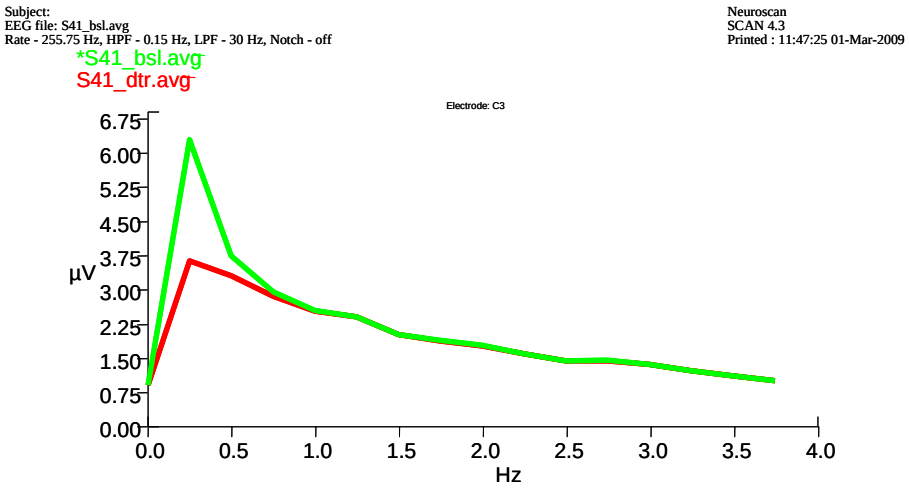

Figure 7.5.: Linear detrending versus baseline correction for subject 41 at electrode C3. Similar damping of frequency content below 1 Hz was observed at all electrodes for the specific subject.

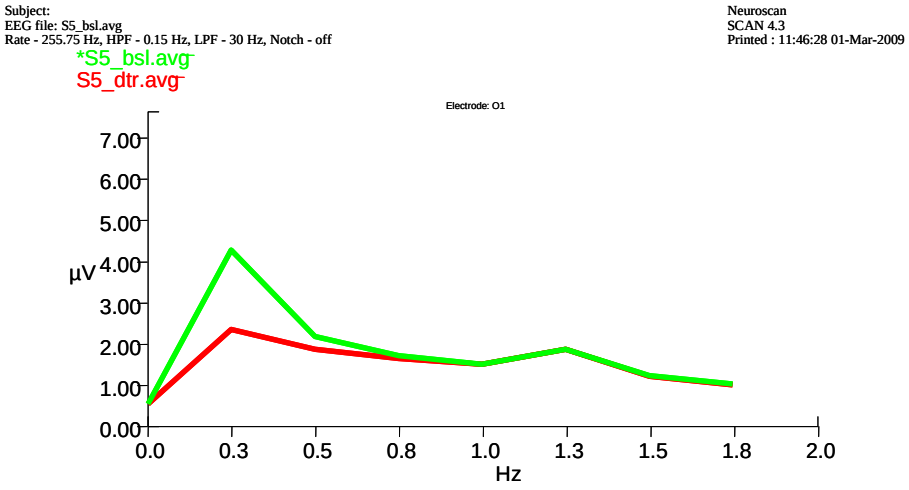

Figure 7.6.: Linear detrending versus baseline correction for subject 5 at electrode O1. Similar damping of frequency content below 1 Hz was observed at all electrodes for the specific subject.

or alpha increase in the resting EEG. It was also identified that the baseline activity during the Sham exposure was lower than during any other experimental interval be it baseline or otherwise. This lower score seems to give rise to most of the reported significant findings. In an attempt to clarify this ambiguity some hypotheses as to why the baseline would score lower have been investigated but no clear indication has been obtained that would point to artefactual contamination of the Sham baseline. It therefore remains unclear whether the reported finding is a real suppression of alpha activity during exposure or was the result of some unidentified artifact. Finally the limitations of the current study were identified along with their potential influence on the outcome.

8. Conclusions

8.1. General conclusions

The public concern about possible health effects that may arise from mobile phone use is ongoing. With the GSM system being in use for more than a decade, numerous studies have been conducted that investigated both the possibility of short and long term effects. The studies that investigated the EEG after brief exposures (usually less than 40 minutes) during awake and sleep were reviewed in Chapter 2 of the present thesis and by others, (see Section 2.1 and references [51, 26, 133]). The general trend in findings points to a small increase of alpha activity in the order of $1\mu V$ during and shortly after exposure to radiation. Additionally short exposures before sleep resulted in increases in spindle frequency activity. Despite the common trends that are observed, there are differences between studies that render comparisons difficult. For example some studies used exposure characteristics that are not representative of real mobile phone use. Another major problem that prevents any evidence from being conclusive is the absence of replication studies (that is identical protocols repeating identical outcomes).

As a precursor to the main study, described in Chapters 5 - 7, the study presented in Chapter 3 had a small sample size of 12 and a relatively remote possibility of detecting subtle EEG changes. No changes in the eyes closed resting EEG under either CW or PM RF exposures of 14 minute durations were observed.

The main human study described in the current thesis (see Chapters 5-7) attempted to detect

changes in the classical EEG bands and in non linear measures of the EEG with realistic exposures and using a sample size of 72, rendering it the second largest study in the field.

This subsequent study employed an improved protocol, incorporated an ELF exposure, used longer exposure durations and made use of better equipment. Exposure characteristics replicated those of mobile phones in terms of SAR magnitude and spatial distribution, and spectral content. To identify which feature of the signals might be responsible for changes to brain activity the GSM signal was broken into three components, a CW RF field, a PM RF field and a pulsed ELF field. Although CW RF exposure does not occur in GSM signals, its inclusion in the protocol allowed to assess the importance of the pulse modulated nature of the real GSM signal through comparison of possible effects of PM RF versus CW RF. This approach was chosen following evidence that pulsing of RF signals is necessary to elicit changes in resting brain activity [58, 114, **?**]. Lastly, pulsed ELF fields arise from the currents circulating within GSM handsets and the potential influence of those fields was assessed in the present experiment for the first time. Since the pulsing of the ELF and PM RF signals are the same, a comparison of changes under these two exposures can reveal information about differences or similarities between the nature of the two interactions.

The study corrected for multiple comparisons and found significant decreases of alpha activity during PM RF exposure (global effect), CW RF exposure (laterality effect) and ELF exposure (laterality effect). The global nature of the PM RF result may suggest that the effect was more robust in comparison to the effect under CW RF and ELF exposures. Additional trend level changes were detected for the delta, theta and beta bands, (see Table 6.11). There is a certain degree of ambiguity to these results that arises from the fact that the majority of changes were caused by the lower baseline during the Sham condition in comparison to the other conditions. At least partly, this occurrence caused the Sham difference (during exposure minus baseline) to appear larger than the respective differences of active exposures. This was translated to a decreasing alpha activity under exposure and is contradictory to the increasing alpha activity that is predominantly observed

in literature. A thorough investigation did not reveal any artefactual influence on the Sham baseline and therefore the result appears to be real. However, the presence of an artefactual event cannot be categorically excluded. An alternative analysis that excluded the baseline periods revealed no statistical changes in the alpha band, however the reduced sensitivity of that approach should not be overlooked.

Possible explanations for the discrepancy between the current findings and those of other studies were discussed in Chapter 7. They included the reduced SAR during the PM RF exposure, (0.06 W/kg versus 0.5 up to 1 W/kg), which may indicate a threshold based effect, and the nature of the protocol which might interact with a non specific mechanism of interaction and thus causing decreases in alpha activity as opposed to the more common increases that have been reported by others, (see Table 2.1).

Therefore the present results in combination with the alpha increases that were demonstrated previously could point towards a SAR or instantaneous peak threshold based effect. It is obvious that such a possibility would need to be tested in an appropriate protocol before proceeding any further with such an argument.

To assess the outcomes of the current thesis the research questions defined in Section 1.3 are answered here.

- Is GSM mobile phone radio frequency radiation capable of causing changes to the human resting EEG?

The current results suggest that changes do occur under both PM RF and CW RF radiation and the observed effect is very small, $\approx 0.03\,\mu V$, and very close to the noise floor of the experimental setup.

- If yes to the above, what is the role of the low frequency modulations of the radio frequency signal in observed results?

The statistical analysis has shown that PM RF signal produced global changes in alpha activity as opposed to the CW RF exposure that produced changes in close proximity to the radiation source. Despite the fact that SAR levels during PM RF were far lower than CW RF PM RF exposure (0.06 W/kg versus 1.95 W/kg) the PM RF seems to have caused a stronger effect as indicated by the presence of global changes versus the trend level changes under CW RF that occurred only close to the source as indicated by the interaction of exposure condition with laterality. Considering the global versus the lateral effect, it may also be speculated that the mechanism of interaction of these two exposure may differ.

Newer technologies such as the one based on the W-CDMA system do not employ signal pulsing and thus would not suffer from such signal pulsing specific effects. If it is indeed proved beyond doubt that signal pulsing is responsible for changes in brain activity, such signal structuring can be avoided in future technologies thus minimizing potential risks.

- Is GSM mobile phone ELF radiation capable of causing changes to the human resting EEG?

The current study is the first to employ ELF radiation exposures and it has shown that pulsed ELF fields are capable of producing measurable decreases in the alpha band of the resting EEG activity. The effect appears at sites that are in close proximity to the exposure source. Since this is the first study to examine the ELF component of GSM exposures, the effect of exposure on brain activity needs to be replicated before more solid statistical conclusions can be drawn.

- What practical significance do these results carry for regular GSM mobile phone users?

As was identified, the nature of these results is ambiguous and therefore to extract conclusions from it about everyday mobile phone use would be premature. A replication of the result is essential to establish more clearly whether it is a real or artefactual one. However when put within the context of previous studies the present results adds to the variability of reported effects, thus causing questions to be raised about the sensitivity of the resting EEG and of the methods used to assess such changes.

Taking this result at face value, that is assuming that it is a real phenomenon of an eyes open resting alpha band EEG activity decrease the following remark can be made. Considering that alpha activity has multiple generating sources and that bidirectional changes can be observed for both reduced or increased mental activity it is difficult to draw conclusions about the impact of such a small change to normal brain functioning (see reference [125], p. 19 on the variety of alpha generators and p. 97 on the paradoxical alpha response). However the mere presence of an effect is sufficient evidence of low-level, mobile phone-like, field interaction with the resting EEG that warrants further scientific investigation.

The current thesis presented two studies that were optimized for acute radiation related effect detection on the resting EEG. As in any other study, limitations did exist and those were identified in Section 7.4. However, none of those limitations were deemed as major enough to give rise to the observed effects. So the importance of these findings is not obscured by those limitations in any way. The next section discusses some recommendations for future research some of which relate to those limitations that were identified.

8.2. Recommendations for future research

With the issue still unresolved, the need for research is still present. Based on the findings reported throughout literature deleterious health effects have yet to be identified. The same cannot be said about biological effects which have been repeatedly demonstrated by independent research groups. As new technologies are introduced it is important for these investigations to continue and to encompass these new technologies as they are introduced. It is also true that as wireless devices multiply in both home and work environments, (wireless Internet, new mobile phone technologies bluetooth etc), the impact of low-level long term exposures from multiple sources also needs to be addressed.

With respect to human volunteer studies it is possible that the variability in results is inevitable, due to the magnitude of the reported effect which is so close to the normal variation of resting brain activity. An alternative approach that has the potential to demonstrate the consistency that is lacking is one based on case studies. A case study where a single subject is tested repeatedly provides the opportunity to demonstrate an effect consistently, or alternatively allows for an effect that arises due to the normal EEG variation to average out (a random fluctuation of the EEG in a regression to the mean manner will tend closer to the average with larger number of samples). The same approach has the potential of demonstrating individual sensitivity to exposures, a factor that potentially adds to the variability.

Future experiments on resting brain activity can benefit from employing vigilance controlled as opposed to pure resting EEG recordings. There are two reasons for this. First, long exposure periods are preferred because they allow for possible cumulative effects to take place and additionally allow for superior signal to noise ratios. However by increasing the time interval of recording sessions vigilance fluctuations become larger and thus cause more variance in results. Considering that alpha activity is strongly correlated with vigilance changes, error variance can be considerably reduced by employing vigilance controlled EEG through for example psycho-motor vigilance tasks (see McEvoy et al. for an example [101]). Through vigilance monitoring subject screening can also be performed before subjects are included in final analyses. In addition, a possibility of improved delta band analysis has been identified through the implementation of linear detrending. However the impact of this signal processing method needs to be further assessed before implemented on resting EEG data.

It seems that there are two schools of thought when it comes to designing controlled exposure environments for wireless technology risk assessment. Some prefer to maximize exposure in a manner that reduces the inter-subject variability and uncertainty of exposures, but the trade off of an exposure that deviates from the actual mobile phone-like one cannot be neglected. Others, including

those involved in the studies of the present thesis, prefer to employ exposures that closely replicate those of actual mobile phone devices. The increased inter-subject variability and uncertainty on the magnitude of exposure is the resulting trade off. It is suggested that these two approaches are complimentary to each other, and in conjunction they have the potential of providing more information regarding both possible bio-effects from mobile phone use as well as more robust information about the nature of the interaction.

8.3. Concluding remarks on the possibility of non-thermal effects on the human EEG

In the absence of any demonstrated mechanism of interaction of low-level fields with brain activity it is very difficult to identify beyond doubt whether any effects do exist. This is particularly true when the purported effects demonstrate very small consistency and are very close to the normal EEG variation.

A possibility that has not been considered previously is that the inability to demonstrate effects consistently may arise because the methods used thus far are not sensitive enough. In particular, as was demonstrated in the present thesis and in other studies, the magnitude of the effect is so small that is comparable in magnitude to the noise floor of the measurement setup. It should be noted that the main experiment described in this thesis utilized standard equipment, so similar noise levels should be expected in other studies. As a result, the effect may only occasionally exceed the noise fluctuation thus appearing with equal frequency. In a similar manner the effect may be very close to the resting EEG variability, and as a result it is masked in a random manner (that is approximately 50% of the time it is detected and 50% it is not). On the contrary the result is demonstrated with more consistency during sleep than during the awake resting EEG, (see Table 2.2). Since the sleep EEG demonstrates more structure that the resting EEG it provides for a less

noisy environment in which small changes can be observed more reliably. An additional variable that could be masking results is the potentially transitory nature of the effect whereby it manifests in short time intervals which may vary between individuals. If indeed this is the case then reliable results would be very difficult to identify. However this difficulty may be overcome through the conduct of case studies as opposed to population based studies.

In conclusion, the possibility of low level radiation interactions with the human EEG is real, as highlighted by the changes that the current study and some of those reviewed in Chapter 2 revealed. All active exposures, (PM RF, CW RF and ELF), caused decreases in alpha activity during exposure. Additional changes were observed in the delta, theta, and beta bands. The possibility of any health effects arising from these changes is not immediately obvious. The absence of any plausible mechanism that can explain the observed changes adds to the obscurity of the findings. Considering the absence of any replication studies, future research should concentrate on such studies in an attempt to produce the repeatable findings that are currently lacking. Upon reliable demonstration of any biological effect or perhaps through identification of the mechanism of interaction, such knowledge can be used to design wireless communication systems that minimize any potential risk. In addition, if the possible interaction mechanism is understood it has the potential of being used in a beneficial manner.

References

[1] Guidance on determining compliance of exposure to pulsed and complex non-sinusoidal waveforms below 100 kHz with ICNIRP guidelines. *Health Phys.*

[2] Guidelines for limiting exposure to time varying electric, magnetic, and electromagnetic fields (up to 300 GHz). *Health Phys*, 74(4):494–522, 1998.

[3] Radiation protection standard for maximum exposure levels to radiofrequency fields - 3 kHz to 300 GHz. *ARPANSA*, 2002.

[4] *Exposure to Static and Low Frequency Electromagnetic Fields, Biological Effects and Health Consequences (0-100 kHz) - Review of the Scientific Evidence and Health Consequences. International Commission on Non-Ionizing Radiation Protection.* 2003. ICNIRP 13/2003.

[5] IEEE recommended practice for determining the Peak Spatial-Average Specific Absorption Rate (SAR) in the human head from wireless communications devices: Measurement techniques. *IEEE Std 1528-2003*, pages 1–149, 2003.

[6] IEEE standard for safety levels with respect to human exposure to radio frequency electromagnetic fields, 3 kHz to 300 GHz. 2005.

[7] GSM Association Press Releases 2006. Gsm hits two billion milestone. $http://www.gsmworld.com/news/press_2006/press06_29.shtml$, 2006. retrieved July 2008.

[8] S. D. Dubey A. J. Sankoh, M. F. Huque. Some comments on frequently used multiple endpoint adjustment methods in clinical trials. *Statistics in Medicine*, 16(22):2529–2542, 1997.

[9] K. Takeuchi T. Tamura M. Sekine K. Nakamura T. Matsumoto Y. Higashi T. Ohtsubo Y. Haruta M. Shimogawara A. Koudabashi, T. Fujimoto. Spatiotemporal characteristics of MEG and EEG entrainment with photic stimulation in schizophrenia. *Conf Proc IEEE Eng Med Biol Soc.*, 6:4465–8, 2004.

[10] D. Abasolo, R. Hornero, P. Espino, J. Poza, C. I. Sanchez, and R. de la Rosa. Analysis of regularity in the EEG background activity of Alzheimer's disease patients with Approximate Entropy. *Clin Neurophysiol*, 116(8):1826–34, 2005.

[11] A. Aftab. Data communication principles: For fixed and wireless networks. 2002. Kluwer Academic Publishers Norwell, MA, USA.

[12] A. P. Anokhin, N. Birbaumer, W. Lutzenberger, A. Nikolaev, and F. Vogel. Age increases brain complexity. *Electroencephalogr Clin Neurophysiol*, 99(1):63–8, 1996.

[13] J.R. Jennings Anthony, B.J. In P.K. Ackles and M.G.H. Coles. In the blink of an eye: implications of reflex modification for information processing. *Advances In Psychophysiology*, 1985.

[14] S. Elsas B. S. Oken, M. Salinsky. Vigilance, alertness or sustained attention: physiological basis and measurement. *Clinical Neurophysiology*, 117(9):1885–1901, 2006.

[15] M. Bachmann, M. Sakki, J. Kalda, J. Lass, V. Tuulik, and H. Hinrikus. Effect of 450 mhz microwave modulated with 217 hz on human EEG in rest. *The Environmentalist*, 25(2):165–171, 2005.

[16] J. Bhattacharya. Complexity analysis of spontaneous EEG. *Acta Neurobiol Exp (Wars)*, 60(4), 2000.

[17] A. A. Borbely, R. Huber, T. Graf, B. Fuchs, E. Gallmann, and P. Achermann. Pulsed high-frequency electromagnetic field affects human sleep and sleep electroencephalogram. *Neuroscience Letters*, 275(3):207–210, 1999.

[18] C. M. Boutry, S. Kuehn, P. Achermann, A. Romann, J. Keshvari, and N. Kuster. Dosimetric evaluation and comparison of different rf exposure apparatuses used in human volunteer studies. *Bioelectromagnetics*, 29(1):11–9, 2008.

[19] M. Breakspear. Nonlinear phase desynchronisation in human electroencephalographic data. *Hum Brain Mapp*, 15:175–198, 2002.

[20] Sporns O. Lysaker P. H. O'Donnell B. F. Brenner, C. A. EEG synchronization to modulated auditory tones in schizophrenia, schizoaffective disorder, and schizotypal personality disorder. *Am J Psychiatry*, 160:2238–40, 2003.

[21] N. Burioka, G. Cornelissen, Y. Maegaki, F. Halberg, D. T. Kaplan, M. Miyata, Y. Fukuoka, M. Endo, H. Suyama, Y. Tomita, and E. Shimizu. Approximate entropy of the electroencephalogram in healthy awake subjects and absence epilepsy patients. *Clin EEG Neurosci*, 36(3):188–93, 2005.

[22] N. Burioka, M. Miyata, G. Cornelissen, F. Halberg, T. Takeshima, D. T. Kaplan, H. Suyama, M. Endo, Y. Maegaki, T. Nomura, Y. Tomita, K. Nakashima, and E. Shimizu. Approximate entropy in the electroencephalogram during wake and sleep. *Clin EEG Neurosci*, 36(1):21–4, 2005.

[23] C. C. Dechaux and R. Scheller. What are GSM and DCS. *Electrical Communication*, 2nd quarter:118–127, 1993.

[24] L. J. Challis. Mechanisms for interaction between rf fields and biological tissue. *Bioelectromagnetics*, Suppl 7:S98–S106, 2005.

[25] H. C. Christensen, J. Schuz, M. Kosteljanetz, H. S. Poulsen, J. Thomsen, and C. Johansen. Cellular telephone use and risk of acoustic neuroma. *Am J Epidemiol*, 159(3):277–83, 2004.

[26] C. M. Cook, D. M. Saucier, A. W. Thomas, and F. S. Prato. Exposure to ELF magnetic and elf-modulated radiofrequency fields: the time course of physiological and cognitive effects observed in recent studies (2001-2005). *Bioelectromagnetics*, 27(8):613–27, 2006.

[27] C. M. Cook, D. M. Saucier, A.W. Thomas, and F. S. Prato. Changes in human EEG alpha activity following exposure to two different pulsed magnetic field sequences. *Bioelectromagnetics*, 30(1):9–20, 2008.

[28] C. M. Cook, A. W. Thomas, L. Keenliside, and F. S. Prato. Resting EEG effects during exposure to a pulsed elf magnetic field. *Bioelectromagnetics*, 26(5):367–76, 2005.

[29] C. M. Cook, A. W. Thomas, and F. S. Prato. Human electrophysiological and cognitive effects of exposure to ELF magnetic and elf modulated rf and microwave fields: a review of recent studies. *Bioelectromagnetics*, 23(2):144–57, 2002.

[30] C. M. Cook, A. W. Thomas, and F. S. Prato. Resting EEG is affected by exposure to a pulsed elf magnetic field. *Bioelectromagnetics*, 25(3):196–203, 2004.

[31] M. Corsi-Cabrera, L. Galindo-Vilchis, Y. del Rio-Portilla, C. Arce, and J. Ramos-Loyo. Within-subject reliability and inter-session stability of eeg power and coherent activity in women evaluated monthly over nine months. *Clin Neurophysiol*, 118(1):9–21, 2007.

[32] R. J. Croft and R. J. Barry. EOG correction of blinks with saccade coefficients: a test and revision of the aligned-artefact average solution. *Clin Neurophysiol*, 111(3):444–51, 2000.

[33] R. J. Croft, J. S. Chandler, R. J. Barry, N. R. Cooper, and A. R. Clarke. EOG correction: a comparison of four methods. *Psychophysiology*, 42(1):16–24, 2005.

[34] R. J. Croft, J. S. Chandler, A. P. Burgess, R. J. Barry, J. D. Williams, and A. R. Clarke. Acute mobile phone operation affects neural function in humans. *Clinical Neurophysiology*, 113(10):1623–1632, 2002.

[35] R. J. Croft, D. L. Hamblin, J. Spong, A. W. Wood, R. J. McKenzie, and C. Stough. The effect of mobile phone electromagnetic fields on the alpha rhythm of human electroencephalogram. *Bioelectromagnetics*, 29(1):1–10, 2008.

[36] G. Curcio, M. Ferrara, F. Moroni, G. D'Inzeo, M. Bertini, and L. De Gennaro. Is the brain influenced by a phone call?: An EEG study of resting wakefulness. *Neuroscience Research*, 53(3):265–270, 2005.

[37] J. Daels. Proceedings: Microwave heating of the uterine wall during parturition. *J Microw Power*, 11(2):166–7, 1976.

[38] H. D'Costa, G. Trueman, L. Tang, U. Abdel-rahman, W. Abdel-rahman, K. Ong, and I. Cosic. Human brain wave activity during exposure to radiofrequency field emissions from mobile phones. *Australas Phys Eng Sci Med*, 26(4):162–7, 2003.

[39] A. Delorme and S. Makeig. EEGLAB: an open source toolbox for analysis of single-trial eeg dynamics including independent component analysis. *J Neurosci Methods*, 134(1):9–21, 2004.

[40] C. L. Ehlers, J. Havstad, D. Prichard, and J. Theiler. Low doses of ethanol reduce evidence for nonlinear structure in brain activity. *J Neurosci*, 18(18):7474–86, 1998.

[41] J. Fell, J. Roschke, K. Mann, and C. Schaffner. Discrimination of sleep stages: a comparison between spectral and nonlinear EEG measures. *Electroencephalogr Clin Neurophysiol*, 98(5):401–10, 1996.

[42] G. Pasqualetti P. De Gennaro L. Fini R. Rossini P. M. Ferreri, F. Curcio. Mobile phone emissions and human brain excitability. *Ann Neurol*, 60(2):188–96, 2006.

[43] A. A. Fingelkurts, A. A. Fingelkurts, V. A. Ermolaev, and A. Y. Kaplan. Stability, reliability and consistency of the compositions of brain oscillations. *Int J Psychophysiol*, 59(2):116–26, 2006.

[44] K. R. Foster and M. H. Repacholi. Biological effects of radiofrequency fields: does modulation matter? *Radiat Res*, 162(2):219–25, 2004.

[45] G. Fritzer, R. Goder, L. Friege, J. Wachter, V. Hansen, D. Hinze-Selch, and J. B. Aldenhoff. Effects of short- and long-term pulsed radiofrequency electromagnetic fields on night sleep and cognitive functions in healthy subjects. *Bioelectromagnetics*, 28(4):316–25, 2007.

[46] G. L. Gebber, S. Zhong, C. Lewis, and S. M. Barman. Human brain alpha rhythm: nonlinear oscillation or filtered noise? *Brain Res*, 818(2):556–60, 1999.

[47] F.M. Greene. NBS field-strength standards and measurements (30 hz to 1000MHz). In *Proc. IEEE*, volume 55, pages 970–981, 1967.

[48] T. Koenig H. Lehmann A. Minder R. Berz H. Kleinlogel, T. Dierks. Effects of weak mobile phoneÂ -Â electromagnetic fields (GSM, UMTS) on well-being and resting EEG. *Bioelectromagnetics*, 29(6):479–487, 2008.

[49] C. Haarala, S. Aalto, H. Hautzel, L. Julkunen, J. O. Rinne, M. Laine, B. Krause, and H. Hamalainen. Effects of a 902 MHz mobile phone on cerebral blood flow in humans: a pet study. *Neuroreport*, 14(16):2019–23, 2003.

[50] D. L. Hamblin, R. J. Croft, A. W. Wood, C. Stough, and J. Spong. The sensitivity of human event-related potentials and reaction time to mobile phone emitted electromagnetic fields. *Bioelectromagnetics*, 2006.

[51] D. L. Hamblin and A. W. Wood. Effects of mobile phone emissions on human brain activity and sleep variables. *Int J Radiat Biol*, 78(8):659–69, 2002.

[52] D. L. Hamblin, A. W. Wood, R. J. Croft, and C. Stough. Examining the effects of electromagnetic fields emitted by GSM mobile phones on human event-related potentials and performance during an auditory task. *Clin Neurophysiol*, 115(1):171–8, 2004.

[53] M. Hietanen, T. Kovala, and A. M. Hamalainen. Human brain activity during exposure to radiofrequency fields emitted by cellular phones. *Scand J Work Environ Health*, 26(2):87–92, 2000.

[54] H. Hinrichs, H. Heinze, and M. Rotte. Human sleep under the influence of a GSM 1800 electromagnetic far field. *Somnologie - Schlafforschung und Schlafmedizin*, 9(4):185–191, 2005.

[55] H. Hinrikus, M. Parts, J. Lass, and V. Tuulik. Changes in human EEG caused by low level modulated microwave stimulation. *Bioelectromagnetics*, 25(6):431–40, 2004.

[56] R. Huber, T. Graf, K. A. Cote, L. Wittmann, E. Gallmann, D. Matter, J. Schuderer, N. Kuster, A. A. Borbely, and P. Achermann. Exposure to pulsed high-frequency electromagnetic field during waking affects human sleep EEG. *Neuroreport*, 11(15):3321–5, 2000.

[57] R. Huber, J. Schuderer, T. Graf, K. Jutz, A. A. Borbely, N. Kuster, and P. Achermann. Radio frequency electromagnetic field exposure in humans: Estimation of SAR distribution in the brain, effects on sleep and heart rate. *Bioelectromagnetics*, 24(4):262–76, 2003.

[58] R. Huber, V. Treyer, A. A. Borbely, J. Schuderer, J. M. Gottselig, H.-P. Landolt, E. Werth, T. Berthold, N. Kuster, A. Buck, and P. Achermann. Electromagnetic fields, such as those from mobile phones, alter regional cerebral blood flow and sleep and waking EEG. *J Sleep Res*, 11(4):289–295, 2002.

[59] R. Huber, V. Treyer, J. Schuderer, T. Berthold, A. Buck, N. Kuster, H. P. Landolt, and P. Achermann. Exposure to pulse-modulated radio frequency electromagnetic fields affects regional cerebral blood flow. *Eur J Neurosci*, 21(4):1000–1006, 2005.

[60] C. S. Hung, C. Anderson, J. A. Horne, and P. McEvoy. Mobile phone 'talk-mode' signal delays EEG-determined sleep onset. *Neurosci Lett*, 421(1):82–6, 2007.

[61] R. J. McKenzie M Abramson I. Inyang, G. Benke. Comparison of measuring instruments for radiofrequency radiation from mobile phone telephones in epidemiological studies: implications for exposure assessment. *J Expo Sci Environ Epidemiol*, 18(2):134–142, 2008.

[62] L. D. Iasemidis. Epileptic seizure prediction and control. *IEEE Trans Biomed Eng*, 50(5):549–58, 2003.

[63] IEGMP. Report of the Group (the Stewart Report). *Independent Expert Group on Mobile Phones*, 2000.

[64] S. Ilvonen, A. P. Sihvonen, K. Karkkainen, and J. Sarvas. Numerical assessment of induced elf currents in the human head due to the battery current of a digital mobile phone. *Bioelectromagnetics*, 26(8):648–56, 2005.

[65] S. Iskra and I.P. MacFarlane. H-field sensor measurement errors in the near-field of a magnetic dipole source. *Electromagnetic Compatibility, IEEE Transactions on*, 31(3):306–311, 1989.

[66] R. M. Salas C. M Salas J. L. Cantero, M. Cantienza. Alpha eeg coherence in different brain states: an electrophysiological index of the arousal level in human subjects. *Neuroscience Letters*, 271(3):167–170, 1999.

[67] S. Jenvey. Measurements of the effectiveness of antenna screens for protection of the head from mobile phone radiation. *2nd international Conference on Bioelectromagnetism*, pages 201–202, 1998.

[68] L. Jing, W. Jin, G. Guozhen, G. Yao, and JLW Zhong. Effects of electromagnetic pulses on approximate entropy of multichannel EEG in freely moving rats. *Asia-Pacific Conference on Environmental Electromagnetics CEEM 2003 Nov. 47 Hangzhou .China*, 2003.

[69] J. B. Johnson. Thermal agitation of electricity in conductors. *Phys. Rev.*, 32(1):97, Jul 1928.

[70] K. Jokela. Restricting exposure to pulsed and broadband magnetic fields. *Health Physics*, 79:373–388, 2000.

[71] K. Jokela. Assessment of complex EMF exposure situations including inhomogeneous field distribution. *Health Phys*, 92(6):531–40, 2007.

[72] L. Sihvonen A. Jokela, K. Puranen. Assessment of the magnetic field exposure due to the battery current of digital mobile phones. *Health Physics*, 86((1)):56–66, 2004.

[73] J.H. Jessell T.M. Kandel ER, Schwartz. Principles of neural science. *Connecticut: Apple and Lange*, 1991.

[74] Choo M. L. Acharya U. R. Kannathal, N. and P.K. Sadasivan. Entropies for detection of epilepsy in EEG. *Comput Meth Prog Bio*, 80:187–194, 2005.

[75] Furman M. I. Pincus S. M. Ryan S. M. Lipsitz L. A. Kaplan, D. T. and A. L. Goldberger. Aging and the complexity of cardiovascular dynamics. *Biophys J*, 59:945–949, 1991.

[76] Vainikainen P. Kivekas O., Lehtiniemi T. On the general energy-absorption mechanism in the human tissue. *Microwave and optical technology letters*, 43(3):195–201, 2004.

[77] V. J. Knott. Quantitative EEG methods and measures in human psychophrmacological research. *Hum. Psychopharmacol. Clin. Exp.*, 15:479–498, 2000.

[78] T. Kobayashi, K. Misaki, H. Nakagawa, S. Madokoro, H. Ihara, K. Tsuda, Y. Umezawa, J. Murayama, and K. Isaki. Non-linear analysis of the sleep EEG. *Psychiatry Clin Neurosci*, 53(2):159–61, 1999. Journal Article Australia.

[79] Le-Wei L. Mook-Seng. Leong Tat-Soon Yeo Pang-Shyan Kooi. Specific absorption rates in human head due to handset antennas: A comparative study using FDTD. *Journal of Electromagnetic Waves and Applications*, 14(7):987–1000, 2000.

[80] A. V. Kramarenko and U. Tan. Effects of high-frequency electromagnetic fields on human EEG: a brain mapping study. *Int J Neurosci*, 113(7):1007–19, 2003.

[81] N. Kuster and F. Schonborn. Recommended minimal requirements and development guidelines for exposure setups of bio-experiments addressing the health risk concern of wireless communications. *Bioelectromagnetics*, 21(7):508–14, 2000.

[82] N. Kuster, J. Schuderer, A. Christ, P. Futter, and S. Ebert. Guidance for exposure design of human studies addressing health risk evaluations of mobile phones. *Bioelectromagnetics*, 25(7):524–9, 2004.

[83] Q. Kuster, N. Balzano. Energy absorption mechanism by biological bodies in the near fieldof dipole antennas above 300 MHz. *Vehicular Technology, IEEE Transactions on*, 41(1):17–23, 2000.

[84] J. Lass, H. Hinrikus, M. Bachmann, and V. Tuulik. Microwave radiation has modulation frequency dependent stimulating effect on human EEG rhythms. In *Engineering in Medicine and Biology Society, 2004. EMBC 2004. Conference Proceedings. 26th Annual International Conference of the*, volume 2, pages 4225–4228, 2004.

[85] N. N. Lebedeva, A. V. Sulimov, O. P. Sulimova, T. I. Korotkovskaya, and T. Gailus. Investigation of brain potentials in sleeping humans exposed to the electromagnetic field of mobile phones. *Crit Rev Biomed Eng*, 29(1):125–33, 2001.

[86] N. N. Lebedeva, A. V. Sulimov, O. P. Sulimova, T. I. Kotrovskaya, and T. Gailus. Cellular phone electromagnetic field effects on bioelectric activity of human brain. *Crit Rev Biomed Eng*, 28(1-2):323–37, 2000.

[87] T. Linde and K. H. Mild. Measurement of low frequency magnetic fields from digital cellular telephones. *Bioelectromagnetics*, 18(2):184–6, 1997.

[88] E. Parts M. Lipping, T. Olejarczyk. Analysis of photo-stimulation and microwave stimulation effects on EEG signal using higuchi's fractal dimension method. *Optical Methods, Sensors, Image Processing and Visualization in Medicine, Proc of SPIE*, 5505(2):188–96, 2004.

[89] Olejarczyk E. andParts M. Lipping, T. Fractal dimension analysis of the effects of photic and microwave stimulation on the brain function. *World Cong. Med. Phys. and Biomed. Eng., Sydney, Australia*, 18:paper 3695, 2003. ISBN 1877040142.

[90] S. P. Loughran, A. W. Wood, J. M. Barton, R. J. Croft, B. Thompson, and C. Stough. The effect of electromagnetic fields emitted by mobile phones on human sleep. *Neuroreport*, 16(17):1973–6, 2005.

[91] D. A. Wolfe M. Hoolander. Nonparametric statistical methods. *Wiley series in propability and statistics, John Wiley and Sons, Inc*, Second Edition, 1999.

[92] J. Schuderer N. Kuster M. Tuor, S. Ebert. Assesment of ELF exposure from GSM handsets and developemnt of an optimized rf/elf exposure setup for studies of human volunteers. *Technical Report, ITIS Foundation*, 2005.

[93] E. Maby, R. Le Bouquin Jeannes, G. Faucon, C. Liegeois-Chauvel, and R. De Seze. Effects of GSM signals on auditory evoked responses. *Bioelectromagnetics*, 26(5):341–50, 2005.

[94] S. Makeig and M. Inlow. Lapses in alertness: coherence of fluctuations in performance and EEG spectrum. *Electroencephalogr Clin Neurophysiol*, 86(1):2335, 1993.

[95] Inlow M. Makeig S. Lapses in alertness: coherence of fluctuations in performance and eeg spectrum. *Electroencephalogr Clin Neurophysiol*, 86(1):23–35, 1993.

[96] Inlow M. Makeig S. Individual changes in human EEG caused by 450 MHz microwave modulated at 40 and 70 Hz. *Journal The Environmentalist*, 27(4):511–517, 2005.

[97] K. Mann, H. Bauer, C. Hiemke, J. Roschke, H. Wetzel, and O. Benkert. Acute, subchronic and discontinuation effects of zopiclone on sleep eeg and nocturnal melatonin secretion. *Eur Neuropsychopharmacol*, 6(3):163–8, 1996.

[98] K. Mann, T. Klingler, S. Noe, J. Roschke, S. Muller, and O. Benkert. Effects of yohimbine on sexual experiences and nocturnal penile tumescence and rigidity in erectile dysfunction. *Arch Sex Behav*, 25(1):1–16, 1996.

[99] K. Mann, W. Maier, P. Franke, J. Roschke, and M. Gansicke. Intra- and interhemispheric electroencephalogram coherence in siblings discordant for schizophrenia and healthy volunteers. *Biol Psychiatry*, 42(8):655–63, 1997.

[100] O. N. Markand. Alpha rhythms. *J Clin Neurophysiol*, 7(2):163–89, 1990.

[101] L. K. McEvoy, M. E. Smith, and A. Gevins. Test-retest reliability of cognitive EEG. *Clin Neurophysiol*, 111(3):457–63, 2000.

[102] S. Mochizuki, S. Watanabe, M. Taki, Y. Yamanaka, and H. Shirai. The size of head phantoms for the standard measurement methods of SAR due to wireless communication devices. *IEICE Trans. Comm.*, J85-B, 2002.

[103] P. S. Myles, K. Leslie, J. McNeil, A. Forbes, and M. T. Chan. Bispectral index monitoring to prevent awareness during anaesthesia: the B-Aware randomised controlled trial. *Lancet*, 363(9423):1757–63, 2004.

[104] R. J. McKenzie I. Cosic N. Perentos, S. Iskra. Simulation of pulsed ELF magnetic fields generated by GSM mobile phone handsets for human electromagnetic bioeffects research. *Australas. Phys. Eng. Sci. Med*, 31(3):235–242, 2008.

[105] Lopes da Silva FH. Niedermeyer E. Electroencephalography: Basic principles, clinical applications and related fields. *Baltimore, USA Urban and Schwarzenberg*, 1987.

[106] T. Lehtiniemi O. KivekÃ€s, J. Ollikainen and P. Vainikainen. Bandwidth, SAR, and efficiency of internal mobile phone antennas. *IEEE Transaction on electromagnetic compatibility*, 46(1):71–87, 2004.

[107] M. Palus. Nonlinearity in normal human EEG: cycles, temporal asymmetry, nonstationarity and randomness, not chaos. *Biol Cybern*, 75(5):389–96, 1996.

[108] Kourtidou-Papadeli C. Bamidis P. D. Maglaveras N. Papadelis, C. and K. Pappas. The effect of hypobaric hypoxia on multichannel EEG signal complexity. *Comput Meth Prog Bio*, 118(1):31–52, 2007.

[109] G.F. Pedersen and J.B. Andersen. RF and ELF exposures from cellular phone handsets: TDMA and CDMA systems. *Radiat Prot Dosimetry*, 83(1-2):131–138, 1999.

[110] N. Perentos, R. J. Croft, R. J. McKenzie, D. Cvetkovic, and I. Cosic. Comparison of the effects of continuous and pulsed mobile phone like RF exposure on the human EEG. *Australas Phys Eng Sci Med*, 30(4):274–80, 2007.

[111] S. Pincus. Approximate entropy as a measure of system complexity. *PNAS*, 88:2297–2301, 1991.

[112] S. Pincus. Approximate entropy (ApEn) as a complexity measure. *Chaos*, 5(1):110–117, 1995.

[113] N. Kannathal T. Chua S. Laxminarayan R. Acharya U, O. Fausta. Non-linear analysis of EEG signals at various sleep stages. *Computer Methods and Programs in Biomedicine*, 80:37–45, 2005.

[114] S. J. Regel, J. M. Gottselig, J. Schuderer, G. Tinguely, J. V. Retey, N. Kuster, H. P. Landolt, and P. Achermann. Pulsed radio frequency radiation affects cognitive performance and the waking electroencephalogram. *Neuroreport*, 18(8), 2007.

[115] S. J. Regel, S. Negovetic, M. Roosli, V. Berdinas, J. Schuderer, A. Huss, U. Lott, N. Kuster, and P. Achermann. UMTS base station-like exposure, well-being, and cognitive performance. *Environ Health Perspect*, 114(8):1270–5, 2006.

[116] H. Reiser, W. Dimpfel, and F. Schober. The influence of electromagnetic fields on human brain activity. *Eur J Med Res*, 1(1):27–32, 1995.

[117] M. H. Repacholi. Low-level exposure to radiofrequency electromagnetic fields: health effects and research needs. *Bioelectromagnetics*, 19(1):1–19, 1998.

[118] M. H. Repacholi. Health risks from the use of mobile phones. *Toxicol Lett*, 120(1-3):323–31, 2001.

[119] M. H. Repacholi and A. Ahlbom. Link between electromagnetic fields and childhood cancer unresolved. *Lancet*, 354(9194):1918–9, 1999.

[120] J. S. Richman and J. R. Moorman. Physiological time-series analysis using approximate entropy and sample entropy. *Am J Physiol Heart Circ Physiol*, 278(6):2039–49, 2000.

[121] J. Roschke, J. Fell, and K. Mann. Non-linear dynamics of alpha and theta rhythm: correlation dimensions and lyapunov exponents from healthy subject's spontaneous eeg. *Int J Psychophysiol*, 26(1-3):251–61, 1997.

[122] M. C. Salinsky, B. S. Oken, and L. Morehead. Test-retest reliability in EEG frequency analysis. *Electroencephalogr Clin Neurophysiol*, 79(5):382–92, 1991.

[123] Shingo Okabe Noritoshi Arai Ritsuko Hanajima Yasuo Terao Toshiaki Frubayashi Yoshikazu Ugawa Satomi Inomata-Terada. Effects of high frequency electromagnetic field (EMF) emitted by mobile phones on the human motor cortex. *Bioelectromagnetics*, 28(7):553–561, 2007.

[124] G. Schmid, S. Cecil, C. Goger, M. Trimmel, N. Kuster, and H. Molla-Djafari. New head exposure system for use in human provocation studies with EEG recording during GSM900- and UMTS-like exposure. *Bioelectromagnetics*, 28(8):636–47, 2007.

[125] J. C. Shaw. *The brain's alpha rhythms and the mind.* 2003.

[126] Booth C B. Spiegel, R. J. and E. L. Bronaugh. A radiation measuring system with potential automotive under-hood application. *IEEE Trans. Electromagn. Compat.*, 25(2):61–69, 1983.

[127] C. J. Stam. Nonlinear dynamical analysis of EEG and MEG: review of an emerging field. *Clin Neurophysiol*, 116(10):2266–301, 2005.

[128] A. Straume, A. Johnsson, G. Oftedal, and J. Wilen. Frequency spectra from current vs. magnetic flux density measurements for mobile phones and other electrical appliances. *Health Phys*, 93(4):279–87, 2007.

[129] R. E. Thayer. The biopsychology of mood and arousal. *New York: Oxford University Press*, 1989.

[130] S. Longtin A. Galdrikian B. Farmer J. D. Theiler, J. Eubank. Testing for nonlinearity in time series: the method of surrogate data. *Physica D*, 58:77–94, 1992.

[131] Longtin A Eubank S Farmer JD. Theiler J, Galdrikian B. Using surrogate data to detect nonlinearity in time series. *Nonlinear modeling and forecasting, SFI studies in the sciences of complexity, proceedings vol. XII. Reading,*, pages 163–188, 1992.

[132] M. Tuor, S. Ebert, S. Schuderer, and N. Kuster. Assessment of ELF magnetic fields from 5 mobile phone handsets. *Bioelectromagnetics Conference, A joint meeting of The Bioelectromagnetics Society and The European Bioelectromagnetics Association*, page 125, 2005.

[133] E. Valentini, G. Curcio, F. Moroni, M. Ferrara, L. De Gennaro, and M. Bertini. Neurophysiological effects of mobile phone electromagnetic fields on humans: a comprehensive review. *Bioelectromagnetics*, 28(6):415–32, 2007.

[134] F. Vecchio, C. Babiloni, F. Ferreri, G. Curcio, R. Fini, C. Del Percio, and P. M. Rossini. Mobile phone emission modulates interhemispheric functional coupling of EEG alpha rhythms. *Eur J Neurosci*, 25(6):1908–13, 2007.

[135] S Verschueren, HG Wieser, and J Dobson. Preliminary analysis of the effects of DTX mobile phone emissions on the human EEG. *Proceedings of the 3rd International Workshop on the Biological Effects of EMFs Kos, Greece, In Press*, 2004.

[136] V. V. Vorobyov, A. A. Galchenko, N. I. Kukushkin, and I. G. Akoev. Effects of weak microwave fields amplitude modulated at elf on eeg of symmetric brain areas in rats. *Bioelectromagnetics*, 18(4):293–8, 1997.

[137] P. Wagner, J. Roschke, K. Mann, J. Fell, W. Hiller, C. Frank, and M. Grozinger. Human sleep EEG under the influence of pulsed radio frequency electromagnetic fields. results from polysomnographies using submaximal high power flux densities. *Neuropsychobiology*, 42(4):207–12, 2000.

[138] P. Wagner, J. Roschke, K. Mann, W. Hiller, and C. Frank. Human sleep under the influence of pulsed radiofrequency electromagnetic fields: a polysomnographic study using standardized conditions. *Bioelectromagnetics*, 19(3):199–202, 1998.

[139] C. J. Whittington and J. V. Podd. Human performance and physiology: a statistical power analysis of ELF electromagnetic field research. *Bioelectromagnetics*, 17(4):274–8, 1996.

A. Approximate Entropy

Theoretical background ApEn represents the mean probability that temporal sections (of length m) of a time series which are 'close' to each other (where 'close' is any distance smaller that a threshold distance r), will remain close for the temporal sections of incremental length m+1.

A.1. ApEn equations

Mathematically, given a time series containing N elements

$$\{x(n)\} = x(1), x(2)...x(N)$$

create vector sequences defined as

$$X(1)...X(N-m+1) \text{ where}$$

$$X(i) = x(i), x(i+1)...x(i+m-1),\ i = 1 \sim N-m+1$$

and m is the vector length, in data points, over which comparisons are made. Define distance d as

A. Approximate Entropy

$$d[X(i), X(f)] = max\Big|x(i) - x(j), x(i+1) - x(j+1)...x(i+m-1) - x(j+m-1)\Big|$$

$$\text{where } j = 1 \sim N - m + 1$$

Now for a given $X(i)$ count the number of $X(j)$s for which

$$d[X(i), X(j)] \leq r.$$

Denote this as $N^m(i)$. Then calculate

$$C_r^m = \frac{N^m(i)}{N-m+1}$$

which represents the portion of vectors that obey the similarity criterion,

$$d \leq r,$$

in comparison to $X(i)$. Repeat this for all $X(i)$s to obtain

$$C_r^m = \sum_i^N \frac{C_r^m}{N-m+1}$$

and define

$$\phi^m(r) = \ln C_r^m.$$

We repeat the above process for $m + 1$ and finally obtain

$$ApEn(m, r) = \phi^m(r) - \phi^{m+1}(r)$$

B. ELF measurements

B.1. Uncertainty in measurements of ELF fields from GSM handsets

Table B.1.: Sources of Uncertainty

Source of Uncertainty	Uncertainty	Standard Uncertainty [a] (ui)
Calibration[b]	±1.74%	0.087
$V_{peak}/217Hz$[c]	±5.00%	0.02887
Amplifier Linearity[d]	±2.83%	0.01633
Loop positioning errors[e]	±7.14%	0.00412
Combined uncertainty[f]	$u_c = \sqrt{\sum_{i=1}^{n} u_i^2}$	±5.36%
Expanded uncertainty[g]	$U = U_c k$, $k = 2$	$\pm 10.7\% C.I. = 95\%$

[a] The value u_i is obtained by dividing the uncertainty in the source by a factor that depends on the probability distribution in the 'true' value. For 'Calibration', the factor is 2 (Normal distribution). For the other uncertainty contributions, the factor is assumed to be $\sqrt{3}$ (rectangular distribution).

[b] Calibration includes uncertainties in the CRO and spectrum analyzer readings, calibration current and deviations from the required geometrical arrangement.

[c] The $V_{peak}/217Hz$ ratio accounts for the uncertainty in deducing the pulse peak from the amplitude of the 217 Hz component.

[d] Linearity in the gain characteristics of the low frequency amplifier.

[e] Includes angle deviation (5^o degrees horizontal and 5^o vertical) from the coaxial loop arrangement and distance errors during measurement.

[f] Combined uncertainty calculated by taking the square root of the sum of squares of the individual standard uncertainties.

[g] Obtained by multiplying the combined standard uncertainty by a coverage factor, k to obtain a specific confidence interval (C.I.). A $k = 2$ will give a C.I. of 95%.

B.2. Pulses of all measured handsets - Time and frequency domains

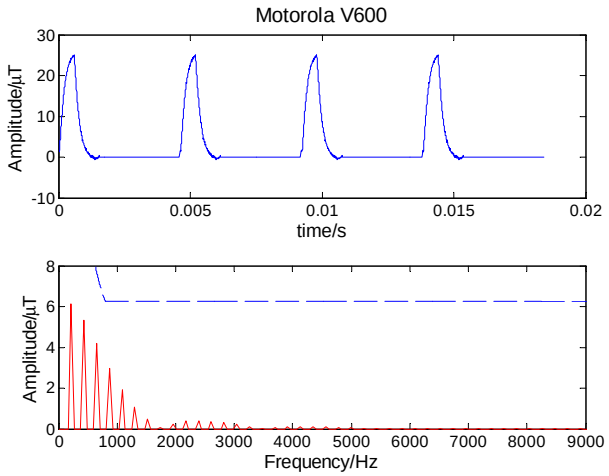

Figure B.1.: Time (top panel) and frequency (bottom panel) characteristics of recorded ELF fields for the Motorola V600 mobile phone handset. Bottom panel-Blue dashed line; ICNIRP reference peak reference levels and Bottom panel-Red dashed line; Spectral peak amplitude data of the GSM pulse train.

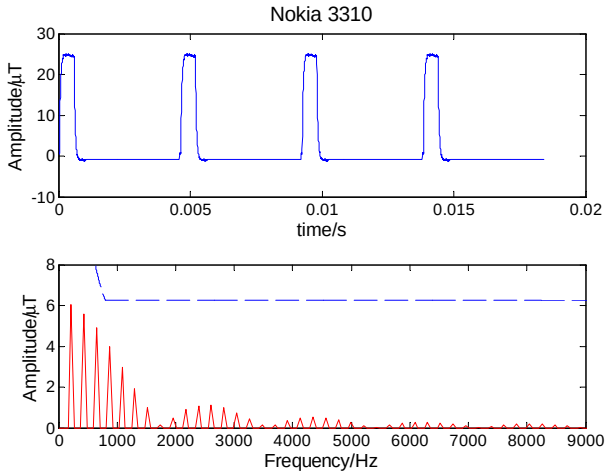

Figure B.2.: Time (top panel) and frequency (bottom panel) characteristics of recorded ELF fields for the Nokia 3110 mobile phone handset. Bottom panel-Blue dashed line; ICNIRP reference peak reference levels and Bottom panel-Red dashed line; Spectral peak amplitude data of the GSM pulse train.

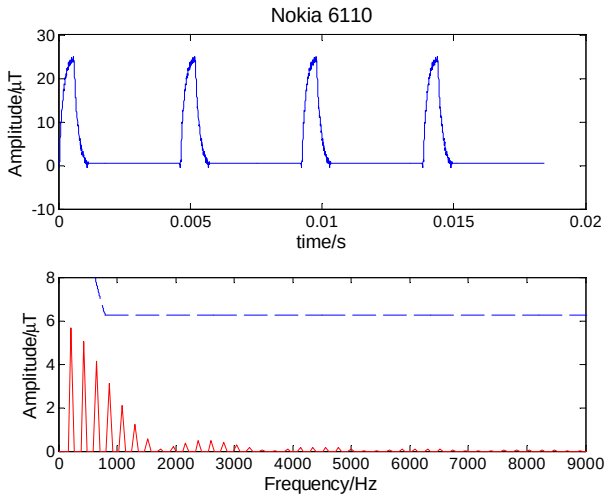

Figure B.3.: Time (top panel) and frequency (bottom panel) characteristics of recorded ELF fields for the Nokia 6110 mobile phone handset. Bottom panel-Blue dashed line; ICNIRP reference peak reference levels and Bottom panel-Red dashed line; Spectral peak amplitude data of the GSM pulse train.

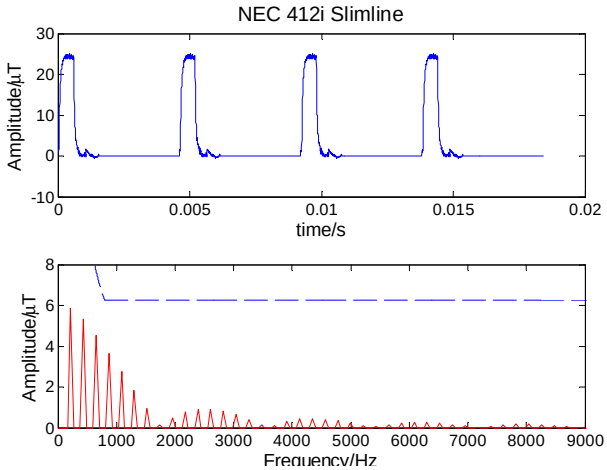

Figure B.4.: Time (top panel) and frequency (bottom panel) characteristics of recorded ELF fields for the Motorola V600 mobile phone handset. Bottom panel-Blue dashed line; ICNIRP reference peak reference levels and Bottom panel-Red dashed line; Spectral peak amplitude data of the GSM pulse train.

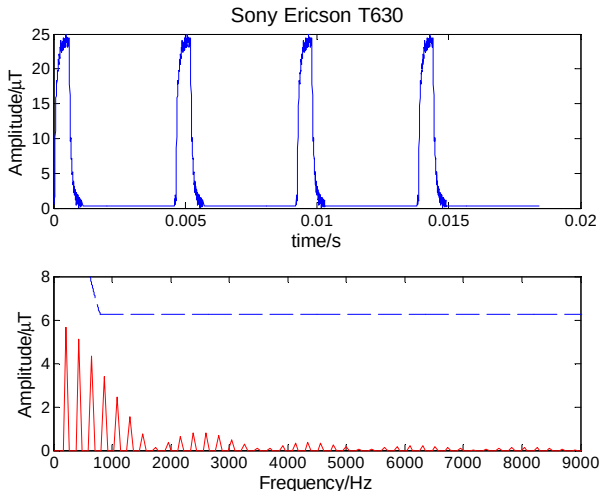

Figure B.5.: Time (top panel) and frequency (bottom panel) characteristics of recorded ELF fields for the Sony Ericsson T630 mobile phone handset. Bottom panel-Blue dashed line; ICNIRP reference peak reference levels and Bottom panel-Red dashed line; Spectral peak amplitude data of the GSM pulse train.

B.3. Induced Current density cross-sectional averaging- Mathematical development

The ICNIRP Guidelines state that induced current densities should be averaged over a cross-section of 1cm^2 before being compared to the corresponding limits. In addition, the ARPANSA standard defines that this 1cm^{2}area should be a circular cross-section. Both standards define that this cross-section must be perpendicular to the direction of current flow. To define this plane and the corresponding cross-section of interest, the following vectorial analysis is developed:

Consider a point C residing in 3-dimensional space, $C(x_C, y_C, z_C)$, with a current density given by vector $N(x_N, y_N, z_N)$.

Obtain the unit vector of N as

$$\hat{n} = \frac{\hat{x}N_x + \hat{y}N_y + \hat{z}N_z}{\sqrt{N_x^2 + N_y^2 + N_z^2}}$$

Define the equation of the plane containing point C and is perpendicular to $\hat{n}$ as

$$x_{\hat{n}} \cdot (x - x_o) + y_{\hat{n}} \cdot (y - y_o) + z_{\hat{n}} \cdot (z - z_o) = 0 \tag{B.1}$$

Define a unit vector from point C on the plane to an arbitrary point P on the plane by first defining the coordinates of point U by setting $x_U = y_U = 0$. Then, by substitution into Equation B.1 obtain z_U.

Obtain the unit vector of U as

$$\hat{u} = \frac{\hat{x}U_x + \hat{y}U_y + \hat{z}U_z}{\sqrt{U_x^2 + U_y^2 + U_z^2}}$$

Define the equation of a circle in 3 dimensional space using the parametric equation

$$P = R \cdot cos(t) \cdot \hat{u} + R \cdot sin(t) \cdot \hat{n} \times \hat{u} + C \tag{B.2}$$

Where R is the radius of the circle of interest.

C. Miscellaneous

C.1. Exposure Sequences

Table C.1.: Exposures sequences. Each exposure condition occurs 1^{st}, 2^{nd}, 3^{rd} and 4^{th} and equal amount of times. Each sequence occurred 3 times, adding up to a fully counterbalanced sample size of 72.

30 minute interval / Sequence Number	1^{st}	2^{nd}	3^{rd}	4^{th}
1	ELF	SHAM	PM_RF	CW_RF
2	CW_RF	SHAM	PM_RF	ELF
3	PM_RF	SHAM	CW_RF	ELF
4	PM_RF	SHAM	ELF	CW_RF
5	ELF	SHAM	CW_RF	PM_RF
6	CW_RF	SHAM	ELF	PM_RF
7	ELF	PM_RF	SHAM	CW_RF
8	CW_RF	PM_RF	SHAM	ELF
9	PM_RF	CW_RF	SHAM	ELF
10	PM_RF	ELF	SHAM	CW_RF
11	ELF	CW_RF	SHAM	PM_RF
12	CW_RF	ELF	SHAM	PM_RF
13	ELF	PM_RF	CW_RF	SHAM
14	CW_RF	PM_RF	ELF	SHAM
15	PM_RF	CW_RF	ELF	SHAM
16	PM_RF	ELF	CW_RF	SHAM
17	ELF	CW_RF	PM_RF	SHAM
18	CW_RF	ELF	PM_RF	SHAM
19	SHAM	PM_RF	CW_RF	ELF
20	SHAM	PM_RF	ELF	CW_RF
21	SHAM	CW_RF	ELF	PM_RF
22	SHAM	ELF	CW_RF	PM_RF
23	SHAM	CW_RF	PM_RF	ELF
24	SHAM	ELF	PM_RF	CW_RF

C.2. Consent Form

HREC Form 2a

RMIT HUMAN RESEARCH ETHICS COMMITTEE

Prescribed Consent Form For Persons Participating In Research Projects Involving Tests and/or Medical Procedures

PORTFOLIO OF: Science Engineering and Technology (SET)
SCHOOL OF: Electrical and Computer Engineering
Name of participant:
Project Title: ELF modulated RF signal influence on central nervous system

Name(s) of investigators: (1) Prof Irena Cosic Phone: 9925 1971
(2) Mr Nicholas Perentos Phone: 9925 3025

1. I have received a statement explaining the tests/procedures and questionnaire involved in this project.
2. I consent to participate in the above project, the particulars of which - including details of tests, procedures and questionnaire - have been explained to me.
3. I authorise the investigator or his or her assistant to use with me the tests, procedures and questionnaires referred to in 1 above.
4. I acknowledge that:
   (a) The possible effects of the tests or procedures have been explained to me to my satisfaction.
   (b) I have been informed that I am free to withdraw from the project at any time and to withdraw any unprocessed data previously supplied (unless follow-up is needed for safety).
   (c) The project is for the purpose of research and/or teaching. It may not be of direct benefit to me.
   (d) The privacy of the personal information I provide will be safeguarded and only disclosed where I have consented to the disclosure or as required by law.
   (e) The security of the research data is assured during and after completion of the study. The data collected during the study may be published and a report of the project outcomes will be provided to Prof Irena Cosic. Any information which will identify me will not be used.

Participant's Consent

Name: _____ **Date:** _____
(Participant - Name and Signature)

Name: _____ **Date:** _____
(Witness –Name and Signature)

Participants should be given a photocopy of this consent form after it has been signed.

Any complaints about your participation in this project may be directed to the Secretary, RMIT Human Research Ethics Committee, University Secretariat, RMIT, GPO Box 2476V, Melbourne, 3001. The telephone number is (03) 9925 1745.
Details of the complaints procedure are available from the above address.

RMIT University
RMIT

Document: HREC Form 2a_Edited to include 2b_04-2005.doc/Nicholas Perentos
Save Date: 26-10-2007
Page 1 of 1

C.3. Screening Questionnaire

QUESTIONNAIRE

Personal information shall not be disclosed to anyone other than the individual concerned upon request.

Participant No_____

Please answer the following questions.

Date: __/__/__

Age:

Gender: ☐ **Male** ☐ **Female**

Do you have any installed pacemakers or metal implants?
☐**Yes** ☐**No**

Have you ever experienced serious head injury?
☐**Yes** ☐**No**

Do you have any known health conditions that affect your brain?
☐**Yes** ☐**No**

Are you currently taking any prescription medicines?
☐**Yes** ☐**No**

Have you had any caffeine intake today?
☐**Yes** ☐**No**

Do you normally have caffeine on an everyday basis?
☐**Yes** ☐**No**

Are you a regular smoker?
☐**Yes** ☐**No**

Have you smoked today?
☐**Yes** ☐**No**

Have you used your mobile phone today?
☐**Yes** (proceed to subsections a. and b.)
☐**No** (go to next question)

a. Time of last phone call: _____hours and _____minutes ago (approximately)

b. Duration of last phone call:
☐ **up to 5 minutes**
☐ **up to 30**
☐ **more than 30**

Do you feel that you had adequate sleep last night?
☐**Yes** ☐**No**

C.4. AD/ACL

Time 1

Activation-Deactivation Adjective Checklist (AD ACL)

definitely feel	(vv)	v	?	no
feel slightly	vv	(v)	?	no
cannot decide	vv	v	(?)	no
definitely do not feel	vv	v	?	(no)

active	vv	v	?	no
placid	vv	v	?	no
sleepy	vv	v	?	no
jittery	vv	v	?	no
energetic	vv	v	?	no
intense	vv	v	?	no
calm	vv	v	?	no
tired	vv	v	?	no
vigorous	vv	v	?	no
at-rest	vv	v	?	no
drowsy	vv	v	?	no
fearful	vv	v	?	no
lively	vv	v	?	no
still	vv	v	?	no
wide-awake	vv	v	?	no
clutched-up	vv	v	?	no
quiet	vv	v	?	no
full-of-pep	vv	v	?	no
tense	vv	v	?	no
wakeful	vv	v	?	no

D. List of Publications

1. N. Perentos, R.J. Croft, R.J. McKenzie, D. Cvetkovic and I. Cosic, "The Effects of GSM like ELF Radiation on the Alpha Band of the Human Resting EEG", *30th Annual International Conference IEEE Engineering in Medicine and Biology Society* (EMBS), Vancouver, Canada, 2008.

2. Perentos, N., Iskra, S., McKenzie, R. J., and Cosic, I., "Simulation of pulsed ELF magnetic fields generated by GSM mobile phone handsets for human electromagnetic bioeffects research", *Australas Phys Eng Sci Med*, 31(3): 235-42, 2008

3. Perentos, N., Croft, R. J., McKenzie, R. J., Cvetkovic, D. and Cosic, I. "Comparison of the effects of continuous and pulsed mobile phone like RF exposure on the human EEG", *Australas Phys Eng Sci Med*, 30(4): 274-80, 2007

4. Perentos, N, Iskra, S, McKenzie, RJ & Cosic, I. "Characterization of pulsed ELF magnetic fields generated by GSM mobile phone handsets", *WC2006 World Congress on Medical Physics and Biomedical Engineering*, Seoul, Korea, 2006

5. Perentos, N, Cosic, I & Cvetkovic, D., "Characterization of magnetic fields generated by mobile phone handsets and their batteries", *World Health Organization (WHO) Regional Workshop on Radio Frequency Fields*, Melbourne, 2005